NNT/NL : 0000AIXM0000/000ED000

THÈSE DE DOCTORAT

Soutenue à Aix-Marseille Université
Le 15 décembre 2022 par

Malak ZOAITER

Analyse culturomique: Description de nouvelles espèces bactériennes et potentiel de résistance à la colistine

Discipline
Biologie santé

Spécialité
Maladies infectieuses

École doctorale
ED 62-Sciences de la vie et de la santé

Laboratoire/Partenaires de recherche
VITROME/ MEPHI /AP-HM /IRD

Composition du jury

Pr. Max MAURIN Université de Grenoble	Rapporteur
Pr. Eid AZAR Université de Balamand	Rapporteur
Pr. Florence FENOLLAR Université d'Aix-Marseille	Présidente du jury
Pr. Pierre-Edouard FOURNIER Université d'Aix-Marseille	Directeur de thèse

Affidavit

Je soussignée, Malak ZOAITER, déclare par la présente que le travail présenté dans ce manuscrit est mon propre travail, réalisé sous la direction scientifique de Professeur Pierre-Edouard Fournier dans le respect des principes d'honnêteté, d'intégrité et de responsabilité inhérents à la mission de recherche. Les travaux de recherche et la rédaction de ce manuscrit ont été réalisés dans le respect à la fois de la charte nationale de déontologie des métiers de la recherche et de la charte d'Aix-Marseille Université relative à la lutte contre le plagiat.

Ce travail n'a pas été précédemment soumis en France ou à l'étranger dans une version identique ou similaire à un organisme examinateur.

Fait à Marseille, le 10 novembre 2022

Malak

Cette œuvre est mise à disposition selon les termes de la Licence Creative Commons Attribution - Pas d'Utilisation Commerciale - Pas de Modification 4.0 International.

Liste de publications

Liste des publications réalisées durant la période de thèse :

1. **Article 1:** *Streptococcus bouchesdurhonensis* sp. nov. isolated from a bronchoalveolar lavage of a patient with pneumonia (under review in Archives of Microbiology)
   Malak Zoaiter, Reham Magdy Wasfy, Aurelia Caputo, Florence Fenollar , Zaher Zeaiter, Pierre-Edouard Fournier, Linda Houhamdi

2. **Article 2:** Description of *Brucella senegalensis* sp. nov. isolated from a senegalese chimpanzee using the taxono-genomic approach (ready to be submitted)
   Malak Zoaiter, Jamal Saad, Babacar Mbaye, Edmond Kuete, Oleg Mediannikov, Bernard Davoust, Cheikh Ibrahima Lo, Florence Fenollar, Zaher Zeaiter, Didier Raoult, Pierre-Edouard Fournier

3. **Article 3:** Taxono-genomic description of *Brucella troglodytis* sp. nov. isolated from senegalese Chimpanzee (ready to be submitted)
   Malak Zoaiter, Rita Zgheib, Hacene Medkour, Louis Kangale, Edmond Kuete, Oleg Mediannikov, Bernard Davoust, Cheikh Ibrahima Lo, Florence Fenollar, Zaher Zeaiter, Didier Raoult, Pierre-Edouard Fournier

4. **Article 4:** Draft genomes of two *Fusobacterium simiae* strains (submitted in Microbiology Resource Annoucements)
   Malak Zoaiter, Florence Fenollar , Pierre-Edouard Fournier, Linda Houhamdi

5. **Article 5:** Intrinsic resistance to polymyxins (to be submitted)
   Malak Zoaiter, Zaher Zeaiter, Eric Ghigo, Pierre-Edouard Fournier

6. **Article 6:** Carbonyl cyanide m-chlorophenyl hydrazone (CCCP) restores the colistin sensitivity in *Brucella intermedia* (submitted in International Journal of Molecular Sciences)
   Malak Zoaiter, Zaher Zeaiter, Michel Drancourt, Cheikh Sokhna, Oleg Mediannikov, Pierre-Edouard Fournier

7. **Article 7:** Description of *Agathobaculum massiliensis* sp. nov. isolated from human stool (submitted in Archives of Microbiology).
   Reham Magdy Wasfy, **Malak Zoaiter**, Cheikh Ibrahima LO, Stéphane Alibar, Florence Fenolla , Didier Raoult, Pierre-Edouard Fournier, Matthieu Million

8. **Article 8**: Description of *Ornithinibacillus timonensis* sp. nov., *Thalassobacillus timonensis* sp. nov., *Sutcliffiella maliensis* sp. nov., *Pseudalkalibacillus massiliomalei* sp. nov., *Halobacillus maliensis* sp. nov., *Virgibacillus cacae* sp. nov., *Lentibacillus ihumii* sp. nov., *Rossellomorea faecium* sp. nov., eight moderate halophilic new species isolated from Malian healthy children (to be submitted)
   Salimata Konate, **Malak Zoaiter**, Aminata Camara, Ogobara Doumbo, Abdoulaye Djimde, Safiatou Niare, Abdoulaye Kassoum Kone, Issa Traore, Pierre-Edouard Fournier, Mahamadou Ali Thera, Maryam Tidjani Alou, Didier Raoult, Matthieu Million

Résumé

Au cours de ma thèse, nous avons isolé quinze espèces bactériennes à partir d'échantillons animaux et humains. Douze des espèces, appartenant à dix genres bactériens se sont révélées être des nouvelles espèces qui ont fait l'objet de descriptions officielles dans cinq articles. Nous avons également étudié le mécanisme à l'origine de la résistance à la colistine de six souches de *Brucella intermedia* isolées de selles de chimpanzés. En utilisant le cyanure de carbonyle 3-chlorophénylhydrazone (CCCP), nous avons montré que la sensibilité à la colistine pouvait être restaurée, à la différence de trois autres inhibiteurs de pompes à efflux. Les résultats ont montré que la résistance de *B. intermedia* à la colistine était causée par un mécanisme d'efflux et ont suggéré que l'utilisation d'une combinaison de colistine et d'inhibiteur de pompes à efflux représentait une piste thérapeutique contre la résistance à la colistine chez les *Brucella*. Les analyses génomiques ont permis l'identification des gènes potentiellement impliqués dans le mécanisme de résistance. La prédiction des pompes à efflux candidates pourrait donc avoir une incidence clinique. Un effet inhibiteur du CCCP en combinaison avec la colistine a été observé aussi sur la formation du biofilm. D'autres investigations seront à poursuivre pour confirmer cet effet observé sur la formation de biofilm. Nos résultats suggèrent que la résistance à la colistine est réversée par le CCCP et que le mécanisme inhibé par le CCCP, probablement médié par les pompes à efflux, est essentiel à la survie des *Brucella intermedia.*

Mots clés : Culturomique, *Brucella intermedia*, nouvelles espèces bactériennes, taxono-génomique, résistance à la colistine, chimpanzés.

Abstract

During my thesis, I isolated fifteen bacterial species from animal and human samples. Twelve of the species, belonging to ten bacterial genera, were found to be new species and have been formally described in five papers. I also investigated the mechanism behind colistin resistance in six strains of *Brucella intermedia* isolated from chimpanzee feces. Using the carbonyl cyanide 3-chlorophenylhydrazone (CCCP), I showed that susceptibility to colistin could be restored, unlike the use of another three efflux pump inhibitors. The results showed that the resistance of *B. intermedia* to colistin was caused by an efflux mechanism and suggested that the use of a combination of colistin and efflux pump inhibitor represented a therapeutic approach against colistin resistance in *Brucella*. Genomic analyses allowed the identification of genes involved in the resistance mechanism. Prediction of candidate efflux pumps may have clinical implications. An inhibitory effect of CCCP in combination with colistin was also observed on biofilm formation. Further investigations to elucidate the effect shown on biofilm formation. My results suggest that colistin resistance is reversed by CCCP and that the CCCP-inhibited mechanism, probably mediated by efflux pumps, is essential for the survival of *Brucella intermedia*.

Keywords: Culturomics, *Brucella intermedia*, new bacterial species, taxono-genomics, colistin resistance, chimpanzee.

Remerciements

D’abord, je tiens à remercier chacun des membres du jury, le Professeur **Max Maurin** et le Professeur **Eid Azar** de m’avoir faite l’honneur d’être les rapporteurs de ma thèse et également la Professeure **Florence Fenollar** d’avoir accepté de faire partie de mon jury de thèse. Veuillez accepter l’expression de ma profonde reconnaissance.

J’exprime ma sincère gratitude au Professeur **Pierre-Edouard Fournier** de m’avoir donnée l’opportunité de faire une thèse à l’« IHU - Méditerranée Infection » et de m’avoir accueillie dans son équipe. J’étais chanceuse d’être sous votre supervision. Merci pour votre gentillesse, votre humanité, votre disponibilité permanente, et votre calme dans les situations stressantes. Je vous suis très reconnaissante pour tout ce que vous m’avez apportée sur le plan scientifique et personnel. infiniment le

Je remercie Professeur **Didier Raoult** de m’avoir acceuillie au sein de l’Institut Hospitalo Universitaire - Méditerranée Infection.

Je remercie également Professeur **Eric Ghigo**, de m'avoir tellement encouragée, merci pour vos conseils bienveillants.

Je tiens à exprimer ma reconnaissance particulière à **Yasmine Dergham, Rita Jaafar** et **Ahmad Joshkon**. À l’ensemble de **mes amis et collègues de l’IHU**, en particulier **Aznavour**, merci pour les bons moments passés ensemble, les rires et les pauses-café. Ce fut un plaisir de faire partie de cette famille. Je m’excuse de ne pas vous mentionner individuellement mais vous savez qui vous êtes.

Pour mon chéri Zaher , mes remerciements ne pourront jamais égaler ton grand cœur qui m'a apporté du soutien au moment où j'avais besoin. Merci pour ton soutien continu et ton amour, pour ta fidélité et ta patience.

Enfin, je remercie profondément **mon père Mostafa**, **ma mère Wissam**, **mes sœurs et mon frère** auxquels je dédie ce travail. Je suis reconnaissante pour votre amour et soutien éternels et inconditionnels.

Pour ma grande mère **Niaam,** je suis tellement reconnaissante de t’avoir eu dans ma vie, je sais que tu me gardes un œil du ciel. Tu me manques profondément.

Affidavit **2**

Liste des publications et participation aux conférences **3**

Résumé **5**

Abstract **6**

Remerciements **7**

Table de matière **8**

Introduction **9**

Objectifs et structure de la thèse **17**

Chapitre I : Description de nouvelles espèces bactériennes en utilisant l'approche polyphasique de la taxono-génomique **19**

Avant-propos **20**

Article 1 : *Streptococcus bouchesdurhonensis* sp. nov. isolated from a bronchoalveolar lavage of a patient with pneumonia **22**

Article 2: Description of *Brucella senegalensis* sp. nov. isolated from a senegalese chimpanzee using the taxono-genomic approach **45**

Article 3 : Taxono-genomic description of *Brucella troglodytis* sp. nov. isolated from senegalese Chimpanzee **73**

Article 4 : Draft genomes of two *Fusobacterium simiae* strains **101**

Chapitre II : Etude de la résistance à la colistine chez les souches de *Brucella intermedia* **107**

Avant-propos **108**

Article 5 : Intrinsic resistance to polymyxins **110**

Article 6 : Carbonyl cyanide m-chlorophenyl hydrazone (CCCP) restores the colistin sensitivity in *Brucella intermedia.* **149**

Conclusions et perspectives **179**

Annexes **186**

Bibliographie **229**

Introduction

Introduction

Les procaryotes sont ubiquitaires dans l'environnement et interagissent en permanence avec les autres êtres vivants, dont l'homme [1]. L'évaluation de cette biodiversité et de son impact sur la santé humaine nécessitent l'isolement, la caractérisation et la classification des espèces bactériennes qui interagissent avec l'homme. La découverte accrue de nombreuses nouvelles espèces au cours des dernières décennies pourrait être utile pour un nombre considérable d'applications dans les domaines de la biomédecine, de la surveillance de l'environnement et de la biosécurité. Le nombre d'espèces bactériennes était en 1980, de 1791 espèces. En 2022, il est de 18674 espèces validées [2]. Ce répertoire bactérien a augmenté grâce à différentes approches dont la culturomique, la génomique, et la métagénomique.

La culturomique, stratégie basée sur la diversification des conditions de culture, a été introduite pour la culture des espèces réputées non-cultivables [3]. La renaissance de la culture a été initiée par les microbiologistes de l'environnement qui ont été les premiers à développer des méthodes de culture et des milieux qui imitent l'environnement naturel des micro-organismes [4]. Dans certaines études, ceci a permis d'augmenter 300 fois le nombre de colonies isolées [5]. Une autre piste d'optimisation de la culture bactérienne, la co-culture en présence d'une autre bactérie connue, a démontré son utilité en fournissant des facteurs sécrétés favorisant la croissance des bactéries qui en sont déficientes et non-cultivables pour cette raison [3]. Enfin, l'élucidation des voies de communication inter-bactérienne a permis l'identification des carences en nutriments dans les milieux standards, qui sont nécessaires pour la croissance bactérienne, et qui pourraient par la suite être ajoutées à la formulation des milieux [6]. En 2012, la

culturomique a permis l'isolement d'un nombre record de bactéries du microbiote humain en adoptant des protocoles de culture optimisés et innovants [7, 8]. En diversifiant les atmosphères, températures, pH, nutriments, minéraux, antibiotiques et phages, des populations minoritaires de bactéries ont été détectées dans les échantillons étudiés. Ces populations peuvent inclure des bactéries pathogènes comme *Salmonella Typhimurium, Tropheryma whipplei* et *Yersinia enterocolitica* [7, 9]. De même, la culturomique a contribué à la découverte d'un monde microbien inexploré, connu sous le nom de « matière noire microbienne », en augmentant le nombre de nouvelles espèces bactériennes cultivées [10, 11].

Ce paradigme est devenu possible grâce au progrès remarquable de la spectrométrie de masse (MALDI-TOF MS). Cette dernière a permis une identification précise à la fois aux niveaux du genre et de l'espèce des bactéries. Cette identification est basée sur la comparaison des profils peptidiques à des bases de données. Sa première utilisation en routine a été rapportée en 2009 dans des laboratoires de microbiologie clinique [12]. La spectrométrie MALDI-TOF MS a réduit le temps d'identification bactérienne à quelques heures et les coûts d'au moins un facteur de 5 en comparaison avec la plupart des méthodes d'identification phénotypique conventionnelle [13]. Caractérisée par sa rentabilité, sa rapidité, sa reproductibilité, elle est devenue une méthode de référence pour l'identification bactérienne en microbiologie clinique [13]. A côté de l'application de la spectrométrie MALDI-TOF MS, l'utilisation de la méthode universelle d'identification basée sur le séquençage des gènes essentiels comme la sous-unité 16S de l'ARN ribosomal est réalisée surtout pour les nouvelles espèces non identifiées avec la spectrométrie MALDI-TOF MS [14].

L'identification de nouvelles espèces peut avoir des effets bénéfiques sur la santé, notamment en détectant de futurs candidats à la bactériothérapie sous forme de probiotiques [15]. L'exploration des relations entre le monde bactérien et la santé humaine nécessite, tant pour les modèles expérimentaux que pour les stratégies thérapeutiques, la culture pure des bactéries. La culturomique reste la meilleure méthode pour capturer la biodiversité fonctionnelle et viable.

L'approche génomique a élargi notre compréhension de la diversité bactérienne. Elle a conféré la caractérisation génétique des espèces bactériennes. La génomique a été appliquée dans la caractérisation et la surveillance des agents pathogènes [16]. De plus, des études ont fait la preuve de concept de l'intérêt de l'utilisation du séquençage de nouvelle génération (NGS) en routine dans les laboratoires de microbiologie clinique [17]. La production de génomes multiples par ces laboratoires a créé une source de données qui sera utilisée pour étudier l'évolution des agents pathogènes, l'étude des populations, les mécanismes d'échange génétique, l'identification des gènes de virulence, des gènes de résistance aux antibiotiques et la mise au point des vaccins [18]. La génomique a contribué à développer des milieux de culture spécifiques pour les bactéries non-cultivables sur milieux axéniques en identifiant leurs voies métaboliques incomplètes, comme pour *T. whipplei*, l'agent de la maladie de Whipple pour lequel l'identification des voies métaboliques déficientes a conduit à la mise au point d'un milieu axénique complémenté [19, 20].

De plus, la génomique a été utilisée comme outil taxonomique permettant l'étude de la diversité et les relations entre les bactéries [21]. L'analyse génomique est devenue obligatoire pour la description des nouvelles espèces bactériennes. Initialement, la classification bactérienne était basée sur le pouvoir pathogène des bactéries, des caractères morphologiques, physiologiques et biochimiques [22]. Dans les années 1980s,

le séquençage du gène codant l'ARNr 16S, a été recommandé pour la description des nouvelles espèces bactériennes [23]. Une similarité de séquence d'ARNr 16S de 95-98,65% entre deux souches indique qu'elles appartiennent au même genre [24]. Bien que cette révolution ait restructuré la taxonomie bactérienne, elle reste une méthode problématique pour les espèces étroitement apparentées, comme c'est le cas du groupe *mitis* des *Streptococcus* [25]. Des gènes de référence alternatifs à l'ARNr 16S, comme les gènes codant pour les sous-unités alpha et bêta de l'ARN polymérase *(rpoA, rpoB),* la sous-unité bêta de l'ADN gyrase **(***gyrB),* la protéine chaperonne *(groEl),* l'enzyme recombinase A *(recA)* et d'autres, ont été utilisés pour répondre à des questions taxonomiques du niveau de l'espèce, voire de rang inférieur [26, 27].

Plusieurs algorithmes, basés sur les degrés de similarité entre séquences génomiques, ont servi à la taxonomie tel que l'hybridation digitale ADN-ADN, et la moyenne de l'identité nucléotidique (ANI) [21, 28]. Jusqu'à présent, l'hybridation ADN-ADN est restée le critère de référence pour estimer l'identité génétique entre les procaryotes [29]. Une valeur de 70 % a été recommandée comme le seuil qui permet de définir des nouvelles espèces. La même valeur est utilisée comme seuil pour la méthode d'hybridation digitale ADN-ADN. Une valeur ANI de 95% entre deux génomes bactériens a été proposée comme étant équivalente à la valeur 70% d'hybridation ADN-ADN [30]. Actuellement, une approche polyphasique, sous le nom de taxono-génomique, est utilisée pour classifier les bactéries, rassemblant à la fois des caractères phénotypiques et génomiques [31]. L'hybridation ADN-ADN, la séquence d'ARNr 16S et la composition en G+C restant les principaux critères génotypiques [32] [33].

L'approche métagénomique a servi pour acquérir une connaissance approfondie des communautés bactériennes dans les milieux environnementaux et cliniques. Elle permet une identification des micro-organismes dans un environnement spécifique. Elle

se différencie de la culturomique par sa capacité à détecter les micro-organismes non cultivables [34]. Elle est basée sur le criblage fonctionnel de gènes ou l'analyse de séquençage, indépendamment de la culture des bactéries [34]. Les principaux domaines d'application de la recherche en métagénomique sont la diversité microbienne, la structure des populations, les relations génétiques et évolutives, l'activité fonctionnelle, les relations de coopération et les relations avec l'environnement. En médecine, la métagénomique a été largement utilisée dans l'étude du microbiome humain et la détection des agents pathogènes médicaux comme *Neisseria meningitidis* [14, 35]. Beaucoup de recherches métagénomiques se concentrent, de nos jours, sur l'étude des bactéries résistantes aux antibiotiques et les gènes impliqués dans cette résistance [36] [37]. Elle a joué aussi un rôle important dans la bioremédiation environnementale en identifiant des gènes fonctionnels qui peuvent dégrader des polluants organiques dans l'environnement [38].

Les approches métagénomiques ont considérablement élargi la diversité microbienne, aussi bien dans le domaine clinique que dans les écosystèmes microbiens environnementaux; mais elles présentent certaines limitations et de nombreuses séquences restent non-attribuées, correspondant à des espèces non identifiées [10]. Cependant, à cause de leur biais de profondeur, elles sont incapables de détecter des petites populations de bactéries dans les populations polymicrobiennes [39]. Ce qui rend la culturomique l'approche idéale complémentaire aux études métagénomiques [8].

La résistance aux antibiotiques est devenue un problème majeur qui menace la santé animale et humaine. En 2013, l'Organisation Mondiale de la Santé (OMS) a déclaré la situation de la résistance aux antibiotiques comme particulièrement préoccupante [40]. Pour un nombre croissant d'infections, comme les pneumonies, la tuberculose, les septicémies, la gonorrhée et les infections d'origine alimentaire, le traitement devient

plus difficile, voire impossible parfois, du fait de la perte d'efficacité des antibiotiques [41]. La disponibilité des approches culturomique, génomique et métagénomique peut servir à l'étude de la résistance aux antibiotiques et par conséquence à avoir une incidence clinique.

La culture et l'isolement d'agents pathogènes cibles porteurs de gènes d'intérêt sont également essentiels pour déterminer les phénotypes de résistance aux antibiotiques. La culture reste la principale méthode utilisée par les laboratoires cliniques pour effectuer les tests de susceptibilité aux antibiotiques [42]. Récemment, les méthodes de culture à haut débit ont augmenté les capacités de traitement, la production et l'analyse des données basées sur la culture [14]. Compte tenu de la découverte récente de nouveaux agents antimicrobiens produits par des commensaux humains, une telle collection de souches pourrait faciliter l'identification de nouveaux antibiotiques [43]. De même, étudier les mécanismes de résistance se base initialement sur la culture des micro-organismes [44]. Des expériences in vitro en présence et en absence d'antibiotiques permettent de mieux comprendre le monde complexe de la résistance aux antibiotiques. Les études fondées sur la culture peuvent permettre d'identifier les liens entre la résistance aux antibiotiques mesurée dans l'environnement et la résistance aux antibiotiques détectée chez des isolats cliniques et humains [34].

La génomique a permis des études plus approfondies sur la diversité et l'abondance des gènes de résistance aux antibiotiques. Elle a amélioré la détection de l'émergence des clones à haut risque, qui ont tendance à disséminer rapidement, et de surveiller leur propagation. Prenons l'exemple de l'émergence du gène de résistance à la colistine mcr-1 (gène mobilisé de la résistance à la colistine) en Allemagne [45,46]. Cette approche a offert la possibilité de fournir des prédictions rapides, cohérentes et précises concernant les gènes de résistance du phénotype résistant détecté. Les données peuvent

être partagées dans des bases de données publiques comme celle hébergée par le Centre Nationale d'Information Biologique (NCBI).

La métagénomique a été utilisée pour comprendre la dynamique du transfert latéral de gènes de résistances dans des écosystèmes donnés comme les bactéries résistantes peuvent potentiellement diffuser largement leurs gènes de résistance parmi les membres de la communauté endogène [47]. Cette approche a montré un rôle dans l'identification des « hotspot » pour la génération d'éléments de résistance tels que les équipements de l'aquaculture [48].

Au cours de notre travail de thèse, nous avons caractérisé douze nouvelles espèces bactériennes isolées selon la stratégie de culturomique, et avons étudié le mécanisme de résistance à la colistine de *Brucella intermedia*.

Objectifs et structure de la thèse

Dans notre travail de thèse, les approches culturomique et génomique ont servi à analyser mes échantillons et ayant pour but :

1- D'élargir nos connaissances sur les micro-organismes pouvant coloniser l'homme et l'animal, spécifiquement les chimpanzés.

2- D'étudier le mécanisme de résistance à la colistine des souches *Brucella intermedia* isolées chez les chimpanzés.

Le manuscrit présenté ici est divisé en deux chapitres :

- **Chapitre I : Description de nouvelles espèces bactériennes en utilisant l'approche polyphasique de la taxono-génomique**

Dans ce chapitre, nous avons utilisé l'approche polyphasique de taxono-génomique pour caractériser et décrire plusieurs nouveaux taxons bactériens. Nous avons pu décrire trois espèces différentes, dans un travail primaire, dont une a été isolée de chez l'homme **(Article 1)** et les deux autres des selles de chimpanzés du Sénégal **(Articles 2 et 3)** et neuf nouvelles espèces dans un travail secondaire **(Annexes 7 et 8)**. Nous avons également caractérisé les génomes de deux souches *Fusobacterium simiae* (y compris la souche type) en raison de l'absence de génome disponible pour l'espèce. **(Article 4)**.

- **Chapitre II : Etude de la résistance à la colistine chez les souches de *Brucella intermedia***

Dans le deuxième chapitre, nous avons écrit une revue rassemblant les mécanismes connus impliqués dans la résistance naturelle aux polymyxines chez des espèces bactériennes naturellement résistantes, y compris le genre *Brucella* ***(Article 5)***.

De plus, nous avons étudié l'effet de la molécule inhibitrice des pompes à efflux, le cyanure de carbonyle 3-chlorophénylhydrazone (CCCP), sur la résistance à la colistine chez six souches *Brucella intermedia* (auparavant *Ochrobactrum intermedium*), isolées de selles de chimpanzés. **(Article 6)**.

- Chapitre I -

Déscription de nouvelles espèces bactériennes en utilisant l'approche polyphasique de la taxono-génomique

Avant-Propos

L'application de la culture à haut débit a permis l'isolement de nombreuses souches bactériennes nécessitant, pour celles représentant des nouveaux taxons, une identification et une caractérisation précises. Par conséquent, une approche taxono-génomique, polyphasique, a été développée dans notre institut et largement utilisée pour décrire les bactéries nouvellement isolées [14].

La mise en œuvre de cette stratégie débute lorsqu'une souche n'est pas identifiée par la spectrométrie MALDI-TOF MS (score inférieur à 2,0). Cela pourrait signifier que la souche appartient à une nouvelle espèce et/ou que son spectre n'est pas disponible dans la base de données MALDI-TOF MS. Pour mieux identifier la souche, le gène codant l'ARNr 16S doit être séquencé et comparé à la base de données nucléotidique du NCBI. Une similarité de séquence l'ARNr 16S inférieure à 98,65 % avec des espèces relativement proches indique que la souche pourrait appartenir à une nouvelle espèce (ou à un nouveau genre avec une similarité de moins de 95 %) [24, 49]. La méthode basée sur le gène ARNr 16S reste un problème chez certaines espèces étroitement apparentées, comme c'est le cas de *Streptococcus bouchesdurhonensis* **(Article 1).**

Actuellement, l'approche taxono-génomique intègre aussi des méthodes basées sur des analyses génomiques. Celles-ci comprennent des analyses phylogénétiques basées sur le génome et la détermination de l'indice OGRI (Overall Genome Relatedness Index). Ce dernier est calculé en utilisant plusieurs algorithmes disponibles en ligne dont l'Average Nucleotide Identity (ANI) (seuil d'espèce 95-96%), l'Average Amino acid Identity (AAI) (seuil d'espèce 95-96%) et l'Hybridation digitale ADN -ADN (dDDH) (seuil d'espèce 70%) notamment [50,51].

En parallèle des analyses génomiques, les propriétés phénotypiques doivent également être déterminées et comparées à celles des espèces les plus proches. Il s'agit notamment de caractéristiques morphologiques (forme cellulaire, spores, flagelles, coloration de Gram et caractéristiques des colonies), conditions de croissance, tests biochimiques (en utilisant les galeries API convenables) et la composition membranaire en acides gras.

Dans ce chapitre, nous avons décrit douze nouvelles espèces bactériennes suivant l'approche taxono-génomique :

- **Dans un travail primaire**, nous avons décrit les trois nouvelles espèces suivantes:

Streptococcus bouchesdurhonensis sp. nov., *Brucella troglodytis* sp. nov. et *Brucella senegalensis* sp. nov.

- **Dans un travail secondaire (Annexe)**, nous avons décrit les neuf nouvelles espèces suivantes :

Agathobaculum massiliensis sp. nov., *Ornithinibacillus timonensis* sp. nov., *Thalassobacillus timonensis* sp. nov., *Sutcliffiella maliensis* sp. nov., *Pseudalkalibacillus massiliomalei* sp. nov., *Halobacillus maliensis* sp. nov., *Virgibacillus cacae* sp. nov., *Lentibacillus ihumii* sp. nov. et *Rossellomorea faecium* sp. nov.

Article 1

Streptococcus bouchesdurhonensis sp. nov. isolated from a bronchoalveolar lavage of a patient with pneumonia

Malak Zoaiter, Reham Magdy Wasfy, Aurelia Caputo, Florence Fenollar, Zaher Zeaiter, Pierre-Edouard Fournier, Linda Houhamdi

-under review in Archives of Microbiology-

Streptococcus bouchesdurhonensis sp. nov. isolated from a bronchoalveolar lavage of a patient with pneumonia

Malak Zoaiter[1,2], Reham Magdy Wasfy[1,3], Aurelia Caputo[1,3], Florence Fenollar[1,2] , Zaher Zeaiter[4], Pierre-Edouard Fournier[1,2], Linda Houhamdi [1,2*]

[1] IHU-Méditerranée-Infection, Marseille, France

[2] Aix-Marseille Univ, IRD, AP-HM, SSA, VITROME, Marseille, France

[3]Aix-Marseille Univ, IRD, AP-HM, MEPHI, Marseille, France

[4] Lebanese University LU, Department of Biology, Faculty of Sciences, Beirut, Lebanon

[*]**Corresponding author:** Linda HOUHAMDI

1) IHU Méditerranée-Infection, Assistance Publique-Hôpitaux de Marseille (AP-HM),

2) IHU Méditerranée-Infection, VITROME, Aix-Marseille Université, Service de Santé des Armées, IRD

19-21 Boulevard Jean Moulin 13385 Marseille cedex 05, France.

Phone: +33 (0) 413 732 401. Fax: +33 (0) 413 732 402

E-mail: linda.houhamdi@ap-hm.fr / lhouhamdi@yahoo.fr

Abstract

Strain Marseille-Q6994 was isolated from a 72 year-old patient with pneumonia from Bouches-du-Rhône department, in France. Cells were Gram positive, non-motile, catalase and oxidase-negative cocci. The major fatty acids were hexadecanoic (47.4%) and tetradecanoic acids (28.3%). 16S rRNA gene sequence comparison suggested that strain Marseille-Q6994 was affiliated to the *Streptococcus* genus. *GroEL* phylogenetic analysis separated strain Marseille-Q6994 in a distinct branch from the closely related *Streptococcus* type strains with standing in nomenclature. Whole genome sequencing-based methods (OrthoAverage Nucleotide Identity, digital DNA-DNA hybridization and pangenome analysis) supported the classification of the strain into a novel species. Therefore, based on the phenotypic, genomic, and phylogenetic analyses, we propose the name *Streptococcus bouchesdurhonensis* sp. nov for which strain Marseille-Q6994^{T} (CSUR Q6994 =DSMZ 113892) is the type strain.

Keywords: *groEL* phylogenetic analysis, *Streptococcus bouchesdurhonensis*, Bouches du Rhône, pneumonia, Whole genome sequencing.

Introduction

Streptococcus species are Gram positive, catalase-negative cocci that belong to the *Streptococcaceae* family, within the order *Lactobacillales* (Martínez-Lamas et al. 2020). The list of prokaryotic names with Standing in Nomenclature contains 151 *Streptococcus* species validly published at the time of writing https://lpsn.dsmz.de/genus/streptococcus. Many classification schemes were proposed over the years to better describe the genus (Hardie and Whiley 1997; Ferretti and Köhler 2016). In 1995, *Streptococcus* species were categorized into six phylogenetic groups based on 16S rDNA sequences: *pyogenes*, *anginosus*, *salivarius*, *mitis*, *bovis*, and *mutans* (Kawamura et al. 1995). The *mitis* group contains twenty species with validly published names including one of the leading pathogens, *S. pneumoniae*, which is a major agent of pneumonia (Park et al. 2019; Lannes-Costa et al. 2021). However, several misidentifications were reported within the group, especially between the commensal species *Streptococcus mitis*, *Streptococcus pseudopneumoniae* and the pathogenic *S. pneumoniae* (Kilian et al. 2008; Kikuchi al. 2015; Sadowy et al. 2020). Due to the high similarities in 16S rDNA sequences, several housekeeping genes, *sodA*, *rpoB* and *groEL* were reported to be helpful for *Streptococcus* species identification (Tian et al. 2019; Mühldorfer et al., 2020). The *groEL* gene showed the highest discriminatory power for inter and intra-species differentiation (Glazunova et al. 2009). More recently, whole genome sequencing-based methods, including Average Nucleotide Identity (ANI), OrthoAverage Nucleotide Identity (OrthoANI), and digital DNA-DNA Hybridization (dDDH) (Goris et al. 2007) provided an important advance in the genomic field and served to delineate a large number of species within the *mitis* group. However, these tools also suffered limitations due the intra-species variation of the group (Jensen et al. 2016). In this study, we used a polyphasic approach based on culturomics and whole genome sequencing analysis to define a novel *Streptococcus* species.

Materials and methods

Strain isolation and Maldi-TOF identification

Strain Marseille-Q6994 was isolated from a bonchoalveolar lavage (BAL) of a 72 year-old male admitted to the Timone hospital on January 1st, 2022. The patient suffered from respiratory diseases. He gave an informed consent for this study. BAL culture enabled detection of monomorphic colonies. Six individual colonies were screened by the Matrix-assisted laser-desorption/ionization time-of-flight mass spectrometry (Maldi-TOF-MS) using a Microflex spectrometer (Bruker Daltonics, Leipzig, Germany) as previously described (Carbonnelle et al. 2011).

Phenotypic and biochemical characterization

Culture assays were carried out on 5% sheep-blood enriched Columbia agar. Various temperatures were tested (25, 28, 37, 45, and 56°C) in aerobic, anaerobic and microaerophilic atmospheres using GENbag systems (bioMérieux) within 24 hours of incubation. Bacterial growth was also tested in various NaCl concentrations [5, 5.5, 7.5, 10, 15, and 20%] and pH levels [5, 5.5, 6, 6.5, 7, 7.5, 8, 8.5]. Morphological features were observed using scanning electron microscope (Hitachi, Tokyo, Japan). Biochemical characteristics of strain Marseille-Q6994 were determined using different API strips, API 50CH, API ZYM and API 20 STREP according to the manufacturer's instructions (bioMérieux). The fatty acid methyl ester (FAME) analysis was explored by gas chromatography/mass spectrometry (GC/MS), as previously reported (Sasser 2006). FAMEs were separated using an Elite 5-MS column and monitored by mass spectrometry (Clarus 500-S8S, Perkin Elmer, Courtaboeuf, France). Spectra were compared with those in repertory databases

using MS Search 2.0 operated with the Standard Reference Database 1A (NIST, Gaithersburg, USA) and the FAMEs mass spectral database (Wiley, Chichester, UK).

DNA extraction and Sequencing

Genomic DNA (gDNA) was extracted using the EZ1 advanced XL biorobot (Qiagen, Hilden, Germany) using the EZ1 DNA Tissue kit. In early steps of extraction, glass beads (Sigma, France) were added to the lysis buffer G2 (Qiagen-EZ1 DNA tissue kit) containing one colony of the strain and required a previous acid wash using a FastPrep-24™ 5G Grinder instrument (mpBio) at maximum speed. Then, the sample was treated with lysozyme for 30 min to make the DNA more accessible. Quantification was assessed by a Qubit assay with the high sensitivity kit (Thermofisher Scientific). gDNA of strain Marseille-Q6994 was sequenced on a MiSeq sequencer (Illumina Inc, San Diego, CA, USA) using the Nextera XT DNA sample prep kit (Illumina) (Ravi et al. 2018). Paired-end library was prepared by tagmentation and then normalized on specific beads (Beckman Coulter Inc, Fullerton, CA, USA) according to the Nextera XT protocol (Illumina). Sequencing was performed in a single 39-hour run in 2x250-bp with the Miseq reagent Kit (V2-500 cycles-Illumina). To improve Miseq assembly, a run was performed with a GRIDION sequencer (Oxford Nanopore Technologies) using the 1D genomic DNA by ligation kit (Oxford Nanopore Technologies). The Library was constructed without fragmentation and was loaded on a flow cell Mk 1 Spot-ON Pk.1 via the Spot-ON port.

Housekeeping genes phylogenies

Phylogenies were inferred from several housekeeping genes including Superoxide dismutase [Mn] (*sodA*), RNA polymerase subunit Beta (*rpoB*), DNA gyrase subunit Alpha (*gyrA*), and the gene coding for the chaperonin 60 kDa (*groEL*), and from the 16S rRNA gene (Glazunova et al. 2009). 16S rRNA sequences were extracted from genomes using the online Contamination

Estimator by 16S (Contest16S) algorithm (Lee et al. 2017). For the other genes, sequences were extracted from annotated genomes. Phylogenetic trees were inferred using the Molecular Evolutionary Genetic Analysis (MEGA) software version 7.0.26. Sequences were aligned using MUSCLE. Trees were rooted using the maximum likelihood method. The phylogenetic distances between sequences were calculated using Tamura-Nei's model. *S. agalactiae* NCTC 8181^{T} was used as outgroup for the mitis group within the *Streptococcus* genus (Sitkiewicz and Hryniewicz 2010).

Genomic annotation and comparison

The genome from strain Marseille-Q6994 was assembled using Spades version 3.14.0 (Bankevich et al. 2012). All *Streptococcus* type strain genomes were downloaded from Genbank (http//:www.ncbi.nlm.nih.gov/) and annotated using Prokka version 1.14.5 (Seemann 2014). Pangenome analysis was inferred using the Roary software (Page et al. 2015). The detail of RNA genes was obtained using ARAGORN version 1.2 (Laslett and Canback 2004). The Orthologous ANI tool (OAT) was used to calculate OrthoANI values by reciprocal comparison between strain Marseille-Q6994 and the related type strains (Lee et al. 2016). Digital DNA-DNA hybridization values were obtained by the Genome to Genome Distance Calculator (GGDC) under distance formula 2 available in Type Strain Genome Server (TYGS) plateform (https://ggdc.dsmz.de). Accession numbers of S*treptococcus* type strains are present in **Table.1**

Results

Identification and phylogeny

Using Maldi-TOF MS, strain Marseille-Q6994 was identified as *S. mitis*. Blast of its 16S rRNA sequence against those deposited in Genbank confirmed that it belonged to the *Streptococcus* mitis group. It shared more than 99% sequence similarity with *S. mitis, Streptococcus oralis, S.*

pseudopneumoniae, S. pmeumoniae, Streptococcus downii, Streptococcus gwangjuense, and *Streptococcus chosunense*. Nucleotide sequences of its housekeeping genes *groEL, rpoB, sodA,* and *gyrA* were also highly similar to the corresponding genes from *S. mitis* strain NCTC 12261^{T} as follows, 93.72%, 98.18%, 96.23%, 97.59% respectively. All phylogenetic analyses confirmed the affiliation of strain Marseille-Q6994 to the *Streptococcus* mitis group. Phylogenetic inferences based on 16S rRNA, *rpoB, sodA,* and *gyrA* genes showed that strain Marseille-Q6994 clustered with *S. mitis.* However, in the *groEL*-based tree, strain Marseille-Q6994 formed a distinct taxon, well separated from *S. mitis* and the other related type strains. Only 16S rRNA and *groEL*-based phylogenetic trees are shown in **Fig.1**.

Phenotypic characteristics and comparison

Strain Marseille-Q6994 colonies were observed after 24 hours of incubation in both aerobic and microaerophilic atmospheres at 28°C and 37°C. Very small colonies appeared at 28°C in anaerobic atmosphere. In the tested range pH range, growth occurred at pH 7. Regarding NaCl tolerance, our strain showed no salt tolerance to the tested NaCl concentration ranges. In optimal growth conditions on blood-enriched Columbia agar (37°C, aerobic atmosphere, PH7, no NaCl), colonies appeared to be small (0.6 mm), white, with regular edges and surrounded by an alpha hemolysis halo. SEM micrographs revealed a coccus shaped bacteria with septa, with an average size of 649 nm in diameter and 694 nm in length (**Fig.1S**). Phenotypic characteristics of our isolate compared with those of the closest bacterial species are c in **Table.3**. According to FAME analysis, the major fatty acids of strain Marseille-Q6994 were even-chained saturated structures **(Table.1S)**. Minor amounts of unsaturated and odd-chained saturated fatty acids were detected. The most abundant fatty acid were the hexadecenoic acid (palmitic acid) as previously described (Drucker et al. 1974; Labbé et al. 1985). Strain Marseille-Q6994 differed from *S. mitis* and *S. pseudopneumoniae* by the

positive assimilation of starch and its inability to assimilate ribose sugar. A positive alkaline phosphatase activity differentiated it from *S. mitis*. In addition, positive activity to alpha-galactosidase and a negative activity to beta-galactosidase differentiated it from *S. pseudopneumoniae*, in addition to the positive assimilation of mannose.

Genome characteristics and comparison

The strain Marseille-Q6994 genome was 3,766,235-bp long with G+C content of 40.1 %. It contained 4031 genes. Among them, 3927 were protein-coding genes, and 104 were RNA (84 were tRNAs, 1 was an mRNA, 6 were 16S rRNAs, 7 were 23S rRNAs and 6 were 5S rRNAs). Its genome size (3.7 Mb) was larger than those of the closest species which ranged from 1.8 Mb to 2.1 Mb **(Table.1)**. Using Orthologous ANI tool, the strain exhibited 86.18 % of similarity with *S. downii* strain CECT 9732T and 95.83 % with *S. pseudopneumoniae* strain CCUG 49455T **(Fig.2)**. Taken into consideration that ANI can be not sufficient to circumscribe a novel species in the mitis group as previously described (Jensen et al. 2016), digital DDH was in support of the decision to propose strain Marseille-Q6994 as a novel species. dDDH values ranged from 31.8 % with *S. downii* strain CECT 9732T to 64.1 % **(Table.2)**. These values were lower than the 70% threshold recommended to delineate a novel bacterial species (Goris et al. 2007). Genome-based phylogenetic analysis revealed the closest relationship of the studied strain with *S. pseudopneumoniae* strain CCUG 49455T as confirmed by OrthoANI and DDH values **(Fig.3)**. The pangenome analysis demonstrated that strain Marseille-Q6994 was clearly distinct from other compared Streptococcus species **(Fig.4).**

Conclusion

According to our findings, strain Marseille-Q6994 which exhibits several unique characteristics among *Streptococcus* species, may be classified within a new species for which we propose the name *Streptococcus bouchesdurhonensis* sp. nov.

Description of *Streptococcus bouchesdurhonensis* sp. nov.

Streptococcus bouchesdurhonensis (*bou.ches.du.rho.nen'sis* N.L. masc. adj., bouchesdurhonensis of Bouches-du-Rhône of the French territory where the strain Marseille-Q6994 was characterized). Growth occurs at 37°C, after 24h of incubation under aerobic conditions on 5% sheep blood-enriched Columbia agar. Cells are aerobic and anaerobic facultative. Growth pH is 7. No salt tolerance is observed. Colonies are small, white and show alpha hemolysis on sheep blood-agar. Mean length of bacterial cell is 694 nm and the mean width is 649 nm. Using an API 50CH strip, positive reactions were obtained for D-Galactose, D-Glucose, D-Fructose, D-Mannose, N-Acetylglucosamine, D-Maltose, D-Lactose, D-Saccharose, D-Raffinose, starch and Glycogen. Positive activities were observed for esterase (C-4), leucine arylamidase, valine arylamidase, α-chymotrypsin, phosphatase acid, naphtol phosphohydrolase, α-galactosidase and α-glucosidase using API Zym strip. The API 20 STREP strip showed positive results with 6-bromo-2-naphthylα-D-galactopyranoside, L-leucine-ß-naphthylamide, D-lactose (bovine origin) and D-raffinose. The major fatty acids are the hexadecanoic (47.4%) and tetradecanoic acids (28.3%). The genome size is 3,766,235-bp long with G+C content of 40.1 %. Strain Marseille-Q6994^{T} caused pneumonia in the index patient.

Strain Marseille-Q6994^{T} isolated from a bronchoalveolar lavage of an hospitalized 72 year-old patient, was deposited in the Collection de Souches de l'Unité des Rickettsies, CSUR - Marseille as strain Marseille-Q6994 and in the German Collection of Microorganisms and Cell Cultures (Deutsche Sammlung von Mikroorganismen und Zellkulturen - Braunschweig) as DSMZ=113892.

Accession numbers

16S rRNA and genome of strain Marseille-Q6994^{T} were deposited in Genbank under accession numbers OX216967 and CALYYQ010000000, respectively.

196 **Acknowledgements**

197 We sincerely thank Hitachi High-Tech Corporation (Tokyo, Japan) and Sara Bellali for the SEM
198 micrographs of strain Marseille-Q6994 obtained using a SU5000 microscope.

References

Bankevich A, Nurk S, Antipov D, et al (2012) SPAdes: a new genome assembly algorithm and its applications to single-cell sequencing. J Comput Biol 19:455–477. https://doi.org/10.1089/cmb.2012.0021

Carbonnelle E, Mesquita C, Bille E, et al (2011) MALDI-TOF mass spectrometry tools for bacterial identification in clinical microbiology laboratory. Clin Biochem 44:104–109. https://doi.org/10.1016/j.clinbiochem.2010.06.017

Drucker DB, Griffith CJ, Melville TH (1974) Fatty acid fingerprints of streptococci: variability due to carbohydrate source. Microbios 9:187–189. https://doi.org/10.1128/aem.33.2.221-226.1977

Ferretti J, Köhler W (2016) History of Streptococcal Research. In: Ferretti JJ, Stevens DL, Fischetti VA (eds) Streptococcus pyogenes : Basic Biology to Clinical Manifestations. University of Oklahoma Health Sciences Center, Oklahoma City (OK)

Glazunova OO, Raoult D, Roux V (2009) Partial sequence comparison of the rpoB, sodA, groEL and gyrB genes within the genus Streptococcus. Int J Syst Evol Microbiol 59:2317–2322. https://doi.org/10.1099/ijs.0.005488-0

Goris J, Konstantinidis KT, Klappenbach JA, et al (1995) DNA–DNA hybridization values and their relationship to whole-genome sequence similarities. Int J Syst Evol Microbiol 57:81–91. https://doi.org/10.1099/ijs.0.64483-0

Hardie JM, Whiley RA (1997) Classification and overview of the genera Streptococcus and Enterococcus. Soc Appl Bacteriol Symp Ser 26:1S-11S. https://doi.org/10.1046/j.1365-2672.83.s1.1.x

Jensen A, Scholz CFP, Kilian M (2016) Re-evaluation of the taxonomy of the Mitis group of the genus Streptococcus based on whole genome phylogenetic analyses, and proposed reclassification of Streptococcus dentisani as Streptococcus oralis subsp. dentisani comb. nov., Streptococcus tigurinus as Streptococcus oralis subsp. tigurinus comb. nov., and Streptococcus oligofermentans as a later synonym of Streptococcus cristatus. Int J Syst Evol Microbiol 66:4803–4820. https://doi.org/10.1099/ijsem.0.001433

Kawamura Y, Hou XG, Sultana F, et al (1995) Determination of 16S rRNA sequences of Streptococcus mitis and Streptococcus gordonii and phylogenetic relationships among members of the genus Streptococcus. Int J Syst Bacteriol 45:406–408. https://doi.org/10.1099/00207713-45-2-406

Kikuchi K, Enari T, Totsuka K, Shimizu K (1995) Comparison of phenotypic characteristics, DNA-DNA hybridization results, and results with a commercial rapid biochemical and enzymatic reaction system for identification of viridans group streptococci. J Clin Microbiol 33:1215–22. https://doi.org/10.1128/JCM.33.5.1215-1222.1995

Kilian M, Poulsen K, Blomqvist T, et al (2008) Evolution of Streptococcus pneumoniae and Its Close Commensal Relatives. PLOS ONE 3:e2683. https://doi.org/10.1371/journal.pone.0002683

Labbé M, Van der Auwera P, Glupczynski Y, et al (1985) Fatty acid composition ofStreptococcus milleri. Eur J Clin Microbiol 4:391–393. https://doi.org/10.1007/BF02148689

Lannes-Costa P s., de Oliveira J s. s., da Silva Santos G, Nagao P e. (2021) A current review of pathogenicity determinants of Streptococcus sp. J Appl Microbiol 131:1600–1620. https://doi.org/10.1111/jam.15090

Laslett D, Canback B (2004) ARAGORN, a program to detect tRNA genes and tmRNA genes in nucleotide sequences. Nucleic Acids Res 32:11–16. https://doi.org/10.1093/nar/gkh152

Lee I, Chalita M, Ha S-M, et al (2017) ContEst16S: an algorithm that identifies contaminated prokaryotic genomes using 16S RNA gene sequences. Int J Syst Evol Microbiol 67:2053–2057. https://doi.org/10.1099/ijsem.0.001872

Lee I, Ouk Kim Y, Park S-C, Chun J (2016) OrthoANI: An improved algorithm and software for calculating average nucleotide identity. Int J Syst Evol Microbiol 66:1100–1103. https://doi.org/10.1099/ijsem.0.000760

Lefort V, Desper R, Gascuel O (2015) FastME 2.0: A Comprehensive, Accurate, and Fast Distance-Based Phylogeny Inference Program. Mol Biol Evol 32:2798–2800. https://doi.org/10.1093/molbev/msv150

Lim YK, Park S-N, Shin JH, et al (2019) Streptococcus chosunense sp. nov., Isolated from Human Postoperative Maxillary Cyst. Curr Microbiol 76:1193–1198. https://doi.org/10.1007/s00284-019-01746-0

Liu D, Xiao C, Li X, et al (2021) Streptococcus shenyangsis sp. nov., a New Species Isolated from the Oropharynx of a Healthy Child from Shenyang China. Curr Microbiol 78:2821–2827. https://doi.org/10.1007/s00284-021-02500-1

Martínez-Lamas L, Limeres-Posse J, Diz-Dios P, Álvarez-Fernández M (2020) Streptococcus downii sp. nov., isolated from the oral cavity of a teenager with Down syndrome. Int J Syst Evol Microbiol 70:4098–4104. https://doi.org/10.1099/ijsem.0.004180

Mühldorfer K, Szentiks CA, Wibbelt G, et al (2020) Streptococcus catagoni sp. nov., isolated from the respiratory tract of diseased Chacoan peccaries (Catagonus wagneri). Int J Syst Evol Microbiol 70:5734–5739. https://doi.org/10.1099/ijsem.0.004471

Page AJ, Cummins CA, Hunt M, et al (2015) Roary: rapid large-scale prokaryote pan genome analysis. Bioinforma Oxf Engl 31:3691–3693. https://doi.org/10.1093/bioinformatics/btv421

Park S-N, Lim YK, Shin JH, et al (2019) Streptococcus gwangjuense sp. nov., Isolated from Human Pericoronitis. Curr Microbiol 76:799–803. https://doi.org/10.1007/s00284-019-01687-8

Ravi RK, Walton K, Khosroheidari M (2018) MiSeq: A Next Generation Sequencing Platform for Genomic Analysis. Methods Mol Biol 1706:223–232. https://doi.org/10.1007/978-1-4939-7471-9_12

Sadowy E, Bojarska A, Kuch A, et al (2020) Relationships among streptococci from the mitis group, misidentified as Streptococcus pneumoniae. Eur J Clin Microbiol Infect Dis 39:1865–1878. https://doi.org/10.1007/s10096-020-03916-6

Sasser M (2006) Bacterial identification by gas chromatographic analysis of fatty acids methyl esters (GC-FAME). Newark NY Microb ID

Seemann T (2014) Prokka: rapid prokaryotic genome annotation. Bioinforma Oxf Engl 30:2068-2069. https://doi.org/10.1093/bioinformatics/btu153

Sitkiewicz I, Hryniewicz W (2010) Pyogenic streptococci--danger of re-emerging pathogens. Pol J Microbiol 59:219–226. https://doi.org/10.33073/PJM-2010-034

Tian Z, Lu S, Jin D, et al (2019) Streptococcus chenjunshii sp. nov. isolated from feces of Tibetan antelopes. Int J Syst Evol Microbiol 69:1237–1243. https://doi.org/10.1099/ijsem.0.003303

Author's contribution

Malak Zoaiter drafted the manuscript and analyzed the data, Reham Magdy Wasfy carried out the technical characterization of strain Marseille-Q6994. Aurelia Caputo submitted the genome sequence to Genbank. Zaher Zeaiter and Florence Fenollar conceived the study. Pierre-Edouard Fournier revised the manuscript. Linda Houhamdi supervised the project.

Funding

This study was funded by the Institut-hospitalo Universitaire (IHU) Méditerranée Infection.

Conflict of interest

The authors declare that they have no conflicts of interest.

Fig.1 Phylogenetic analysis showing the position of strain Marseille-Q6994^T compared to closely related *Streptococcus* genus based on the 16S rRNA gene **(a)** and *groEL* gene **(b)** sequences. Sequences were aligned by MUSCLE. Phylogenetic inferences were obtained using the maximum likelihood method within the Mega software. Values at the nodes are bootstrap values obtained using 1000 replicates. *Halobacillus halophilus* DSM 2266^T served as an outgroup of the genus (Accesion number: HE717023.1). The scale bars indicate 2% and 5% sequence divergences for 16S rRNA and *groEL*, respectively

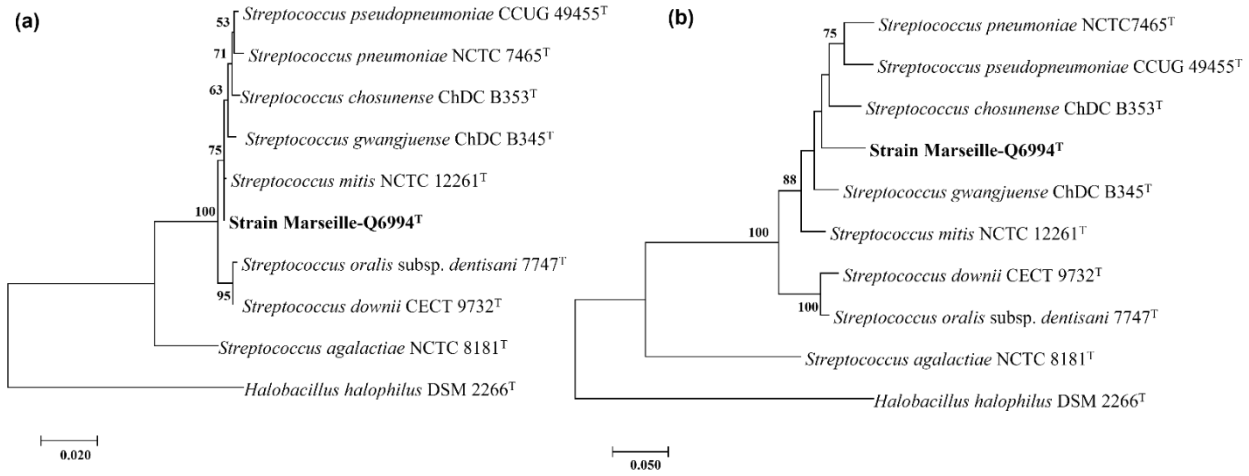

305 **Fig.2** Heatmap generated with OrthoANI values using the OAT software version 0.93.1 between

306 Marseille-Q6994^{T} and related *Streptococcus* species

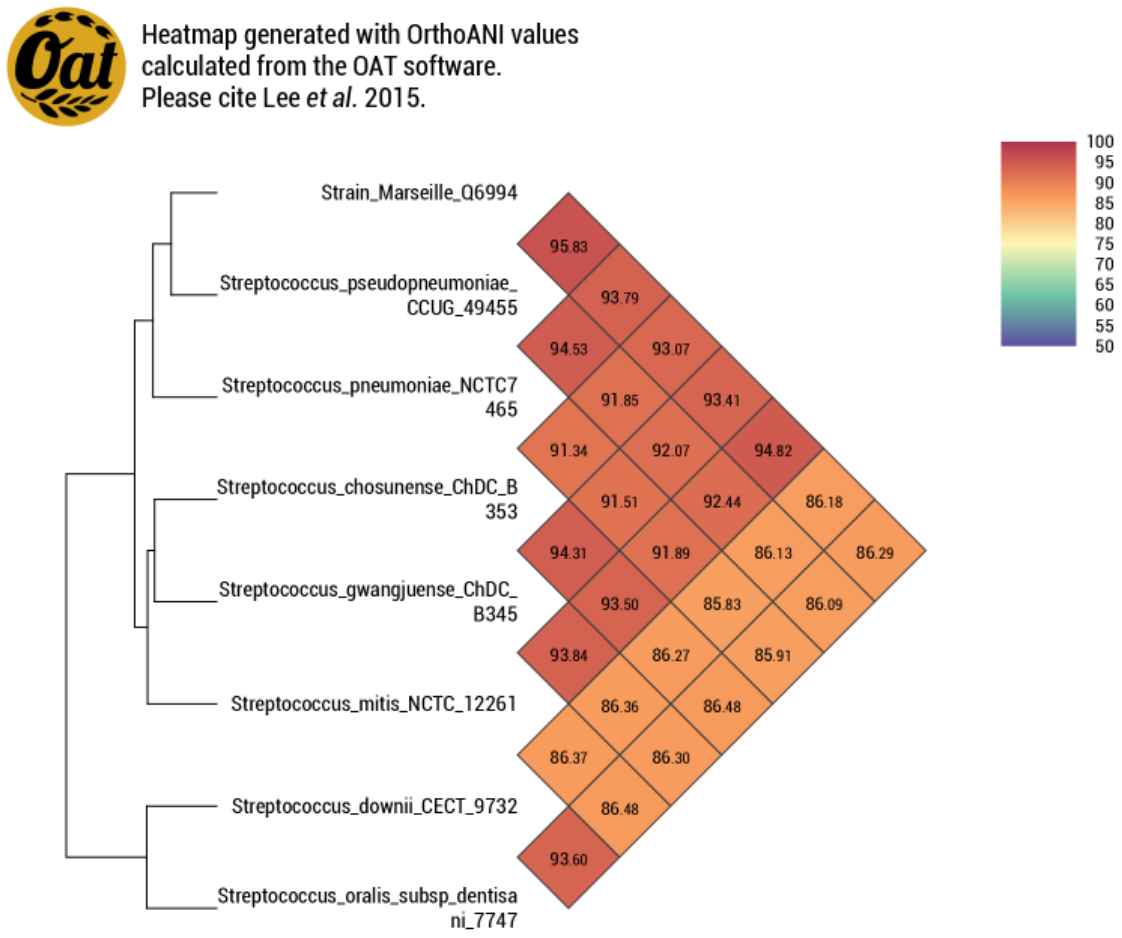

307

308 **Fig.3** Genome-based tree inferred with FastME version 2.1.6.1 (Lefort et al. 2015). Distances
309 were calculated using the Genome Blast Distance Phylogeny (GBDP) approach. The tree was
310 rooted with midpoint. The scale bar represents a 1 % nucleotide divergence

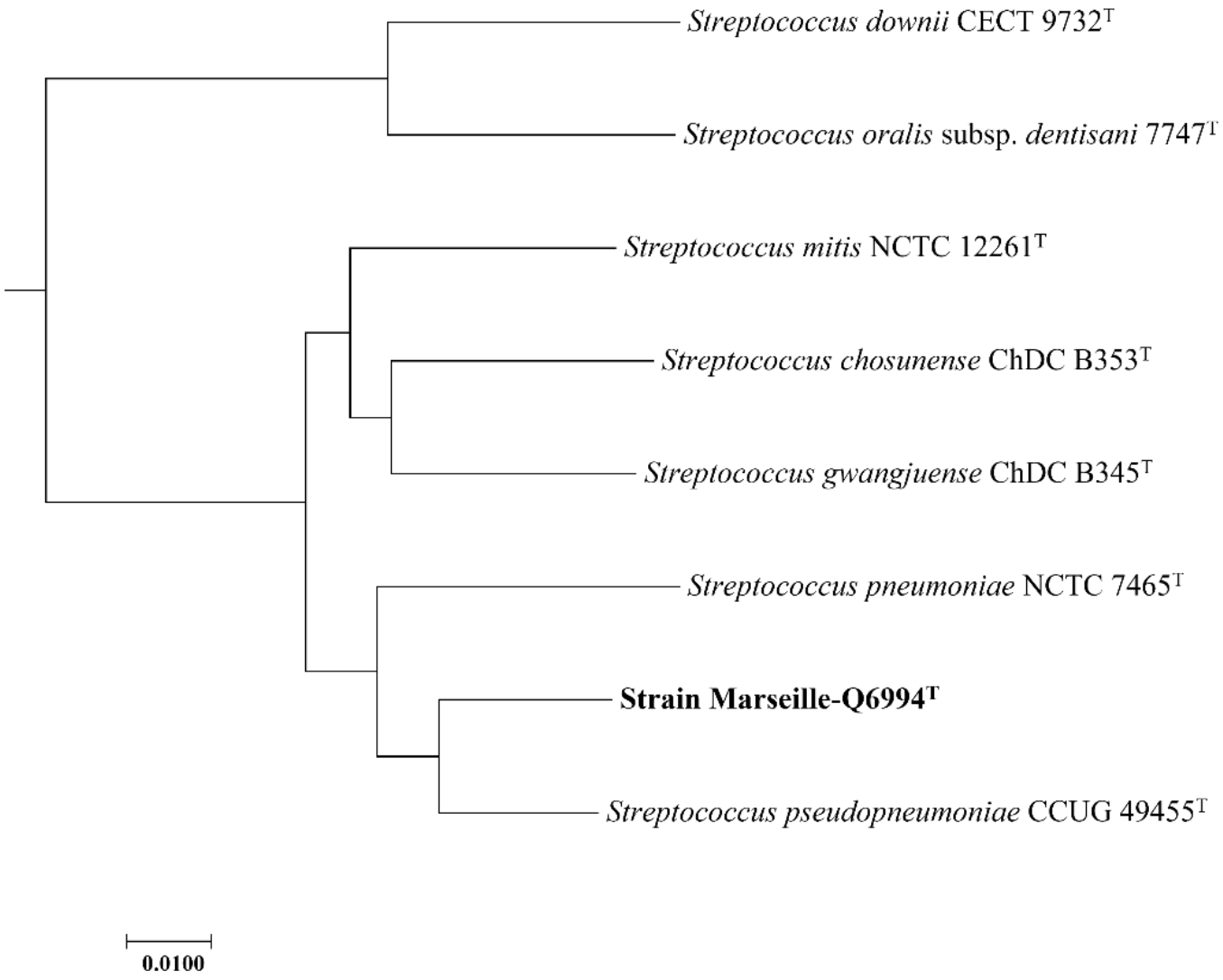

311

Fig.4 Pangenome-based tree showing the position of Marseille-Q6994^{T} among related *Streptococcus* species. Pangenomic analysis was carried out using the Roary software. The scale represents a 10% nucleotide sequence divergence

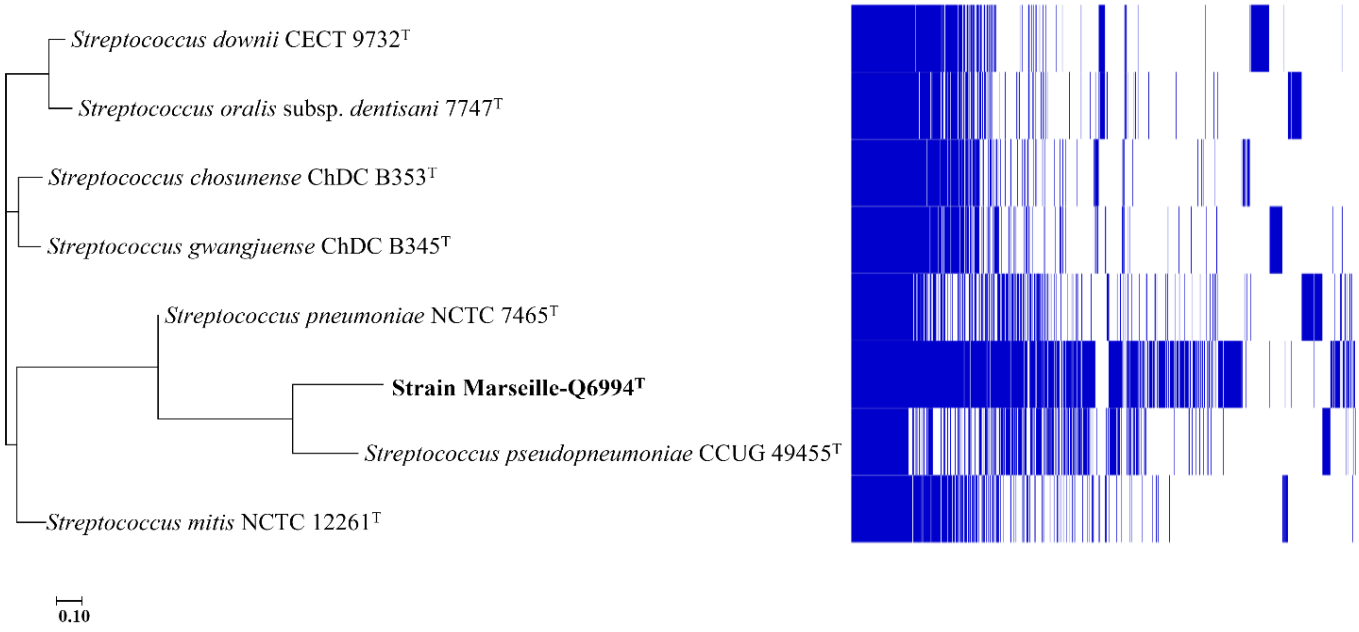

316 **Table.1** S*treptococcus* type strains used in this study.

Species	Type strain	Size (bp)	G+C	Accession numbers
Streptococcus chosunense	ChDC B353	1,902,053	40.10%	RBCK00000000.1
Streptococcus downii	CECT 9732	1,922,750	41.10%	MZNX00000000.1
Streptococcus gwangjuense	ChDC B345	1,972,481	40.20%	NZ_CP032621.1
Streptococcus mitis	NCTC 12261	1,879,851	40.50%	UHFS00000000.1
Streptococcus oralis subsp. d*entisani*	7747	1,884,389	40.80%	CAUK00000000.1
Streptococcus pneumoniae	NCTC7465	2,110,968	39.70%	LN831051.1
Streptococcus pseudopneumoniae	CCUG 49455	2,172,620	39.80%	MWSM00000000.1
Streptococcus agalactiae	NCTC 8181	2,448,053	35.70%	UAVB01000001.1

317

Table.2 Digital DNA-DNA hybridization values (%) between strain Marseille-Q6994^T and related streptococci using formula 2 of the GGDC web server (Estimation was based on identities /HSP length)

	Q6994	**SC**	**SD**	**SG**	**SM**	**SO**	**SP**	**SPS**
Q6994	**100**	51.4	31.8	52.4	57.7	32.2	53.9	**64.1**
SC		**100**	31.2	56.3	53.2	31.1	45.2	46.4
SD			**100**	31.6	31.5	52.2	30.9	31.5
SG				**100**	54.1	31.3	46.1	47.6
SM					**100**	31.7	46.7	48.3
SO						**100**	31.2	31.4
SP							**100**	58.9
SPS								**100**

SC: *S. chosunense,* SD: *S. downii*, SG: *S. gwangjuense*, SM: *S. mitis*, SO: *S. oralis* subsp. *dentisani*, SP: *S. pneumoniae*, SPS: *S. pseudopneumoniae*, Q6994: strain Marseille-Q6994

Table.3 Phenotypic characteristics of strain Marseille-Q6994^{T} compared to other members of the 'mitis group' (Lim et al. 2019; Martínez-Lamas et al. 2020; Liu et al. 2021)

SC: *S. chosunense,* SD: *S. downii*, SG: *S. gwangjuense*, SM: *S. mitis*, SO: *S. oralis* subsp. *dentisani*, SP: *S. pneumoniae*, SPS: *S. pseudopneumoniae*, Q6994: strain Marseille-Q6994.

Properties	*Q6994*	*SD*	*SO*	*SC*	*SG*	*SP*	*SPS*	*SM*
Source	Bronchoalveolar lavage	Dental plaque	Carrie-free tooth	Maxillary cyst	Pericoronitis lesion	NA	Human sputum	NA
Gram stain	+	+	+	+	+	+	+	+
Cell shape	Cocci	Cocci	Cocci	cocci	Cocci	cocci	cocci	cocci
Motility	-	-	-	-	-	-	-	-
Endospore	-	-	-	-	-	-	-	-
Catalase	-	-	-	-	-	-	-	-
Hemolysis	α	α	α	α	α	α	α	α
Temperature	28°C-37°C	37°C	37°C	30 °C-37 °C	37 °C-40 °C	37°C	37°C	37°C
Oxygen tolerance	Microaerophilic	Aerobic	Microaerophilic	Facultative anaerobic	Facultative anaerobic	Microaerophilic	Microaerophilic	Facultative anaerobic
Incubation	24H	24H	24-48H	48H	48H	24-48H	24-48H	24-48H
Salt tolerance	-	NA	0.79%	0.50%	0.50%	NA	NA	NA
Optimum pH	7	7	6-7.5	7-7.5	7-7.5	NA	NA	NA
Alkaline Phosphatase	+	+	+	NA	NA	-	+	-
Esculin	-	-	-	-	-	v	-	-
Arginine	-	-	NA	-	-	+	-	v
α-galactosidase	+	+	+	-	-	+	-	+
β-Galactosidase	-	+	-	+	+	+	+	-
B-glucosidase	-	NA	-	-	-	-	v	-
Ribose	-	NA	-	-	-	-	v	v
Mannose	+	+	+	NA	NA	NA	-	+
Mannitol	-	NA	-	-	-	v	v	-
Sucrose	+	+	+	NA	NA	+	v	+
Raffinose	+	+	+	-	-	+	-	v
Glycogen	V	-	NA	NA	NA	NA	NA	-
Starch	+	-	-	+	-	v	-	-
Lactose	+	+	+	+	+	+	+	+

328 +: Positive, -: Negative, v: Variable, NA: Not determined

Article 2

Description of *Brucella senegalensis* sp. nov. isolated from a senegalese chimpanzee using the taxono-genomic approach

Malak Zoaiter, Jamal Saad, Babacar Mbaye, Edmond Kuete , Oleg Mediannikov, Bernard Davoust, Cheikh Ibrahima Lo, Florence Fenollar, Zaher Zeaiter, Didier Raoult, Pierre-Edouard Fournier

-Ready to be submitted-

Description of Brucella senegalensis sp. nov. isolated from a senegalese chimpanzee using the taxono-genomic approach.

Zoaiter M[1,2], Saad J[1,3], Babacar M[1,3], Kuete E[1,3], Mediannikov O[1,2], Davoust B[1,3], Lo CI[1,2], Fenollar F[1,2], Zeaiter Z[4], Raoult D[1,3], Fournier PE[1,2]*

[1]IHU-Méditerranée-Infection, Marseille, France

[2]Aix-Marseille Univ, IRD, AP-HM, SSA, VITROME, Marseille, France

[3]Aix-Marseille Univ, IRD, AP-HM, MEPHI, Marseille, France

[4]Lebanese University LU, Department of Biology, Faculty of sciences, Beirut, Lebanon

***Corresponding author:** Pierre-Edouard Fournier

Aix-Marseille Université, Institut Hospitalo-Universitaire Méditerranée Infection,

19-21 Boulevard Jean Moulin 13385 Marseille cedex 05, France.

Phone: +33(0)413732401. Fax: +33(0)413732402

E-mail: pierre-edouard.fournier@univ-amu.fr

Abstract

Gram-negative, non-fermenting aerobic bacilli, strain Q0168 was isolated from the stool of a healthy chimpanzee from Senegal. It was catalase negative and oxidase positive. Bacterial cells were motile, rod-shaped and asporogenous. The predominant fatty acid was C_{18}: 1_w. The strain exhibited 98, 85% 16S RNA sequence similarity with *Brucella anthropi* strain ATCC 49188. The genome size was 5,122,895-bp long with a 56.9% G+C content. Using Orthologous Average Nucleotide Identity (OrthoANI) and digital DNA-DNA hybridization (dDDH) estimation against *Brucella* related species with standing in nomenclature, values are ranged from 77.25% to 81.38%, and from 21,2% to 25.1% respectively. Pangenome and core genome analysis supported his affiliation to the genus *Brucella.* Thus, on the basis of its genomic, phylogenetic and phenotypic properties, we propose the creation of the new species *Brucella Senegalensis* sp. nov. with $Q0168^T$ as the type strain.

Keywords: *Brucella senegalensis, Pan troglodytes,* culturomics, taxonomic position, reclassified *Ochrobactrum.*

Introduction

Brucella genus is a gram negative, facultative intracellular bacteria that belongs to the alpha-*Proteobacteria* (Suárez-Esquivel et al. 2020). Members of *Brucella* represent the etiological agents of brucellosis, a worldwide zoonoses that can be transmitted to humans. Predominantly, *Brucella melitensis*, *Brucella abortus*, and *Brucella suis* are the most virulent species for humans (Celli 2019). *Brucella* species differ by host specificity, despite the closely genetic relationship. For a long time, the genus has been classified into six species : *B. melitensis, B. abortus, B. suis, Brucella neotomae, Brucella ovis* and *Brucella canis* (Godfroid et al. 2005) . Then, it has been extended to 12 species by the description of *Brucella pinnipedialis*, *Brucella microti*, *Brucella inopinata*, *Brucella ceti*, *Brucella papionis*, and *Brucella vulpis*. Currently, according to the phylogenetic study of Hördt and al. , the entire *Ochrobactrum* genus was reclassified into the genus of *Brucella* (Hördt et al. 2020) **(Figure.2).** So, at the time of writing *Brucella* genus consists of 33 species (http://www.bacterio.net/brucella.html). In this study, we describe a novel isolate from a chimpanzee during a culturomic study on stool samples. Based on 16S rRNA gene analysis, the isolate was most closely related to *Brucella anthropi* ATCC 49188 (98.85%), to *Brucella lupini* LUP21T (98.78%) and *Brucella cytisi* ESC1 (98.78%). Hence, genomic and phenotypic analysis (Fournier et al. 2015) supports its affiliation to the genus of *Brucella* with a novel taxonomic position. So, we propose the name of *Brucella senegalensis* sp. nov. with Q0168^{T}, the type strain.

Materials and methods

Isolation and MALDI-TOF MS analysis

In 2016, an unidentified bacterial strain was isolated from the stool of a specimen healthy *Pan troglodytes* chimpanzee. Samples were collected on June 6th, 2016 in the Dindefelo Community Nature Reserve (12°22'01.4"N12°18'00.0"W) in south-eastern Senegal. After 24h of incubation of the feces sample in aerobic atmosphere at 37°C, a screening of isolated colonies was made by MALDI-TOF MS (Matrix-assisted laser-desorption/ionization time-of-flight mass spectrometry). Protein analysis was performed using a Microflex spectrometer (Bruker Daltonics, Leipzig, Germany), as previously reported (Seng et al. 2009). All obtained MS spectra were compared using the MALDI Biotyper 3.0 software (Bruker Daltonics) and analyzed against the main spectra of the bacteria included in two databases (Bruker and constantly updated URMS databases, (http://www.mediterraneeinfection.com/article.php?larub=280&titre=urms-database).

16S phylogenetic analysis

To achieve identification of strain Q0168, the 16S rRNA gene was amplified using the primer pair FD1 and RP2 (Eurogentec, Angers, France) and sequenced using the Big Dye® Terminator v1.1 Cycle Sequencing Kit and an ABI Prism 3130x1 Genetic Analyzer capillary 3500xL sequencer (Termofisher, Saint-Aubin, France), as previously described (Morel et al. 2015). The 16S rRNA nucleotide sequence was assembled and corrected using the CodonCode Aligner software (http://www.codoncode.com). The obtained sequence was compared with *Brucella* sequences in GenBank (Altschul et al. 1990) and were aligned using the Clustal W software (Thompson et al. 1997). Phylogenetic relationship were inferred using the maximum likelihood model (Saitou and

Nei 1987) in the MEGA 7.09 software (Kumar et al. 2016). Evolutionary distances were computed using the Tamura-3 parameter algorithm (Tourasse and Gouy 1997).

DNA extraction and genome sequencing

To extract the genomic DNA (gDNA) from the strain Q0168, suspended colonies were treated with acid-washed beads by using the FastPrep BIO 101 automate (Qbiogene, Strasbourg, France), and then incubated with lysozyme for 30 min at 37°C. The g DNA was then extracted using the EZ1 biorobot with the EZ1 DNA tissue kit (Qiagen, Hilden, Germany). DNA quantification was done by the Qubit assay with the high sensitivity kit (Life Technologies, Carlsbad, CA, USA). Sequencing was performed on a Miseq Sequencer (Illumina Inc, San Diego, CA, USA) with two strategies: paired-end and mate-pair. The gDNA was barcoded with the Nextera Mate-Pair sample prep kit (Illumina). Paired-end libraries were fragmented and tagged. The fragmentation profile was validated on a Agilent 2100 Bioanalyzer (Agilent Technologies, Santa Clara, CA, USA) with a DNA 7500 labchip. Six hundred ng of tagmented DNA with no size selection was circularized and sheared to small fragments on a S2 Covaris device (Covaris, Woburn, MA, USA) in microtubes with an optimal size of 993 bp. The library profile was visualized on a high Sensitivity BioAnalyser LabChip (Agilent, Technologies). The libraries were normalized at 2 nmol/L and pooled. Samples were denaturated and diluted at 15 pM. The pool of libraries was loaded onto the reagent cartridge and then onto the instrument along with the flow cell. A single run was done for cluster generation and sequencing in a 2 x 151 bp.

Genome annotation and comparison

The genome was assembled using the SPADES software (Bankevich et al. 2012) and annotated by Prokka as previously described (Seemann 2014). In addition, to estimate the similarity between

compared genomes, we used the Genome to Genome Distance Calculator (GGDC) formula 2 available in the web server (http://ggdc.dsmz.de). The mean levels of relatedness between the genome sequence from strain Q0168 and the other related species was also measured using OrthoAni (Orthologous Average Nucleotide Identity) (https://www.ezbiocloud.net/tools/orthoani) (Lee et al. 2016). The Roary pangenome pipeline in the Galaxy software (https://usegalaxy.org.au./) was used for the pangenomic analysis and to extract the core genome of compared *Brucella* genomes. Phylogenetic inferences were obtained Tygs (https://tygs.dsmz.de/) and NG phylogeny (NGPhylogeny.fr) web servers.

Phenotypic tests

Culture assays were performed on 5% sheep blood-enriched Columbia agar (bioMérieux). Growth of strain Q0168 was tested under different PH (6, 6.5, 7, 7.5, 8, 8.5), different salinity concentrations (50 g/l, 75 g/l, 100 g/l et 150 g/l) and different temperatures (20°C, 28°C, 37°C, 42°C and 56°C).

Preliminary identification of the strain Q0168 was performed using gram staining method as previously described (Bartholomew and Mittwer 1952). Cell morphology was observed using electronic microscopy. Colonies were immersed and fixed into 2.5% glutaraldehyde. A drop of cell suspension was deposited on a poly-L-lysine-coated microscope slide for 5 minutes, treated with 1% phosphotungstic acid aqueous solution (pH 2.0) for 2 minutes, washed in water; air-dried and then evaluated using a TM4000 scanning microscope (Hitachi, Tokyo, Japan). Fresh colonies was suspensed in PBS then heated at 80°C for 20 min in order to test sporulation. API ZYM, API 50CH and API NE strips (bioMérieux), were used for enzyme activity and carbohydrate metabolism respectively, as recommended by the manufacturer's instructions and performed in duplicate.

Fatty acid test

Cellular fatty acid methyl ester (FAME) analysis was performed by gas chromatography/mass spectrometry (GC/MS). FAMES were prepared as described in 2006 (Santos et al. 2018). GC/MS analyses were carried out as described before (Dione et al. 2016). Two samples were prepared with approximately 80 mg of bacterial biomass per tube harvested from several culture plates. Briefly, fatty acid methyl esters were separated using an Elite 5-MS column and monitored by mass spectrometry (Clarus 500-SQ 8 S, Perkin Elmer, Courtaboeuf, France). Spectral database search was performed using MS Search 2.0 operated with the Standard Reference Database 1A (NIST, Gaithersburg, USA) and the FAMEs mass spectral database (Wiley, Chichester, UK).

Results and discussion

MALDI -TOF MS and 16S RNA phylogenetic analysis

The MALDI-TOF MS identification of strain Q0168 failed with a maximum score of 1.7 (Hsueh et al. 2014). A reference mass spectrum was added to the URMS database (Bruker, daltonics) (**Figure.1**). Using BLAST (https://blast.ncbi.nlm.nih.gov), strain Q0168 exhibited a 98,85% sequence identity with *B. anthropi* ATCC 49188^{T} , 98.78% with *B. lupini* LUP21^{T} and 98.78% to *B. cytisi* ESC1^{T}. Phylogenetic analysis showed that strain Q0168 forms a separate branch from the closest related *B. anthropi*, *B. lupini* and *B.cytisi*. **(Figure.2).**

Genome characteristics and comparison

The genome size of strain Q0168 is 5,122,898 bp long with a 56.9% G+C content. Of the predicted genes, 4773 are protein-coding genes and 58 are RNAs (3rRNAs, 54 tRNAs and 1 mRNA).

Strain Q0168 exhibited orthoANI values ranging from 77.25% with *B. gallinifaecis* strain ISO 196^{T} to 81.38% with *B. ciceri* strain DSM 22292 ^{T} **(Figure.4)**. DDH values ranging from 21.2% with *B. gallinifaecis* strain ISO 196 ^{T} to 25.1% with *B. lupini* strain LUP21^{T} **(Table.1).** Pangenomic analysis allowed that strain Q0168 was clustered with *B. gallinifaecis* strain ISO 196^{T} (**Figure.6).**

Besides**,** phylogenetic trees based either on DDH of the closest *Brucella* genomes or on conserved genes in the core genome confirmed that the new strain was branched separately to the related species and was represented respectively in **Figures 5** and **7.**

Therefore, according to the fact that the threshold of dDDH and OrthoANI values for distinguishing different species are 70% and 95%–96%, respectively (Meier-Kolthoff et al. 2013)-

(Richter and Rosselló-Móra 2009), these data confirm the classification of strain Q0168 in a distinct species within *Brucella* genus in the family *Brucellaceae* for which the name *Brucella senegalensis* sp. nov. is proposed.

It should be noted that all genomic analysis showed a high genomic similarity between *B. anthropi* strain *NCTC 12168* ^{T} and *B. lupini* strain LUP21 ^{T} and between *B. ciceri* strain DSM 22293 ^{T} and *B. intermedia* strain NCTC 12171 ^{T} . So, *B. anthropi* strain *NCTC 12168* ^{T} exhibited an ortho-ANI and DDH values respectively 97.98% and 83.9% with *B. lupini* LUP21^{T} which validated the reclassification of *B. lupini* as heterotypic synonym of *B. anthropi* (Gazolla Volpiano et al. 2019). Phylogenetic trees based on DDH values and on the core genome confirmed this affiliation. Hence, we see the same case for *B. intermedia* strain NCTC 12171 ^{T} that showed 98.32% and 85.4% with *B. ciceri* strain DSM 22293 ^{T} as values for orthoANI and DDH respectively.

Phenotypic characteristics

Cells grow from 20°C to 37°C under aerobic conditions, and under PH 6-8 (optimum 8-8.5) without NaCl supplement. No growth is observed at 42°C and 56°C neither for different tested NaCl concentrations. The optimal growth of the isolated strain is obtained after 24 hours of culture on 5% sheep blood enriched Columbia (bioMérieux) in aerobic conditions at 37°C. Colonies were observed to be translucent, convex and mucoid. Cells were Gram-negative, rod-shaped, peritriche, asporogenous, non-hemolytic. The Rods had a length of about 1.99 µm and a width of about 0.56 µm **(Figure.3)**. Strain Q0168 shows catalase negative and oxidase positive activities.

Using API ZYM strips, positive reactions are obtained for Esterase C-4, Leucine arylamidase, and phosphatase acid, but negative reactions are observed for Esterase C-8, alkaline phosphatase with esterase lipase, lipase, valine arylamidase, cystine arylamidase, α-chymotrypsin, α-galactosidase,

ß-galactosidase, ß-glucuronidase, α-glucosidase, ß-glucosidase, N-acetyl-ß-glucosaminidase, α-mannosidase and α-fucosidase.

Using API NE strips, strain Q0168 exhibits β-glucosidase activity. Negative reactions are detected for reduction of potassium nitrate, indole production from tryptophan, glucose fermentation, arginine hydrolysis, and metabolism of aesculin, gelatin, and p-nitrophenyl-ßD-galactopyranoside. Assimilation tests were positive for L-arabinose, N-acetyl glucosamine, malate, weakly for D-mannose , Glucose, D-maltose and negative for mannitol, gluconate, caprate, adipate, citrate and phenyl-acetate. Using API 50CH strips, cells exhibit negative reactions for all fermentation of substrates belonging to the carbohydrate family and their derivatives after 24 hours except for Esculin. The most abundant fatty acid is 11-Octadecenoic acid (49.1 %) 18:1n7 such as described previously for *Brucella* strains (3). Traces of Eicosenoic, Hexadecanoic, 2-hexyl-Cyclopropaneoctanoic and Pentadecanoic acids are characteristics of the strain Q0168 **(Table.3).** Biochemical characteristics of strain Q0168 are described in **Table.2**. It differs from the closest related *Brucella* species by the negative catalase production.

Conclusion

On the basis of unique phenotypic features, including MALDI-TOF MS spectrum, a 16S rRNA sequence divergence of >1.3%, an OrthoANI value < 95% and a DDH value < 70% with the phylogenetically closest species with standing in nomenclature, we formally propose strain Q0168^T as the type strain of *Brucella senegalensis* sp. nov. which is a new species in the genus *Brucella*.

Description of *Brucella senegalensis* sp. nov.

Brucella senegalensis (CSUR=Q0168^T) (se.ne.gal.e'n.sis. L.gen. masc., meaning originating from Senegal, the country from which the stool sample was collected).

The optimal growth is obtained after 24 hours of culture on 5% sheep blood enriched Columbia (bioMérieux) in aerobic conditions at 37°C without NaCl supplement and with a pH range from 8 to 8.5. Colonies were observed to be translucent, convex and mucoid. Gram-negative and rod-shaped cells are peritrichous, asporogenous and non-hemolytic. The Rods had a length of about 1.99 µm and a width of about 0.56 µm and show catalase negative and oxidase positive activities. Positive reactions are obtained for Esterase C-4, Leucine arylamidase, and phosphatase acid using API ZYM strips and β-glucosidase activity using API NE strips. Positive reaction only for Esculin using API 50CH. The most abundant fatty acid is 11-Octadecenoic acid (49.1 %) 18:1n7.

The strain Q0168 isolated from a stool sample of a chimpanzee (*Pan troglodytes)* from Senegal, in 2016 was deposited under number CSUR (Collection Souches Unité des Rickettsies) Q0168^T. The 16S rRNA gene sequence, and genome sequences of *Brucella senegalensis* strain Q0168^T are deposited in GenBank under accession numbers: MW310689 and JAELXQ000000000, respectively.

Ethics statement

The permit to collect stool samples from chimpanzee was given by the Environment and Durable Development Ministry of Senegal (001914/DEF/DGF de la Direction des Eaux, Forêts, Chasses et de la Conservation des Sols).

Figure.1 MALDI-TOF reference mass spectrum of strain Q0168. Spectra from 12 isolated colonies were compared and a reference spectrum generated.

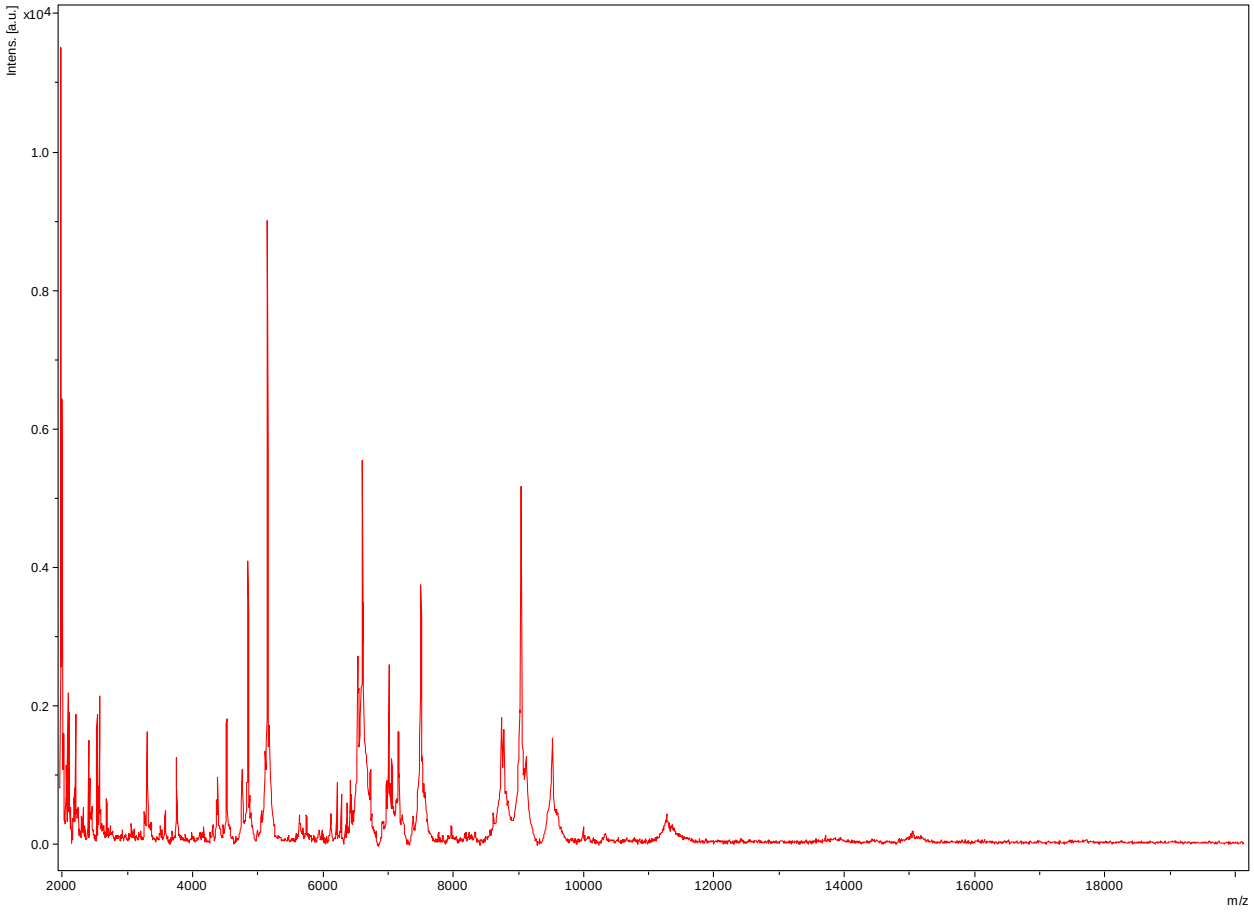

Figure.2 Phylogenetic tree highlighting the position of strain Q0168 in *Brucella* genus based on 16S rRNA gene sequences. Sequences were aligned using clustal w, phylogenetic inferences were obtained using the maximum likelihood method and Mega software version 7. Accession numbers are indicated in parentheses. *Brevundimonas vesicularis* strain CIP 101035^{T} was used as out group. The scale bar represents 1% sequence divergence

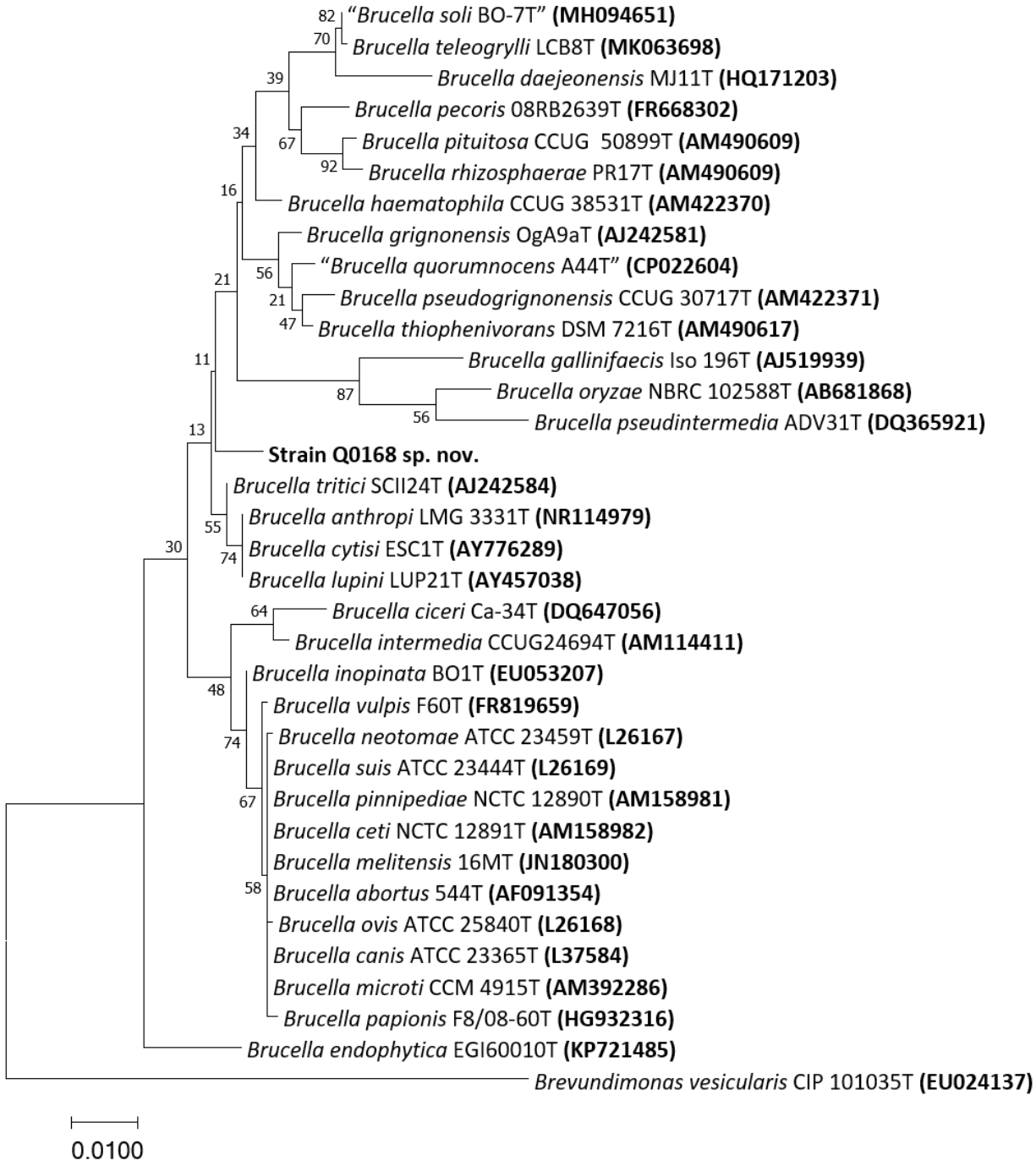
82
70
39
34
67
92
16
56
21
21
47
11
87
56
13
55
30
74
64
48
74
67
58
"Brucella soli BO-7T" (MH094651)
Brucella teleogrylli LCB8T (MK063698)
Brucella daejeonensis MJ11T (HQ171203)
Brucella pecoris 08RB2639T (FR668302)
Brucella pituitosa CCUG 50899T (AM490609)
Brucella rhizosphaerae PR17T (AM490609)
Brucella haematophila CCUG 38531T (AM422370)
Brucella grignonensis OgA9aT (AJ242581)
"Brucella quorumnocens A44T" (CP022604)
Brucella pseudogrignonensis CCUG 30717T (AM422371)
Brucella thiophenivorans DSM 7216T (AM490617)
Brucella gallinifaecis Iso 196T (AJ519939)
Brucella oryzae NBRC 102588T (AB681868)
Brucella pseudintermedia ADV31T (DQ365921)
Strain Q0168 sp. nov.
Brucella tritici SCII24T (AJ242584)
Brucella anthropi LMG 3331T (NR114979)
Brucella cytisi ESC1T (AY776289)
Brucella lupini LUP21T (AY457038)
Brucella ciceri Ca-34T (DQ647056)
Brucella intermedia CCUG24694T (AM114411)
Brucella inopinata BO1T (EU053207)
Brucella vulpis F60T (FR819659)
Brucella neotomae ATCC 23459T (L26167)
Brucella suis ATCC 23444T (L26169)
Brucella pinnipediae NCTC 12890T (AM158981)
Brucella ceti NCTC 12891T (AM158982)
Brucella melitensis 16MT (JN180300)
Brucella abortus 544T (AF091354)
Brucella ovis ATCC 25840T (L26168)
Brucella canis ATCC 23365T (L37584)
Brucella microti CCM 4915T (AM392286)
Brucella papionis F8/08-60T (HG932316)
Brucella endophytica EGI60010T (KP721485)
Brevundimonas vesicularis CIP 101035T (EU024137)
0.0100

223

Figure.3 Scanning electron microscopy (SEM) of stained strain Q0168 using a tabletop microscope (Hitachi, TM4000). Scales and acquisition settings are shown in the figure. The scale bar indicates 10µm.

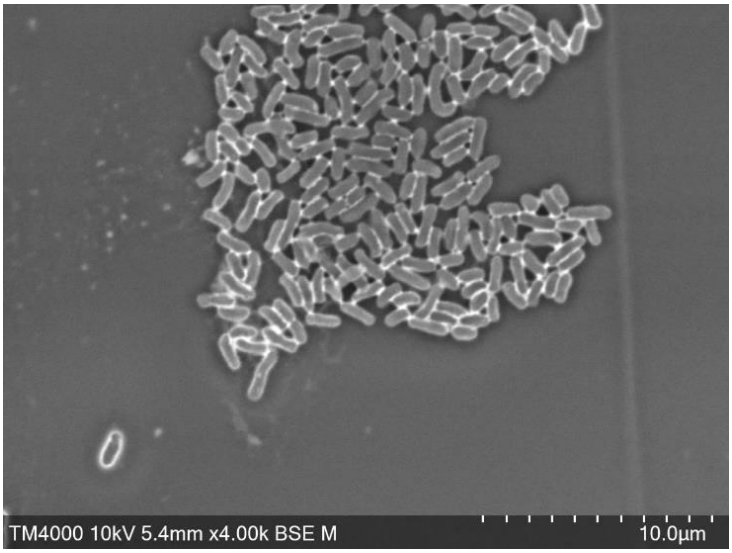

Figure.4 Heatmap generated with ORTHOANI values using OAT software for the strain Q0168 against genomes of the closest *Brucella* species with standing in nomenclature.

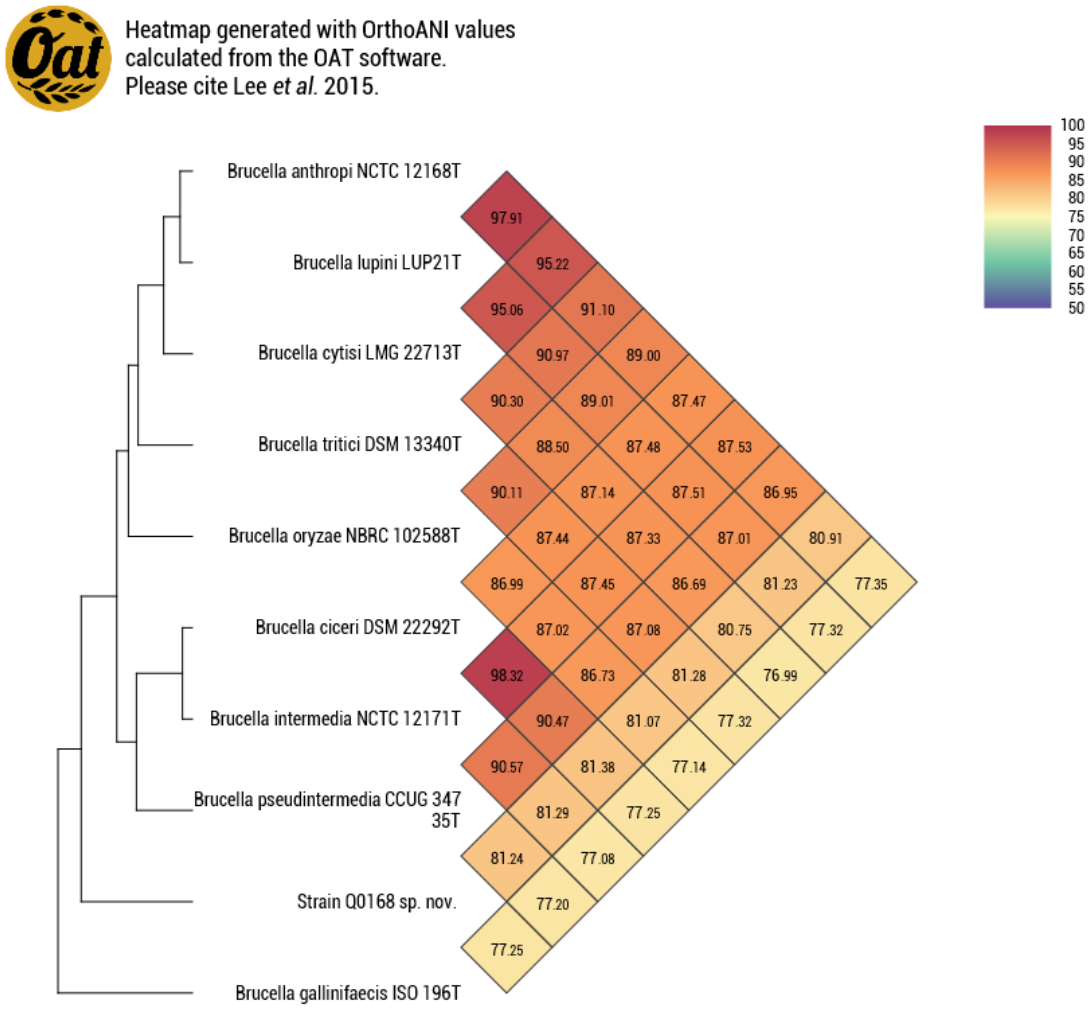

Table.1 Digital DNA-DNA hybridization between strain Q0168 and related *Brucella* species using GGDC, formula 2 (DDH estimates based on identities /HSP length).

	BA	**BCC**	**BC**	**BG**	**BI**	**BL**	**BO**	**BP**	**Q0168**	**BT**
BA	100	33.3	63.1	21.7	33.6	**83.9**	37.5	32.3	24.7	43.6
BCC		100	32.8	21.3	**85.4**	33.5	32.3	40.6	24.8	33.5
BC			100	21.3	33	62.9	36	31.5	24.6	41.9
BG				100	21.3	21.4	21.2	21.1	21.2	21.5
BI					100	33.7	32.3	40.9	25	33.5
BL						100	37.3	32.2	25.1	42.9
BO							100	31.9	24.9	40.2
BP								100	24.4	32.4
Q0168									100	24.9
BT										100

BA : *B. anthropi* NCTC 12168^{T} (UGSA00000000.1); **BCC :** *B. ciceri* DSM 22292^{T} (JAAVLR000000000.1); **BC :** *B. cytisi* LMG 22713 ^{T} (JAAVLQ000000000.1); **BG :** *B. gallinifaecis* ISO 196^{T} (VEWJ00000000.1); **BI :** *B. intermedia* NCTC12171^{T} (UGSH00000000.1); **BL :** *B. lupini* LUP21^{T} (NNRN00000000.1) ; **BO :** *O. Oryzae* NBRC 102588^{T} (JAAVLL000000000.1); **BP :** *B. pseudintermedia* CCUG 34735 (WBWE00000000.1); **Q0168 :** strain Q0168 sp. nov. ; **BT :** *B. tritici DSM 13340* ^{T} (JAAXZB000000000.1).

Figure 5. Phylogenetic tree inferred using FastME 2.1.6.1 (Lefort et al. 2015) from GBDP distances calculated from genome sequences. Numbers at the nodes are GBDP pseudo-bootstrap support values > 60 % from 100 replications, with an average branch support of 96.7 %. The tree was rooted at midpoint (Boykin et al. 2010). Bar represents 0.02 substitutions per nucleotide position divergence.

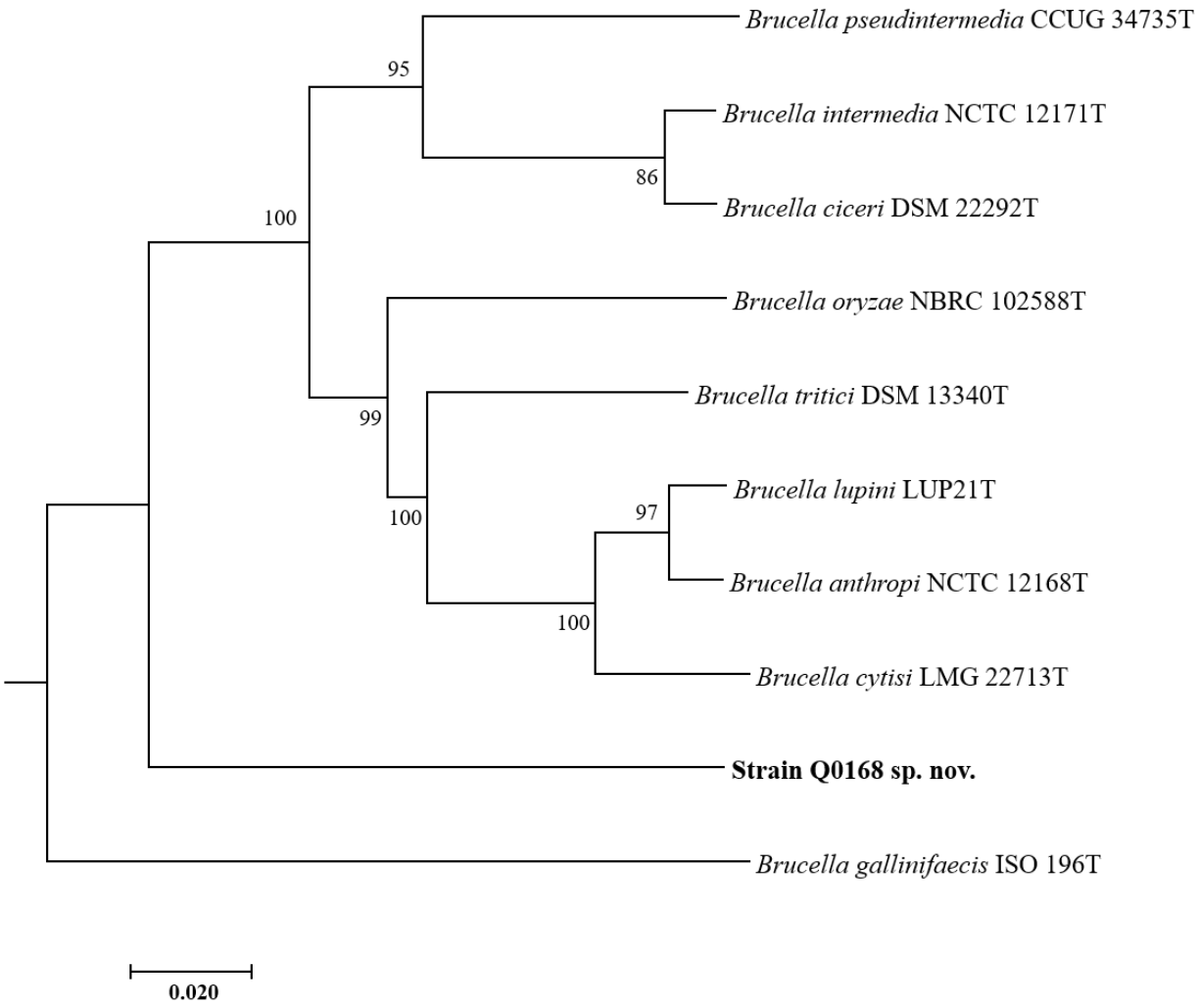

Fig 6. Pangenome tree of strain Q0168 among the closest *Brucella* species obtained using Roary software. Scale bar represents 5% nucleotide sequence divergence.

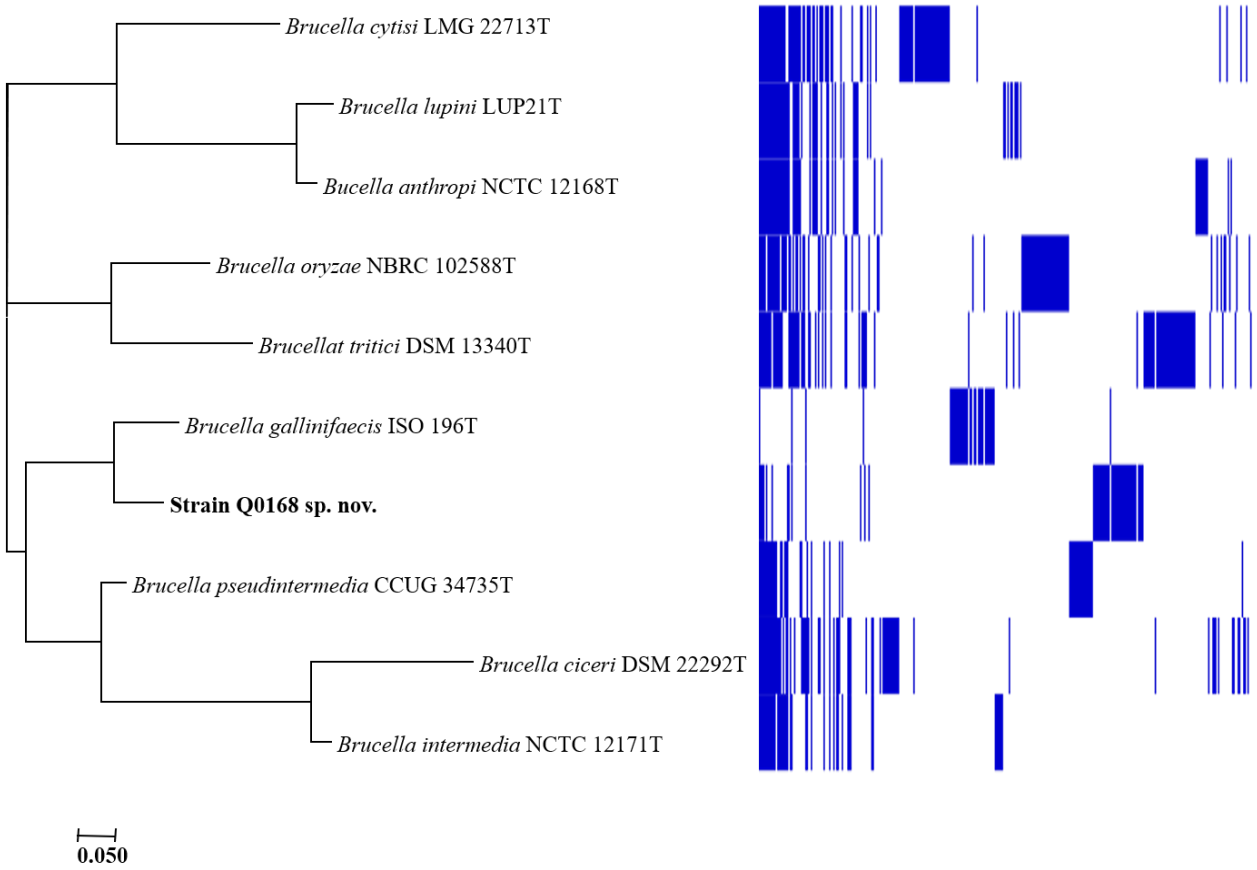

Figure 7. Core-genome-based phylogenetic relationships of strain Q0168 and related *Brucella* species. Genomes were annotated using Prokka and phylogenetic inferences using https://ngphylogeny.fr (Lemoine et al. 2019). Scale bar represents 2 % nucleotide divergence.

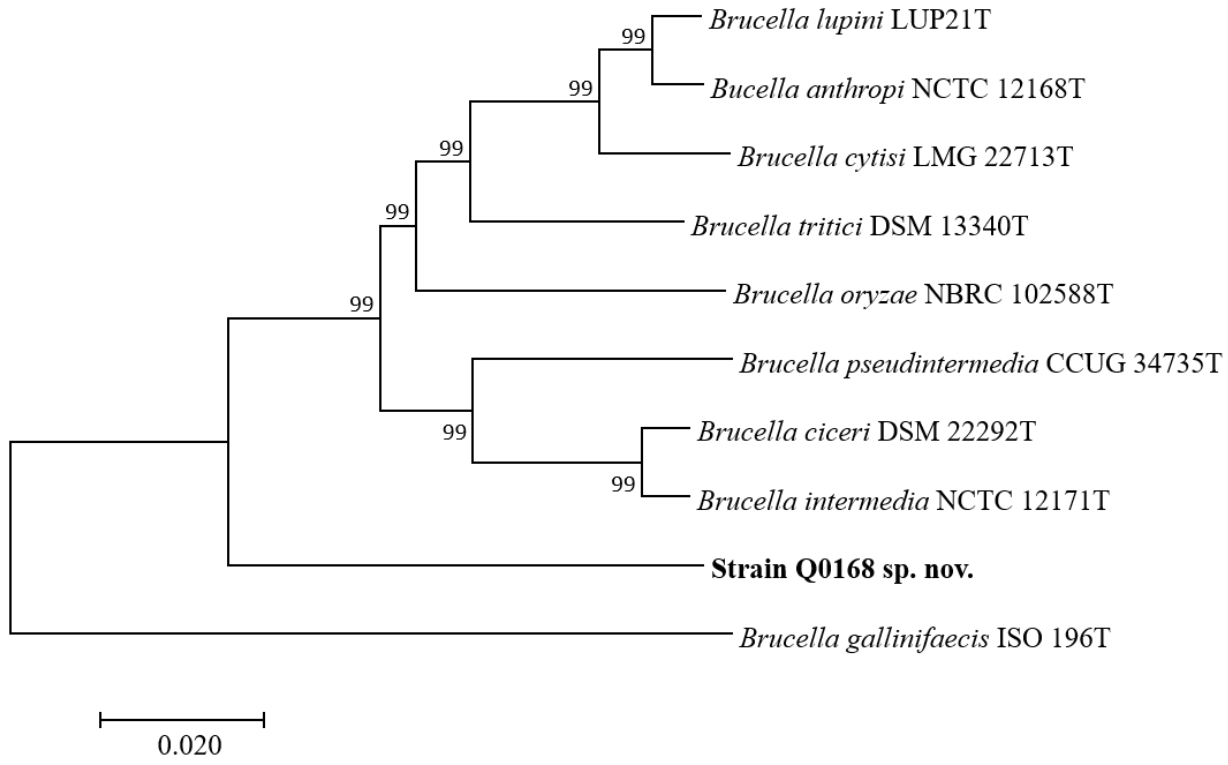

Table 2. Differential characteristics of strain Q0168 with the closest *Brucella* species.

1. Q0168 : strain Q0168 sp. nov. ; **2**. **BCC :** *B. ciceri* DSM 22292^{T}, **3. BA :** *B. anthropi* NCTC 12168 ^{T} , **4.** ; **BO :** *B. Oryzae* NBRC 102588^{T}, **5. BP :** *B. pseudintermedium* DSM 17490^{T} **6. BC :** *B. cytisi* LMG 22713 ^{T}, **7. OT :** *B. tritici DSM 13340* ^{T}, **8. BL :** *O. lupini* LUP21^{T}, **9. BI :** *B. intermedia* NCTC12171^{T} **10. BG :** *B. gallinifaecis* ISO 196^{T}.

	1	2	3	4	5	6	7	8	9	10
Isolation source	Chimpanzee	Nodules of chickpea	Human	Deep water Rice	Human	*Cytisus scoparius*	Wheat rhizoplane	Root nodules	Human blood	Chicken faeces
Colony description	Translucent Mucoid	Off-white Mucoid	Viscous Pale	Translucent Milky	Mucoid Opaque	Beige Pigmented	Highly confluent	Mucoid White	Smooth Shiny	Shiny Translucent
Temperature range (°C)	20-37	28-37	20-34	10-37	37	15-35	4-40	25-27	18-37	10-37
Gram-strain	–	–	–	–	–	–	–	–	–	–
Motility	+	+	+	+	+	+	+	–	+	–
Endospores forming	–	–	–	–	–	–	–	–	–	–
Aerobic	+	+	+	+	+	+	+	+	+	+
Catalase	–	+	ND	+	+	+	+	+	+	ND
Oxidase	+	+	ND	+	+	+	+	+	+	+
Urease	+	+	–	ND	–	+	+	+	+	ND
Arginine Dihydrolase acitivity	+	+	+	ND	–	+	–	ND	–	ND
Gelatin hydrolysis	–	+	–	–	–	–	–	–	–	–
Indole production	–	–	–	–	–	–	–	–	–	–
D-Glucose,	+	+	+	+	+	+	+	+	+	+
D-maltose	(+)	+	+	+	+	+	(+)	+	+	–
L-arabinose	+	+	+	+	+	+	–	+	–	+
Malate	+	+	+	+	+	+	+	+	+	+
D-mannose	(+)	+	+	+	+	N	–	+	–	+
N-acetyl glucosamine	+	+	+	+	+	+	+	+	+	–
D-sorbitol	+	+	+	+	+	+	–	–	+	–
L-rhamnose	+	+	–	+	ND	+	+	+	+	–
D-melibiose	+	–	–	–	ND	–	–	+	–	+
D-inositol	+	+	+	+	ND	+	+	–	+	–

260 - : Negative + : Positive (+) : Weakly positive ND : No data available

261 **Table 3**. Fatty acid methyl ester profile of strain Q0168 sp. nov.

262

Fatty acid Name	Mean relative %
11-Octadecanoic acid	49.1
2-octyl-Cyclopropaneoctanoic acid	23.1
Hexadecanoic acid	6.8
Heptadecanoicacid	0.8
3-hydroxy-Octadecanoic acid	TR
Eicosenoic acid	TR
9-Hexadecanoic acid	TR
14-methyl-Hexadecanoic acid	TR
14-methyl-Pentadecanoicacid	TR
2-hexyl-Cyclopropaneoctanoic acid	TR

263

264 TR: trace amounts < 1 %

References

Altschul SF, Gish W, Miller W, et al (1990) Basic local alignment search tool. J Mol Biol 215:403–410. https://doi.org/10.1016/S0022-2836(05)80360-2

Bankevich A, Nurk S, Antipov D, et al (2012) SPAdes: a new genome assembly algorithm and its applications to single-cell sequencing. J Comput Biol J Comput Mol Cell Biol 19:455–477. https://doi.org/10.1089/cmb.2012.0021

Bartholomew JW, Mittwer T (1952) THE GRAM STAIN. Bacteriol Rev 16:1–29

Boykin LM, Kubatko LS, Lowrey TK (2010) Comparison of methods for rooting phylogenetic trees: A case study using Orcuttieae (Poaceae: Chloridoideae). Mol Phylogenet Evol 54:687–700. https://doi.org/10.1016/j.ympev.2009.11.016

Celli J (2019) The intracellular lifecycle of Brucella spp. Microbiol Spectr 7:. https://doi.org/10.1128/microbiolspec.BAI-0006-2019

Dione N, Sankar SA, Lagier J-C, et al (2016) Genome sequence and description of Anaerosalibacter massiliensis sp. nov. New Microbes New Infect 10:66–76. https://doi.org/10.1016/j.nmni.2016.01.002

Fournier P-E, Lagier J-C, Dubourg G, Raoult D (2015) From culturomics to taxonomogenomics: A need to change the taxonomy of prokaryotes in clinical microbiology. Anaerobe 36:73–78. https://doi.org/10.1016/j.anaerobe.2015.10.011

Gazolla Volpiano C, Hayashi Sant'Anna F, Ambrosini A, et al (2019) Reclassification of Ochrobactrum lupini as a later heterotypic synonym of Ochrobactrum anthropi based on whole-genome sequence analysis. Int J Syst Evol Microbiol 69:2312–2314. https://doi.org/10.1099/ijsem.0.003465

Godfroid J, Cloeckaert A, Liautard J-P, et al (2005) From the discovery of the Malta fever's agent to the discovery of a marine mammal reservoir, brucellosis has continuously been a re-emerging zoonosis. Vet Res 36:313–326. https://doi.org/10.1051/vetres:2005003

Hördt A, López MG, Meier-Kolthoff JP, et al (2020) Analysis of 1,000+ Type-Strain Genomes Substantially Improves Taxonomic Classification of Alphaproteobacteria. Front Microbiol 11:. https://doi.org/10.3389/fmicb.2020.00468

Hsueh P-R, Lee T-F, Du S-H, et al (2014) Bruker Biotyper Matrix-Assisted Laser Desorption Ionization–Time of Flight Mass Spectrometry System for Identification of Nocardia, Rhodococcus, Kocuria, Gordonia, Tsukamurella, and Listeria Species. J Clin Microbiol 52:2371–2379. https://doi.org/10.1128/JCM.00456-14

Huber B, Scholz HC, Kämpfer P, et al (2010) Ochrobactrum pituitosum sp. nov., isolated from an industrial environment. Int J Syst Evol Microbiol 60:321–326. https://doi.org/10.1099/ijs.0.011668-0

Kumar S, Stecher G, Tamura K (2016) MEGA7: Molecular Evolutionary Genetics Analysis Version 7.0 for Bigger Datasets. Mol Biol Evol 33:1870–1874. https://doi.org/10.1093/molbev/msw054

Lee I, Ouk Kim Y, Park S-C, Chun J (2016) OrthoANI: An improved algorithm and software for calculating average nucleotide identity. Int J Syst Evol Microbiol 66:1100–1103. https://doi.org/10.1099/ijsem.0.000760

Lefort V, Desper R, Gascuel O (2015) FastME 2.0: A Comprehensive, Accurate, and Fast Distance-Based Phylogeny Inference Program. Mol Biol Evol 32:2798–2800. https://doi.org/10.1093/molbev/msv150

Lemoine F, Correia D, Lefort V, et al (2019) NGPhylogeny.fr: new generation phylogenetic services for non-specialists. Nucleic Acids Res 47:W260–W265. https://doi.org/10.1093/nar/gkz303

Li L, Li Y-Q, Jiang Z, et al (2016) Ochrobactrum endophyticum sp. nov., isolated from roots of Glycyrrhiza uralensis. Arch Microbiol 198:171–179. https://doi.org/10.1007/s00203-015-1170-8

Meier-Kolthoff JP, Auch AF, Klenk H-P, Göker M (2013) Genome sequence-based species delimitation with confidence intervals and improved distance functions. BMC Bioinformatics 14:60. https://doi.org/10.1186/1471-2105-14-60

Morel A-S, Dubourg G, Prudent E, et al (2015) Complementarity between targeted real-time specific PCR and conventional broad-range 16S rDNA PCR in the syndrome-driven diagnosis of infectious diseases. Eur J Clin Microbiol Infect Dis 34:561–570. https://doi.org/10.1007/s10096-014-2263-z

Richter M, Rosselló-Móra R (2009) Shifting the genomic gold standard for the prokaryotic species definition. Proc Natl Acad Sci U S A 106:19126–19131. https://doi.org/10.1073/pnas.0906412106

Saitou N, Nei M (1987) The neighbor-joining method: a new method for reconstructing phylogenetic trees. Mol Biol Evol 4:406–425. https://doi.org/10.1093/oxfordjournals.molbev.a040454

Santos IC, Smuts J, Choi W-S, et al (2018) Analysis of bacterial FAMEs using gas chromatography - vacuum ultraviolet spectroscopy for the identification and discrimination of bacteria. Talanta 182:536–543. https://doi.org/10.1016/j.talanta.2018.01.074

Seemann T (2014) Prokka: rapid prokaryotic genome annotation. Bioinforma Oxf Engl 30:2068–2069. https://doi.org/10.1093/bioinformatics/btu153

Seng P, Drancourt M, Gouriet F, et al (2009) Ongoing revolution in bacteriology: routine identification of bacteria by matrix-assisted laser desorption ionization time-of-flight

mass spectrometry. Clin Infect Dis Off Publ Infect Dis Soc Am 49:543–551. https://doi.org/10.1086/600885

Suárez-Esquivel M, Chaves-Olarte E, Moreno E, Guzmán-Verri C (2020) Brucella Genomics: Macro and Micro Evolution. Int J Mol Sci 21:. https://doi.org/10.3390/ijms21207749

Thompson JD, Gibson TJ, Plewniak F, et al (1997) The CLUSTAL_X windows interface: flexible strategies for multiple sequence alignment aided by quality analysis tools. Nucleic Acids Res 25:4876–4882. https://doi.org/10.1093/nar/25.24.4876

Tourasse NJ, Gouy M (1997) Evolutionary distances between nucleotide sequences based on the distribution of substitution rates among sites as estimated by parsimony. Mol Biol Evol 14:287–298. https://doi.org/10.1093/oxfordjournals.molbev.a025764

Ochrobactrum pecoris sp. nov., isolated from farm animals | Microbiology Society. https://www.microbiologyresearch.org/content/journal/ijsem/10.1099/ijs.0.027631-0. Accessed 9 Sep 2019

Article3

Taxono-genomic description of *Brucella troglodytis* sp. nov. isolated from senegalese Chimpanzee

Malak Zoaiter, Rita Zgheib, Hacene Medkour, Louis Kangale, Edmond Kuete, Oleg Mediannikov, Bernard Davoust, Cheikh Ibrahima Lo, Florence Fenollar, Zaher Zeaiter, Didier Raoult, Pierre-Edouard Fournier

-Ready to be submitted-

Taxonogenomic description of *Brucella troglodytis* sp. nov. isolated from senegalese Chimpanzee.

Zoaiter M[1,2], Zgheib R[1,2], Medkour H[1,3], Kangale L[1,2], Kuete E[1,3] , Mediannikov O[1,2], Davoust B[1,3], Lo CI[1,2], Fenollar F[1,3], Zeaiter Z[4], Raoult D[1,3] , Fournier PE[1,2]*

[1]IHU-Méditerranée-Infection, Marseille, France

[2]Aix-Marseille Univ, IRD, AP-HM, SSA, VITROME, Marseille, France

[3]Aix-Marseille Univ, IRD, AP-HM, MEPHI, Marseille, France

[4] Lebanese University LU, Department of Biology, Faculty of sciences, Beirut, Lebanon

***Corresponding author:** Pierre-Edouard Fournier

Aix-Marseille Université, Institut Hospitalo-Universitaire Méditerranée Infection,

19-21 Boulevard Jean Moulin 13385 Marseille cedex 05, France.

Phone: +33(0)413732401. Fax: +33(0)413732402

E-mail: pierre-edouard.fournier@univ-amu.fr

Abstract

Gram-stain-negative, motile, non-spore-forming and rod-shaped bacterium, strain Q0166 was isolated from a stool specimen of a healthy chimpanzee from Senegal. It was catalase-positive and oxidase-negative. Optimal growth occured at 37°C in aerobic atmosphere. The most abundant fatty acid was 11-octadecenoic acid (88%) as was described for *Brucella* species. Based on 16S rRNA gene phylogenetic analysis, Q0166 was clustered with *Brucella pseudogrignonensis* strain CCUG 30717^{T}, the most closely related species with standing in nomenclature. Its genome was 4,398,462-bp-long with 52.1% G+C content, and genome-based pairwise comparison (digital DNA–DNA hybridization, and OrthoANI analyses) confirmed this phylogenetic relationship. These results enabled the classification of strain Q0166 as a type strain of a new *Brucella* species for which we propose the name *Brucella troglodytis* sp. nov.

Keywords: *Brucella* reclassification, *Brucella troglodytis*, culturomics, chimpanzee, Senegal, taxono-genomics,

Introduction

The *Brucella* genus was created in 1920 by Meyer and Shaw (Meyer and Shaw 1920). It belongs to the α subclass of *Proteobacteria*, and the family *Brucellaceae* that includes the genera *Pseudochrobactrum*, *Falsochrobactrum*, *Ochrobactrum* and *Brucella* (Suárez-Esquivel et al. 2020). In april 2020, Hordt A et al., proposed the reclassification of *Ochrobactrum* species within the *Brucella* genus based on gene-content analysis, despite differences in genome size (Hördt et al. 2020). Currently, *Brucella* genus includes 33 species (http://www.bacterio.net/brucella.html). *Brucella* species have been detected from a wide variety of terrestrial, and marine mammals, and amphibians as primary hosts (Celli 2019). Members of *Brucella* genus vary in host preferences, zoonotic potential and pathogenicity. *B. melitensis*, *B.abortus*, *B.suis*, *B.canis*, are the most pathogenic for human (Rajendhran 2021). However, they exhibit high levels of nucleotide similarity and are divided in two phylogenetic clusters (**Figure.2**). The classical group is characterized by 99% genome similarity with *B. melitensis* (Guzmán-Verri et al. 2019). The non-classical group displays 97% genomic similarity. Initially, non-classical *Brucella* isolates were identified as *Ochrobactrum*, the closest relative genus, based on metabolic capabilities (Scholz et al. 2010).

By studying a stool sample from a chimpanzee in Senegal as part of a culturomics project, we isolated a strain Q0166 that was not identified by MALDI-TOF MS. 16S rRNA sequence comparison showed that the strain was affiliated to the *Brucella* genus. Species belonging to this genus are Gram-negative, motile, asporogenous, catalase-positive and oxidase-negative. In order to better understand the relationship of strain Q0166 with its phylogenetic neighbors, we used a

polyphasic taxono-genomic approach that involves multiple comparisons (genomic, phenotypic, biochemical)(Ramasamy et al. 2014) with the closest relative species

Materials and methods

Isolation and MALDI-TOF-MS

An unidentified strain Q0166, was isolated from chimpanzee feces collected on June 6 th , 2016 in the Dindefelo Community Nature Reserve (12°22'01.4"N12°18'00.0"W) in south-eastern Senegal. The strain identification was attempted using Matrix-assisted laser-desorption/ionization time-of-flight mass spectrometry (MALDI-TOF MS) on a Microflex LT spectrometer (Bruker Daltonics, Bremen, Germany) as previously described (7). The obtained spectra were imported in the MALDI Biotyper 3.0 software (Bruker Daltonics) and analyzed against the main spectra of the bacteria included in two databases (Bruker and the constantly updated URMS databases (http://www.mediterraneeinfection.com/article.php?larub=280&titre=urms-database).

Strain identification

After isolation and screening by MALDI-TOF MS, 16S rRNA amplification and sequencing was performed in order to classify this bacterium (Lagier et al. 2012), using the primer pair FD1 and RP2 (Eurogentec, Angers, France). Sequencing was performed using the Big Dye® Terminator v1.1 Cycle Sequencing Kit and an ABI Prism 3130x1 Genetic Analyzer capillary 3500xL sequencer (Termofisher, Saint-Aubin, France), as previously described (Morel et al. 2015). The 16S rRNA nucleotide sequence was assembled and corrected using the CodonCode Aligner software (http://www.codoncode.com). Phylogenetic analysis was performed using the MEGA 7 software (Kumar et al. 2016). The evolutionary history was inferred using the maximum likelihood method.

Genome sequencing

Genomic DNA was extracted using the EZ1 biorobot with the EZ1 DNA tissue kit (Qiagen, Hilton, Germany) and then sequenced on a MiSeq sequencer (Illumina, San Diego, CA, USA) with the Nextera Mate Pair sample prep kit (Illumina), as previously described (Diop et al. 2016). Sequence assembly was obtained with a pipeline incorporating several softwares (Velvet) (Zerbino and Birney 2008), Spades (Bankevich et al. 2012) and Soap Denovo (Luo et al. 2012), on trimmed (MiSeq and Trimmomatic softwares) (Bolger et al. 2014) or untrimmed data (only MiSeq software). GapCloser was used to reduce assembly gaps. Scaffolds <800 base pair (bp) with a depth value lower than 25% of the mean depth were deleted. The best assembly was selected by using different criteria (number of scaffolds, N50, number of N).

Genome annotation and comparison

The genome was annotated as previously described (Medkour et al. 2019). Open reading frames (ORFs) were predicted using PRODIGAL (Hyatt et al. 2010) with default parameters, but predicted ORFs were excluded if they spanned a sequencing gap region. The predicted bacterial protein sequences were searched against the GenBank database using BLASTP and the Clusters of Orthologous Groups (COG) database using COGNITOR (Tatusov et al. 2000). The prediction of RNA genes, including rRNAs, tRNAs, and other RNAs, was carried out using the RNAmmer (Lagesen et al. 2007) and ARAGORN (Laslett and Canback 2004) algorithms. The transmembrane helices and signal peptides were identified using TMHMM (Krogh et al. 2001) and Signal P (Petersen et al. 2011), respectively.

Phenotypic tests

In order to determine the optimal growth conditions, culture assays were performed on 5% sheep blood-enriched Columbia agar (bioMérieux, Marcy-l'Étoile, France) under different atmospheres

including aerobic, anaerobic and microaerophilic (GENbag, bioMérieux) conditions, and different temperatures including 20°C, 28°C, 37°C, 45°C and 56 °C. Cell morphological features were observed under electron microscopy. Isolated colonies were immersed and fixed into 2.5% glutaraldehyde. A drop of the suspension was deposited on a poly-L-lysine-coated microscope slide for 5 minutes, treated with 1% phosphotungstic acid aqueous solution (pH 2.0) for 2 minutes, washed in water, air-dried and then evaluated on a TM4000 scanning microscope (Hitachi, Tokyo, Japan). Gram-staining was performed according to the Hucker method as previously described (Bartholomew and Mittwer 1952). Sporulation test was assessed by thermic shock of fresh colonies at 80°C for 20 min. The E-test gradient strip method (bioMérieux) was used to test Antimicrobial susceptibility with the following agents : colistin, fosfomycin, vancomycin, amoxicillin, ceftriaxone, ceftazidime, imipenem, cefotaxime, amikacin, ciprofloxacin, doxycycline, trimethoprim +sulfamethoxazole, rifampicin, and gentamicin to determine the minimal inhibitory concentration (MIC) of each tested antibiotic on blood Columbia agar. Biochemical characterization was assessed by standardized systems using API ZYM, API 50 CH, API NE, and API E strips (bioMérieux) for 24h – 48h at 37°C according to the manufacturer's instructions.

Fatty acid profile

Cellular fatty acid methyl ester (FAME) analysis was performed by gas chromatography/mass spectrometry (GC/MS). Two samples were prepared with approximately 25 mg of bacterial biomass per tube harvested from culture plates. Briefly, fatty acid methyl esters were separated using an Elite 5-MS column and monitored by mass spectrometry (Clarus 500-SQ 8 S, Perkin Elmer, Courtaboeuf, France). Spectral database search was performed using MS Search 2.0 operated with the Standard Reference Database 1A (NIST, Gaithersburg, USA).

Results and discussion

MALDI-TOF MS and phylogenetic analysis

MALDI-TOF MS failed to detect the bacterial strain and gave a score of 1.6. So, all obtained protein spectra were loaded into the MALDI Biotyper Software (Bruker Daltonics) **(Figure.1)**. To achieve identification for unidentified colonies, the 16S rRNA gene was sequenced using fD1-rP2 primers and the obtained sequence was matched against the NCBI database using the BLAST algorithm (https://blast.ncbi.nlm.nih.gov). Strain exhibited a 98.03% sequence identity with *Brucella grignonensis strain OgA9aT*. As suggested, the 16S rRNA gene sequence similarity value was lower than 98.65%. .Based on the complete 16S rRNA sequences 1450 pb, phylogenetic tree highlight the position of strain Q0166 related to other closed *Brucella* genus. It was clustered with *Brucella pseudogrignonensis* strain CCUG 30717^{T} **(Figure.2).**

Genome characteristics and comparison

The genome size of the strain Q0166 was 4,398462 bp long with a 52.1% G+C content. The NGS sequencing covered 65.9224807692% of the genome. Of the 4,224 predicted genes, 4161 were protein-coding genes and 63 were RNAs (3rRNAs, 59 tRNAs and 1 mRNA). A total of 2743 genes (65.92%) were assigned a putative function and 1,418 genes (34.07%) were annotated as hypothetical proteins.

The degree of genomic similarity of strain Q0166 with the closest species within the *Brucella* genus with standing in nomenclature was estimated using ORTHOANI (Ortho Average Nucleotide Identity) software (Lee et al. 2016). Values are ranged from 77.17% between *B. pecoris* strain 08RB2639^{T} and *B. gallinifaecis* strain ISO^{T} 196 to *9*2.27% between *B. grignonensis* strain OgA9a ^{T} and *B. pituitosa* strain CCUG 50899 ^{T}. When the isolate was compared to these species, values

147 ranged from 80.91% with *B. rhisosphaerae* strain PR17 ^{T} to 85.98% *B. pseudogrignonensis* strain
148 CCUG 30717 ^{T} **(Figure.4).** As 95–96 % is considered as the species boundaries of OrthoANI
149 (Richter and Rosselló-Móra 2009), strain Q0166 is distinct from these other tested bacterial taxa.
150 Moreover, digital DNA-DNA hybridization estimation of strain Q0166 against the genomes of the
151 closest species, were obtained by GGDC software based on pairwise genome comparison. Values
152 were ranged from 22% between strain Q0166 and *B. haematophila* strain CCUG 38531^{T}, *B.*
153 *pecoris* strain 08RB2639^{T}and *B. thiophenivorans* strain DSM 7216^{T} to 47.9% between *B.*
154 *grignonensis* strain OgA9a^{T} and *B. pituitosa* strain CCUG 50899^{T}.When strain Q0166 was
155 compared to these closely species, values ranged from 22% with *B. haematophila* strain CCUG
156 38531^{T} to 32.4% with *B. pseudogrignonensis* strain CCUG 30717^{T} **(Table.1).** These values are
157 lower than 70% the cut-off used for delineating prokaryotic species (Meier-Kolthoff et al. 2013).
158 In addition, phylogenetic tree using Tygs (https://tygs.dsmz.de/) based on DDH of all genomes
159 showed that strain was related to *B. pseudogrignonensis* strain CCUG 30717 ^{T} **(Figure.5)**.
160 Cumulatively, the above data suggest that strain Q0166 represents a novel species within *Brucella*
161 genus in the family *Brucellaceae*

162 **Phenotypic characteristics**

163 Growth of strain Q0166 is obtained after 24 hours of culture on 5% sheep blood enriched Columbia
164 agar (bioMérieux) in aerobic atmospheres at 37°C. Cells are Gram-negative, rod-shaped, motile,
165 non-sporulating, non-hemolytic, ranging in length from 1.09 µm and in width from 680nm
166 **(Figure.3)**. Colonies observed on Columbia agar are circular, smooth, opaque, and raised with
167 entire edges. Cells exhibit catalase-positive and oxidase- negative activities.
168 Biochemical characteristics were performed under aerobic conditions at 37°C. Using API ZYM
169 strips (bioMérieux), positive reactions are obtained for Esterase C-4, Esterase C-8, Leucine

arylamidase, phosphatase acid, and Naphtol-ASBI phosphohydrolase, but negative reactions are observed for alkaline phosphatase with esterase lipase, lipase, valine arylamidase, cystine arylamidase, trypsin, α-chymotrypsin, α-galactosidase, ß-galactosidase, ß-glucuronidase, α-glucosidase, ß-glucosidase, N-acetyl-ß-glucosaminidase, α-mannosidase and α-fucosidase.

Using API 20E strips, positive reactions are observed for urease, arginine dihydrolase activity and negative reactions for 2-nitrophenyl- ßD-galactopyranoside, lysin decarboxylase, ornithin decarboxylase, citrate utilization, H2S production, tryptophan deaminase, indole production, acetoin production, gelatinase. The strain produces acid from the following substrates D-glucose, D-mannitol, D-inositol, D-sorbitol, D-saccharose, L-rhamnose, D-melibiose, amygdaline, and weakly from L-arabinose after 48 hours of incubation. Using an API NE strips, strain Q0166 exhibits a positive reaction for urease activity, and negative reactions for reduction of potassium nitrate, indole production from tryptophan, glucose fermentation, arginine hydrolysis, and metabolism of aesculin, gelatin, and p-nitrophenyl-ßD-galactopyranoside. Assimilation tests are positive for L-arabinose, D-mannose, N-acetyl glucosamine, malate, weak for glucose and negative for mannitol, maltose, gluconate, caprate, adipate, citrate and phenyl-acetate. Cells exhibit negative reactions for fermentation of all substrates belonging to the carbohydrate family and its derivatives after 24 hours (API 50CH). The 11-octadecanoic acid is the most abundant fatty acid produced by strain Q0166, as described previously for other *Brucella* strains (31). When compared to other *Brucella* species, strain Q0166 differs in oxidase production, and shows the highest percentage of octadecanoic acid (88.4%) in the cell membrane. In addition, short fatty acid 5 :0 iso (3-methyl-butanoic acid) was also characteristic for strain $Q0166^{T}$.

Strain Q0166 is resistant to colistin, fosfomycin, vancomycin and susceptible to amoxicillin, ceftriaxone, ceftazidime, imipenem, cefotaxime, amikacin, ciprofloxacin, doxycycline, trimethoprim +sulfamethoxazole, rifampicin, gentamicin.

Conclusion

Based on the results from chemotaxonomic and phenotypic characteristics, including MALDI-TOF spectrum, a 16S rRNA sequence divergence >1.3%, an ORTHOANI value < 95% and a DDH value < 70% with the phylogenetically closest species with standing in nomenclature, we proposed strain Q0166 of *Brucella troglodytis* as a new species within the genus of *Brucella* in the family of *Brucellaceae.*

Description of *Brucella troglodytis* sp. nov.

Brucella troglodytis (tro.glo.dy'tis, L. adj. fem., troglodytis of *Pan troglodyte*s, the latin name of chimpanzee from the stool of which strain Q0166 was cultivated).

Growth is obtained after 24 hours of culture on 5% sheep blood enriched Columbia agar (bioMérieux) in aerobic atmospheres at 37°C. Cells are Gram-negative, rod-shaped, motile, non-sporulating, non-hemolytic, ranging in length from 1.09 µm and in width from 680nm. Colonies observed on Columbia agar are circular, smooth, opaque, and raised with entire edges. Cells exhibit catalase-positive and oxidase- negative activities.

Cells exhibit negative reactions for fermentation of all substrates belonging to the carbohydrate family and its derivatives after 24hours (API 50CH). The most abundant fatty acid in cell membrane is 11-octadecanoic acid. A short fatty acid 5 :0 iso (3-methyl-butanoic acid) was also characteristic for the species.

Strain Q0166, isolated from the feces of a healthy chimpanzee from Senegal in 2016, is the type strain of *B. troglodytis* sp. nov. and was deposited in the CSUR Collection under reference CSUR-Q0166.

Nucleotide sequence accession number. The 16S rRNA gene sequence, and genome sequences of *Brucella troglodytis* Q0166 sp. nov. were deposited in GenBank under the following accession numbers : MT859931 and JACJUO000000000, respectively.

Ethics statement

The permit to collect chimpanzee stool samples samples was given by the Environment and Durable Development Ministry of Senegal under reference 001914/DEF/DGF (Direction des Eaux, Forêts, Chasses et de la Conservation des Sols).

Figure.1 MALDI-TOF reference mass spectrum of strain Q0166 sp. nov. Spectra from 12 isolated colonies were compared and a reference spectrum generated.

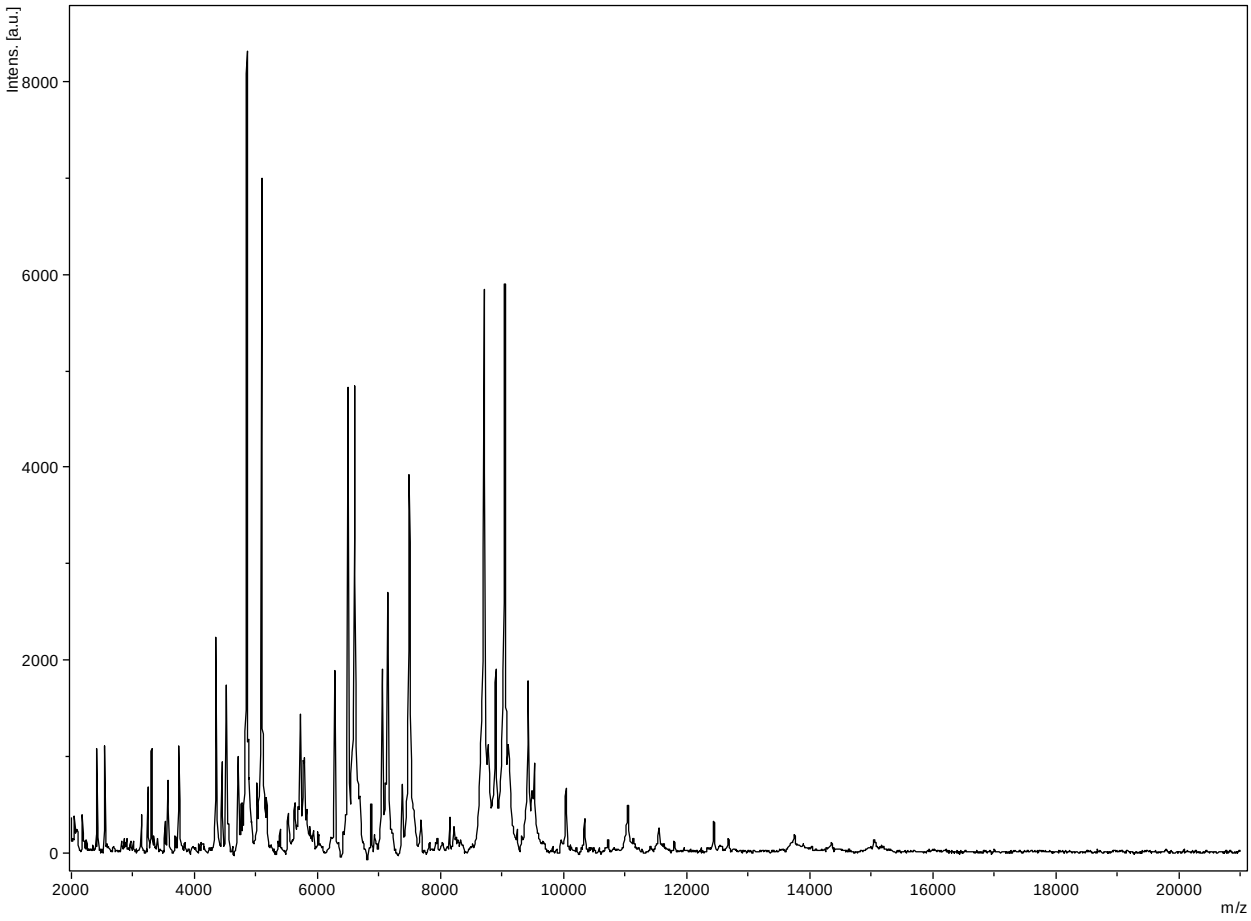

Figure.2 Phylogenetic tree constructed based on the comparison 16S rRNA gene sequences using the maximum likelihood method. The evolutionary distances were computed using the Tamura-Nei algorithm. Strain Q0166 is shown in bold letters. The respective GenBank accession numbers are in parentheses. *Brevundimonas vesicularis* strain CIP 101035^{T} was used as outgroup. scale bar represents a 1% sequence divergence.

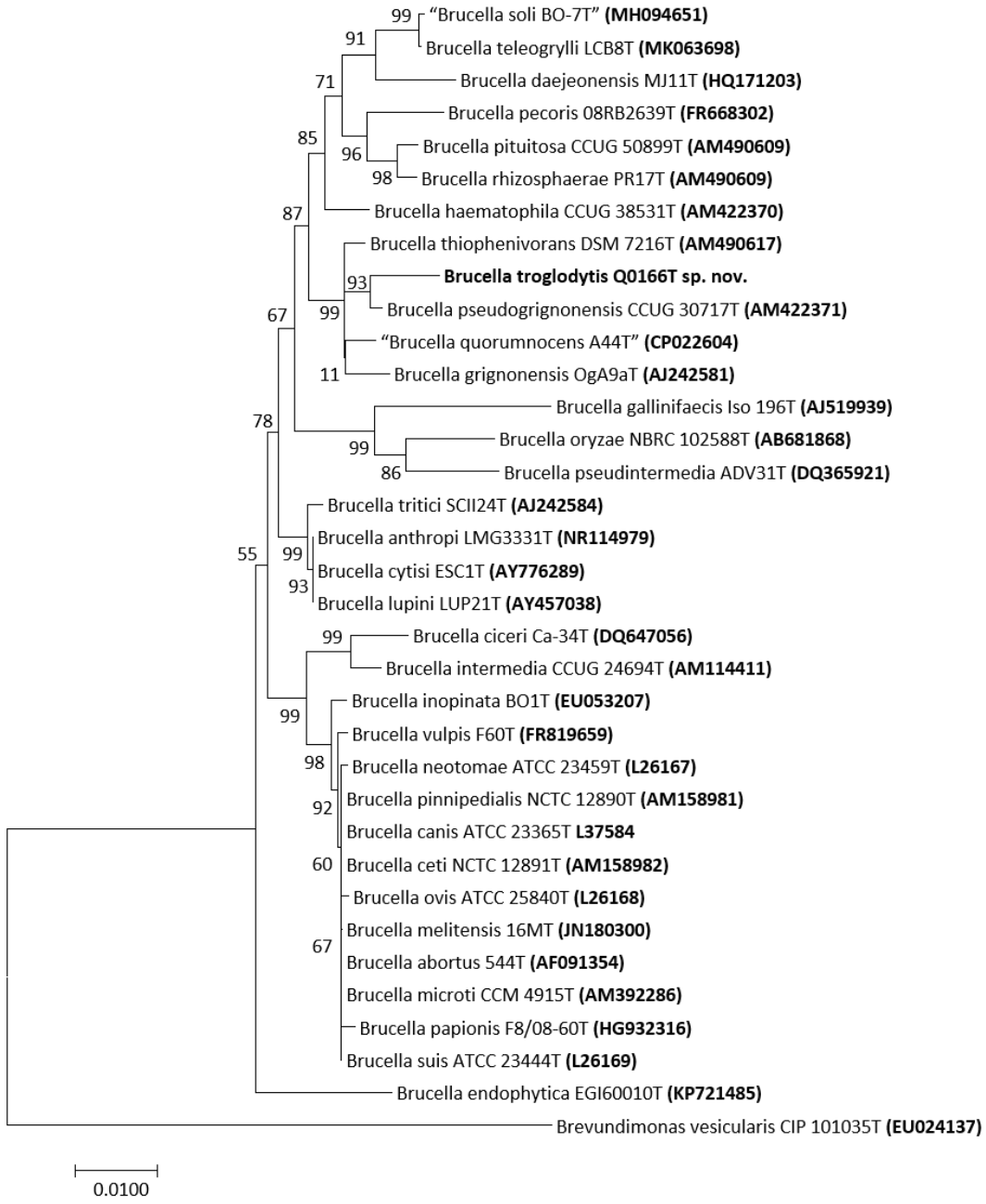
99 "Brucella soli BO-7T" (MH094651)
91 Brucella teleogrylli LCB8T (MK063698)
71 Brucella daejeonensis MJ11T (HQ171203)
Brucella pecoris 08RB2639T (FR668302)
85 96 Brucella pituitosa CCUG 50899T (AM490609)
98 Brucella rhizosphaerae PR17T (AM490609)
87 Brucella haematophila CCUG 38531T (AM422370)
Brucella thiophenivorans DSM 7216T (AM490617)
93 Brucella troglodytis Q0166T sp. nov.
67 99 Brucella pseudogrignonensis CCUG 30717T (AM422371)
"Brucella quorumnocens A44T" (CP022604)
11 Brucella grignonensis OgA9aT (AJ242581)
Brucella gallinifaecis Iso 196T (AJ519939)
78 99 Brucella oryzae NBRC 102588T (AB681868)
86 Brucella pseudintermedia ADV31T (DQ365921)
Brucella tritici SCII24T (AJ242584)
55 99 Brucella anthropi LMG3331T (NR114979)
Brucella cytisi ESC1T (AY776289)
93 Brucella lupini LUP21T (AY457038)
99 Brucella ciceri Ca-34T (DQ647056)
Brucella intermedia CCUG 24694T (AM114411)
99 Brucella inopinata BO1T (EU053207)
Brucella vulpis F60T (FR819659)
98 Brucella neotomae ATCC 23459T (L26167)
92 Brucella pinnipedialis NCTC 12890T (AM158981)
Brucella canis ATCC 23365T L37584
60 Brucella ceti NCTC 12891T (AM158982)
Brucella ovis ATCC 25840T (L26168)
67 Brucella melitensis 16MT (JN180300)
Brucella abortus 544T (AF091354)
Brucella microti CCM 4915T (AM392286)
Brucella papionis F8/08-60T (HG932316)
Brucella suis ATCC 23444T (L26169)
Brucella endophytica EGI60010T (KP721485)
Brevundimonas vesicularis CIP 101035T (EU024137)
0.0100

230

Figure.3 Scanning electron microscopy strain Q0166 sp. nov. using a tabletop scanning microscope (Hitachi SU5000). Acquisition settings are shown in the Figure. The scale bar indicates 20µm.



Figure.4 Heatmap generated with ORTHOANI values using the OAT software for strain Q0166 sp. nov. with other related species in the *Brucella* genus with standing in nomenclature.

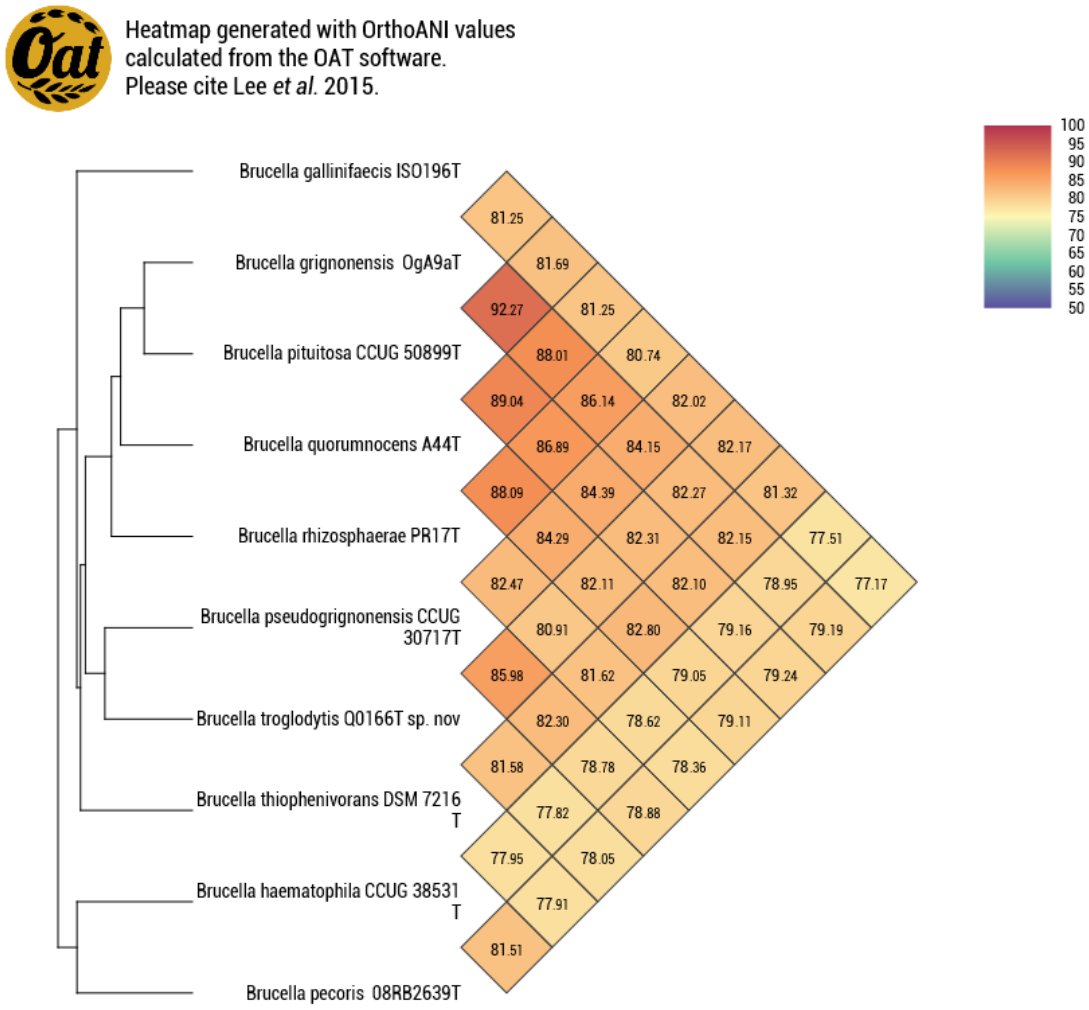

238 **Table 1.** Percentage of DDH values between strain Q0166 sp. nov. and the closest related *Brucella*

239 type strains.

240

	BGA	BG	BH	BP	BPI	BPG	BQ	BR	BTP	Q0166
BGA	100	24.5	21.9	21.3	25.3	25.4	23.8	24	24.3	25
BG		100	23.1	24.1	47.9	28.1	34.5	30.9	25.5	25.7
BH			100	25.8	23.9	23.4	22.8	23.3	21.8	22
BP				100	23.9	23.3	22.7	22.5	22	22.3
BPI					100	28.7	37	32.5	25.7	25.7
BPG						100	27.4	25.7	25.9	32.4
BQ							100	34.4	25.8	24.9
BR								100	24.8	23.6
BTP									100	24.6
Q0166										100

241 **BGA :** *B. gallinifaecis* Iso 196^{T} (VEWJ00000000.1); **BG :** *B. grignonensis* OgA9a^{T}

242 (NNRL00000000.1); **BH :** *B. haematophila* CCUG 38531^{T} (VCPE00000000.1); **BP :** *B. pecoris*

243 08RB2639^{T} (VEWK00000000.1); **BPI :** *B. pituitosa* CCUG 50899^{T} (PYSY00000000.2); **BPG :** *B.*

244 *pseudogrignonensis* CCUG 30717^{T} (NNRM00000000.1) ; **BQ :** *B. Quorumnocens* A44^{T}

245 (CP022604.1); **BR :** *B. rhizosphaerae* PR17^{T} (NNRK00000000.1); **BTP :** *B. thiophenivorans* DSM

246 7216 ^{T} (NNRJ00000000.1); **Q0166:** strain Q0166

Table.2 Comparison of the phenotypic and biochemical characteristics of strain Q0166 sp. nov. with those of phylogenetically close *Brucella* species.

1. Strain Q0166 sp. nov. ; **2.** *B. pseudogrignonensis* strain CCUG 30717^{T} ; **3.** *B. thiophenivorans* strain DSM 7216^{T} ; **4.** *B. grignonensis* strain OgA9a^{T} ; **5.** *B. pecoris* strain 08RB2639^{T} ; **6.** *B. pituitosa* strain CCUG 50899^{T} ; **7.** *B. haematophila* strain CCUG 38531^{T}; **8.** *B. rhizospherae* PR-17^{T} ; **9.** *B. gallinifaecis* strain *ISO 196*^{T} ; **10.** *B. qorumnocens* strain A44^{T} .

	1	2	3	4	5	6	7	8	9	10
Isolation	Chimpanzee	Human Blood	Wastewater	Grignon Soil	Sheep	Industrial environment	Human blood	Potato rhizosphere	Chicken faeces	Potato rizhosphere
Colonies	Circular Opaque	Translucent	Translucent Beige	Opaque Isolated	Beige tanslucent	Small Beige	Beige Translucent	Beige Translucent	Shiny Translucent	Round Smooth
Gram-strain	_	_	_	_	_	_	_	_	_	_
Motility	+	_	_	+	_	+	_	+	_	+
Endospores forming	_	_	_	ND	_	_	_	_	_	_
Aerobic	+	+	+	+	+	+	+	+	+	+
Catalase	+	ND	ND	+	ND	+	ND	ND	ND	+
Oxidase	_	+	+	+	+	+	+	+	+	+
Urease	+	ND	ND	_	ND	ND	ND	ND	ND	_
Arginine Dihydrolase acitivity	+	ND	ND	_	ND	ND	ND	ND	ND	_
Indole production	_	_	_	_	_	_	_	_	_	_
D-Glucose	(+)	+	+	(+)	+	+	+	+	+	+
D-maltose	_	_	_	_	+	+	+	+	_	_
L-arabinose	+	+	+	+	+	+	+	+	+	+
Malate	+	+	+	ND	+	+	+	+	+	+
D-mannose	+	+	+	+	+	+	+	+	+	+
N-acetyl glucosamine	+	_	(+)	_	+	+	+	(+)	_	+
D-sorbitol	+	+	+	_	+	+	+	+	_	_
L-rhamnose	+	+	_	_	_	+	+	+	_	+
D-melibiose	_	_	_	+	_	_	_	_	+	_
D-inositol	+	+	+	_	(+)	+	+	+	_	+

253

254 - : Negative + : Positive (+) : Weakly positive ND : No data available

255 **Table.3** Fatty acid methyl ester profiles of the strain Q0166 and the closest relatives species.

256 **1.** Strain Q0166, **2.** *B. pseudogrignonensis* CCUG 30717 ^{T} , **3.** *pituitosa* CCUG 50899 ^{T} , **4.** *B. rhizospherae* PR-17 ^{T},

257 **5.** *B. quorumnocens* A44 ^{T}, **6.** *B. grignonensis* OgA9a ^{T}.

258

	1	2	3	4	5	6
C5 : 0 iso	2.5	_	_	_	_	_
C14:0	_	0.4	_	_	_	0.3
C16:0	4.4	13.7	0.7	7.7	7.8	5.3
C17:0	_	_	0.4	_	0.6	0.4
C18:0	3.2	12.1	2.1	15.8	12.4	11.4
C16:1	1.5	2.4	7.5	2.6	1.9	1.7
C18:1	88.4	67.6	75.3	73.9	73.3	79.4

259

Figure.5 Phylogenetic tree inferred using FastME 2.1.6.1 (Lefort et al. 2015) from GBDP distances calculated among the closest genome sequences. The numbers at the nodes are GBDP pseudo-bootstrap support values > 60 % from 100 replications, with an average branch support of 91.6 %. The tree was rooted at midpoint (Kinene et al. 2016). The scale bar represents the evolutionary distances in the units of the number of base substitutions per site.

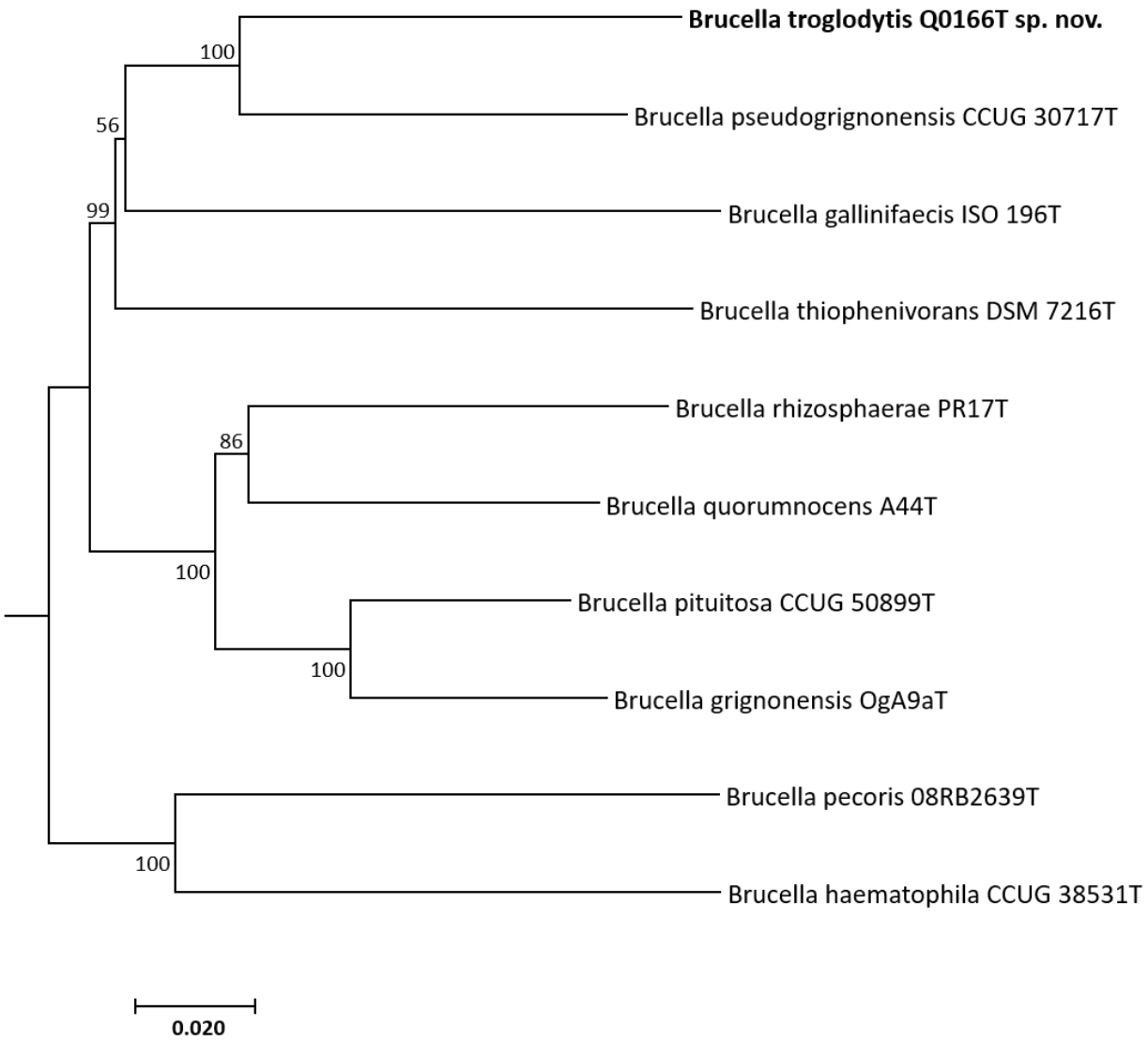

Table.4 Classification and general features of strain Q0166.sp. nov.,

Property	Terms
Current classification	Domain : *Bacteria* Phylum : *Proteobacteria* Class : *Alphaproteobacteria* Order : *Rhizobiales* Family : *Brucellaceae* Genus : *Brucella* Species : *Brucella troglodytis* Type : Strain Q0166
Gram stain	Positive
Cell shape	Rod
Motility	Motile
Sporulation	Asporogenous
Temperature range	20 -40°C
Optimum temperature	37°C
PH	Unknown
Oxygen requirement	Aerobic
Carbon source	Unknown
Habitat	Chimpanzee gut
Biotic relationship	Free-living
Pathogenicity	Unknown

Figure.6 Comparative distribution of protein-coding genes of strain Q0166 and *Brucella* species in the different COGs categories.

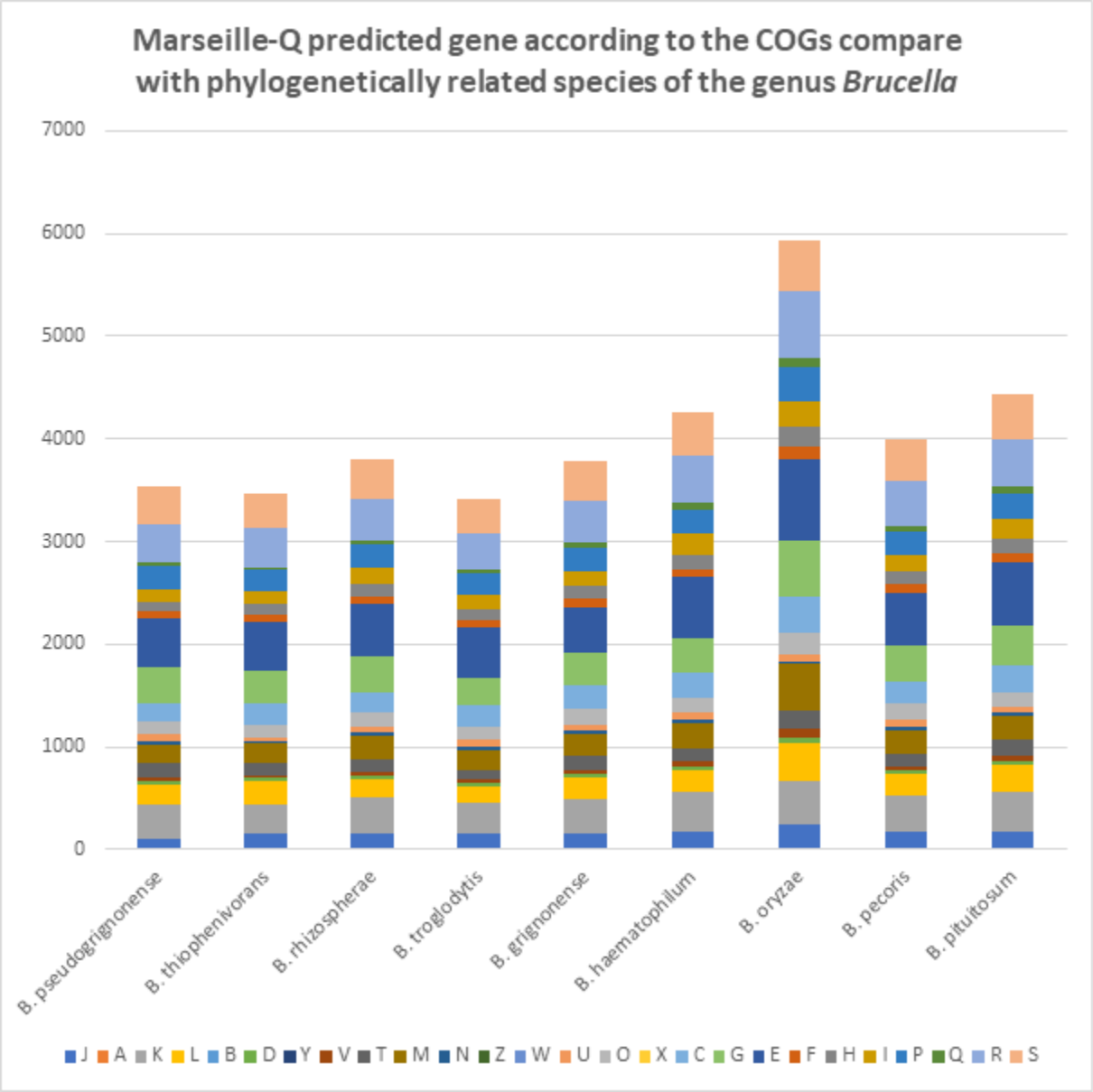

Table.5 Functional annotation of the predicted genes of strain Q0166 according to the COGs database.

Information storage and processing		
[J]	169	Translation, ribosomal structure, and biogenesis
[A]	0	RNA processing and modification
[K]	347	Transcription
[L]	221	Replication, recombination, and repair
[B]	1	Chromatin structure and dynamics
Cellular processes and signaling		
[D]	36	Cell cycle control, cell division, chromosome partitioning
[V]	0	Defense mechanisms
[T]	81	Signal transduction mechanisms
[M]	190	Cell wall/membrane/envelope biogenesis
[N]	197	Cell motility
[Z]	77	Cytoskeleton
[W]	0	Extracellular structures
[U]	0	Intracellular trafficking, secretion, and vesicular transport
[O]	30	Posttranslational modification, protein turnover, chaperones
[X]	125	Mobilome: prophages, transposons
Metabolism		
[C]	181	Energy production and conversion
[G]	444	Carbohydrate transport and metabolism
[E]	308	Amino acid transport and metabolism
[F]	92	Nucleotide transport and metabolism
[H]	120	Coenzyme transport and metabolism
[I]	137	Lipid transport and metabolism
[P]	205	Inorganic ion transport and metabolism
[Q]	47	Secondary metabolites biosynthesis, transport, and catabolism
Poorly characterized		
[R]	469	General function prediction only
[S]	403	Function unknown

References

Bankevich A, Nurk S, Antipov D, et al (2012) SPAdes: a new genome assembly algorithm and its applications to single-cell sequencing. J Comput Biol J Comput Mol Cell Biol 19:455–477. https://doi.org/10.1089/cmb.2012.0021

Bartholomew JW, Mittwer T (1952) THE GRAM STAIN. Bacteriol Rev 16:1–29

Bolger AM, Lohse M, Usadel B (2014) Trimmomatic: a flexible trimmer for Illumina sequence data. Bioinformatics 30:2114–2120. https://doi.org/10.1093/bioinformatics/btu170

Celli J (2019) The intracellular lifecycle of Brucella spp. Microbiol Spectr 7:. https://doi.org/10.1128/microbiolspec.BAI-0006-2019

Diop A, Khelaifia S, Armstrong N, et al (2016) Microbial culturomics unravels the halophilic microbiota repertoire of table salt: description of Gracilibacillus massiliensis sp. nov. Microb Ecol Health Dis 27:32049. https://doi.org/10.3402/mehd.v27.32049

Guzmán-Verri C, Suárez-Esquivel M, Ruíz-Villalobos N, et al (2019) Genetic and Phenotypic Characterization of the Etiological Agent of Canine Orchiepididymitis Smooth Brucella sp. BCCN84.3. Front Vet Sci 6:. https://doi.org/10.3389/fvets.2019.00175

Hördt A, López MG, Meier-Kolthoff JP, et al (2020) Analysis of 1,000+ Type-Strain Genomes Substantially Improves Taxonomic Classification of Alphaproteobacteria. Front Microbiol 11:. https://doi.org/10.3389/fmicb.2020.00468

Hyatt D, Chen G-L, Locascio PF, et al (2010) Prodigal: prokaryotic gene recognition and translation initiation site identification. BMC Bioinformatics 11:119. https://doi.org/10.1186/1471-2105-11-119

Kinene T, Wainaina J, Maina S, Boykin LM (2016) Rooting Trees, Methods for. In: Encyclopedia of Evolutionary Biology. Elsevier, pp 489–493

Krogh A, Larsson B, von Heijne G, Sonnhammer EL (2001) Predicting transmembrane protein topology with a hidden Markov model: application to complete genomes. J Mol Biol 305:567–580. https://doi.org/10.1006/jmbi.2000.4315

Kumar S, Stecher G, Tamura K (2016) MEGA7: Molecular Evolutionary Genetics Analysis Version 7.0 for Bigger Datasets. Mol Biol Evol 33:1870–1874. https://doi.org/10.1093/molbev/msw054

Lagesen K, Hallin P, Rødland EA, et al (2007) RNAmmer: consistent and rapid annotation of ribosomal RNA genes. Nucleic Acids Res 35:3100–3108. https://doi.org/10.1093/nar/gkm160

Lagier J-C, Armougom F, Million M, et al (2012) Microbial culturomics: paradigm shift in the human gut microbiome study. Clin Microbiol Infect 18:1185–1193. https://doi.org/10.1111/1469-0691.12023

Laslett D, Canback B (2004) ARAGORN, a program to detect tRNA genes and tmRNA genes in nucleotide sequences. Nucleic Acids Res 32:11–16. https://doi.org/10.1093/nar/gkh152

Lee I, Ouk Kim Y, Park S-C, Chun J (2016) OrthoANI: An improved algorithm and software for calculating average nucleotide identity. Int J Syst Evol Microbiol 66:1100–1103. https://doi.org/10.1099/ijsem.0.000760

Lefort V, Desper R, Gascuel O (2015) FastME 2.0: A Comprehensive, Accurate, and Fast Distance-Based Phylogeny Inference Program. Mol Biol Evol 32:2798–2800. https://doi.org/10.1093/molbev/msv150

Li L, Li Y-Q, Jiang Z, et al (2016) Ochrobactrum endophyticum sp. nov., isolated from roots of Glycyrrhiza uralensis. Arch Microbiol 198:171–179. https://doi.org/10.1007/s00203-015-1170-8

Luo R, Liu B, Xie Y, et al (2012) SOAPdenovo2: an empirically improved memory-efficient short-read de novo assembler. GigaScience 1:18. https://doi.org/10.1186/2047-217X-1-18

Medkour H, Ibrahima LO C, Anani H, et al (2019) Bartonella massiliensis sp. nov., a new bacterial species isolated from an Ornithodoros sonrai tick from Senegal. New Microbes New Infect 100596. https://doi.org/10.1016/j.nmni.2019.100596

Meier-Kolthoff JP, Auch AF, Klenk H-P, Göker M (2013) Genome sequence-based species delimitation with confidence intervals and improved distance functions. BMC Bioinformatics 14:60. https://doi.org/10.1186/1471-2105-14-60

Meyer KF, Shaw EB (1920) A Comparison of the Morphologic, Cultural and Biochemical Characteristics of B. Abortus and B. Melitensis*: Studies on the Genus Brucella Nov. Gen. I. J Infect Dis 27:173–184. https://doi.org/10.1093/infdis/27.3.173

Morel A-S, Dubourg G, Prudent E, et al (2015) Complementarity between targeted real-time specific PCR and conventional broad-range 16S rDNA PCR in the syndrome-driven diagnosis of infectious diseases. Eur J Clin Microbiol Infect Dis 34:561–570. https://doi.org/10.1007/s10096-014-2263-z

Petersen TN, Brunak S, von Heijne G, Nielsen H (2011) SignalP 4.0: discriminating signal peptides from transmembrane regions. Nat Methods 8:785–786. https://doi.org/10.1038/nmeth.1701

Rajendhran J (2021) Genomic insights into Brucella. Infect Genet Evol J Mol Epidemiol Evol Genet Infect Dis 87:104635. https://doi.org/10.1016/j.meegid.2020.104635

Ramasamy D, Mishra AK, Lagier J-C, et al (2014) A polyphasic strategy incorporating genomic data for the taxonomic description of novel bacterial species. Int J Syst Evol Microbiol 64:384–391. https://doi.org/10.1099/ijs.0.057091-0

Richter M, Rosselló-Móra R (2009) Shifting the genomic gold standard for the prokaryotic species definition. Proc Natl Acad Sci U S A 106:19126–19131. https://doi.org/10.1073/pnas.0906412106

Scholz HC, Nöckler K, Göllner C, et al (2010) Brucella inopinata sp. nov., isolated from a breast implant infection. Int J Syst Evol Microbiol 60:801–808. https://doi.org/10.1099/ijs.0.011148-0

Suárez-Esquivel M, Chaves-Olarte E, Moreno E, Guzmán-Verri C (2020) Brucella Genomics: Macro and Micro Evolution. Int J Mol Sci 21:. https://doi.org/10.3390/ijms21207749

Tatusov RL, Galperin MY, Natale DA, Koonin EV (2000) The COG database: a tool for genome-scale analysis of protein functions and evolution. Nucleic Acids Res 28:33–36. https://doi.org/10.1093/nar/28.1.33

Zerbino DR, Birney E (2008) Velvet: Algorithms for de novo short read assembly using de Bruijn graphs. Genome Res 18:821–829. https://doi.org/10.1101/gr.074492.107

Article 4

Draft genomes of two *Fusobacterium simiae* strains

Malak Zoaiter, Florence Fenollar, Pierre-Edouard Fournier, Linda Houhamdi

-Submitted in Microbiology Resource Annoucements-

Draft genomes of two *Fusobacterium simiae* strains

Malak Zoaiter[a,b], Pierre-Edouard Fournier[a,b], Linda Houhamdi[a,b#]

[a] IHU-Méditerranée-Infection, Marseille, France

[b] Aix-Marseille Univ, IRD, AP-HM, SSA, VITROME, Marseille, France

[#]Corresponding author: Linda HOUHAMDI

1) IHU Méditerranée-Infection, Assistance Publique-Hôpitaux de Marseille (AP-HM),

2) IHU Méditerranée-Infection, VITROME, Aix-Marseille Université, Service de Santé des Armées, IRD

19-21 Boulevard Jean Moulin 13385 Marseille cedex 05, France.

Phone: +33(0)413 732 401. Fax: +33(0)413 732 402

E-mail: lhouhamdi@yahoo.fr

Abstract

Here, we report the draft genomes of *Fusobacterium simiae* strain DSM 19848^T initially isolated from monkey dental plaque and the closely related bacterium strain Marseille-Q7035 cultivated from an intra-abdominal abscess puncture fluid of a 68-year-old woman, post-appendectomy. The genome size of strain DSM 19848^T was 2,4 Mb and that of strain Marseille-Q7035 was 2,5Mb. G+C content were 27.1% and 27.2%, respectively.

Fusobacterium simiae, a Gram-negative, rod-shaped bacillus, belonging to the *Fusobacteriaceae* family, was described in 1982 (1). The type strain was first isolated from Monkey dental plaque (*Macaca arctoides*) (2). As no genome sequence was available in Genbank, we purchased the type strain DSM 19848^{T} from the Deutsche Sammlung von Mikroorganismen und Zellkulturen GmbH (DSMZ). Strain Marseille-Q7035, a closely related strain, was isolated from a 68-year-old woman's intra-abdominal abscess puncture fluid on May 1st, 2022, following an appendectomy, in Marseille, France. The patient gave an informed consent for this study. We performed a whole genome sequencing for the two strains to be compared. Both were grown at 37˚C in anaerobic conditions on 5% sheep blood-enriched Columbia agar (bioMérieux, Marcy l'Etoile, France) after 24H of incubation in our laboratory.

The genomic DNA(gDNA) was extracted on a EZ1 BioRobot (Qiagen, Hilden, Germany) using the EZ1 DNA Tissue Kit. A single colony of each strain was treated mechanically and chemically using glass beads and lysozyme, respectively, before the DNA extraction step. The DNA quantification was assessed using Qubit assay (Thermofisher Scientific). Sequencing was performed on a Miseq sequencer (Illumina, Inc., San Diego, CA, USA) using the Nextera XT DNA sample prep kit (Illumina) and the mate pair strategy (3). Tagmentation was achieved using the Nextera XT transposome which added index adapter sequences on the ends of the fragmented gDNA, allowing PCR amplification.The latter was performed with twelve limited cycles and introduced dual-index barcodes.The libraries were purified using AMPure XP beads (Beckman Coulter Inc, Fullerton, CA, USA), and normalized using a bead-based procedure according to the kit protocol. Standardized libraries were combined, denaturated, diluted, and then pooled for sequencing. A single run was perfomed for cluster generation and paired-end sequencing in a 2 x 250 bp with the Miseq reagent Kit (V2-500 cycles) (Illumina).

Data information of 6.2526 Gb for strain DSM 19848^T were obtained from a 640 k/mm^2 cluster density with 97.1% clusters passing quality control filters. The index representation within the run was 5.78%. A total of 1,674,862 reads were produced by illumina Miseq sequencing. For strain Marseille-Q7035, 9.287 Gb of data were obtained from a 1577 K/ mm^2 cluster density with 63,5% clusters passing quality control filters. The index representation was 9.05%. A number of 1,469,874 reads was obtained. The forward and reverse reads of the two strains were quality checked using FastQC version 0.11.9 with default parameters (4). They were trimmed on the Galaxy Europe server available online using the Trimmomatic tool version 0.38.1(5). They were assembled using Spades version 3.14.0 (6). The genomes were annotated using Prokka version 1.14.5 (7). Strain Marseille-Q7035 had a genome size of 2,578,792 bp with a G+C content of 27.2%. Strain DSM 19848 ^{T} had a genome size of 2,481,730 bp with a G+C content of 27.1%. The genome-based comparison methods confirmed that strain Marseille-Q7035 was also affiliated to the *F. simiae* species.

Strain DSM 19848^T was deposited in the Collection de Souches de l'Unité des Rickettsies, CSUR, as Q7974 (DSM 19848 ^{T} = CSUR Q7974) and strain Marseille-Q7035 was deposited in the CSUR collection as Q7035 and in the Spanish Type Culture Collection as CECT 30592 (Marseille-Q7035=CECT 30592).

Data availability

Genomes sequences of the two *F. simiae* strains Marseille-Q7035 and DSM 19848^T were deposited in Genbank under accession numbers CALYGX010000000 and JAOXXL000000000, respectively, and the raw reads of each under accession numbers ERR10314471 and SRR21745855, respectively.

Acknowledgments

This work was funded by the Fondation Méditerranée Infection.

References

1. Robinson A, Wilde J, Allen-Vercoe E. 2020. Chapter 6 - Fusobacteria: physiology, form, and function. p. 95–134. *In* Floch, MH (ed.), Colorectal Neoplasia and the Colorectal Microbiome. Academic Press.

2. Slots J, Potts TVY 1982. Fusobacterium simiae, a New Species from Monkey Dental Plaque. Int J Syst Evol Microbiol 32:191–194.

3. Ravi RK, Walton K, Khosroheidari M. 2018. MiSeq: A Next Generation Sequencing Platform for Genomic Analysis. Methods Mol Biol Clifton NJ 1706:223–232.

4. Wingett SW, Andrews S. 2018. FastQ Screen: A tool for multi-genome mapping and quality control. F1000Research 7:1338.

5. Bolger AM, Lohse M, Usadel B. 2014. Trimmomatic: a flexible trimmer for Illumina sequence data. Bioinforma Oxf Engl 30:2114–2120.

6. Bankevich A, Nurk S, Antipov D, Gurevich AA, Dvorkin M, Kulikov AS, Lesin VM, Nikolenko SI, Pham S, Prjibelski AD, Pyshkin AV, Sirotkin AV, Vyahhi N, Tesler G, Alekseyev MA, Pevzner PA. 2012. SPAdes: a new genome assembly algorithm and its applications to single-cell sequencing. J Comput Biol J Comput Mol Cell Biol 19:455–477.

7. Seemann T. 2014. Prokka: rapid prokaryotic genome annotation. Bioinforma Oxf Engl 30:2068–2069.

-Chapitre II -

Etude de la résistance à la colistine chez les souches de *Brucella intermedia*

Avant-propos

Dans un projet de culturomique, six souches de *Brucella intermedia* (auparavant *Ochrobactrum intermedium*) ont été isolées des selles de chimpanzés vivant dans la réserve naturelle de Dindefelo au sud-est du Sénégal. Les colonies résistantes à la colistine ont été sélectionnées sur des géloses sélectives, puis identifiées par spectrométrie de masse MALDI-TOF MS. La colistine est un antibiotique de dernier recours pour traiter les infections causées par les bactéries Gram-négatives (GNB) multirésistantes, en particulier les bactéries résistantes aux carbapénèmes [52]. Cet antibiotique agit au niveau du lipopolysaccharide (LPS), chargé négativement, de la membrane externe des GNB [53]. Le mécanisme de résistance le plus commun est la modification du LPS de la membrane des GNB. Ce qui conduit à une réduction de la charge négative de la membrane, indispensable à l'interaction avec la colistine [54]. Des mécanismes qui incluent l'activité des pompes à efflux et la présence de la capsule chez certaines espèces ont été rapportés [55, 56]. L'espèce *Brucella intermedia*, non fermentative, multirésistante aux antibiotiques, est occasionnellement isolée d'infections humaines [57]. Sa résistance naturelle à la colistine induit un échec des traitements colistine-dépendants [58].

L'exportation des antibiotiques par l'activité des pompes à efflux joue un rôle important dans la résistance intrinsèque et acquise des GNB multirésistantes. Récemment, plusieurs études ont démontré que la résistance à la colistine pouvait être réversée par le cyanure de carbonyle 3-chlorophénylhydrazone (CCCP) chez les *Enterobacteriaceae* [59], *Acinetobacter baumannii*, et *Stenotrophomonas maltophilia* [60]. Le CCCP est un puissant découpleur de la phosphorylation oxydative qui perturbe la force motrice des protons (PMF) et la production d'ATP, nécessaires à l'activité des pompes à efflux. Cependant, le mécanisme exact de synergie avec la colistine est encore inconnu.

L'utilisation de CCCP a été limitée à tester expérimentalement l'activité des pompes à efflux dans la résistance aux antibiotiques ou dans la formation de biofilm chez les bactéries [60, 61].

Dans ce chapitre, nous avons rapporté d'abord, dans une revue, les mécanismes connus et impliqués dans la résistance aux polymyxines, y compris la colistine, chez des espèces intrinsèquement résistantes et d'intérêt médical. Ensuite, dans le but d'étudier le mécanisme de résistance à la colistine chez *Brucella intermedia*, nous avons testé l'effet de CCCP comme inhibiteur des pompes à efflux. La colistine, antibiotique de dernier recours contre les GNB multirésistantes, agit sur la membrane externe bactérienne, perturbant son intégrité et entraînant la mort cellulaire. Il est inactif contre les bactéries intrinsèquement résistantes à la colistine dont les espèces de *Brucella* (39), suggérant un rôle de la paroi cellulaire dans le mécanisme de résistance. Et comme les pompes à efflux font partie de la paroi cellulaire, nous avons choisi la CCCP pour investiguer leur implication dans le mécanisme de résistance intrinsèque à la colistine.

C'est le premier travail qui montre l'effet du CCCP sur le genre *Brucell*a et plus particulièrement sur l'espèce *Brucella intermedia.* Nous avons montré que la combinaison CCCP/colistine est capable de réverser la résistance à la colistine. Nos analyses pangénomiques ont permis la prédiction de certaines pompes à efflux conservées chez les *Brucella intermedia*, et potentiellement impliquées dans le mécanisme de résistance naturelle à la colistine.

Article 5

Intrinsic resistance to polymyxins

Malak Zoaiter, Zaher Zeaiter, Eric Ghigo, Pierre-Edouard Fournier

- to be submitted-

Intrinsic resistance to polymyxins

Malak Zoaiter[1,2], Zaher Zeaiter[4] , Eric Ghigo[1,5], Pierre-Edouard Fournier[1,2]*

[1] IHU Méditerranée Infection, Marseille, France

[2] Aix-Marseille Univ, IRD, AP-HM, SSA, VITROME, Marseille, France

[3]Aix-Marseille Univ, IRD, AP-HM, MEPHI, Marseille, France

[4] Lebanese University LU, Department of Biology, Faculty of sciences, Beirut, Lebanon

[5] Techno Jouvence, Marseille, France.

***Corresponding author:** Pierre-Edouard Fournier

Aix-Marseille Université, Institut Hospitalo-Universitaire Méditerranée Infection,

19-21 Boulevard Jean Moulin 13385 Marseille cedex 05, France.

Phone: +33(0)413732401. Fax: +33(0)413732402

E-mail: pierre-edouard.fournier@univ-amu.fr

DRAFT REVIEW

Abstract

Polymyxins (PX) belong to cationic antimicrobial peptide that derived from different species of soil bacterium in the genus of *Bacillus.* PXs were used to treat multi-drug resistant infections especially carbapenemase mediated Gram-negative bacteria. Diverse human pathogenic genus were known to be intrinsically resistant to polymyxin B (PXB) and polymyxin E (PXE), the two available forms in medicine. This characteristic is independent of a previous antibiotic exposure and not caused by a horizontal transfer gene. Recently, the researches carried out on the interest of intrinsic resistance genes as these genetic products can predict the future emergence of resistant pathogens and provide therapeutic targets for the development of new adjuvants. In this review, we summarize the known intrinsic PX resistance mechanisms in several bacterial genus of medical interest. In total, there are no well-defined resistance mechanisms. Changes in membrane composition and integrity such as membrane porins, biosynthesis of isoprenoids and hopanoids, and capsule production contribute to the level of intrinsic susceptibility of bacterial pathogens. In addition, the efflux pumps, which reduce effectively the PX's intracellular concentration, as well as metabolic enzymes involved in basic bacterial metabolisms seems to confer the intrinsic trait of resistance to PX. We discuss the intrinsic genes at the origin of PX resistance. In total, there are no well-defined PX resistance mechanisms and more experimental studies are needed to expanding our knowledge.

Keywords: Intrinsic resistance, Polymyxins E and B, LPS, cell membrane remodeling, efflux pumps, PX resistant-bacteria

DRAFT REVIEW

Introduction

In the last 70 years, people have moved from the glory days of Antibiotics to the age of Antibiotic resistance that threats health care systems worldwide. At an alarming rate, the number of infections caused by multidrug resistant Gram-negative (MDR-GNB) pathogens is rising (1). Antibiotic resistance evolves over time and has received considerable attention due to the rapid expansion in the pathogenic bacteria. This problem arises to longer human hospitalization, additional doctor visits, increased mortality rates, more complications in patients undergoing surgery, organ transplantation, cancer chemotherapy, and dialysis and etc. (2). As result, antibiotic resistance imposes an increased rate in healthcare costs. According to World Bank team, an economic simulation found that antimicrobial resistance AMR cost could exceed $ 2 trillion annually by 2050 in a optimistic case of low-AMR impact and it can be three times higher in the second scenario of high-AMR impact (3).

Antibiotic resistance is frequently thought to be acquired by formerly susceptible bacteria, the basis of which can be attributed to the horizontal acquisition of new genes or the occurrence of spontaneous mutations within chromosomally located genes that are then transmitted vertically as the bacteria replicates (4) (5). In fact, antibiotic resistance predates the antibiotic era and represent an ancient phenomenon. There have been many studies that reveal the presence of diverse resistance elements in microorganisms collected from pristine environments, unimpacted by anthropogenic antibiotics, such Lechuguilla Cave (6), remote Antarctic soils (7), Hanford site in Washington as a deep Terrestrial subsurface (8), and Antarctic waters (9). Therefore, in addition to the acquired resistance, bacteria also possess an inherent resistance to diverse antibiotics .This characteristic is independent of a previous antibiotic exposure and not caused by a horizontal transfer gene. The impermeability of the

DRAFT REVIEW

Gram-negative outer membrane OM and the active efflux pumps which reduce effectively the drug's intracellular concentration contribute to the level of intrinsic susceptibility of bacterial pathogens. The therapeutic options for treating infections caused by Gram-negative pathogens are severely constrained by the intrinsic resistance of Gram-negative bacteria. To predict the antibiotic resistance phenomenon, its clinical threat and the rising incidence of bacteria that are resistant to multiple drugs and reduce its potential consequences required the consideration of both acquired and intrinsic antibiotic resistance.

Polymyxin B (B) and E (PE), the two clinically available forms of polymyxins (PX), are polypeptide antibiotics that were effective against MDR especially carbapenem resistant. Several human pathogenic bacteria are known to be intrinsically or naturally resistant to PX such as *Neisseria, Proteus, Providencia, Burkholderia,* and *Brucella* genera and *Serratia marcescens, Morganella morganii, Helicobacter pylori,* and *Vibrio cholerae* species (3) (4). Their intrinsic polymyxin resistance is largely unknown. The ability to resist to PX in different host niches increases their pathogenicity and contributes to their virulence. In this review, we summarize the known mechanisms underlying the PX resistance in the following bacterial species as they represent a medical interest.

Polymyxins overview

Polymyxins (PX), discovered in 1947, belongs to cationic antimicrobial peptides (CAMP) and derived from different species of soil bacterium in the genus of *Bacillus*. Only PE or colistin and PB are the only two clinically available forms. Over the past decades, PXs have been replaced by newer antibiotics due to the adverse renal and neurological effects. Currently, the increased occurrence of infections caused by MDR-GNB and the shortage of new antibiotics led to the re-emergence of PX use as the last resort antibiotic in clinical medicine.

DRAFT REVIEW

Noteworthy, new evidence showed that PX use is associated to less toxicity compared to old studies (12). Apart from the potential treatment for Gam-positive bacteria, it was highly effective against selected susceptible GNB including *Klebsiella pneumoniae, Acinetobacter baumannii, Pseudomonas aeruginosa* and *Enterobacter* species (1)(13). PXs having detergent-like properties, affect the bacterial membrane selective permeability. They act by binding to the lipopolysaccharide (LPS), rich in negatively-charged lipid A and penetrates the outer membrane (OM) through a "self-promoted uptake" mechanism required by displacing the divalent cations Ca^{2+} and Mg^{2+} that stabilized the LPS structure. Subsequently, the membrane integrity is destroyed, leading to an outflow of cellular components and bacterial cell death (14). PE and PB share the same mechanism of action against GNB, the same mechanisms of resistance and have similar applications. However, they differ in the chemical structure and pharmacokinetic properties (14).

Overview of the involved pathways in PX resistance

Bacterial pathogens undergo different strategies to overcome the antimicrobial activity of PX including incorporation of cationic groups to LPS, export of the PX via efflux pump, production of proteases that cleave PX, release of proteins that could adsorb extracellular PX. Modifications of LPS, the first point of attack by PX, via cationic substitution are the most common among PX resistance mechanisms. It can be achieved by replacing the phosphate groups of lipid A moiety of LPS by 4-amino-4-deoxy-L-arabinose (L-Ara4N) (15), phosphoethanolamine (PEtn) (16), or galactosamine (GalN) (17) in the OM of GNB. Each modification functions to mask the negative charge presented by the native lipid A then disrupting the electrostatic interactions of PX for their initial interaction with lipid A. Noteworthy, the addition of L-Ara4N is the most ubiquitous of all lipid A modifications that

DRAFT REVIEW

confer PX resistance and is more effective than that of PEtn moiety (18). It decreases more the net lipid charge (19). Glycosylation of lipid A with GalN was observed in *A. baumannii* (17) in addition to a complete loss of LPS production (20). LPS modifications is regulated mostly by the two-component systems (TCS). The most studied are PhoP/Q and PmrA/B (21). PhoQ and PmrB are transmembrane histidine kinase sensors and can change the expression patterns of the TCS in response to environmental signals. PhoP and PmrA are the response regulators. PhoQ senses acid PH, low concentrations of Mg 2+, cationic peptides (22), extracellular DNA (23), and PmrB senses high concentrations of Al 3+ or Fe2+(24). In addition to stress conditions, mutations in the genes encoding TCS give rise to constitutive stimulation of the LPS modification pathway (25). Regulations of PhoP/Q and PmrA/B have been found to overlap. Upon stimulation of PmrB, phosphorylated PmrA activates the transcription of PmrCAB operon. PmrC (PEtn) is a phosphotransferase that is responsible of the incorporation of PEtn into lipid A (26). This network is found in *A. Baumanii* (27), *Salmonella enterica* (28). Likewise, PmrA activates Pmr HFIJKLM operon which is involved in the addition of L-Ara-4N to lipide A. PhoP/Q can interact directly with the PmrA/B as shown in *P. aeruginosa* (29) and indirectly as characterized in *S. enterica* via a local regulator PmrD which stabilizes the phosphorylation of PmrA (30). Another TCS have been reported to mediate resistance in *P. aeruginosa*. were ParRS, ColRS, and CprRS (31).

Intrinsic resistance mechanisms

Burkholderia sp.

The genus *Burkholderia* sp. including ***B**urkholderia **C**epacia* **C**omplex (BCC) exhibits high intrinsic resistance to PX (32). Since 1970, it was recognized as an opportunistic pathogen particularly in patients with cystic fibrosis (CF) or chronic granulomatous disease(CGD) (33).

DRAFT REVIEW

As mentioned previously, the mechanism of resistance is linked to the presence of the sugar L-Ara4N in both the lipid A and an unusual glycerol-talo-octulosonic acid (Ko) residue in the LPS inner core (34). A putative gene cluster encoding for a constitutive L-Ara4N was found in *B. cenopacia* and it is essential for bacterial viability. These genes are highly similar to those acquired in *Salmonella* and other bacteria. It corresponds to arnT (Ara4N transferase), arnB (UDP-4'-ketopentose aminotransferase), arnC (Ara4N Und-P transferase), arnA1(UDP-Ara4N formyltransferase), arnA2 (UDP-4'-keto-5'-carboxypentose decarboxylase), BCAL1930 and BCAL1935 equivalent to pmrLM and pmrJ respectively with unknown function (35). However, the exact mechanism remain unknown. LptG, protein of Lpt pathway, is involved in the export of L-Ara4N modified lipid A from the inner to the outer membrane remain also to be elucidate (36). Additionally, Bmul_2133 (hpnJ) and Bmul_2134 (hpnI) have been shown to increase resistance to PB and colistin with 8-16 fold respectively in *Burkholderia multivorans (Bm)*, a member of BCC using a transposon mutant library. These genes, not expressed in all bacteria, were required for the hopanoid biosynthesis, analogues of sterols in eukaryotic membranes. The abrogation of hopanoid enhances specifically PX susceptibility by increasing the OM permeability supposing its involvement in the membrane stability (37). LytB also called ispH (BCAL2710) is required for isoprenoids biosynthesis in both *Burkholderia pseudomallei* and *B. cenocepacia* and could confer resistance to PX by affecting phospholipid and peptidoglycan biosynthesis of the inner membrane (38). *B. cenocepacia* showed additional determinants of PX resistance. The major one is linked to a sigma factor RpoE that could control the expression of several critical genes for PX resistance at 37°C not at 30°C (39). Another major determinant is the increasing in PX sensitivity in response to a truncated LPS core oligosaccharide including the severe truncation

DRAFT REVIEW

which leads to loss of the L-glycero-D-manno-heptose and the following residues (40). Also, Ugd gene (BCAL2945), UDP-glucose dehydrogenase, highly expressed gene, that acts as a component of the L-Ara4N synthesis pathway is implicated in PX resistance (38). It was found that NorM, Na^+ coupled multidrug efflux transporter, member of MATE (multidrug and toxic compound extrusion) family contributes to PX resistance in *Burkholderia vietnamiensis*, a member of BCC (41). MucD (periplasmic protease), ZmpA, ZmpB (two zinc-metalloproteases), BCAL2831 protein regulator of TCS, ispH (BCAM2738) display also a role in resistance to PX (39). In 2016, two-component regulatory system MgrS/MgrR have been identified in clinical isolates of *B. pseudomallei* which mutations in MgrS were found to be responsible for acquired not naturel colistin resistance (42).

Proteus tribe

Proteus genus consists on a member of *proteeae* tribe that comprises three genera *Proteus*, *Providencia* and *Morganella* (43). These organisms are ubiquitous in the environment and become a non-negligent opportunistic pathogens that cause nosocomial infections and may lead to mortality in severe conditions (44). The *proteeae* tribe are usually known that is inherently resistant to PX. The presence of L-Ara4N in the LPS outer membrane is common for *P. mirabilis*, *M. morgani* and *P. rettgeri* (45).

P. mirabilis cause human infections mainly in the urinary tract (46). It was found that L-Ara4N was incorporated in the core and lipid A of *P. mirabilis* (47). Similarly, it was established a role of PMI3104 gene as an ethanolamine phosphotransferase C (eptC) involved in the transfer of PEtn to the O-6 of L-glycero-D-mano-heptose II in the LPS core (48). Using transposon mutagenesis Tn5, TCS *RppA/RppB*, homologous to *PmrA/B* and *PhoP/Q* in *Salmonella* have been identified in *P. mirabilis* mutants **(Figure.1b)**. RppA was upregulated

DRAFT REVIEW

179 in response to PX and a low Mg2+ levels. *RppA* and *RppB* mutants exhibit super-swarming
180 and PX-sensitive phenotype suggesting PX resistance and swarming regulation in *P.*
181 *mirabilis*. Further, LPS lacks L-ara4N in RppA knock out model. Homologues to *PagP*
182 (incorporation of palmitate into the lipid A) and *pmrH* (encoding an aminotransferase) genes
183 in *Salmonella* were less expressed in the mutant than the wild type. Together, this supports
184 that *RppA* controls LPS modification and resulting in PX resistance. Genes involved in the
185 swarming migration, the flagellin biosynthesis, the hemolysin cytotoxic activity were
186 modulating negatively through *RppA*-dependent pathway in the presence of PX (49). It was
187 found in another study, that *Ugd* (UDP-glucose deshydrogenase) and *GalU* (UDP-glucose
188 pyrophosphorylase) mutants express a PX-sensitive phenotype which is RppA dependent. The
189 latest activates *GalU* and *Ugd* in response to PX. It was known that the two enzymes are
190 involved in the production of L-Ara4N leading to the alteration of LPS profile and eventually,
191 inducing PX resistance. The ability to express virulence factors and swarming behavior are
192 affecting negatively in the mutants which is explained by the activation of the sigma factor
193 RpoE that in fact responds to stress factors including LPS alteration (50). An additional gene
194 can be under the control of RppA and confers PX resistance is UDP-glucuronic acid
195 decarboxylase PpmrI (Proteus pmrI). Similar to GalU, it was demonstrate that RppA, induced
196 by PX, can stimulates *PpmrI* (ArnA) by direct binding to its promoter. *PpmrI* is equivalent to
197 *pmrF* operon in *E.coli* and *S. enterica* which is required for the synthesis and addition of L-
198 Ara4N to the lipid A moiety. Apart from LPS changes, *PpmrI* mutant caused an alteration in
199 biofilm formation and a reduced urothelial cell invasion ability suggesting that the LPS
200 changes influence the bacterial adherence and invasion into host cells in *P. mirabilis.* As we
201 have shown above that RppA/RppB regulates several genes involved in the PX resistance but

202 the detailed mechanisms remain elusive (51). Moreover, previous work showed that Genes,
203 homologues to sapD in *Salmonella* and to ATP-synthase showed an increase in sensitivity to
204 PX *P. mirabilis* mutant. Tn5- disrupted locus of an O-acetyl transferase reduces 320 fold the
205 resistance to PX. It seems to be essential for the addition of L-ara4N to lipid A but the
206 mechanism still unknown. Together, the three mutants were involved directly or indirectly in
207 LPS modifications leading to abolish the ability of *P. mirabilis* to swarming across the
208 surfaces (52). Recent study has been reported a comparative genomic, transcriptomic and
209 proteomic approaches between an unusual colistin susceptible *P. vulgaris* and another
210 resistant one. The susceptible strain had an inactivated arnBCADTEF operon which lacked L-
211 Ara4N in the lipid A moiety. It was postulated that the colistin sensitive *P. vulgaris*, isolated
212 as a mixed population with colistin resistant *P. mirabilis* from a human urine sample, to be
213 interpreted as heteroresistant strain. Several genes are absent such as TCS genes involved in
214 copper regulation, genes involved in sialic acid metabolism , in the LPS biosynthesis, in the
215 O-antigen biosynthesis, and others (53). In addition, a downregulation of the expression of
216 *arnB* and *arnT* is attributed to the alteration of the sugar fixation strain. It should noted also
217 that an *arnD* gene cloned in the colistin-susceptible strain increases 32 times the resistance to
218 colistin demonstrating its role in *Proteus* genus (53).

219 To note, lipid A of *Morganella morgani* shares closest features within the *Proteeae* tribe,
220 containing PEtn in addition to L-Ara4N. Based on genomic analysis of a colistin-resistant
221 strain, a large panel of genes LPX mediating lipid A synthesis, arn and eptB genes involved in
222 the synthesis of cationic groups and their addition to LPS were detected. The TCS
223 PhoP/PhoQ and its feedback inhibitor mgrB were found to govern the LPS modification
224 pathway. Likewise, *qseB/C* and *rssA/B*, another TCS might have been contributed indirectly

in PX resistance. It was noticed that *pmrA/B* was absent in all *Proteeae* members and two copy of *arnT* were present, suggesting a distinct factor contributing to their same possible intrinsic PX resistance mechanism (54).

Serratia marcescens

Serratia marcescens is a nosocomial pathogen, intrinsically resistant to PX, can cause infections notably in the urinary tract (55). In 2014, mechanism of PX resistance has been reported for the first time using *S. marcescens arnB*, *arnC* and *PhoP* mutants (56). PX resistance is induced through the expression of *arn* operon which are controlled by the TCS *PhoP/Q* to modify LPS. PX and low Mg 2+ (1µg/ml) promote the activation of *PhoP* that binds directly to *arn* promoter in a way that doesn't require *Pho-P* activated *PmrD* protein similarly to *yersinia pestis* (57). Different species of *Serratia* exhibited Pho-P conserved binding site in the *arn* promoter confirming the correspondent pathway. In addition, it was investigated that *ugd* gene, encoding the L-Ara4N precursor, responds also to the PX signal through *PhoP* pathway. Different *S. marcescens* clinical isolates that were resistant to PX ,undergo a high expression of *ArnA* versus the susceptible strains. Therefore, this suggest that *arnBCADTEF* operon is essential to induce PX resistance through PhoP-dependent modification in *S. marcescens* (56).

Brucella sp.

Brucella are facultative intracellular bacteria that can infect both animals and humans (58). These organisms are naturally resistant to polymyxin. Previously, it have been shown that both the core lipid A and the O-chain of *Brucella* LPS are related to resistance to bactericidal cationic peptides such PX (59). *Brucella spp.* presents a branched LPS core structure. Two

247 glycosyltransferases were required for the synthesis of the core branch not linked to the O-
248 polysaccharide. WadC is a mannosyltransferase able to transfer mannose residue to lipid A-
249 kdo. In a later step, WadB acts as glucosamine transferase on the mannose units. Disruption
250 of these two genes in *Brucella abortus*, increases the sensitivity to polycationic peptide
251 including PX, and to serum complement confirming a defective core LPS keeping intact O-
252 PS chain and lipid A. The two bacterial mutants are not able to multiply in dendritic cells
253 (DC). It was also demonstrated that WadC mutant could activate DC and induce their
254 maturation through increase binding to MD2-TLR4 (52)-(61). In this context, wadB and
255 wadC appear to be targets for brucellosis vaccine. BvrS/BvrR, a well characterized TCS in
256 *Brucella* virulence, seems to be involved in PX resistance in *B. abortus.* BvrS/BvrR mutant
257 evolved an underacylation at lipid A levels, an increasing in acyl-chain fluidity and therefore
258 a high affinity to complement and PX binding. But, these alterations do not affect the
259 immunostimulatory activity and the expression of genes implicated in lipid A acylation
260 (acPXL, LPXXL, bac-A) (62). However, a dysfunction of bac-A, that was postulated to be a
261 putative peptide transporter, induced an alteration in the lipid A with the very-long-chain fatty
262 acid (VLCFA) >22C leading to increase the sensitivity to antibiotics and detergents through
263 BvrS/BvrR-independent pathway (63). A virulence gene VirB2 allows also a PX resistance
264 and it was controlled positively by a quorum-sensing related regulator *vjbR* (64).Tn-5
265 transposon, Omp31 (BR1622) and *pgm* (BRA0348) mutants induce an decrease in PX
266 resistance in *B. suis* resulting either from a membrane destabilization or from the alteration of
267 LPS structure. It should be noted that Omp31 is an outer membrane lipoprotein and *pgm* a
268 putative phosphoglucomutase (BRA0348) responsible to the conversion of glucose-6-P to
269 glucose-1-P. Using In vitro system, the two genes were resistant also to the action of the

γ9δ2T lymphocytes that consists to reducing the intramacrophagic multiplication of bacteria in the presence of activated T lymphocytes. This suggests that the two genes might impair the interaction between activated lymphocytes and infected macrophages (65). In a further study, low PEtn abundance was underlying the PX resistance in *B. melitensis.* The mechanism was maintained by the activity of a phospholipase-A1 *bveA* (BMEII0681) that is broadly conserved within *Brucella spp*. *BveA* (Brucella-virulence esterase A) mutant becomes more sensitive to PX and reveals an accumulation of PEtn in the cell envelope but did not affect the LPS composition. It also enhances the bacterial fitness during persistent infections (66). In response to PX, gene expression of the *yejABEF* operon, encoding a putative ABC transporter was up-regulated in *B. melitensis* inducing PX resistance. Accordingly, a *yejABEF* mutant appears more sensitive to PX and to acidic conditions than the intact wild-type. Otherwise, mutant displays a reduced invasion and replication abilities in macrophages cells. Thus, resistance to CAMP plays a key role in maintaining persistent infection by brucella pathogens (67). Furthermore, three genes involved in the remodeling of the brucella cell envelope have been identified LptA (transferase), LPXE (phosphatase) and LPXO Acyl hydroxylase). Only LptA encodes a PEtn transferase that modified lipid A and showed an increase in PX resistance in *Brucella*. The tested mutants of these genes did not affect their interactions , their immunogenic capacity, and their virulence functions within the host cells (68). Recently, based on MS/MS analysis, the lipid A structure isolated from *B. abortus* and *B. suis* LPS contains a diGLcN backbone bearing one phosphate and one pyrophosphorylethanolamine that may contribute to PX resistance (69). In addition, MapB (BR0049), homologue to TamB (Translocation and Assembly Module B), a large protein inserted in the IM, seems to play a critical role in the cell integrity in *B. ovis.* Hence, deletion of MapB displays an increase in the

sensitivity to the lytic effect of lysozyme and from 5 to 14 fold to PX. It was found that the mutant did not affect greatly LPS structure, instead mapB appears to be responsible to the correct insertion of OMP with adhesion activity in the OM and their stability such Omp25, Omp31 and BamB autotransporter. Besides, an aberrant cell division and a defect in the internalization in macrophages at early stages were observed during mapB deletion (70).

Vibrio cholerae

Some strains of *Vibrio cholerae* have an epidemic potential and can cause cholera, a severe diarrheal illness. *Vibrio cholerae* O1 is the predominant cholera pathogen serogroup (71). O1 Vc strains were subdivided into two distinct biotypes, classical and El Tor, which differ phenotypically in resistance to PX. Classical strains are sensitive while El Tor strains are strongly resistant (72). The mechanism underlying PX resistance in El Tor depends on the tripartite system AlmEFG that mediates the attachment of one or two residues of glycine to the El Tor lipid A domain **(Figure.1a)**. The lipid A glycylation was described as a unique modification strategy among GNB and resembling to teichoic acid modification by D-alanine in gram positive (73). AlmE (Vc1579), AlmF (Vc1578), AlmG (Vc1577) are the enzymes products. AlmE, a dual aminoacyl transferase/carrier protein ligase, activates glycine, generates the intermediate glycyl-AMP and then ligates glycine onto holo-AlmF (modified AlmF from an Apo-AlmF precursor). AlmF, a glycyl carrier protein which serves as a aminoacyl donor to AlmG (73). AlmG, an acyltransferase, esterifies the glycine onto the secondary hydroxylauryl acyl chain harbored by an acyl carrier protein acpP (Vc2020) (74). Furthermore, LPXN (Vc 0212), also known as msbB (72), transfers in turn the hydroxylaurate from ACP to the glucosamine disaccharide of lipid A generating the hexa-acylated lipid A (75). Glycine-modified lipid A, a potent activator of MsbA flippase , was translocated from

316 the inner membrane to the periplasm side (76), then was transported to the bacterial surface
317 through Lpt essential proteins (77). As result, lipid A glycylation reduces the net anionic
318 charge of LPS and thus the permeability barrier properties of the OM which provides
319 resistance to PX. Besides, the addition of glycine to lipid A is also required for intestinal
320 colonization (78). The expression of AlmEGF operon is activated TCS VprAB, also designed
321 as CarRS (vc1320/vc1319), which responds to PX ,bile and mildly acidic PH (70-71).The
322 latest acts also as a negative regulator of the biofilm formation by repressing the extracellular
323 matrix components genes such as vibrio polysac2charides genes VpsA,VpsL (80). It is proven
324 that a downregulation on the CarR expression was observed in response to high calcium
325 levels >1mM and to an acidic PH <5. Ultimately, it was followed by a decrease in the
326 expression of CarR-regulated genes almEGF, vpsA, et vpsL. Mutants defective of each *Alm*
327 operon, VprAB, and LPXN increased LPS sensitivity to PX in El Tor *V. cholerae.*, the
328 emergence of a novel PX-sensitive VC O1 el Tor biotype employs an acquired mechanism
329 found to be a point mutation in CarR altering therefore environmental parameters (79). In
330 addition, Classical biotype of V. cholerae appears to have lost a functional AlmEFG pathway
331 due to the encoding of a truncated AlmF that lacks the site required for carrier protein
332 function (4'-phosphopanteetheinyl) (73). Herrera and colleagues, were identified a EptA (Vc
333 1102) orthologue in EL Tor O1 *V.cholerae* that displays a high similarity with EptA proteins
334 in *Enterobacteriaceae* (81). EptA is activated under mildly acidic conditions. Although the
335 PEtn addition in El Tor strains was independent on VprA, a 100-fold decrease in resistance
336 has been shown in VprA mutants. These findings suggest that VprA coordinatly controls the
337 LPS modification systems with additional regulators at PH acid (81). A GalU mutant, which
338 provides a defect in the core oligosaccharide in O1 El Tor strain, expresses a PB-sensitive

phenotype. The mechanism still unresolved because any studies were reported the presence of L-Ara4N modification. Together, GalU and GalE also was investigated to be essential for exopolysaccharide (VPS) production in the biofilm formation in a rugose variant limiting the acces of antimicrobial peptides (82).

Other mutants in genes gspI (Vc 2728), gspF(Vc 2731), gspE (Vc 2732) encoding the components of the type II secretion system exhibit a PX sensitive phenotype (78). Previous study was reported the implication of a VC major porin, OmpU in PX resistance. In response to a sublethal doses of CAMP including PX, OmpU enhances the expression of the sigma factor RpoE through DegS-mediated proteolytic cascade. The OmpU acts as sensor to the damage induced by PX which induced conformational changes in the porin. Thus, the exposed C-terminal YXF motif of OmpU in the periplasm interacts with the PDZ domain of the periplasmic protease DegS promoting a cascade cleavage that release the sigma factor σ^E from the inner membrane and activate it (73). It should be note that each of the OmpU and RpoE mutants confers PX resistance and a decrease in the RpoE amount was displayed in the OmpU mutant (73). Apart LPS modifications, it was found that RND efflux pump (resistance-nodulation-division) are required for resistance to antimicrobial peptides, bile secretion, fatty acids, detergents and others in VC. It was shown that especially VexB (VC0164) contributes to PX resistance. Furthermore, it was investigate that RND efflux pump is essential for bacterial colonization in a mouse model and can be linked to virulence factor production. A reduced transcription of TcpP and ToxT that regulate the cholera toxin genes (CT) and toxin-coregulated pilus (TCP) were observed in a RND-null mutant in addition to PX resistance. Together, it was confirmed that VC RND efflux pump play role in VC pathogenesis (83) .

Helicobacter pylori

H. pylori infect more than 50% of human stomach in the world mostly without manifestation of syndromes. It can evade the immune system and persist for several years to cause chronic infection in absence of antibiotic treatment. Peptic ulcer and gastric cancer including Mucosa-associated lymphoid tissue lymphoma (MALT) lymphoma and gastric adenocarcinoma, represent the severe outcomes of the chronic infection (84). The enzymatic machinery for LPS biosynthesis is well conserved in GNB and has been identified in H pylori (85). However, modification enzymes were reported to remodeling the LPS of the OM in order to survive in the gastric mucosa and giving rise to PX resistance. Of note, *H. pylori* requires a constitutive modification of LPS which provides a single form of lipid A and lacks an environmental regulation, differently to other bacterial pathogens (86). A highly modified lipid A is produced via five step enzymatic pathway **(Figure.2).** LPXE (Hp0021), a lipid A 1-phosphatase, removes 1-phosphate group from the disaccharide backbone of lipid A. It is followed by an attachment of PEtn residue catalyzed by an EptA transferase (Hp0022), forming a phosphodiester linkage, unlike a number of GNB which add the PEtn directly to the lipid A phosphate group in a pyrophosphate linkage. Then, a kdo hydrolase (Hp0579/Hp0580) cleaves the terminal kdo sugar. Subsequently, LPXF (Hp1580) a second phosphatase, becomes responsible for the dephosphorylation of lipid A 4'-phosphate group. At the final step, a deacylation activity of two acyl chains was catalyzed by LPXR (Hp0694), giving rise to a tetra-acylated lipid A (87). Previous studies have been reported a 1020 fold increase in the sensitivity to CAMP including PX in LPXE/F mutants (88). Moreover, it has been showed that these mutants have a greatest impact but not the only one in the appearance of the low endotoxicity in *H. pylori* (through the attenuation of hTLR4-MD2 complex activation) and in effective host colonization. Similarly, a 180 to 250 fold decrease in PB minimal

inhibitory concentration MIC was observed in a kdo hydrolase mutant which can also generate changes in the expression of the O-antigen (89). However, the LPXR mutant exhibits CAMP CMI that found to be comparable to that of wild type strain suggesting that the deacylation of Lipid A did play no role in the CAMP resistance (88).

Furthermore, LPS modification in *H. pylori* might be also cholesterol-dependent and contributes to antibiotic resistance (90) in addition to its role in virulence. The bacterium steals host cholesterol, modifies it by glycosylation through cholesterol glycosyltransferase (cgt). Then, the cholesteryl glucoside is incorporated into its membrane which enhances the resistance to many antimicrobial compounds including PB and PE. *Cgt* knockout strain showed an increase in colistin susceptibility but retained resistance to most antibiotics. This suggests its involvement in the lipid A modification. Thus, it has been found that a LPXE mutant displayed a loss of the cholesterol-dependent resistance to PXB and colistin. Consequently, LPXE plays an essential role in cholesterol-dependent resistance to colistin and PXB but the mechanism remains unknown (90).Moreover, a recent study reports that the deletion of the O-antigen ligase (WaaL) and the putative Heptose III transferase of the LPS core domain (HP1284) lead to a moderate susceptibility to PX with loss of host colonization (91). Based on these results, HP1284 and WaaL are unlikely to affect lipid A modification process.

Neisseria sp.

Neisseria genus colonize mucosal surfaces of animals and humans. The genus includes commensal and pathogenic species. Two species are known to be human pathogenic *N. meningitidis (Nm)* and *N. gonorrhoeae (Ng)* and colonize the respiratory and the uro-genital tracts respectively. The latest pathogens were agents of epidemic meningitis and gonorrhea

and they are intrinsically highly resistant to CAMP such as PX. Constitutive PEtn substitution is the critical strategy used by *Neisseria* to maintain resistance to cationic cyclic polypeptide antibiotic, and PX as it lacks the essential machinery to synthesize L-Ara4N modification conferring PX resistance in many GNB. Previous studies describe several PEtn transferases in *Neisseria*. Lpt-3 (NMB2010) (92) and Lpt-6 (NMA0408) that are required for the addition of PEtn on the distal heptose-II residue at the position 3-6 respectively within the inner core of the oligosaccharide (93). LptA (NMB1638) catalyzes the esterification of the lipid A head groups (1 and 4' positions) by PEtn **(Figure.3)** (94). It was reported that PEtn substitution from the heptose-II at the position 6 mediates susceptibility to both normal human serum (NHS) and PX in *Nm*, no effect was observed in *Ng*. However, lipid A substitution with PEtn correlates high-levels of PX resistance in both species. LptA is also important in enabling *Ng* to resist to NHS through complement mediated killing pathway in contrast to *Nm* (95). It should be noted that LptA contributes broadly to promoting *Neisseria* infections through undergoing an essential role in CAMP resistance including PX and other biological functions to evade innate defenses rendering it a vaccine candidate: It mediates meningococcal adhesion to human endothelial and epithelial cells, this action might be masked in encapsulated meningococci (96). In addition, it was found that PEtn-lipid A decoration in *Ng* by LptA plays a protective effect against complement-mediated bactericidal activity and an immunostimulatory role through TLR4 within the host (97). LptA in Ng confers also a resistance to bactericidal activity of neutrophils (98) and evade autophagy in murine and in human macrophages (99). Moreover, it was demonstrated that *Ng* PEtn in lipid A catalyzed by LptA provides a survival advantage in mouse and human during infection and enhances the fitness of the bacterium (100). LptA gene was found only in *Ng*, *Nm* and two commensal

species *N. lactamica* and one strain of *N. polysaccharea* which hypothesized that the absence of lipid A-PEtn, allows commensal species to survive for a long time by reducing the inflammatory potential of the LOS, contributing then to their commensalism (101). Recent evidence demonstrates that LptA of *Ng* behaves as a Phase-Variable gene which can highly modulate CAMP resistance and results in resistance to PX within the phase-off (102). Previous work in *Nm* (103) elicits a critical contribution basically of both LptA and the MtrCDE efflux pump in PX and CAMP resistance, using mariner-transposon mutagenesis (104). It is important to note that the mtr multidrug efflux pump promotes the survival of Ng in murine genital tract (105). Another genes have been reported to influence positively PX resistance: the *pilMNOPQ* operon involved in type IV pilin secretion and biogenesis; PorB an outer membrane protein which decreases a 16-fold MIC of PXB; LPXL1/2 late acetyltransferases of lipid A confirm the role of the deacylation in PX resistance , a putative outer membrane lipoprotein in KA2025 mutant homologue to OlmA in *P. aeruginosa* that was defined to maintain membrane integrity (106), and genes encoding metabolic enzymes such *GshB* a glutathione synthase, and *fbp* fructose 1,6-biphosphatase which might have an indirect impact on PX resistance. Of note, *fbp* reduces the outer membrane content of lipid A suggesting to increase in its permeability (103). Recent evidence has shown that MisR protein component of the TCS MisR/MisS in *Ng*, contributes to constitutive and inducible PX resistance independently of MisS (107). MisR, unresponsive to $Mg2^{+}$, provides resistance through regulation of permeability genes of the cell envelope and does not influence neither the expression of PEtn on lipid A nor that of the MtrCDE efflux pump. The closest orthologues of MisR are elucidated by CPXR in *V.cholerae* and AmgR in *P.aeruginosa* which known to confer intrinsic CAMP and aminoglycoside resistance. Likewise, it shares

100% identity with MisR (NM0595) in *Nm* (107).Several studies were investigated the stability of LptA by oxidoreductase enzymes, the role of capsule and the effect of polyamines on PX resistance in the two pathogen strains. In E.coli, neisserial LptA induces PX resistance when co-expressed with oxidoreductase DsbA. So, in the absence of DsbA, LptA is rapidly degraded suggesting a preventive effect from the proteolytic degradation in the periplasm. Based on this finding, the role of neisserial oxidoreductases in the stability of LptA and PX resistance in *Nm* was evaluated. Unlike to *E.coli*, it was shown that Dsb3 only contributes to the activity of LptA but does not appear to complete loss of LptA and the latest remains stable although in the absence of the three enzymes. Further, each of the triple oxidoreductases DsbA1/ DsbA2/ DsbA3 mutants undergo increase in resistance to PX. The combination of the three mutations displayed an additive sensitivity to PX. This suggest that others factors are involved in the stability of lipid A and the enzymes exhibit other mechanisms to resist to PX (108). Another study has been demonstrated that small, positively-charged polyamines which bathe urogenital mucosal surfaces and involved in key cellular functions, impair *Ng* interaction with antimicrobials. It was known that polyamines bind to bacterial surfaces contributing, in a reversible manner, to increase gonococcal resistance to NHS, CAMP such PXB and was dose-dependent (109). Further investigation about the capsule role showed that the meningococcal capsule bears a protective effect for bacteria in the intracellular environment through enhancing the resistance to PX. Thus, the unencapsulated meningococci was more sensitive to PX than the encapsulated bacteria (110). This finding prompted to investigate if the capsular polysaccharide of *Neisseria* mediates resistance to PX such *K. pneumoniae* (111). Noteworthy, the expression of capsular genes (SiaD, cps) and MtrC-MtrD-MtrE involved in CAMP resistance was up-regulated during the intracellular phase of

bacterial infection (110). Recently, stable PB and PE heteroresistance was emerged in a unique meningococcal clade that causes urethritis US_NmUC (112). It was shown, using direct mutagenesis and whole genome sequencing analysis, that the heteroresistance is linked to mutations in pilM and pilQ of the *pilMNOPQ* operon which encodes for pilin biogenesis. It should be noted, PilM a cytoplasmic ATP-binding protein, exhibited a polar effect on the expression of pilQ in its mutant. PilQ, the major component of the outer membrane, has been expected to block the entry of antibiotics in pilQ mutant. Both, pilM and pilQ mutants conferred also competence deficiency. The heteroresistance phenotype requires the intrinsic components of PX resistance: the Mtr efflux pump and the LptA transferase and show a cross-resistance to several antibiotics (112).

Conclusion

Intrinsic resistance is independent of the selective pressure, imposed by the clinical use of antibiotics. It reduces the pool of antibiotics that can treat human infections and afterwards the therapeutic options for infections caused by MDR pathogens. Intrinsic resistant elements can be transferred between bacterial communities. So, the intrinsic resistance in non-pathogenic bacteria can be transferred to a pathogenic bacterium which restrict the treatment options for infections induced by these bacteria. Targeting such components of the resistome may reduce the potential for human toxicity and offers a more tailored approach to antibiotic chemotherapy and adjuvant development. Therefore, the intrinsic resistome of bacteria become a new therapeutic target which give crucial knowledge into bacterial physiology considering clinical threat by Gram-negative pathogens.

DRAFT REVIEW

References

1. Antibiotic resistance [Internet]. [cited 2022 Nov 14]. Available from: https://www.who.int/news-room/fact-sheets/detail/antibiotic-resistance

2. Huemer M, Mairpady Shambat S, Brugger SD, Zinkernagel AS. Antibiotic resistance and persistence-Implications for human health and treatment perspectives. EMBO Rep. 2020 Dec 3;21(12):e51034.

3. 114679-REVISED-v2-Drug-Resistant-Infections-Final-Report.pdf [Internet]. [cited 2020 Jul 28]. Available from: https://openknowledge.worldbank.org/bitstream/handle/10986/26707/114679-REVISED-v2-Drug-Resistant-Infections-Final-Report.pdf?sequence=1&isAllowed=y

4. Ogunlana L, Shaw L, Kaur D, Jangir P, Walsh T, Uphoff S, et al. Regulatory fine-tuning and horizontal gene transfer stabilize mobile colistin resistance [Internet]. bioRxiv; 2022 [cited 2022 Nov 14]. p. 2022.11.04.515217. Available from: https://www.biorxiv.org/content/10.1101/2022.11.04.515217v1

5. Martinez JL, Baquero F. Mutation frequencies and antibiotic resistance. Antimicrob Agents Chemother. 2000 Jul;44(7):1771–7.

6. Bhullar K, Waglechner N, Pawlowski A, Koteva K, Banks ED, Johnston MD, et al. Antibiotic Resistance Is Prevalent in an Isolated Cave Microbiome. Aziz RK, editor. PLoS ONE. 2012 Apr 11;7(4):e34953.

7. Van Goethem MW, Pierneef R, Bezuidt OKI, Van De Peer Y, Cowan DA, Makhalanyane TP. A reservoir of 'historical' antibiotic resistance genes in remote pristine Antarctic soils. Microbiome [Internet]. 2018 Feb 23 [cited 2020 Jul 30];6. Available from: https://www.ncbi.nlm.nih.gov/pmc/articles/PMC5824556/

8. Brown MG, Balkwill DL. Antibiotic Resistance in Bacteria Isolated from the Deep Terrestrial Subsurface. Microb Ecol. 2009 Apr;57(3):484–93.

9. De Souza MJ, Nair S, Loka Bharathi PA, Chandramohan D. Metal and antibiotic-resistance in psychrotrophic bacteria from Antarctic Marine waters. Ecotoxicology. 2006 May;15(4):379–84.

10. Colistin: An Update on the Antibiotic of the 21st Century [Internet]. Medscape. [cited 2020 Apr 26]. Available from: http://www.medscape.com/viewarticle/772588

11. Hayakawa K, Marchaim D, Divine GW, Pogue JM, Kumar S, Lephart P, et al. Growing prevalence of Providencia stuartii associated with the increased usage of colistin at a tertiary health care center. Int J Infect Dis IJID Off Publ Int Soc Infect Dis. 2012 Sep;16(9):e646-648.

12. Falagas ME, Kasiakou SK. Toxicity of polymyxins: a systematic review of the evidence from old and recent studies. Crit Care. 2006;10(1):R27.

DRAFT REVIEW

13. Li J, Nation RL, Turnidge JD, Milne RW, Coulthard K, Rayner CR, et al. Colistin: the re-emerging antibiotic for multidrug-resistant Gram-negative bacterial infections. Lancet Infect Dis. 2006 Sep;6(9):589–601.

14. Kwa A, Kasiakou SK, Tam VH, Falagas ME. Polymyxin B: similarities to and differences from colistin (polymyxin E). Expert Rev Anti Infect Ther. 2007 Oct;5(5):811–21.

15. Baron S, Hadjadj L, Rolain JM, Olaitan AO. Molecular mechanisms of polymyxin resistance: knowns and unknowns. Int J Antimicrob Agents. 2016 Dec;48(6):583–91.

16. Lee H, Hsu FF, Turk J, Groisman EA. The PmrA-Regulated pmrC Gene Mediates Phosphoethanolamine Modification of Lipid A and Polymyxin Resistance in Salmonella enterica. J Bacteriol. 2004 Jul;186(13):4124–33.

17. Pelletier MR, Casella LG, Jones JW, Adams MD, Zurawski DV, Hazlett KRO, et al. Unique structural modifications are present in the lipopolysaccharide from colistin-resistant strains of Acinetobacter baumannii. Antimicrob Agents Chemother. 2013 Oct;57(10):4831–40.

18. Quiroga C, Nastro M, Di Conza J. Current scenario of plasmid-mediated colistin resistance in Latin America. Rev Argent Microbiol. 2019 Mar;51(1):93–100.

19. Nikaido H. Molecular Basis of Bacterial Outer Membrane Permeability Revisited. Microbiol Mol Biol Rev. 2003 Dec 1;67(4):593–656.

20. Insertion Sequence ISAba11 Is Involved in Colistin Resistance and Loss of Lipopolysaccharide in Acinetobacter baumannii [Internet]. [cited 2020 May 1]. Available from: https://www.ncbi.nlm.nih.gov/pmc/articles/PMC3101452/

21. Yu Z, Qin W, Lin J, Fang S, Qiu J. Antibacterial Mechanisms of Polymyxin and Bacterial Resistance. BioMed Res Int. 2015;2015:1–11.

22. Bader MW, Sanowar S, Daley ME, Schneider AR, Cho U, Xu W, et al. Recognition of Antimicrobial Peptides by a Bacterial Sensor Kinase. Cell. 2005 Aug 12;122(3):461–72.

23. Johnson L, Horsman SR, Charron-Mazenod L, Turnbull AL, Mulcahy H, Surette MG, et al. Extracellular DNA-induced antimicrobial peptide resistance in Salmonella enterica serovar Typhimurium. BMC Microbiol. 2013 May 24;13:115.

24. Dow M, Newman MA, Roepenack E von. The Induction and Modulation of Plant Defense Responses by Bacterial Lipopolysaccharides [Internet]. https://doi.org/10.1146/annurev.phyto.38.1.241. 2003 [cited 2020 Apr 30]. Available from: https://www.annualreviews.org/doi/abs/10.1146/annurev.phyto.38.1.241

25. Olaitan AO, Morand S, Rolain JM. Mechanisms of polymyxin resistance: acquired and intrinsic resistance in bacteria. Front Microbiol [Internet]. 2014 [cited 2020 May 1];5. Available from: https://www.ncbi.nlm.nih.gov/pmc/articles/PMC4244539/

DRAFT REVIEW

26. Kato A, Chen HD, Latifi T, Groisman EA. Reciprocal control between a bacterium's regulatory system and the modification status of its lipopolysaccharide. Mol Cell. 2012 Sep 28;47(6):897–908.

27. Lesho E, Yoon EJ, McGann P, Snesrud E, Kwak Y, Milillo M, et al. Emergence of colistin-resistance in extremely drug-resistant Acinetobacter baumannii containing a novel pmrCAB operon during colistin therapy of wound infections. J Infect Dis. 2013 Oct 1;208(7):1142–51.

28. Lee H, Hsu FF, Turk J, Groisman E. The PmrA-Regulated pmrC Gene Mediates Phosphoethanolamine Modification of Lipid A and Polymyxin Resistance in Salmonella enterica. J Bacteriol. 2004 Aug 1;186:4124–33.

29. Trimble MJ, Mlynárčik P, Kolář M, Hancock REW. Polymyxin: Alternative Mechanisms of Action and Resistance. Cold Spring Harb Perspect Med. 2016 Oct;6(10):a025288.

30. Johnson MD, Nation RL, Li J. Mechanism of the Antibacterial Activity and Resistance of Polymyxins. In: Mayers DL, Sobel JD, Ouellette M, Kaye KS, Marchaim D, editors. Antimicrobial Drug Resistance: Mechanisms of Drug Resistance, Volume 1 [Internet]. Cham: Springer International Publishing; 2017 [cited 2020 May 1]. p. 333–44. Available from: https://doi.org/10.1007/978-3-319-46718-4_23

31. Baron S, Hadjadj L, Rolain JM, Olaitan AO. Molecular mechanisms of polymyxin resistance: knowns and unknowns. Int J Antimicrob Agents. 2016 Dec;48(6):583–91.

32. Baul SN, De R, Mandal PK, Roy S, Dolai TK, Chakrabarti P. Outbreak of Burkholderia Cepacia Infection: a Systematic Study in a Hematolooncology Unit of a Tertiary Care Hospital from Eastern India. Mediterr J Hematol Infect Dis [Internet]. 2018 Sep 1 [cited 2020 May 7];10(1). Available from: https://www.ncbi.nlm.nih.gov/pmc/articles/PMC6131102/

33. Vinion-Dubiel AD, Goldberg JB. Lipopolysaccharide of Burkholderia cepacia complex. J Endotoxin Res. 2003;9(4):201–13.

34. Isshiki Y, Kawahara K, Zähringer U. Isolation and characterisation of disodium (4-amino-4-deoxy-β-l-arabinopyranosyl)-(1→8)-(d-glycero-α-d-talo-oct-2-ulopyranosylonate)-(2→4)-(methyl 3-deoxy-d-manno-oct-2-ulopyranosid)onate from the lipopolysaccharide of Burkholderia cepacia. Carbohydr Res. 1998 Nov 1;313(1):21–7.

35. Ortega XP, Cardona ST, Brown AR, Loutet SA, Flannagan RS, Campopiano DJ, et al. A Putative Gene Cluster for Aminoarabinose Biosynthesis Is Essential for Burkholderia cenocepacia Viability. J Bacteriol. 2007 May;189(9):3639–44.

36. Hamad MA, Lorenzo FD, Molinaro A, Valvano MA. Aminoarabinose is essential for lipopolysaccharide export and intrinsic antimicrobial peptide resistance in Burkholderia cenocepacia†. Mol Microbiol. 2012 Sep 1;85(5):962–74.

37. Malott RJ, Steen-Kinnaird BR, Lee TD, Speert DP. Identification of Hopanoid Biosynthesis Genes Involved in Polymyxin Resistance in Burkholderia multivorans. Antimicrob Agents Chemother. 2012 Jan;56(1):464–71.

DRAFT REVIEW

38. Burtnick MN, Woods DE. Isolation of polymyxin B-susceptible mutants of Burkholderia pseudomallei and molecular characterization of genetic loci involved in polymyxin B resistance. Antimicrob Agents Chemother. 1999 Nov;43(11):2648–56.

39. Loutet SA, Mussen LE, Flannagan RS, Valvano MA. A two-tier model of polymyxin B resistance in Burkholderia cenocepacia. Environ Microbiol Rep. 2011 Apr;3(2):278–85.

40. Ortega X, Silipo A, Saldías MS, Bates CC, Molinaro A, Valvano MA. Biosynthesis and structure of the Burkholderia cenocepacia K56-2 lipopolysaccharide core oligosaccharide: truncation of the core oligosaccharide leads to increased binding and sensitivity to polymyxin B. J Biol Chem. 2009 Aug 7;284(32):21738–51.

41. Cloning and characterization of the Burkholderia vietnamiensis norM gene encoding a multi-drug efflux protein | FEMS Microbiology Letters | Oxford Academic [Internet]. [cited 2020 Jun 21]. Available from: https://academic.oup.com/femsle/article/215/2/279/491715

42. Kumar M, Gupta A, Sahoo RK, Jena J, Debata NK, Subudhi E. Functional Genome Screening to Elucidate the Colistin Resistance Mechanism. Sci Rep [Internet]. 2016 [cited 2020 May 6];6. Available from: https://www.ncbi.nlm.nih.gov/pmc/articles/PMC4796810/

43. Laupland KB, Parkins MD, Ross T, Pitout JDD. Population-based laboratory surveillance for tribe Proteeae isolates in a large Canadian health region. Clin Microbiol Infect. 2007 Jul 1;13(7):683–8.

44. Gautam V, Gupta V, Joshi RM, Sawhney G, Duhan S. Morganella morganii-Associated Arthritis in a Diabetic Patient. J Clin Microbiol. 2003 Jul;41(7):3451.

45. Basu S, Radziejewska-Lebrecht J, Mayer H. Lipopolysaccharide of Providencia rettgeri. Arch Microbiol. 1986 Apr 1;144(3):213–8.

46. Drzewiecka D. Significance and Roles of Proteus spp. Bacteria in Natural Environments. Microb Ecol. 2016;72(4):741–58.

47. Chemical structure of the lipid A component of the lipopolysaccharide from a Proteus mirabilis Re-mutant - SIDORCZYK - 1983 - European Journal of Biochemistry - Wiley Online Library [Internet]. [cited 2020 May 9]. Available from: https://febs.onlinelibrary.wiley.com/doi/full/10.1111/j.1432-1033.1983.tb07789.x

48. Aquilini E, Merino S, Knirel YA, Regué M, Tomás JM. Functional Identification of Proteus mirabilis eptC Gene Encoding a Core Lipopolysaccharide Phosphoethanolamine Transferase. Int J Mol Sci. 2014 Apr 21;15(4):6689–702.

49. Wang WB, Chen IC, Jiang SS, Chen HR, Hsu CY, Hsueh PR, et al. Role of RppA in the Regulation of Polymyxin B Susceptibility, Swarming, and Virulence Factor Expression in Proteus mirabilis. Infect Immun. 2008 May;76(5):2051.

50. Jiang SS, Lin TY, Wang WB, Liu MC, Hsueh PR, Liaw SJ. Characterization of UDP-Glucose Dehydrogenase and UDP-Glucose Pyrophosphorylase Mutants of Proteus mirabilis:

DRAFT REVIEW

Defectiveness in Polymyxin B Resistance, Swarming, and Virulence. Antimicrob Agents Chemother. 2010 May;54(5):2000–9.

51. Jiang SS, Liu MC, Teng LJ, Wang WB, Hsueh PR, Liaw SJ. Proteus mirabilis pmrI, an RppA-Regulated Gene Necessary for Polymyxin B Resistance, Biofilm Formation, and Urothelial Cell Invasion. Antimicrob Agents Chemother. 2010 Apr;54(4):1564–71.

52. McCoy AJ, Liu H, Falla TJ, Gunn JS. Identification of Proteus mirabilis Mutants with Increased Sensitivity to Antimicrobial Peptides. Antimicrob Agents Chemother. 2001 Jul;45(7):2030–7.

53. Baron S, Leulmi Z, Villard C, Olaitan AO, Telke AA, Rolain JM. Inactivation of the arn operon and loss of aminoarabinose on lipopolysaccharide as the cause of susceptibility to colistin in an atypical clinical isolate of proteus vulgaris. Int J Antimicrob Agents. 2018 Mar;51(3):450–7.

54. Olaitan AO, Diene SM, Gupta SK, Adler A, Assous MV, Rolain JM. Genome analysis of NDM-1 producing *Morganella morganii* clinical isolate. Expert Rev Anti Infect Ther. 2014 Oct;12(10):1297–305.

55. Iguchi A, Nagaya Y, Pradel E, Ooka T, Ogura Y, Katsura K, et al. Genome evolution and plasticity of Serratia marcescens, an important multidrug-resistant nosocomial pathogen. Genome Biol Evol. 2014 Aug;6(8):2096–110.

56. Serratia marcescens arn, a PhoP-Regulated Locus Necessary for Polymyxin B Resistance [Internet]. [cited 2020 May 27]. Available from: https://www.ncbi.nlm.nih.gov/pmc/articles/PMC4135846/

57. Winfield MD, Latifi T, Groisman EA. Transcriptional regulation of the 4-amino-4-deoxy-L-arabinose biosynthetic genes in Yersinia pestis. J Biol Chem. 2005 Apr 15;280(15):14765–72.

58. Cloeckaert A, Tibor A, Zygmunt MS. Brucella Outer Membrane Lipoproteins Share Antigenic Determinants with Bacteria of the Family Rhizobiaceae. Clin Diagn Lab Immunol. 1999 Jul;6(4):627–9.

59. Martínez de Tejada G, Pizarro-Cerdá J, Moreno E, Moriyón I. The outer membranes of Brucella spp. are resistant to bactericidal cationic peptides. Infect Immun. 1995 Aug;63(8):3054–61.

60. Gil-Ramírez Y, Conde-Álvarez R, Palacios-Chaves L, Zúñiga-Ripa A, Grilló MJ, Arce-Gorvel V, et al. The identification of wadB, a new glycosyltransferase gene, confirms the branched structure and the role in virulence of the lipopolysaccharide core of Brucella abortus. Microb Pathog. 2014 Aug;73:53–9.

61. Conde-Álvarez R, Arce-Gorvel V, Iriarte M, Manček-Keber M, Barquero-Calvo E, Palacios-Chaves L, et al. The Lipopolysaccharide Core of Brucella abortus Acts as a Shield Against Innate Immunity Recognition. Tsolis RM, editor. PLoS Pathog. 2012 May 10;8(5):e1002675.

62. Manterola L, Moriyón I, Moreno E, Sola-Landa A, Weiss DS, Koch MHJ, et al. The Lipopolysaccharide of Brucella abortus BvrS/BvrR Mutants Contains Lipid A Modifications and Has Higher Affinity for Bactericidal Cationic Peptides. J Bacteriol. 2005 Aug;187(16):5631–9.

DRAFT REVIEW

63. Ferguson GP, Datta A, Baumgartner J, Roop RM, Carlson RW, Walker GC. Similarity to peroxisomal-membrane protein family reveals that Sinorhizobium and Brucella BacA affect lipid-A fatty acids. Proc Natl Acad Sci U S A. 2004 Apr 6;101(14):5012–7.

64. Martín-Martín AI, Sancho P, de Miguel MJ, Fernández-Lago L, Vizcaíno N. Quorum-Sensing and BvrR/BvrS Regulation, the Type IV Secretion System, Cyclic Glucans, and BacA in the Virulence of Brucella ovis: Similarities to and Differences from Smooth Brucellae. Infect Immun. 2012 May;80(5):1783–93.

65. Liautard J, Ouahrani-Bettache S, Jubier-Maurin V, Lafont V, Köhler S, Liautard JP. Identification and Isolation of Brucella suis Virulence Genes Involved in Resistance to the Human Innate Immune System. Infect Immun. 2007 Nov;75(11):5167–74.

66. Kerrinnes T, Young BM, Leon C, Roux CM, Tran L, Atluri VL, et al. Phospholipase A1 Modulates the Cell Envelope Phospholipid Content of Brucella melitensis, Contributing to Polymyxin Resistance and Pathogenicity. Antimicrob Agents Chemother. 2015 Nov;59(11):6717–24.

67. The ABC transporter YejABEF is required for resistance to antimicrobial peptides and the virulence of Brucella melitensis [Internet]. [cited 2020 May 13]. Available from: https://www.ncbi.nlm.nih.gov/pmc/articles/PMC4994006/

68. Conde-Álvarez R, Palacios-Chaves L, Gil-Ramírez Y, Salvador-Bescós M, Bárcena-Varela M, Aragón-Aranda B, et al. Identification of lptA, lpxE, and lpxO, Three Genes Involved in the Remodeling of Brucella Cell Envelope. Front Microbiol [Internet]. 2018 Jan 10 [cited 2020 May 12];8. Available from: https://www.ncbi.nlm.nih.gov/pmc/articles/PMC5767591/

69. Casabuono AC, Czibener C, Del Giudice MG, Valguarnera E, Ugalde JE, Couto AS. New Features in the Lipid A Structure of Brucella suis and Brucella abortus Lipopolysaccharide. J Am Soc Mass Spectrom. 2017 Dec;28(12):2716–23.

70. Bialer MG, Ruiz-Ranwez V, Sycz G, Estein SM, Russo DM, Altabe S, et al. MapB, the Brucella suis TamB homologue, is involved in cell envelope biogenesis, cell division and virulence. Sci Rep [Internet]. 2019 [cited 2020 Jun 28];9. Available from: https://www.ncbi.nlm.nih.gov/pmc/articles/PMC6377625/

71. Non-O1 and non-O139 Infections | Sources of Infection & Risk Factors | Cholera | CDC [Internet]. 2018 [cited 2020 May 20]. Available from: https://www.cdc.gov/cholera/non-01-0139-infections.html

72. Matson JS, Yoo HJ, Hakansson K, DiRita VJ. Polymyxin B Resistance in El Tor Vibrio cholerae Requires Lipid Acylation Catalyzed by MsbB. J Bacteriol. 2010 Apr 15;192(8):2044–52.

73. Henderson JC, Fage CD, Cannon JR, Brodbelt JS, Keatinge-Clay AT, Trent MS. Antimicrobial Peptide Resistance of Vibrio cholerae Results from an LPS Modification Pathway Related to Nonribosomal Peptide Synthetases. ACS Chem Biol. 2014 Oct 17;9(10):2382.

74. Henderson JC, Herrera CM, Trent MS. AlmG, responsible for polymyxin resistance in pandemic Vibrio cholerae, is a glycyltransferase distantly related to lipid A late acyltransferases. J Biol Chem. 2017 Dec 22;292(51):21205–15.

DRAFT REVIEW

75. Hankins JV, Madsen JA, Giles DK, Childers BM, Klose KE, Brodbelt JS, et al. Elucidation of a novel Vibrio cholerae lipid A secondary hydroxy-acyltransferase and its role in innate immune recognition. Mol Microbiol. 2011 Sep;81(5):1313–29.

76. Raetz CRH, Guan Z, Ingram BO, Six DA, Song F, Wang X, et al. Discovery of new biosynthetic pathways: the lipid A story. J Lipid Res. 2009 Apr;50(Suppl):S103–8.

77. Chimalakonda G, Ruiz N, Chng SS, Garner RA, Kahne D, Silhavy TJ. Lipoprotein LptE is required for the assembly of LptD by the β-barrel assembly machine in the outer membrane of Escherichia coli. Proc Natl Acad Sci U S A. 2011 Feb 8;108(6):2492–7.

78. Herrera CM, Crofts AA, Henderson JC, Pingali SC, Davies BW, Trent MS. The Vibrio cholerae VprA-VprB Two-Component System Controls Virulence through Endotoxin Modification. mBio [Internet]. 2014 Dec 23 [cited 2020 May 20];5(6). Available from: https://www.ncbi.nlm.nih.gov/pmc/articles/PMC4278540/

79. Samanta P, Mandal RS, Saha RN, Shaw S, Ghosh P, Dutta S, et al. A Point Mutation in *carR* Is Involved in the Emergence of Polymyxin B-Sensitive *Vibrio cholerae* O1 El Tor Biotype by Influencing Gene Transcription. Raffatellu M, editor. Infect Immun. 2020 Feb 24;88(5):e00080-20, /iai/88/5/IAI.00080-20.atom.

80. Bilecen K, Fong JCN, Cheng A, Jones CJ, Zamorano-Sánchez D, Yildiz FH. Polymyxin B Resistance and Biofilm Formation in Vibrio cholerae Are Controlled by the Response Regulator CarR. Infect Immun. 2015 Mar;83(3):1199–209.

81. Herrera CM, Henderson JC, Crofts AA, Trent MS. Novel Coordination of Lipopolysaccharide Modifications in Vibrio cholerae promotes CAMP resistance. Mol Microbiol. 2017 Nov;106(4):582–96.

82. Nesper J, Lauriano CM, Klose KE, Kapfhammer D, Kraiß A, Reidl J. Characterization of Vibrio cholerae O1 El Tor galU and galE Mutants: Influence on Lipopolysaccharide Structure, Colonization, and Biofilm Formation. Infect Immun. 2001 Jan;69(1):435–45.

83. Bina XR, Provenzano D, Nguyen N, Bina JE. Vibrio cholerae RND Family Efflux Systems Are Required for Antimicrobial Resistance, Optimal Virulence Factor Production, and Colonization of the Infant Mouse Small Intestine. Infect Immun. 2008 Aug;76(8):3595–605.

84. Sgouros SN, Bergele C. Clinical outcome of patients with Helicobacter pylori infection: the bug, the host, or the environment? Postgrad Med J. 2006 May;82(967):338–42.

85. Raetz CRH, Whitfield C. Lipopolysaccharide Endotoxins. Annu Rev Biochem. 2002;71:635–700.

86. LIPID A MODIFICATION SYSTEMS IN GRAM-NEGATIVE BACTERIA [Internet]. [cited 2020 Jun 3]. Available from: https://www.ncbi.nlm.nih.gov/pmc/articles/PMC2569861/

87. Li H, Liao T, Debowski AW, Tang H, Nilsson HO, Stubbs KA, et al. Lipopolysaccharide Structure and Biosynthesis in *Helicobacter pylori*. Helicobacter. 2016 Dec;21(6):445–61.

DRAFT REVIEW

88. Helicobacter pylori versus the Host: Remodeling of the Bacterial Outer Membrane Is Required for Survival in the Gastric Mucosa [Internet]. [cited 2020 Jun 2]. Available from: https://www.ncbi.nlm.nih.gov/pmc/articles/PMC3245313/

89. Stead CM, Zhao J, Raetz CRH, Trent MS. Removal of the outer Kdo from Helicobacter pylori lipopolysaccharide and its impact on the bacterial surface. Mol Microbiol. 2010 Nov;78(4):837–52.

90. Cholesterol Enhances Helicobacter pylori Resistance to Antibiotics and LL-37 [Internet]. [cited 2020 Jun 4]. Available from: https://www.ncbi.nlm.nih.gov/pmc/articles/PMC3101455/

91. The redefinition of Helicobacter pylori lipopolysaccharide O-antigen and core-oligosaccharide domains [Internet]. [cited 2020 Jun 5]. Available from: https://journals.plos.org/plospathogens/article?id=10.1371/journal.ppat.1006280

92. Mackinnon FG, Cox AD, Plested JS, Tang CM, Makepeace K, Coull PA, et al. Identification of a gene (lpt-3) required for the addition of phosphoethanolamine to the lipopolysaccharide inner core of Neisseria meningitidis and its role in mediating susceptibility to bactericidal killing and opsonophagocytosis. Mol Microbiol. 2002 Feb;43(4):931–43.

93. Wright JC, Hood DW, Randle GA, Makepeace K, Cox AD, Li J, et al. lpt6, a Gene Required for Addition of Phosphoethanolamine to Inner-Core Lipopolysaccharide of Neisseria meningitidis and Haemophilus influenzae. J Bacteriol. 2004 Oct;186(20):6970–82.

94. Cox AD, Wright JC, Li J, Hood DW, Moxon ER, Richards JC. Phosphorylation of the Lipid A Region of Meningococcal Lipopolysaccharide: Identification of a Family of Transferases That Add Phosphoethanolamine to Lipopolysaccharide. J Bacteriol. 2003 Jun;185(11):3270–7.

95. Lewis LA, Choudhury B, Balthazar JT, Martin LE, Ram S, Rice PA, et al. Phosphoethanolamine Substitution of Lipid A and Resistance of Neisseria gonorrhoeae to Cationic Antimicrobial Peptides and Complement-Mediated Killing by Normal Human Serum. Infect Immun. 2009 Mar;77(3):1112.

96. Takahashi H, Carlson RW, Muszynski A, Choudhury B, Kim KS, Stephens DS, et al. Modification of Lipooligosaccharide with Phosphoethanolamine by LptA in Neisseria meningitidis Enhances Meningococcal Adhesion to Human Endothelial and Epithelial Cells. Infect Immun. 2008 Dec;76(12):5777.

97. Phosphoethanolamine Decoration of Neisseria gonorrhoeae Lipid A Plays a Dual Immunostimulatory and Protective Role during Experimental Genital Tract Infection [Internet]. [cited 2020 Jun 18]. Available from: https://www.ncbi.nlm.nih.gov/pmc/articles/PMC4019182/#B14

98. Handing JW, Criss AK. The Lipooligosaccharide Modifying Enzyme LptA Enhances Gonococcal Defense Against Human Neutrophils. Cell Microbiol. 2015 Jun;17(6):910–21.

99. Zughaier SM, Kandler JL, Balthazar JT, Shafer WM. Phosphoethanolamine Modification of Neisseria gonorrhoeae Lipid A Reduces Autophagy Flux in Macrophages. PLoS ONE [Internet].

DRAFT REVIEW

2015 Dec 7 [cited 2020 Jun 18];10(12). Available from: https://www.ncbi.nlm.nih.gov/pmc/articles/PMC4671640/

100. Hobbs MM, Anderson JE, Balthazar JT, Kandler JL, Carlson RW, Ganguly J, et al. Lipid A's structure mediates Neisseria gonorrhoeae fitness during experimental infection of mice and men. mBio. 2013 Nov 19;4(6):e00892-00813.

101. John CM, Liu M, Phillips NJ, Yang Z, Funk CR, Zimmerman LI, et al. Lack of Lipid A Pyrophosphorylation and Functional lptA Reduces Inflammation by Neisseria Commensals. Infect Immun. 2012 Nov;80(11):4014–26.

102. Phase-Variable Expression of lptA Modulates the Resistance of Neisseria gonorrhoeae to Cationic Antimicrobial Peptides [Internet]. [cited 2020 Jun 19]. Available from: https://www.ncbi.nlm.nih.gov/pmc/articles/PMC4068544/

103. Tzeng YL, Ambrose KD, Zughaier S, Zhou X, Miller YK, Shafer WM, et al. Cationic Antimicrobial Peptide Resistance in Neisseria meningitidis. J Bacteriol. 2005 Aug;187(15):5387–96.

104. Hagman KE, Pan W, Spratt BG, Balthazar JT, Judd RC, Shafer WM. Resistance of Neisseria gonorrhoeae to antimicrobial hydrophobic agents is modulated by the mtrRCDE efflux system. Microbiol Read Engl. 1995 Mar;141 (Pt 3):611–22.

105. Jerse AE, Sharma ND, Simms AN, Crow ET, Snyder LA, Shafer WM. A Gonococcal Efflux Pump System Enhances Bacterial Survival in a Female Mouse Model of Genital Tract Infection. Infect Immun. 2003 Oct;71(10):5576–82.

106. Ochsner UA, Vasil AI, Johnson Z, Vasil ML. Pseudomonas aeruginosa fur overlaps with a gene encoding a novel outer membrane lipoprotein, OmlA. J Bacteriol. 1999 Feb;181(4):1099–109.

107. Kandler JL, Holley CL, Reimche JL, Dhulipala V, Balthazar JT, Muszyński A, et al. The MisR Response Regulator Is Necessary for Intrinsic Cationic Antimicrobial Peptide and Aminoglycoside Resistance in Neisseria gonorrhoeae. Antimicrob Agents Chemother. 2016 Jul 22;60(8):4690–700.

108. Piek S, Wang Z, Ganguly J, Lakey AM, Bartley SN, Mowlaboccus S, et al. The Role of Oxidoreductases in Determining the Function of the Neisserial Lipid A Phosphoethanolamine Transferase Required for Resistance to Polymyxin. PLoS ONE [Internet]. 2014 Sep 12 [cited 2020 Jun 15];9(9). Available from: https://www.ncbi.nlm.nih.gov/pmc/articles/PMC4162559/

109. Goytia M, Shafer WM. Polyamines Can Increase Resistance of Neisseria gonorrhoeae to Mediators of the Innate Human Host Defense. Infect Immun. 2010 Jul;78(7):3187–95.

110. Spinosa MR, Progida C, Talà A, Cogli L, Alifano P, Bucci C. The Neisseria meningitidis Capsule Is Important for Intracellular Survival in Human Cells. Infect Immun. 2007 Jul;75(7):3594–603.

111. Campos MA, Vargas MA, Regueiro V, Llompart CM, Albertí S, Bengoechea JA. Capsule Polysaccharide Mediates Bacterial Resistance to Antimicrobial Peptides. Infect Immun. 2004 Dec;72(12):7107.

DRAFT REVIEW

112. Tzeng YL, Berman Z, Toh E, Bazan JA, Turner AN, Retchless AC, et al. Heteroresistance to the model antimicrobial peptide polymyxin B in the emerging Neisseria meningitidis lineage 11.2 urethritis clade: mutations in the pilMNOPQ operon. Mol Microbiol. 2019 Jan;111(1):254.

DRAFT REVIEW

Figure.1 Regulation of the LPS outer membrane OM giving rise to the intrinsic polymyxin resistance. **(a).** VprAB, the two component system activates the expression of the tripartite system AlmEGF responsible for LPS glycylation in *Vibrio cholerae.* LpxN generate a modified lipid A hexa-acylated that will be translocated to the OM by lpt proteins.

(b). RppAB, the two component system regulates the addition of L-Ara4N to *Proteus mirabilis* lipid A. The two genes *Ugd* (UDP glucose dehydrogenase) and GalU (UDP glucose pyrophosphorylase) and arnBCADTEF operon were activated. ArnT transports the modified lipidA to the inner membrane IM which then can be translocated also to the OM by Lpt proteins.

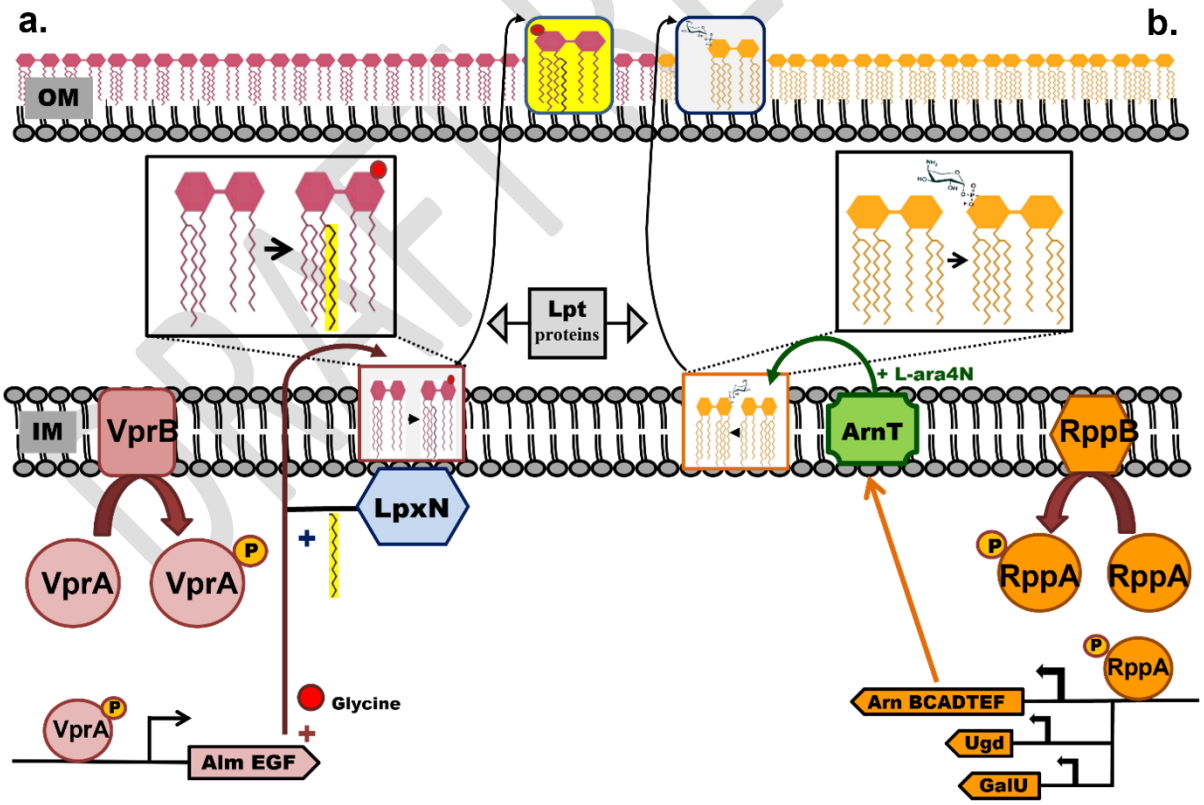

DRAFT PREVIEW

Figure.2 Regulation of LPS modification conferring intrinsic PX resistance in *Helicobacter pylori*.

LpxE removes 1-phosphate group from the lipid A backbone. EptA adds directly a phosphoethanolamine PE group on the lipid A. kdo hydrolase cleaves the terminal kdo sugar. LpxF a second phosphatase which dephosphorylate the 4'-P of lipid A. LpxR catalyse the lipid A diacylation giving rise to a tetra-acylated lipid A.

: 4'-Phosphate : 1'-Phosphate

: deux kdo sugar (3-deoxy-d-manno-oct-2-ulosonic acid)

IM: Inner membrane OM: Outer membrane

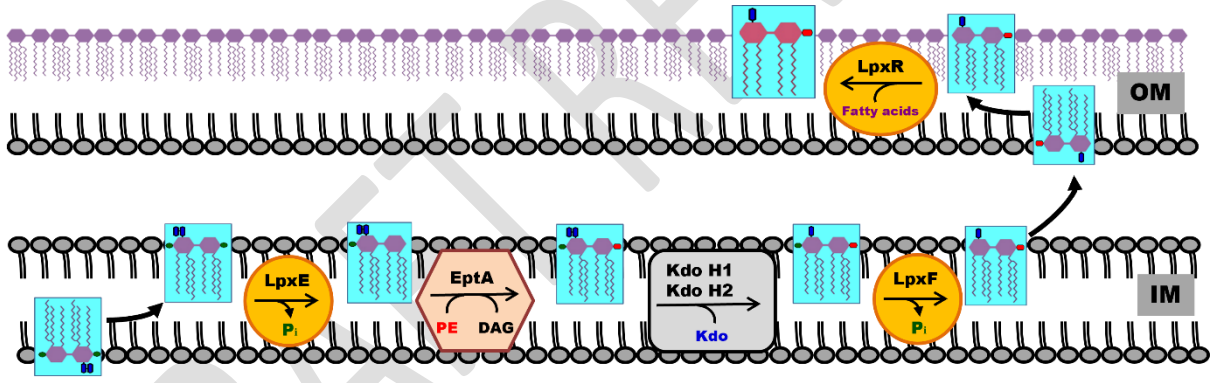

DRAFT REVIEW

Figure.3 High level of LPS modification conferring intrinsic resistance to PX in *Neisseria meningitidis* et *Neisseria gonorrhoeae*.

The LptA enzyme can catalyze the esterification of the lipid A head groups (1' and 4' groups) by the addition of phoshoethanolamine PETN. The hexa-acylated lipid A was then transported to the OM via lpt proteins.

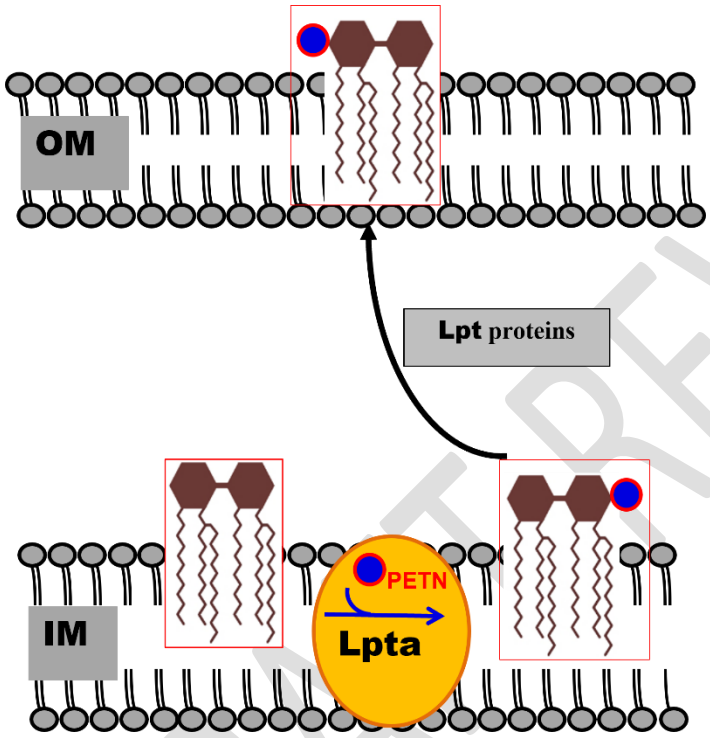

DRAFT REVIEW

871 **Table.1** Intrinsic resistant genes found in the discussed bacterial pathogenes

DRAFT REVIEW

Intrinsic polymyxin resistance mechanisms		Involved determinants	Bacteria	Ref.
Surface remodelling	**L-Ara4N**	Ugd, GalU, PpmrI, arnT, arnD	*Proteus mirabilis*	
		O-acetyl transferase, ATPase , SapD	*Proteus mirabilis*	
		arnT, arnB, arnC, arnA1, arnA2, Ugd (BCAL2945)	*Burkholderia cenopacia*	
		Ugd, arnA, arnB, arnC	*Serratia marescens*	
	P-Etn	EptC (PMI3104)	*Proteus mirabilis*	
		EptB	*Morganella morganii*	
		EptA (Vc1102)/EptA (Hp0022)	*Vibrio cholerae/helicobacter pylori*	
			Neisseria meningitidis/Brucella	
	Pyrophosphorylethanolamine		*Brucella ovis, Brucella abortus*	
	Capsule formation	SiaD, cps	*Neisseria meningitidis*	
	Membrane composition and integrity modifications	PilMNOPQ, PorB	*Neisseria meningitidis*	
		BveA (BMEII0681) , VirB2	*Brucella melitensis*	
		Omp31 (BR1622)	*Brucella suis*	
		MapB	*Brucella ovis*	
		Bmul2133 (hpnj), Bmul2134 (hpnI)	*Burkholderia multivorans*	
		Isph: LytB (BCAL2710), BCAM2738	*Burkholderia pseudomallei*	
		gspI, gspE, gspF, OmpU	*Vibrio cholerae*	
	Two-component systems (TCS)	BvrR/BvrS	*Brucella abortus*	
		MgrR/MgrS	*Burkholderia pseudomallei*	
		MisR/MisS	*Neisseria gonorrhoeae*	
		VprA/VprB or CarR/CarS	*Vibrio cholerae*	
		PhoP/PhoQ	*Serratia marescens*	
		qseB/qseC, rssA/rssB	*Morganella morgani*	
		RppA/RppB	*Proteus mirabilis*	
	LPS /LOS alteration	LpxE, LpxF, Hp0579/Hp0580, WaaL, HP1284	*Helicobacter pylori*	
		LpxL1/2	*Neisseria meningitidis*	
		AlmE, AlmF, AlmG, LpxN=msbB (Vc0212)	*Vibrio cholerae*	

DRAFT REVIEW

		bacA, WadC, WadB	*Brucella abortus*	
		PagP and pmrH homologues	*Proteus mirabilis*	
		pgm	*Brucella suis*	
Efflux and transport	**Efflux**	NorM	*Burkholderia vietnamiensis*	
		VexB	*Vibrio cholerae*	
		MtrCDE	*Neisseria meningitidis*	
		yejABEF	*Brucella melitensis*	
	Transport	MsbA	*Vibrio cholerae*	
		LptG	*Burkholderia*	
Others		MucD, ZmpA, ZmpB, BCAL2831	*Burkholderia cenopacia*	
		cgt	*Helicobacter pylori*	
		ATP synthase	*Proteus mirabilis*	
		DsbA1/DsbA2/DsbA3, GshB, fbp	*Neisseria meningitidis*	
		GalU	*Vibrio cholerae*	
		RpoE	*Vibrio cholerae* *Burkholderia cenopacia*	

872

DRAFT REVIEW

Article 6

Carbonyl cyanide m-chlorophenyl hydrazone (CCCP) restores the colistin sensitivity in *Brucella intermedia*

Malak Zoaiter, Zaher Zeaiter, Michel Drancourt, Cheikh Sokhna, Oleg Mediannikov, Pierre-Edouard Fournier

-Submitted in International Journal of Molecular Sciences-

Carbonyl cyanide m-chlorophenyl hydrazone (CCCP) restores the colistin sensitivity in *Brucella intermedia*

Malak Zoaiter[1,2], Zaher Zeaiter[3] , Oleg Mediannikov[1,4], Michel Drancourt[1,4], Cheikh Sokhna[1,3,5], Pierre-Edouard Fournier[1,2]*

[1] IHU-Méditerranée-Infection, Marseille, France

[2] Aix-Marseille Univ, IRD, AP-HM, SSA, VITROME, Marseille, France

[3]Aix-Marseille Univ, IRD, AP-HM, MEPHI, Marseille, France

[4] Lebanese Univ-section-I, Faculty of sciences, Beirut, Liban

[5] Campus Commun UCAD-IRD of Hann, Dakar, Senegal

***Corresponding author:** Pierre-Edouard Fournier

Aix-Marseille Université, Institut Hospitalo-Universitaire Méditerranée Infection,

19-21 Boulevard Jean Moulin 13385 Marseille cedex 05, France.

Phone: +33(0)413732401. Fax: +33(0)413732402

E-mail: pierre-edouard.fournier@univ-amu.fr

Abstract

Brucella intermedia (formerly *Ochrobactrum intermedium*), a non-fermentative bacterium, has been isolated from animals and human clinical specimens. It is naturally resistant to polymyxins, including colistin (CO), and may cause opportunistic infections in humans. We isolated six *Brucella intermedia* strains from senegalese monkey stool. In order to determine whether an efflux pump mechanism was involved in CO resistance in *B. intermedia*, we evaluated the effects of verapamil (VRP), reserpine (RSP), phe-arg β-naphtylamide dihydrochloride (PAβN) and Carbonyl cyanide m-chlorophenyl hydrazone (CCCP), four efflux pump inhibitors, on these colistin-resistant strains. Using the broth microdilution method, the CO and CCCP combination of 2 µg/ml and10 µg/ml, respectively, significantly reduced the CO minimal inhibitory concentration (MIC) of *B. intermedia* supporting an efflux pump mechanism. In contrast VRP, PAβN, and RSP did not restore CO susceptibility. Time kill assay showed a bactericidal effect of the CO-CCCP combination. Genomic analysis revealed a potential implication in the CO resistance mechanism for some conserved efflux pumps such as YejABEF, NorM, EmrAB, as previously reported in other bacteria. An inhibitory effect of the CO-CCCP combination was observed on the biofilm formation using the crystal violet method. These results suggest that the intrinsic CO resistance in *Brucella intermedia* is linked to an efflux pump mechanism and that CO-CCCP, synergistic effect may open a field to identify new treatments to restore antibiotic efficacy in humans.

Introduction

Colistin (CO) was isolated in 1947 from the Gram-positive bacterium *Bacillus polymyxa* (1). Since 2005, it has been recognized as being bactericidal against Gram-negative aerobic bacteria and several *Mycobacterium* species (2). As a consequence, CO has become a key antibiotic, alone or in combination with other antimicrobial agents (3), to treat multidrug resistant (MDR), especially carbapenemase-producing, bacteria (3). CO binds to the negatively charged lipopolysaccharides (LPS) of Gram-negative bacteria (GNB), and penetrates the outer membrane by a "self-promoted uptake" mechanism. This leads to destabilize the inner membrane integrity, eventually causing cell death (4). Resistance to CO may be explained by several mechanisms: i) The most common is the modification of LPS, the main target of CO. LPS is able to reduce the negative charge of the bacterial surface, thus the electrostatic interactions with CO (5). Such an alteration targets the chromosomally-encoded genes associated with LPS modification, by activating mutational (6) or non-mutational (adaptive) effects in response to environmental signals such as the presence of CO or other inducers (7); ii) CO-degrading enzymes have been identified in CO-producing *Bacillus polymyxa* for self-protection (8) and recently in *Bacillus lichenformis* (9), but it has never been linked to CO resistance in other micro-organisms (10); iii) Since 2015, plasmid-borne mobilized CO resistance (mcr) genes have been reported, initially in China (11). Mcr genes play a role in bacterial outer membrane remodeling and CO-resistance. Such plasmids are easily transmitted and increase the spread of CO resistance; iv) Other strategies include capsule polysaccharide shielding as in Klebsiella pneumoniae (12) and the efflux pump system related to proton motive force (13).

Brucella intermedia (formerly *Ochrobactrum intermedium*) is a non-fermentative bacterium that is widely distributed in soil, plants, water, animals, and polluted or industrial environments (14).

Its presence in the hospital environment and its multi-resistance to antibiotics led to its increasingly frequent isolation in human infections, in particular in immunocompromised patients (15) and cystic fibrosis (16). It is associated with a variety of infections including bacteremia (17), pelvic abscess (18), dyspepsia (19), endocarditis (20), and pneumonia (16). *Brucella intermedia* is naturally resistant to polymyxins, including CO (21). The resistance mechanism in *B. intermedia* is thus probably mediated by the cell envelope (22). The export of antimicrobial agents through the activity of efflux pumps plays an important role in both intrinsic and acquired resistance in MDR bacteria. Recently, several studies have demonstrated that the resistance to CO was reversed by the Carbonyl cyanide 3-chlorophenylhydrazone (CCCP) in *Enterobacteriaceae* (23-15), *Acinetobacter baumannii*, (23) and *Stenotrophomonas maltophilia* (25). CCCP is a strong uncoupler that disrupts proton motive force by affecting the electrochemical transmembrane gradients and reducing the ATP production. Its use was restricted to testing experimentally the active efflux or the biofilm formation (25-26) in resistant bacteria. However, the mechanism of CO-CCCP synergy is still unknown. To date, one report showed a direct antibacterial activity of CCCP against *Mycobacterium abscessus* (28).

In this article, we investigated the role of efflux pumps in the intrinsic mechanism of CO resistance in *B. intermedia*, isolated from a healthy chimpanzee stool, by using CCCP, verapamil (VRP) , reserpine (RSP) and phe-arg β-naphtylamide dihydrochloride (PAβN) as several efflux pump inhibitors (EPI).

Materials and methods

Bacterial isolation and culture conditions

Six *Brucella* strains were isolated from stool chimpanzee collected on the ground on June 6th , 2016, in the Dindefelo Community Nature Reserve (12°22'01.4"N12°18'00.0"W) in south-

eastern Senegal Stools were externally decontaminated with 70% ethanol prior to culture.Then they were enriched in Tryptone Soy Broth (TSB, bioMérieux, France) at 37°C for 72 hours. Ten microliters of culture were inoculated on CO TSB agar. A 4 µg/ml CO concentration was chosen based on the European Committee on Antimicrobial Susceptibility Testing EUCAST guidelines. The plates were then incubated for 24 hours at 37˚C. Individual colonies were replicated on 5% sheep blood-enriched Columbia agar (COS, bioMérieux), and then identified by the Matrix assisted laser desorption/ionization time-of-light mass spectrometry (Maldi-Tof MS).The study of strains was permitted by the Senegalese Nagoya autority under reference 001042.The strains were deposited in the CSUR collection as following: Q1103, Q1105, Q1107, Q1108, Q1109, and Q1111.

Genome sequencing, annotation and phylogenetic analyses

Genomic DNA (gDNA) of *Brucella* strains was extracted using the EZ1 biorobot with the DNA Tissue kit, as recommended by the manufacturer (Qiagen, Hilden, Germany). gDNA was quantified by a Qubit assay with the high sensitive dsDNA kit (Invitrogen**,** Carlsbad**,** US). Sequencing was performed with the Miseq technology and the mate-pair strategy (Illumina Inc, San Diego, CA, USA), as previously described (29). Genomes were assembled using Spades version 3.14.0 and were annotated by PROKKA version 1.14.5. Pangenomic analysis was performed using Roary software version 3.10.5 and was visualized on the available phandango website phandango (jameshadfield.github.io) (30) (31). 16S rRNA sequences were extracted from the genomes using contEst16S EZbiocloud ContEst16S | Ezbiocloud.net. Two *Brucella intermedia* genomes were downloaded from NCBI (NCTC12171 and LMG3301) to be compared to those of chimpanzee strains. Their accession numbers were UGSH00000000.1 and ACQA00000000.1, respectively. *recA* gene sequences, also extracted from genome sequences,

were used to confirm the affiliation of the strains. The sequences were aligned by Clustal W (32). Evolutionary analyses were inferred using the Maximum Likelihood method based on the Tamura-Nei model, and were conducted in MEGA Version 7.0.26 (33).

Brucella strains were deposited in Genbank database under the following accession numbers: Q1103: JAOXXK000000000 Q1105: JAOXXJ00000000 Q1107: JAOXXI000000000 Q1108: JAOXXH000000000 Q1109: JAOXXG000000000 Q111: JAOXXF000000000

Chemicals and stock solution

CO sulphate salt (CO) was purchased from MP-Biomedicals (Illkirch-Graffenstaden, France). All efflux pump inhibitors, CCCP, verapamil (VRP) , reserpine (RSP) and phe-arg β-naphtylamide dihydrochlorid (PAβN) were purchased from Sigma Aldrich (Lyon, France). CCCP and RSP were dissolved in DMSO at 5mg/ml. VRP was dissolved in ethanol 99% at 5mg/ml. PAβN was diluted to 5 mg/ml in deionized Water. All stock solutions were preserved at -20˚C. The final concentration of PaβN, RSP and VRP was 50 µg/ml.

Minimal inhibitory concentrations (MICs) determination

Currently, broth microdilution method is the recommended technique to determine the susceptibility to CO (34). Susceptibility testing was performed according to the EUCAST guidelines using the Cation-adjusted Mueller Hinton broth CAMHB (BD-ThermoFisher, Bourgoin-Jallieu**,** France). MICs were evaluated in the presence of CO alone and with the four efflux pump inhibitors. CO was diluted to final concentrations ranging from 0.25 to 256 µg/ml. Efflux pump inhibitor concentrations ranged from 2.5 to 100 µg/ml. To test the effect of efflux pump inhibitors on CO MIC of the tested strains, a sub-MIC of 10 µg/ml for CCCP and 50

µg/ml for each of VRP, RSP and PAβN were combined with the various CO concentrations mentioned above (24) (35).

A mcr-mediated CO-resistant *E.coli* strain, used as positive control, became susceptible when adding 10 µg/ml CCCP as previously described (24).

For each tested strain, the inoculum was prepared by resuspending three to five colonies in 0.85% NaCL medium to obtain the standard turbidity 0.5 MacFarland. Then, 5.10^5 CFU/ml was added in each well of a 96-well plate containing tested antibiotic dilutions. Plates were incubated at 37°C and MIC results were visualized after 16h-18h by adding iodonitrotetrazolium (Sigma-Aldrich S.A.R.L, Lyon, France). MIC testing for each strain was carried out in duplicate in three independent experiments.

MIC fold change and synergy index

The MIC fold change after CO-CCCP combination was defined by the ratio of the CCCP-free CO to that of CCCP-added CO. The mean fold change was calculated following the equation:

$$[1/n\ ] \times \Sigma[\text{MIC fold change} \times \text{frequency of fold change}]$$

The influence of an efflux pump on the CO MIC for a bacterial strain was defined as an MIC reduction of at least 8-fold in the presence of CCCP (24). The effect of CO looked reversed when a strain became susceptible with a MIC $\leq$2 µg/ml , according to the EUCAST (24). The interaction between the two molecules was determined by calculating the fractional inhibitory concentration index (FICI). The fractional inhibitory concentration FIC was derived from the lowest concentration of CO and CCCP combination permitting no visible growth of *Brucella intermedia* in the wells. The FIC value for each agent was calculated according to the formula:

$$\text{FIC CO} = (\text{MIC of combination}/\text{MIC of CO})$$

FIC CCCP = (MIC of combination/MIC of CCCP)

To calculate the FIC index, the following formulas were used : FICI =FIC (CO) + FIC (CCCP). The combination was classified as synergistic if the FIC indices were lower than or equal to 0.5, additive if the FIC indices were greater than 0.5 and lower than or equal to 1, indifferent if FIC were greater than 1 and lower than or equal to 2 , and antagonistic if FIC were greater than 2 (28) - (29).

Effect of CCCP on CO-MIC on agar plates

The effect of CCCP on CO-MIC was assessed on CAMH agar plates. CCCP was added at a final concentration of 10 µg/ml . Commercial diffusion 50 µg CO disks were deposited on the plates (bioMérieux). Plates without CCCP were prepared with DMSO 0.2%. Agar plates were incubated under aerobic conditions at 37 ˚C for 18h to 24h. The density of the inoculum was standardized at 0.5 MacFarland. All experiments were performed in triplicate.

Crystal blue assay

Brucella intermedia culture was performed using the same method of MIC microdilution, in a 96-well polystyrene microtiter plate. Biofilm formation was assessed under static growth in Mueller Hinton. After 48h of incubation, the supernatant was removed. Wells were washed with phosphate-buffered saline (PBS) three times to remove the planktonic bacteria. The plate was well dried. Adherent biofilms were stained with 125 µL of 0.1% crystal violet in water .The microtiter plate was incubated for 10 -15 min at room temperature. The dye was removed and three washes were performed with water to eliminate all excess cells and dye. The plate was turned upside-down and air-dried for a few hours. Dye that bound to adherent cells was re-solubilized with 125 µl of 30% acetic acid in water for 10-15 min. Absorbance was measured at

550 nm in a plate reader using 30% acetic acid in water blank. Tests were repeated in three separate times to confirm reproducibility.

Growth curves

Plates were prepared as described above.

Bacterial growth was measured by optical density (OD 600) using a Gen-5 microplate reader (Agilent-Biotek, Les ULIS, France). CO concentration ranged from 256 to 0.5µg/ml. CCCP was fixed at 10µg/ml. PaβN, RSP and VRP were used at 50 µg/ml. Strains Q1103 and Q1105 were grown in Muller Hinton at 37˚C with shaking continuously for 24H to 48H. CO and efflux pump inhibitors were added at the beginning of the experiment.

Time-kill assay

To explore the effect of CCCP alone and in combination with CO, time-kill assays were performed. Two strains were chosen according to their phenotypic characteristics (Q1103 was more viscous than Q1105). 5.10^5 CFU/ml were inoculated in MHCA broth and were incubated for 24H and 48H with shaking. Time-kill analysis was done by adding a combination of 10µg/ml CCCP and 2 µg/ml CO.

Statistical analysis

Data represented the means ± standards deviations for three independent experiments and replicated twice. Data were analyzed using the GraphPad Prism version 8 software. Significant differences among the various treatment conditions were evaluated using the one way Analysis Of Variance (ANOVA) and multiple comparisons were done by the non-parametric student's t-test. Differences were considered to be significant at $P<0.05$.

Results

Bacterial isolation and identification

Six *B. intermedia* strains (Q1103-Q1105-Q1107-Q1108-Q1109-Q1111) and one *Brucella tritici* strain (Q1106) were cultivated from the stool sample and identified by Maldi-Tof MS. 16S rRNA and *recA* genes confirmed the affiliation of the five strains to *B. intermedia*. 16S rRNA sequences showed a similarity of > 98.8 % with those of *B. intermedia* strains available in NCBI. *recA* gene sequences exhibited >98.5 % similarity with *B. intermedia*. Phylogenetic trees based on the 16S rRNA and *Rec*A genes confirmed that all isolated *B. intermedia* were clustered together (**Fig.1).**

CO, CCCP and CO/CCCP MIC determination

Using the broth microdilution, all six *B. intermedia* isolates showed a CO-MICs >512 µg/ml , confirming their intrinsic resistance **(Fig.2a).** VRP, RSP and PaβN did not cause any decrease in CO-MIC of *B. intermedia with* the tested concentration. Therefore, only results for CCCP were discussed**.** For the protonophore CCCP, we observed distinct MICs even within the same strain. This led us to think that the population may be heterogeneous with regard to CCCP's response. A successful isolation of colonies for each strain that respond to different concentrations of CCCP (5, 7, 8, 9, 10, 15 µg/ml) confirmed our hypothesis. As a result, we divided each strain into two populations: the first including colonies that were able to survive at 10 µg/ml CCCP and the second those exhibit a CCCP-MIC<10 µg/ml. This CCCP concentration has been chosen according to the literature. In our study, we focused on the colonies with higher CCCP-MIC (>10µg/ml). Strains Q1103 and Q1107 had CCCP-MICs < 30 µg/ml, and strains Q1105, Q1108, Q1109 and Q1111 had MICs < 20 µg/ml. We then assessed the effect of the efflux pump on the antibacterial susceptibility profile to CO, by evaluating the CO-MIC in the presence of CCCP.

The addition of the CCCP inhibitor reduced significatively the MIC of CO to < 2 µg/ml with a mean fold change of 426.66 µg/ml, which is a > 8 fold change, confirming the involvement of the efflux pump in the resistance mechanism **(Table.1)**. FICI of the combination was lower than 0.5, confirming the synergism of the two drugs with the chosen concentration of CCCP 10 µg/ml. **Table.1** summarizes the CO-MICs alone as well as with CCCP, the MIC fold change and the fractional inhibitory concentration. The effect of CCCP on the CO-MIC has also been assessed on agar plates. All plates showed that CCCP had an effect alone on *Brucella* growth. Likewise, the CCCP revived the activity of CO by the appearance of the circular inhibition zone. The diameters were measured at 21 to 23 mm for all strains except Q1103 that exhibited a 19 mm diameter **(Fig.2b).**The *E. coli* strain, used as positive control, was resistant to CO and had a known CO-MIC 4-8 µg/ml using broth microdilution. The strain become susceptible to CO with a MIC< µg/ml when µg/ml of CCCP was added. On agar plates, the diameter of the CO inhibition zone increased from 12mm to 15 mm on plates containing CCCP. CCCP alone had no effect on the used *E.coli* strain neither on broth or on agar.

Synergistic effect of CCCP-CO inhibits bacterial growth

To confirm the obtained MIC results and to choose the best CCCP-CO combination, we monitored the growth kinetics of the treated bacterial strains cultures in microtiter plate. Strains Q1105 and Q1103 control curves showed a prolific growth as the populations reached the maximum OD 1.5 after 24 hours **(Fig.3).** Increasing concentrations of CO did not affect the growth of strain Q1105 (P=0.999) **(Fig.3b)** but significantly affected that of the strain Q1103 (P=0.0388) **(Fig.3a).** Furthermore, the addition of CCCP at different concentrations resulted in variable levels of growth inhibition of both strains. The CCCP treatment showed a remarkable dose-dependent effects with an increase in lag phase duration and decrease of the maximum

specific growth rate (P<0.0001) **(Fig.4 c, e).** Complete growth inhibition was observed at the 20 µg/ml and 30 µg/ml on strains Q1105 and Q1103 respectively, confirming MIC results. Growth was suppressed from 2µg/ml of CO with CCCP for both Q1103 and Q1105 strains (P<0.0001) **(Fig.4 d, f).** Unlike CCCP, VRP, RSP and PAβN exhibit an incomplete inhibitory effects in combination with CO on the *B. intermedia* growth **(Fig.S2)**. These growth inhibition assays not only confirmed our MIC results, but also showed that the synergistic effect of CO/CCCP could be bactericidal too. Based on our findings, we decided to perform the time-kill assay with the combination of 2µg/ml CO and 10 µg/ml CCCP.

Bactericidal effect of CCCP-CO

Due to heterogeneous treatment responses to CCCP, time-kill curves were assessed for strains Q1105 and Q1103 which represent both populations (CCCP-MIC>10 µg/ml, CCCP-MIC <10 µg/ml, respectively). For population 1 exhibiting a CCCP-MIC>10 µg/ml, both Q1105 and Q1103 *Brucella* strains had lower growth rates than controls, when treated with CCCP alone **(Fig.5 a, c)**. However, after 24h, a weak bactericidal effect estimated at 19.2% for Q1103 and 29.2% for strain Q1105, was observed in the presence of the CO/CCCP combination. This effect increased much more in strain Q1105 after 48h (23.5% for strain Q1103 and 62.8% for strain Q1105). For population 2 (CCCP-MIC <10 µg/ml), a bactericidal effect was shown for CCCP alone in strains Q1103 and Q1105 (67.8% and 74.5%, respectively) after 24h, and (91% and 99%, respectively) after 48h **(Fig. 5 b, d)**. A complete bactericidal effect was obtained with the CO/CCCP combination after 24h in both strains

Co-treatment with CO/CCCP inhibits biofilm formation of *B. intermedia*

To explain the difference in bactericidal effect at 48h in population 1 between the two strains, we considered the phenotypic differences between them. Strain Q1103 was able to form a matrix on agar plates much more than strain Q1105 which can be considered a biofilm layer. Therefore, biofilm-formation assays were carried out using the crystal violet (CV) method. After 48 hours of incubation time, we found that strain Q1103 adhered to the culture plate much more than strain Q1105 ($P<0.0003$). Biofilm formation capability of both strains was not affected when treated with 10 µg/ml of CCCP or with increasing concentrations of CO (**Fig.6**). Furthermore, treatment of both strains cultures with various CO/CCCP combinations, yielded a dose-dependent decrease in their biofilm formation ability; where clear and significant decrease began at the CO/CCCP combination of 10 µg/ml-2 µg/ml ($P<0.0001$). The inhibitory effect between the CCCP-treated and the non-CCCP-treated groups was statistically significant for strains Q1103 and Q1105 ($P<0.0001$, $P<0.0014$, respectively).Taken together, our data suggest that *B. intermedia* biofilms may play a crucial role in CO resistance.

Pangenomic analysis

Based on our results, the addition of CCCP in combination with CO rescued the intrinsic resistance to CO in studied *B. intermedia* strains. Which led us to assume that efflux pumps may be involved in their resistance mechanism. Through genomic analysis, we decided to identify the common genes encoding for efflux pumps that can be involved in the CO resistance mechanism. The pangenome analysis showed that *B. intermedia* genomes contained 8276 gene clusters and 3546 of these composed the core genome in which, conserved putative efflux pumps were found **(Fig.7).** Some of these have been experimentally shown to be involved in the resistance to polymyxins, including CO, in other bacteria. Among the core genome cluster of *B. intermedia*,

we found ATP-Binding (ABC) transporter such as YejABEF, and LolCDE. These efflux were reported in *Brucella melitensis* and *Acinetobacter baumannii*, respectively (38) (39). NorM, which is a member of Multidrug And Toxic Efflux (MATE) family, was detected in the core genome. It contributed to the polymyxin B intrinsic resistance in *Burkholderia Vietnamiensis* (40). Furthermore, EmrE, a Small Multidrug Resistance (SMR) efflux pump, was conserved within the studied strains and showed more than 60% similarity with that of *Burkholderia stabilis* representing a multi-resistant transporter of cationic drug (www.uniprot.org). Another Emr pump, EmrAB that formed a tripartite complex with the outer membrane protein TolC was also found in *Brucella* strains. It belongs to the Major Facilitator Superfamily (MFS) and was reported in CO resistance mechanism in *Acinetobacter baumannii* (41). *Brucella* genomes contained, in addition, a conserved permease ATP-dependent MapB, a TamB ortholog that was demonstrated to play a role in CO resistance in *Brucella suis* (42). Other conserved multiresistant efflux pumps that may be involved in the resistance to CO mechanism include BepE, YbhRFS, Mdtk, Bmr3, EmrK, and OqxB28.

Discussion

In recent years, CO has been receiving much attention in response to an increasing prevalence of antibiotic resistance worldwide (43). In human medicine, CO has been used as last resource drug to treat MDR bacteria, especially carbapenem resistant ones. CO is inactive against intrinsically-resistant bacteria, including *Brucella* species which suggests a role of the cell wall in this mechanism (44). The conventional mechanisms of intrinsic resistance include the outer membrane impermeability to antibiotics and the activity of multidrug efflux pumps that prevent the access of the drugs to their targets (45). Several EPI have been evaluated to re-establish the CO activity such as VRP, RSP, PABN and CCCP. In our study, VRP, PAβN, and RSP failed to

restore the CO activity in *B. intermedia*, confirming previous studies on MDR-GNB (46). In contrast, a potential synergy between CCCP and CO was observed in reversing CO resistance in *B. intermedia,* as it was reported in *A. baumannii*, *Stenotrophomonas maltophilia* (25), and *Enterobacteriaceae* (44). CCCP reduced CO MIC more than 256 fold, suggesting that the mechanism inhibited by CCCP is essential for their CO resistance. CCCP, a potential nonspecific protonophore uncoupler, acts by dissipating the PMF, the most common source of energy in bacterial cells and subsequently inhibiting their efflux pump activity (47). Our findings, we strongly suggest an efflux pump inhibitory effect for CCCP. Time-kill curves showed that CCCP had a bactericidal effect alone and in combination with CO. Which can be explained that CCCP and CO may share common efflux pumps that are essential for the *Brucella* growth.

It should be noted, that CCCP alone, showed a heterogenous inhibitory effect in tested *Brucella* strains. Such an heterogeneity in CCCP response was reported recently in *E. coli* and explained by a heterogenous dissipation of PMF between cells (48). The heterogeneity in response to CCCP that was observed among cells of a given strain may be explained by the fact that the molecule targetsefflux pumps that acts on itself and exclude it from cells with high efflux pump activity. Therefore, these cells maintain their PMF and the efflux pump activity generating a positive feedback between CCCP and efflux pumps (48).

Based on the pangenome analysis, several efflux pumps such YejABEF , LolCDE , NorM, were identified in the *Brucella* core genome. Previous studies allowed their involvement in CO resistance in other organisms (41), (49). *Emr* (MFS), especially Emr A, a part of the tripartite EmrAB-TolC efflux pump, was demonstrated to confer resistance to CCCP in *E. coli* and to CO in *A. baumannii.* This may explain the common bactericidal effect of CCCP alone and combined with CO (50) (51). TamB provided resistance to CO in *Brucella suis*. It should be noted that the

Mex and Acr efflux pumps that contributed to CO resistance in *Pseudomonas aeruginosa* and *Acinetobacter baumannii* were detected in some *Brucella* strains, but as they were not located in the core genome, their involvement in CO resistance is unlikely (39),(52).

As CCCP blocked the PMF and ATP synthesis, it affects, in addition to the efflux pump activity, the cellular metabolism in all energy-requiring reactions (47). Subsequently, we detected several conserved enzymes that confer resistance to polymyxins such as those involved in the biosynthesis of lipopolysaccharides WadA, WadC (53), LpxM or MsbB (54) EptA (55), and in Carbohydrate pathways such pgm (56).

The biofilm formation can be a second factor for CO resistance mechanism. The inhibitory effect of CO-CCCP combination observed using the crystal violet method may either be explained by an inhibition of the efflux pumps involved in the biofilm formation or by the bactericidal effect induced by the CCCP-CO combination. To elucidate the potential effect of CCCP on biofilm formation and its relation to CO resistance, more experimental analyses including the biomass and the extracellular matrix of treated cells should be carried out.

In summary, we demonstrated for the first time that CO resistance in *B. intermedia* can be reversed by CCCP. The precise mechanism of this antibiotic efficiency restoration require further investigations especially the elucidation of the specific role of each efflux pump system identified by in the pangenome analysis. Additional work is also needed to clarify the effect of CCCP on biofilm formation in *B. intermedia.* Due to its intrinsic cytotoxicity, this molecule cannot be applied in the clinical field but may serve as a model to identify new agents that potentiate the activity of colistin in treating CO-resistant infections.

352 **Table.1** Antibiotic susceptibility of *B. intermedia* strains to CO with and without CCCP by the
353 microdilution method and FIC index interpretation.

354 CO: colistin; CCCP: Carbonyl cyanide m-chlorophenyl hydrazone; MIC: minimal inhibitory
355 concentration FIC index: Fractional inhibitory concentration index.

	Microdilution method					
	MIC (µg/ml)				**FIC index**	
Strains	**CO**	**CCCP**	**CO/CCCP**	**MIC fold change**	**Value**	**Interpretation**
E. coli	> 4-8	> 30	< 1	4—8	0.158-0.28	Synergism
Q1103	> 512	< 30	< 2- 4	128-256	0.070-0.074	Synergism
Q1105	> 512	< 20	< 1	512	0.051	Synergism
Q1107	> 512	< 20	< 2	256	0.053	Synergism
Q1108	> 512	< 15	< 0.5	512	0.068	Synergism
Q1109	> 512	< 20	< 1	512	0.051	Synergism
Q1111	> 512	< 15	< 1	512	0.068	Synergism

356

Fig.1 Phylogenetic trees showing the clustering of *B. intermedia* strains based on 16S rRNA **(a)** et RecA **(b)** genes using the Maximum Likelihood method. The scale bar represents a 1% sequence divergence. *Brevundimonas diminuta* NCTC 8545 was used as outgroup for the 16S rRNA gene. Species in bold letters indicate these for which genomes were downloaded from Genbank.

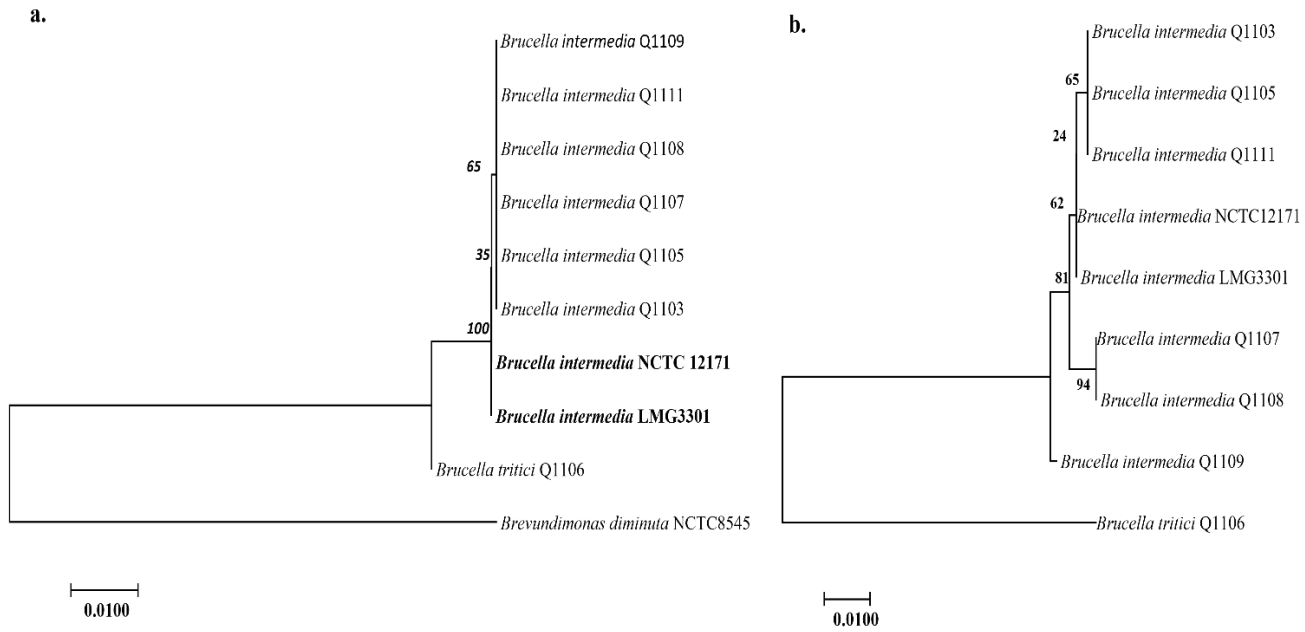

Fig.2 Observation of the effect of CCCP alone and in combination with CO using the liquid method **(a)** and the agar method **(b)** on tested *Brucella* strains. **(a)**: CO-MIC determination by the microdilution method with and without CCCP 10 µg/ml . **(b)**: left, CO inhibition diameter on CAMH plates containing 0.2% DMSO or CCCP 10 µg/ml ; right, growth of strains on CAMH + CCCP 10 µg/ml without CO. Ctrl: negative control. The 2 photographs were not to scale.

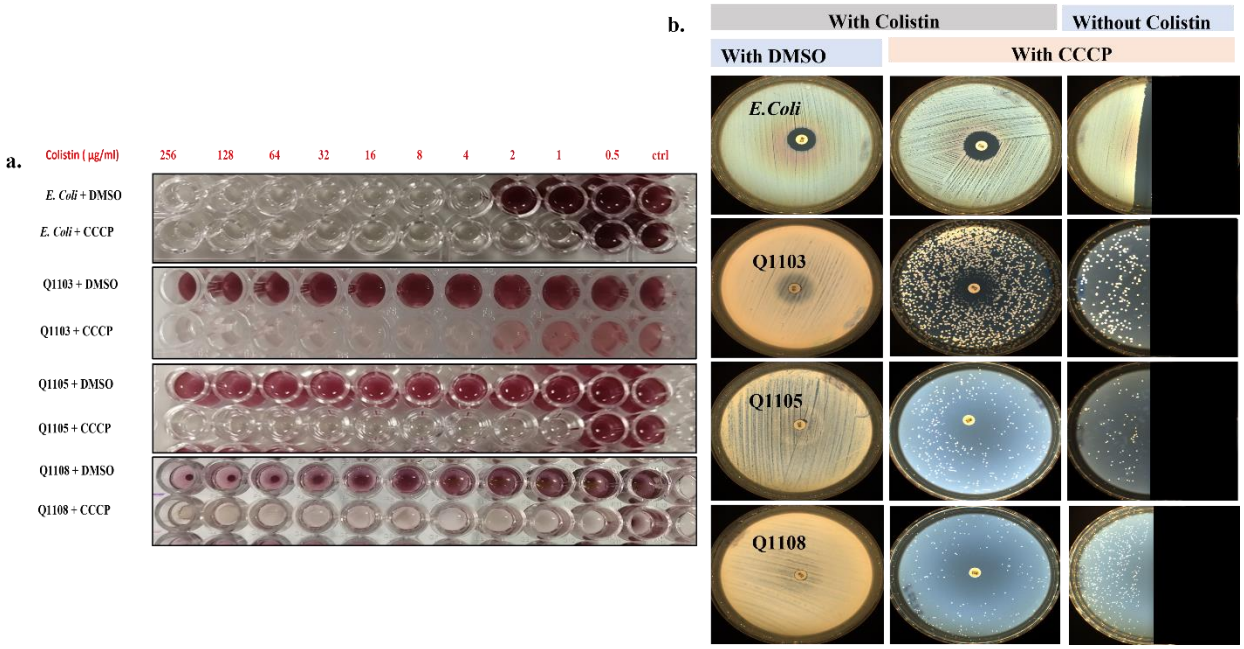

Fig.3 Growth of *B. intermedia* strains treated with different CO concentrations. Growth of strain Q1103 was affected by the increasing concentrations of CO (P<0.0388)*, unlike the strain Q1105 (P=0.999).

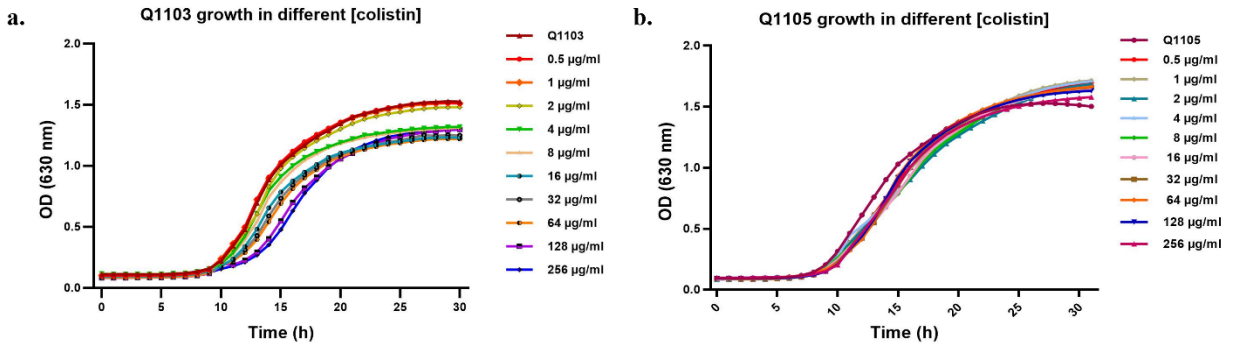

Fig.4 Growth curves of studied strains in different conditions. **(a)** Growth of *E.coli* in different CO concentrations, **(c)** and **(e)** growth of *Brucella* strains Q1103 and Q1105 in different CCCP concentrations **(b)**, **(d)** and **(f)** growth of the three strains in different CO concentrations with CCCP 10 µg/ml. Each graph represents the mean of three independent experiments. (P<0.0001)****

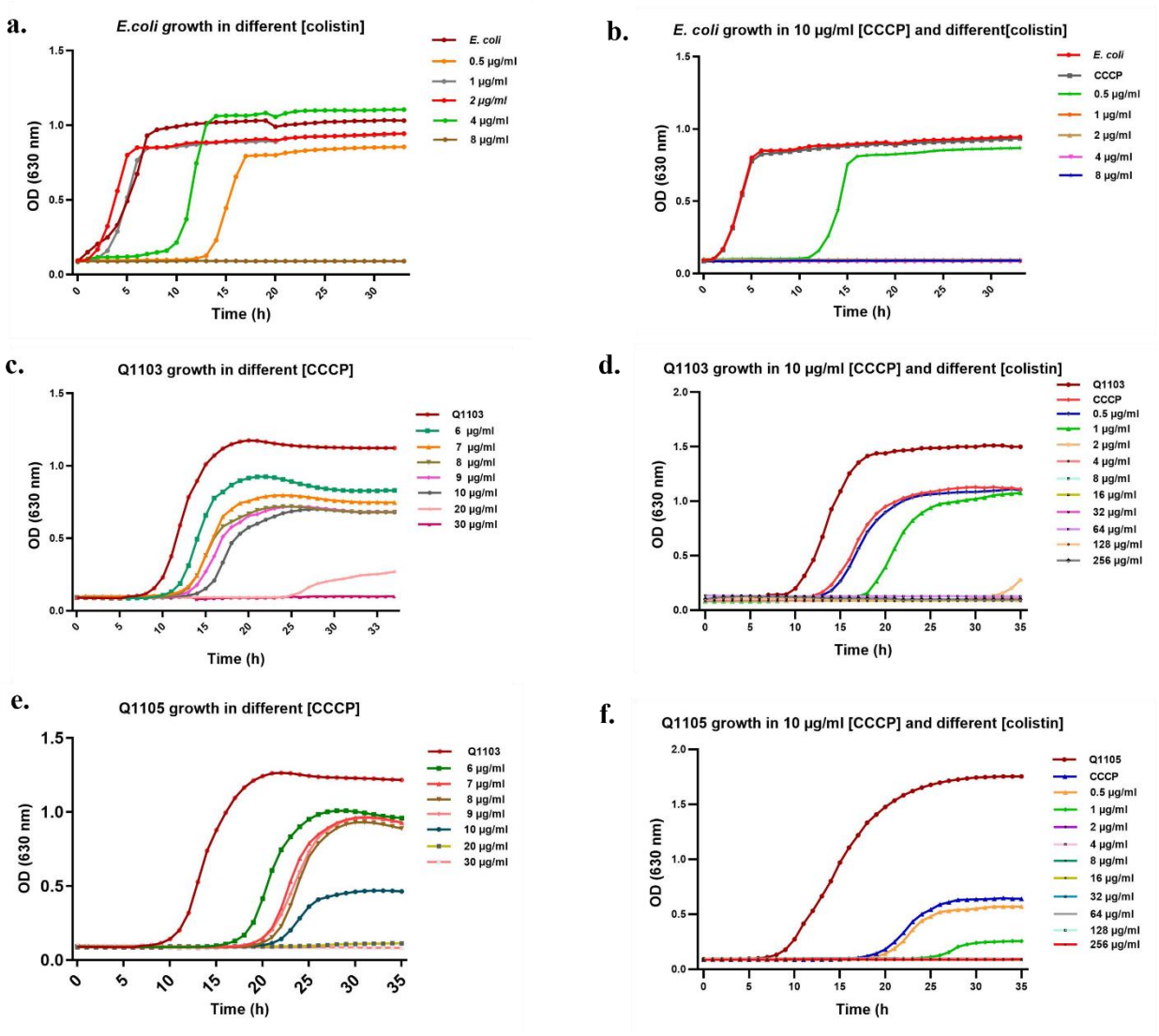

Fig.5 Time-kill curves of the combination of CO 2 µg/ml, and CCCP 10 µg/ml, of populations 1 and 2 of *B. intermedia* strains Q1103 and Q1105. **Population 1:** CCCP-MIC (alone) >10 µg/ml **Population 2:** CCCP-MIC (alone) < 10 µg/ml (P<0.05).

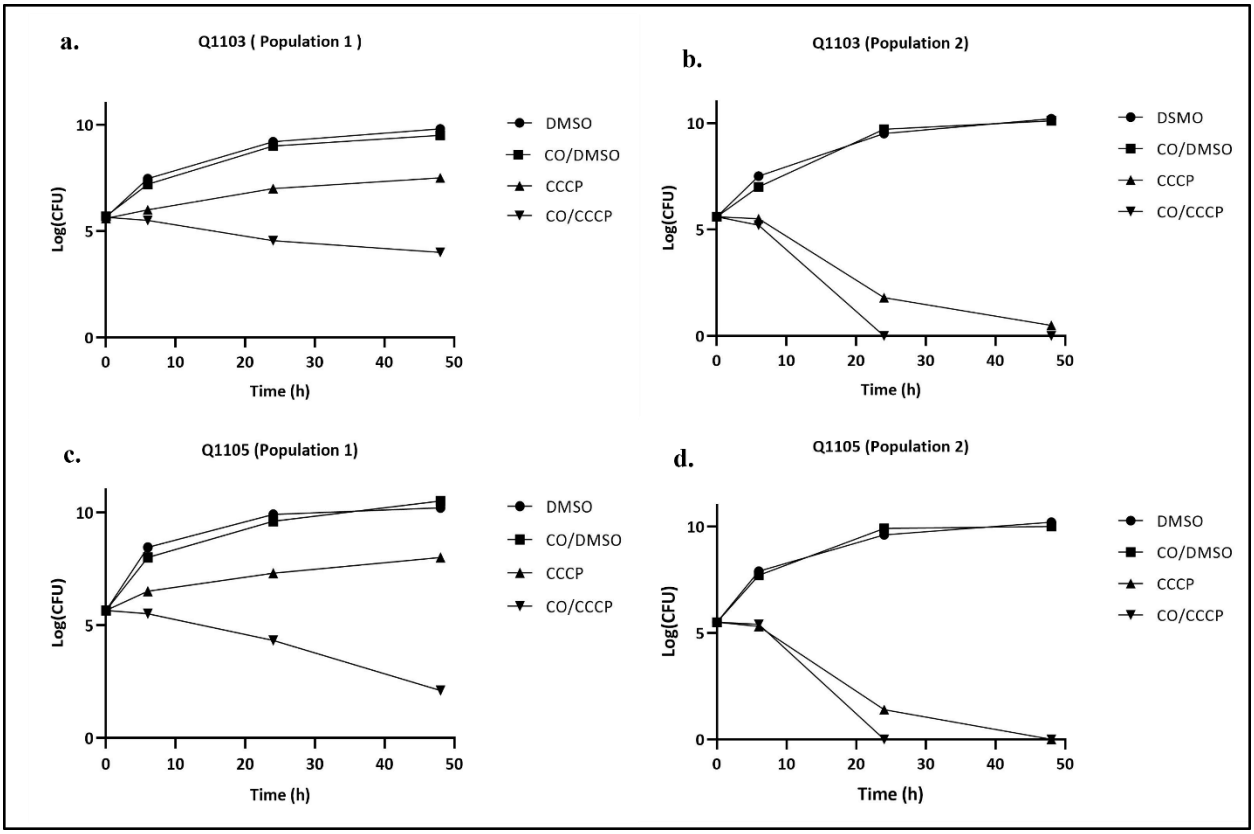

Fig.6 Effect of 10 µg/ml CCCP on biofilm formation in *B. intermedia* strains Q1103 and Q1105 after 48 hours with and without CO (***** and ******: P<0.05; **ns:** non-significant).

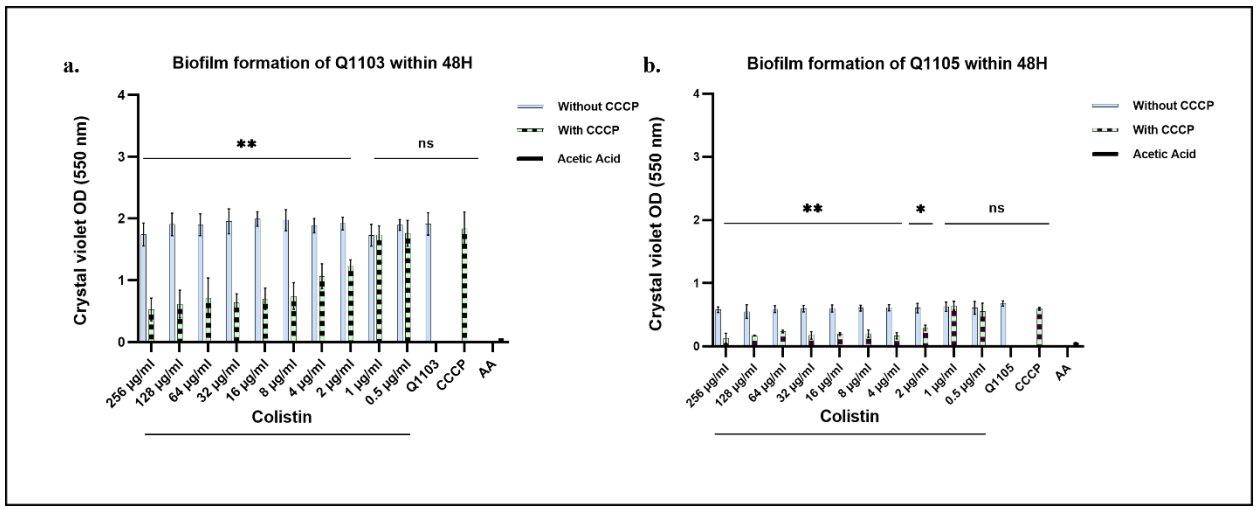

Fig.7 Pangenome analysis of the isolated *B. intermedia* strains carried out using the Roary software. Left: core-genome phylogeny, right: genes heatmap. The scale represents 20% nucleotide sequence divergence.

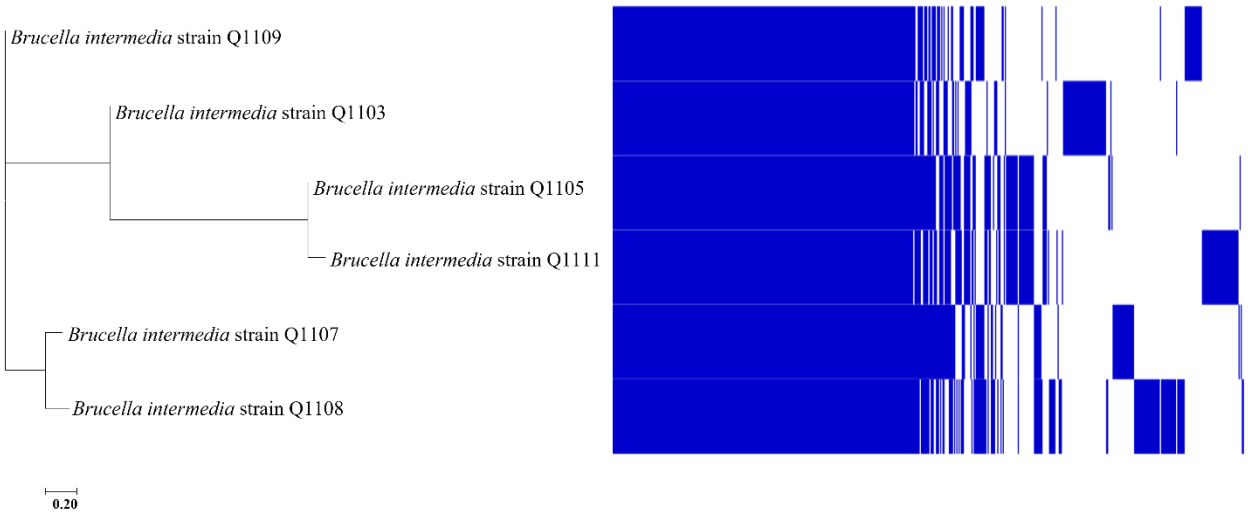

Figure.S1 Observation of the effect of CCCP alone and in combination with CO using the liquid method **(a)** and the agar method **(b)** on Q1107, Q1109 and Q1111 *Brucella* strains. **(a):** CO-MIC

394 determination by the microdilution method with and without CCCP 10 µg/ml . **(b):** left, CO
395 inhibition diameter on CAMH plates containing 0.2% DMSO or CCCP 10 µg/ml ; right, growth
396 of strains on CAMH + CCCP 10 µg/ml without CO. Ctrl: negative control. The 2 photographs
397 were not to scale.

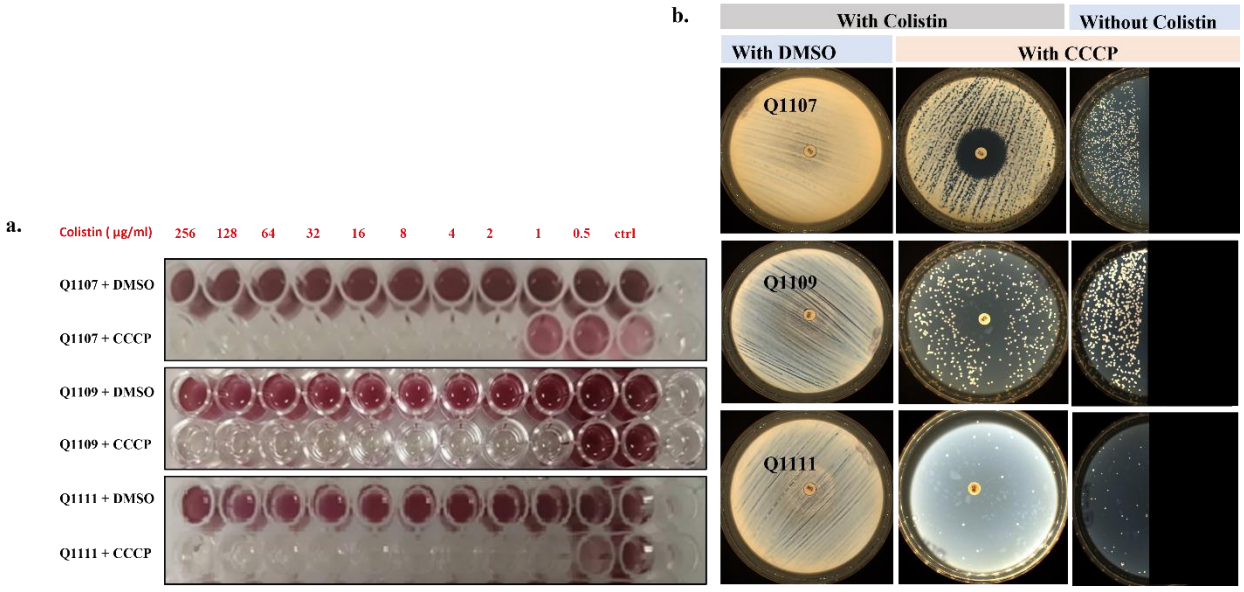

398

Fig.S2 Growth curves of *B. intermedia* strain Q1103 in different CO concentrations with 50 µg/ml of the following efflux pump inhibitors **(a)** PaβN (P<0.022)* **(b)** RSP (P<0.0002)*** and **(c)** VRP (P<0.0011)**.

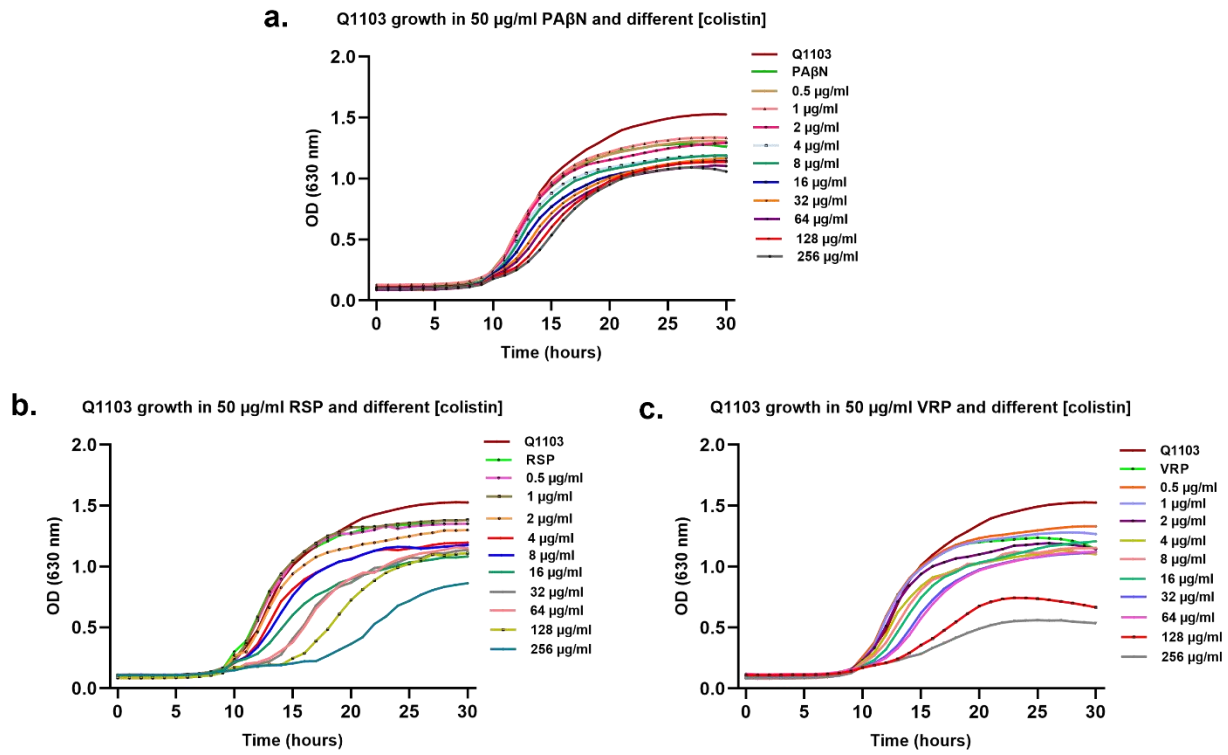

References

1. Storm DR, Rosenthal KS, Swanson PE. Polymyxin and Related Peptide Antibiotics. Annu Rev Biochem. 1977 Jun;46(1):723–63.

2. Falagas ME, Kasiakou SK. Colistin: the revival of polymyxins for the management of multidrug-resistant gram-negative bacterial infections. Clin Infect Dis Off Publ Infect Dis Soc Am. 2005 May 1;40(9):1333–41.

3. Monaco M, Giani T, Raffone M, Arena F, Garcia-Fernandez A, Pollini S, et al. Colistin resistance superimposed to endemic carbapenem-resistant Klebsiella pneumoniae: a rapidly evolving problem in Italy, November 2013 to April 2014. Eurosurveillance. 2014 Oct 23;19(42):20939.

4. Yu Z, Cai Y, Qin W, Lin J, Qiu J. Polymyxin E Induces Rapid Paenibacillus polymyxa Death by Damaging Cell Membrane while Ca2+ Can Protect Cells from Damage. PLoS ONE. 2015 Aug 7;10(8):e0135198.

5. Moffatt JH, Harper M, Boyce JD. Mechanisms of Polymyxin Resistance. In: Li J, Nation RL, Kaye KS, editors. Polymyxin Antibiotics: From Laboratory Bench to Bedside [Internet]. Cham: Springer International Publishing; 2019 [cited 2022 Jan 27]. p. 55–71. (Advances in Experimental Medicine and Biology; vol. 1145). Available from: http://link.springer.com/10.1007/978-3-030-16373-0_5

6. Baron S, Hadjadj L, Rolain JM, Olaitan AO. Molecular mechanisms of polymyxin resistance: knowns and unknowns. Int J Antimicrob Agents. 2016 Dec;48(6):583–91.

7. Fernández L, Gooderham WJ, Bains M, McPhee JB, Wiegand I, Hancock REW. Adaptive Resistance to the “Last Hope” Antibiotics Polymyxin B and Colistin in Pseudomonas aeruginosa Is Mediated by the Novel Two-Component Regulatory System ParR-ParS. Antimicrob Agents Chemother. 2010 Aug;54(8):3372–82.

8. Ito-Kagawa M, Koyama Y. Selective cleavage of a peptide antibiotic, colistin by colistinase. J Antibiot (Tokyo). 1980 Dec;33(12):1551–5.

9. Yin J, Wang G, Cheng D, Fu J, Qiu J, Yu Z. Inactivation of Polymyxin by Hydrolytic Mechanism. Antimicrob Agents Chemother. 2019 May 23;63(6):e02378-18.

10. Hamel M, Rolain JM, Baron SA. The History of Colistin Resistance Mechanisms in Bacteria: Progress and Challenges. Microorganisms. 2021 Feb 20;9(2):442.

11. Liu YY, Wang Y, Walsh TR, Yi LX, Zhang R, Spencer J, et al. Emergence of plasmid-mediated colistin resistance mechanism MCR-1 in animals and human beings in China: a microbiological and molecular biological study. Lancet Infect Dis. 2016 Feb;16(2):161–8.

12. Campos MA, Vargas MA, Regueiro V, Llompart CM, Albertí S, Bengoechea JA. Capsule Polysaccharide Mediates Bacterial Resistance to Antimicrobial Peptides. Infect Immun. 2004 Dec;72(12):7107–14.

13. Lin MF, Lin YY, Lan CY. Contribution of EmrAB efflux pumps to colistin resistance in Acinetobacter baumannii. J Microbiol. 2017 Feb;55(2):130–6.

14. Aujoulat F, Romano-Bertrand S, Masnou A, Marchandin H, Jumas-Bilak E. Niches, Population Structure and Genome Reduction in Ochrobactrum intermedium: Clues to Technology-Driven Emergence of Pathogens. PLOS ONE. 2014 Jan 17;9(1):e83376.

15. Teyssier C, Jumas-Bilak E, Marchandin H, Jean-Pierre H, Jeannot JL, Dusart G, et al. Identification d'espèce et épidémiologie moléculaire des bactéries du genre Ochrobactrum. Pathol Biol. 2003 Feb;51(1):5–12.

16. Teyssier C, Jumas-Bilak E, Counil F, Masnou A, Aleyrangues L, Chiron R, et al. Ochrobactrum and Agrobacterium spp.: emerging opportunistic pathogens in cystic fibrosis patients? J Cyst Fibros. 2009 Jun;8:S47.

17. Apisarnthanarak A, Kiratisin P, Mundy LM. Evaluation of Ochrobactrum intermedium bacteremia in a patient with bladder cancer. Diagn Microbiol Infect Dis. 2005 Oct 1;53(2):153–5.

18. Vaidya SA, Citron DM, Fine MB, Murakami G, Goldstein EJC. Pelvic Abscess Due to Ochrobactrum anthropi in an Immunocompetent Host: Case Report and Review of the Literature. J Clin Microbiol [Internet]. 2007 May [cited 2022 Jan 5]; Available from: https://journals.asm.org/doi/abs/10.1128/JCM.02260-06

19. Dharne MS, Misra SP, Misra V, Dwivedi M, Patole MS, Shouche YS. Isolation of urease-positive Ochrobactrum intermedium in the stomach of a non-ulcer dyspeptic patient from north India. J Microbiol Immunol Infect Wei Mian Yu Gan Ran Za Zhi. 2008 Apr;41(2):183–6.

20. Bharucha T, Sharma D, Sharma H, Kandil H, Collier S. Ochromobactrum intermedium: an emerging opportunistic pathogen—case of recurrent bacteraemia associated with infective endocarditis in a haemodialysis patient. New Microbes New Infect. 2016 Oct 6;15:14–5.

21. Aghapour Z, Gholizadeh P, Ganbarov K, Bialvaei AZ, Mahmood SS, Tanomand A, et al. Molecular mechanisms related to colistin resistance in Enterobacteriaceae. Infect Drug Resist. 2019 Apr 24;12:965–75.

22. Olaitan AO, Morand S, Rolain JM. Mechanisms of polymyxin resistance: acquired and intrinsic resistance in bacteria. Front Microbiol. 2014 Nov 26;5:643.

23. Park YK, Ko KS. Effect of carbonyl cyanide 3-chlorophenylhydrazone (CCCP) on killing Acinetobacter baumannii by colistin. J Microbiol. 2015 Jan;53(1):53–9.

24. Baron SA, Rolain JM. Efflux pump inhibitor CCCP to rescue colistin susceptibility in mcr-1 plasmid-mediated colistin-resistant strains and Gram-negative bacteria. J Antimicrob Chemother. 2018 Jul 1;73(7):1862–71.

25. Ni W, Li Y, Guan J, Zhao J, Cui J, Wang R, et al. Effects of Efflux Pump Inhibitors on Colistin Resistance in Multidrug-Resistant Gram-Negative Bacteria. Antimicrob Agents Chemother. 2016 Apr 22;60(5):3215–8.

26. Tang M, Wei X, Wan X, Ding Z, Ding Y, Liu J. The role and relationship with efflux pump of biofilm formation in Klebsiella pneumoniae. Microb Pathog. 2020 Oct 1;147:104244.

27. Ikonomidis A, Tsakris A, Kanellopoulou M, Maniatis A n., Pournaras S. Effect of the proton motive force inhibitor carbonyl cyanide-m-chlorophenylhydrazone (CCCP) on Pseudomonas aeruginosa biofilm development. Lett Appl Microbiol. 2008;47(4):298–302.

28. Chen S, Teng T, Zhang Z, Shang Y, Xiao H, Jiang G, et al. Carbonyl Cyanide 3-Chlorophenylhydrazone (CCCP) Exhibits Direct Antibacterial Activity Against Mycobacterium abscessus. Infect Drug Resist. 2021 Mar 23;14:1199–208.

29. Ravi RK, Walton K, Khosroheidari M. MiSeq: A Next Generation Sequencing Platform for Genomic Analysis. In: DiStefano JK, editor. Disease Gene Identification: Methods and Protocols [Internet]. New York, NY: Springer; 2018 [cited 2022 Jul 18]. p. 223–32. (Methods in Molecular Biology). Available from: https://doi.org/10.1007/978-1-4939-7471-9_12

30. Page AJ, Cummins CA, Hunt M, Wong VK, Reuter S, Holden MTG, et al. Roary: rapid large-scale prokaryote pan genome analysis. Bioinforma Oxf Engl. 2015 Nov 15;31(22):3691–3.

31. Hadfield J, Croucher NJ, Goater RJ, Abudahab K, Aanensen DM, Harris SR. Phandango: an interactive viewer for bacterial population genomics. Bioinforma Oxf Engl. 2018 Jan 15;34(2):292–3.

32. Thompson JD, Higgins DG, Gibson TJ. CLUSTAL W: improving the sensitivity of progressive multiple sequence alignment through sequence weighting, position-specific gap penalties and weight matrix choice. Nucleic Acids Res. 1994 Nov 11;22(22):4673–80.

33. Kumar S, Stecher G, Tamura K. MEGA7: Molecular Evolutionary Genetics Analysis Version 7.0 for Bigger Datasets. Mol Biol Evol. 2016;33(7):1870–4.

34. Jayol A, Nordmann P, André C, Poirel L, Dubois V. Evaluation of three broth microdilution systems to determine colistin susceptibility of Gram-negative bacilli. J Antimicrob Chemother. 2018 May 1;73(5):1272–8.

35. Lamers RP, Cavallari JF, Burrows LL. The Efflux Inhibitor Phenylalanine-Arginine Beta-Naphthylamide (PAβN) Permeabilizes the Outer Membrane of Gram-Negative Bacteria. PLoS ONE. 2013 Mar 27;8(3):e60666.

36. Odds FC. Synergy, antagonism, and what the chequerboard puts between them. J Antimicrob Chemother. 2003 Jul 1;52(1):1.

37. Terminology relating to methods for the determination of susceptibility of bacteria to antimicrobial agents. Clin Microbiol Infect. 2000 Sep 1;6(9):503–8.

38. Wang Z, Bie P, Cheng J, Lu L, Cui B, Wu Q. The ABC transporter YejABEF is required for resistance to antimicrobial peptides and the virulence of Brucella melitensis. Sci Rep. 2016 Aug 23;6:31876.

39. Cheah SE, Johnson MD, Zhu Y, Tsuji BT, Forrest A, Bulitta JB, et al. Polymyxin Resistance in Acinetobacter baumannii: Genetic Mutations and Transcriptomic Changes in Response to Clinically Relevant Dosage Regimens. Sci Rep. 2016 May 19;6:26233.

40. Fehlner-Gardiner CC, Valvano MA. Cloning and characterization of the Burkholderia vietnamiensis norM gene encoding a multi-drug efflux protein. FEMS Microbiol Lett. 2002;215(2):279–83.

41. Lin MF, Lin YY, Lan CY. Contribution of EmrAB efflux pumps to colistin resistance in Acinetobacter baumannii. J Microbiol. 2017 Feb 1;55(2):130–6.

42. Bialer MG, Ruiz-Ranwez V, Sycz G, Estein SM, Russo DM, Altabe S, et al. MapB, the Brucella suis TamB homologue, is involved in cell envelope biogenesis, cell division and virulence. Sci Rep. 2019 Feb 1;9(1):2158.

43. Binsker U, Käsbohrer A, Hammerl JA. Global colistin use: a review of the emergence of resistant Enterobacterales and the impact on their genetic basis. FEMS Microbiol Rev. 2021 Oct 6;46(1):fuab049.

44. Osei Sekyere J, Amoako DG. Carbonyl Cyanide m-Chlorophenylhydrazine (CCCP) Reverses Resistance to Colistin, but Not to Carbapenems and Tigecycline in Multidrug-Resistant Enterobacteriaceae. Front Microbiol [Internet]. 2017 [cited 2022 Feb 20];8. Available from: https://www.frontiersin.org/article/10.3389/fmicb.2017.00228

45. Nikaido H. Prevention of Drug Access to Bacterial Targets: Permeability Barriers and Active Efflux. Science. 1994 Apr 15;264(5157):382–8.

46. Ni W, Li Y, Guan J, Zhao J, Cui J, Wang R, et al. Effects of Efflux Pump Inhibitors on Colistin Resistance in Multidrug-Resistant Gram-Negative Bacteria. Antimicrob Agents Chemother. 2016 Apr 22;60(5):3215–8.

47. Montville TJ, Bruno MEC. Evidence that dissipation of proton motive force is a common mechanism of action for bacteriocins and other antimicrobial proteins. Int J Food Microbiol. 1994 Dec;24(1–2):53–74.

48. Le D, Krasnopeeva E, Sinjab F, Pilizota T, Kim M. Active Efflux Leads to Heterogeneous Dissipation of Proton Motive Force by Protonophores in Bacteria. mBio. 12(4):e00676-21.

49. Wang Z, Bie P, Cheng J, Lu L, Cui B, Wu Q. The ABC transporter YejABEF is required for resistance to antimicrobial peptides and the virulence of Brucella melitensis. Sci Rep. 2016 Aug 23;6:31876.

50. Borges-Walmsley MI, Beauchamp J, Kelly SM, Jumel K, Candlish D, Harding SE, et al. Identification of Oligomerization and Drug-binding Domains of the Membrane Fusion Protein EmrA *. J Biol Chem. 2003 Apr 11;278(15):12903–12.

51. Lin MF, Lin YY, Lan CY. Contribution of EmrAB efflux pumps to colistin resistance in Acinetobacter baumannii. J Microbiol. 2017 Feb 1;55(2):130–6.

52. El-Sayed Ahmed MAEG, Zhong LL, Shen C, Yang Y, Doi Y, Tian GB. Colistin and its role in the Era of antibiotic resistance: an extended review (2000–2019). Emerg Microbes Infect. 2020 May 6;9(1):868–85.

53. Gil-Ramírez Y, Conde-Álvarez R, Palacios-Chaves L, Zúñiga-Ripa A, Grilló MJ, Arce-Gorvel V, et al. The identification of wadB, a new glycosyltransferase gene, confirms the branched structure and the role in virulence of the lipopolysaccharide core of Brucella abortus. Microb Pathog. 2014 Aug 1;73:53–9.

54. Matson JS, Yoo HJ, Hakansson K, DiRita VJ. Polymyxin B Resistance in El Tor Vibrio cholerae Requires Lipid Acylation Catalyzed by MsbB. J Bacteriol. 2010 Apr;192(8):2044–52.

549 55. Gogry FA, Siddiqui MT, Sultan I, Haq QMohdR. Current Update on Intrinsic and Acquired Colistin
550 Resistance Mechanisms in Bacteria. Front Med [Internet]. 2021 [cited 2022 Aug 31];8. Available from:
551 https://www.frontiersin.org/articles/10.3389/fmed.2021.677720

552 56. Liautard J, Ouahrani-Bettache S, Jubier-Maurin V, Lafont V, Köhler S, Liautard JP. Identification
553 and Isolation of Brucella suis Virulence Genes Involved in Resistance to the Human Innate Immune
554 System. Infect Immun. 2007 Nov;75(11):5167–74.

555

Conclusions et Perspectives

Conclusion et perspectives

Dans notre travail de thèse, nous avons contribué, en premier lieu, à augmenter le répertoire bactérien en caractérisant des nouvelles espèces qui peuvent coloniser l'homme et les primates non humains (PNH). En second lieu, nous avons apporté des informations sur le mécanisme de résistance naturelle à la colistine chez *Brucella intermedia*, pouvant servir à améliorer la prise en charge des infections humaines causées par cette espèce.

Depuis 2012, plus de 800 nouvelles espèces associées à l'homme ont été isolées et caractérisées grâce à la culturomique et à la taxono-génomique. Cette stratégie a permis d'identifier des espèces ayant un potentiel thérapeutique, notamment pour le traitement de certains cancers, en jouant un rôle dans la modulation de la réponse immune et en optimisant l'efficacité de certains anticorps monoclonaux [63]. Grâce à la culturomique, nous avons isolé douze nouvelles espèces bactériennes, six souches de l'espèce *B. intermedia*, une souche de *Brucella tritici* et une souche de *Fusobacterium Simiae*. Nous avons décrit les nouvelles espèces suivant une approche taxono-génomique. Nous avons caracterisé chez l'homme la nouvelle espèce *Streptococcus bouchesdurhonensis,* isolée du lavage broncho-alveolaire d'un patient souffrant de pneumonie. Cette espèce appartient au « groupe *mitis* » du genre *Streptococcus* qui présente une grande similaritité au niveau des séquences d'ARNr 16S [62]. Cette description permet de la différencier des espèces commensales *Streptococcus pseudopneumoniae*, *Streptococccus mitis* et de l'espèce pathogène *Streptococccus pneumoniae,* phylogénétiquement proches. Cette description permet une meilleure discrimination des espèces proches de *Streptococccus pneumoniae*

et offre aux chercheurs le choix d'outils moléculaires adaptés pour différencier les souches pathogènes.

Nous avons aussi isolé une souche de *Fusobacterium simiae* à partir d'un liquide de ponction d'abcès intra-abdominal post-appendicectomie. Le génome de la souche a été séquencé avec celui de la souche type de l'espèce. Ces deux génomes, qui sont les premiers premiers de *F. simiae*, ont été déposés dans la base de données GenBank.

Un autre volet de nos recherches a concerné le Chimpanzé du Sénégal (*Pan troglodytes*). Les PNH sont phylogénétiquement proches des humains et peuvent partager les mêmes agents infectieux. Les échantillons (fèces) que nous avons étudiés ont été collectés d'une manière non-invasive dans une réserve sauvage d'Afrique du Sénégal.

A partir des selles des chimpanzés, nous avons pu caractériser deux nouvelles espèces de *Brucella* (auparavant classées dans le genre *Ochrobactrum*) : *Brucella senegalensis* sp. nov., proche de l'espèce *Brucella anthropi*, un pathogène d'intérêt médical, et *Brucella troglodytis* sp. nov., proche de l'espèce *Brucella pseudogrignonensis.* Actuellement, le statut taxonomique des membres du genre *Ochrobactrum* n'est pas clair. Leur reclassification dans le genre *Brucella* fait débat [64, 65]. En avril 2020, une nouvelle reclassification des alphaprotéobactéries a inclus le genre *Ochobactrum* dans le genre *Brucella* sur la base d'analyses génomiques globales, et notamment d'une grande similarité génomique et d'une équivalence présumée avec d'autres genres contenant des espèces pathogènes et non pathogènes tels que le genre *Mycobacterium* [66]. Cependant, une étude plus récente, en mars 2022, a suggéré que les deux genres *Brucella* et *Ochrobactrum* devraient rester séparés au principe que les équivalences avec les autres genres sont incorrectes et négligent les spécificités épidémio-cliniques des *Brucella* et des *Ochrobactrum*. L'étude a été basée sur le principe que les rangs taxonomiques multi-dimensionnels ne sont pas équivalents aux analyses phylogénétiques donnant une

représentation bi-dimensionnelle. Les organismes vivants ne devraient pas être catégorisés selon les seules règles de la taxonomie bi-dimensionnelle puisqu'il s'agit de systèmes dynamiques multidimensionnels qui évoluent en temps réel selon des contingences spatio-temporelles complexes avec un nombre pratiquement infini de combinaisons génétiques. Les divergences des *Brucella* et *Ochrobactrum* en termes de mode de vie, physiologie, structure de population, pangénome, traits génomiques et pathogénicité les distinguent. Certains auteurs évoquent aussi un risque de confusion pour les autorités de santé publique qui sont confrontées à la brucellose si des espèces environnementales (*Ochrobactrum*) et des espèces hautement pathogènes (*Brucella)* sont associées dans le même genre [67]. Par conséquent, à ce jour, la classification taxonomique des membres des deux genres reste toujours un sujet de discorde.

Dans notre revue de la littérature, nous avons décrit les mécanismes de résistance connus chez des espèces intrinsèquement résistantes aux polymyxines (PX) et d'intérêt médical. Celles-ci incluent les bactéries des genres *Burkholderia, Brucella* et *Neisseria,* de la tribu *Proteus* (*Proteus mirabilis*, *Serratia marcescens, Morganella morganii),* et des espèces *Vibrio cholerae* et *Helicobacter pylori*. La résistance aux PX concerne les deux molécules disponibles en clinique: la polymyxine B (PXB) et la polymyxine E (PXE) ou colistine.

Les connaissances sur la résistance intrinsèque aux PX étant limitées, nous avons listé les mécanismes classiques connus, notamment le remodelage de la surface cellulaire. Il semble le plus répandu mais reste largement méconnu. Des substitutions cationiques sont à l'origine des modifications des lipopolysaccharides (LPS) de la membrane bactérienne telles que la phospho-éthanolamine (PEtn), le 4-amino-4-désoxy-L-arabinose (L-Ara4N) et la glycylation du lipide A [68]. Des systèmes à deux composants (TCS), qui sont des gènes régulateurs, peuvent intervenir dans ces modifications en réponse à des

conditions de stress telles que le PH acide, les faibles concentrations de Mg^{2+}, les peptides cationiques, l'ADN extracellulaire et les concentrations élevées d'Al^{3+} ou Fe^{2+}. Les TCS sont souvent rapportés dans la résistance intrinsèque aux PX tels que MgrS/MgrR (*Burkholderia*), PhoP/Q to (*Serratia marcescens*), BvrS/BvrR (*Brucella*), VprAB (*Vibrio Cholerae*), MisR/MisS (*Neisseria*), *qseB/C* and *rssA/B* (*Morganella*) [69]. Des modifications de la composition et de l'intégrité membranaire telles que les porines membranaires, la biosynthèse des isoprénoïdes et des hopanoides, et la production de capsule confèrent aussi une telle résistance. De plus, des pompes à efflux, faisant partie de la membrane, ainsi que des enzymes métaboliques impliquées dans des métabolismes bactériens de base confèrent une résistance intrinsèque aux PX [70].

Au total, il n'y a pas un mécanisme de résistance bien défini. Il a été décrit que plusieurs facteurs peuvent intervenir dans une même espèce ayant une résistance intrinsèque aux PX. Les recherches actuelles portent sur les gènes de résistance intrinsèque qui pourraient servir de cibles thérapeutiques pour développer de nouveaux médicaments et prédire l'émergence future d'agents pathogènes résistants s'ils sont transmis. Ainsi, une origine environnementale provenant des bactéries intrinsèquement résistantes et portant le gène chromosomial PmrC a été supposée comme étant à l'origine du gène de résistance à la colistine (mcr) [71].

Brucella intermedia a été rapportée dans plusieurs cas d'infection nosocomiale. Cette espèce présente une résistance intrinsèque à la colistine. Pour étudier son mécanisme de résistance, nous avons testé l'effet de différents inhibiteurs de pompes à efflux tels que le CCCP, le vérapamil (VRP), la réserpine (RSP) et le phe-arg β-naphtylamide dihydrochloride (PAβN) sur la résistance à la colistine des six souches isolées. Pour la première fois, j'ai montré que VRP, RSP, et PaβN ne restaurent que très partiellement la croissance de *B. intermedia* en combinaison avec la colistine (vue dans

les courbes de croissance). La molécule CCCP était la seule qui ait pu réverser pleinement la résistance à la colistine. Ce qui a suggéré un rôle des pompes à efflux dans le mécanisme de résistance de cette espèce. Et comme le CCCP est un inhibiteur non spécifique agissant sur la dissipation de l'énergie, un autre mécanisme pourrait être couplé aux pompes à efflux affectant des voies métaboliques essentielles chez les *Brucella*.

L'analyse génomique de *B. intermedia* nous a permis d'identifier des pompes à efflux conservées dans toutes les souches, et qui sont vraisemblablement impliquées dans le mécanisme de résistance d'après la littérature [72, 73]. Le mécanisme concret de résistance à la colistine nécessite des recherches plus approfondies, en particulier pour l'élucidation du rôle spécifique de chaque système de pompe à efflux identifié par l'analyse pangénomique.

Un effet inhibiteur de la combinaison colistine-CCCP a aussi été observé sur la formation du biofilm, qui pourrait être un deuxième facteur jouant un rôle dans la résistance. Pour élucider l'effet potentiel du CCCP sur la formation du biofilm et sa relation avec la résistance à la colistine, d'autres analyses expérimentales incluant la biomasse et la matrice extracellulaire des cellules traitées seront nécessaires.

De nombreuses études sont en cours sur l'effet des inhibiteurs de pompes à efflux. Plusieurs d'entre eux sont capables de potentialiser l'efficacité des antibiotiques sur des souches multi-résistantes mais leur utilisation en pratique clinique reste encore un projet à cause de leur toxicité. L'identification des pompes à efflux cibles des inhibiteurs, et la détermination de leur activité de résistance pourraient conduire à la synthèse de molécules originales inhibitrices des pompes à efflux pour une utilisation clinique. Ce qui pourrait aboutir à un effet thérapeutique efficace dans les infections à bactéries colistine-résistantes. De même, d'autres voies de recherche pourraient consister à modifier les antibiotiques tels que la colistine pour qu'ils ne soient pas reconnus par leurs pompes à

efflux, à jouer sur l'expression génique des pompes ou à cibler leur mode d'assemblage. Pour que ces approches soient envisagées pour un développement ultérieur, il sera nécessaire d'explorer l'activité fonctionnelle des pompes, leur sélectivité pour des substrats, les sites possibles d'interaction et leurs domaines d'affinité pour les substrats.

Pour conclure, la résistance aux antibiotiques est préoccupante à la fois pour la santé humaine et pour la santé animale. De nos jours, au nom du concept « One Heath » nous nous sommes capables d'étudier grâce aux approches génomique, culturomique, et métagénomique, les mécanismes de résistance des antibiotiques, surtout ceux de dernier recours, mais aussi de découvrir de nouveaux antibiotiques grâce à des descriptions croissantes de nouvelles espèces, et de potentialiser l'activité des antibiotiques existants par la combinaison à des adjuvants.

Annexe

Avant-propos

Durant notre thèse, nous avons contribué à travers des travaux secondaires et des collaborations avec d'autres équipes à des projets de description de nouvelles espèces bactériennes isolées d'échantillons humains dans le but de décrire la composition du microbiote humain chez des individus sains et malades. Ces travaux sont regroupés dans cette partie annexe.

Article 7

Description of *Agathobaculum massiliensis* sp. nov. isolated from human stool

Reham Magdy Wasfy, **Malak Zoaiter**, Cheikh Ibrahima LO, Stéphane Alibar, Florence Fenollar, Didier Raoult, Pierre-Edouard Fournier, Matthieu Million

Submitted in Archives of Microbiology

Description of *Agathobaculum massiliense* sp. nov. a new bacterial species isolated from human stool

Reham MAGDY WASFY[1,2], Malak ZOAITER[1,3], Melhem BILEN[4], Maryam TIDJANI ALOU[1,2], Cheikh Ibrahima LO[1,3], Sara BELLALI[1], Stéphane ALIBAR[1,2,5], Claudia ANDRIEU[1,2,5], Aurelia CAPUTO[1,2,5], Didier RAOULT[1,2], Pierre Edouard FOURNIER[1,3,5] and Matthieu MILLION[1,2,5*]

[1]IHU Méditerranée Infection, Marseille 13005, France.

[2]Aix-Marseille-Univ, IRD, MEPHI, IHU Méditerranée Infection, Marseille 13005, France.

[3]Aix Marseille Univ, IRD, AP-HM, SSA, VITROME, Marseille, France

[4]Department of Bioengineering and ChEM-H, Stanford University, Stanford, CA 94305, USA

[5]Assistance Publique-Hôpitaux de Marseille, 13005 Marseille, France

[*]Corresponding author

Contact : Matthieu MILLION

IHU Méditerranée Infection, MEPHI, IRD, 19-12 Bd Jean Moulin 13005 Marseille, France.

Email : matthieumillion@gmail.com

Tel: +33 413 732 401, Fax: +33 413 732 402

ABSTRACT

The novel bacterial strain Marseille-P4005^T was isolated from the stool sample of a healthy donor. It is a Gram-stain negative, non-motile, non-spore-forming rod. It grew optimally at 37°C and at pH 7.0 on 5% sheep blood enriched Columbia agar after preincubation in blood-culture bottle supplemented with rumen and blood. This strain does not ferment monosaccharides (except D-tagatose), disaccharides or polymeric carbohydrates. The major cellular fatty acids were the hexadecenoic (24.6%), octadecanoic (22.8%) and tetradecanoic (20.1%) acids. Next generation sequencing revealed a genome size of 3.2 Mbp with a 56.4 mol% G+C. Phylogenetic analysis based on the 16S rRNA gene highlighted *Agathobaculum desmolans* strain ATCC 43058^T as the closest related strain. The OrthoANI and the digital DNA-DNA hybridization values were below the critical thresholds of 95% and 70%, respectively, to define a novel bacterial species. Based on the phenotypic and genomic data, we describe Strain Marseille-P4005^T (= CSUR P4005^T = CECT 9669^T) a novel bacterial species within the genus *Agathobaculum*, for which the name of *Agathobaculum massiliense* sp. nov. is proposed.

Keywords

Culturomics; human gut; *Agathobaculum massiliense*; microbiota; taxono-genomics

INTRODUCTION

The human microbiota is a very diverse and complex ecosystem which diversity has been highlighted owing to next generation sequencing (NGS). NGS methods also highlighted a high number of uncultivated species including hitherto unknown species as revealed by the high proportion of unassigned sequences. This led to new advances in the field of bacterial culture to isolate and identify previously unknown species (Fontaine *et al.,* 2012; Lagier *et al.*, 2015; Lagier *et al.*, 2012). Culturomics, a high throughout culture approach which was described in 2012, contributed in the identification of a plethora of new bacterial species from human samples (Lagier *et al.,* 2012, 2016; Lagier, Hugon, *et al.,* 2015). In a culturomics project aimed at studying the composition of the human gut microbiota, we isolated strain Marseille-P4005^{T} from a human stool sample. The strain Marseille-P4005^{T} was classified within the *Agathobaculum* genus.

The *Agathobaculum* genus was created in 2016 with the reclassification and description of *Agathobaculum desmolans* initially described as *Eubacterium desmolans* in 1986 by Morris et al. (Ahn *et al.,* 2016). This genus is classified within the Firmicutes phylum and belongs to Oscillospiraceae family, which includes 56 other validly published genera. The *Agathobaculum* genus currently includes four validly published species where the type species is *Agathobaculum butyriciproducens.* Members of the *Agathobaculum* genus are generally Gram-stain-positive, motile or non-motile, non-spores forming, obligately anaerobic, oxidase- and catalase-negative. They have an optimum growth temperature ranging from 30 to 40 °C and the major fermentation end product is butyrate or acetate (Ahn *et al.,* 2016). *A. desmolans* has been first isolated from cat faeces (Morris *et al.,* 1986).

In this study, a novel species named *Agathobaculum massiliense* sp. nov. strain Marseille-P4005^{T} is described using the taxonogenomics approach (Ramasamy *et al.,* 2014)

which applies phenotypic, proteomic, phylogenetic and genomic characteristics to classify new species.

MATERIAL AND METHODS

Sample collection and bacterial identification

Stool samples were collected from a young French healthy female after providing a signed informed consent. The study protocol on the description of the viable human microbiota using the culturomics was approved by the ethics committee of the Institut de Recherche Fédératif 48, under agreement number 09-022. Institut de Recherche Fédératif 48, under agreement number 09-022. The stool samples were cultured according to the culturomics approach previously established in our laboratory (Lagier *et al.*, 2015). Different bacterial colonies were isolated on 5% sheep blood enriched Columbia (COS) agar (BioMérieux, Craponne, France) after preincubation in a blood-culture bottle supplemented with rumen and sheep blood. Isolation was achieved after two days of incubation in an anaerobic atmosphere generated using anaeroGEN generators (Beckton Dickinson, Arcueil, FRANCE). The bacterial colonies were identified using Matrix-Assisted Laser Desorption/Ionization Time-Of-Flight (MALDI-TOF MS) with the Microflex LT instrument instrument (Bruker Daltonics, Bremen, Germany) as previously reported (Seng et al., 2009).

16S rRNA gene phylogeny

The 16S rRNA gene sequences of strain Marseille-P4005^{T} was extracted from its genome using Contest16S available online (www.ezbiocloud.net, last accessed October 2022). The sequence was compared using BLASTn to the NCBI nucleotide database with the NCBI server. A phylogenetic tree was constructed based on the 16S rRNA gene sequences using MEGA 7 version 7.0.26 with the maximum likelihood (ML) method and 1000 bootstraps replications (Kumar *et al.*, 2018).

Phenotypic and biochemical characterization

The optimal culture conditions have been determined by attempted growth of strain Marseille-P4005^T on COS agar at different temperatures (25, 28, 37, 45, and 56°C) in three atmospheres (aerobic, anaerobic and microaerophilic). Bacterial growth was also tested in different NaCl concentrations (5, 5.5, 7.5, 10, 15, and 20%). The salt tolerance of the studied strain was estimated using a medium containing 42 g Columbia agar (Thermo Fisher Scientific, Waltham, Massachusetts, US), 10 g $MgCl_2$, 10 g $MgSO_4$, 4 g KCl, 1 g $CaCl_2$, 0.5 g $NaHCO_3$, 5 g yeast extract and 2 g glucose. Different pH levels were also tested (5, 5.5, 6, 6.5, 7, 7.5, 8, 8.5) using a solid medium consisting of 42 g Columbia agar, 10 g NaCl, 5 g $MgCl_2$, 5 g $MgSO_4$, 2 g KCl, 1 g $CaCl_2$ (VWR, Radnor, Pennsylvania, US) and 2 g glucose (MP biomedicals, Irvine, California, US). The addition of NaOH or HCl solution was used to adjust the pH of the medium.

The morphologic features of strain Marseille-P4005^T was described using scanning electron microcopy (SEM) (SU5000, Hitachi, Tokyo, Japan) as previously described (Bellali *et al.*, 2022). Bacterial length and width were measured from sets of SEM micrographs using ImageJ. Furthermore, biochemical characteristics were assessed using different API strips: API 50CH, API ZYM and API 20A (bioMérieux, Craponne, France) according to bioMérieux instructions (BioMérieux France, 2022).

The fatty acid methyl ester (FAME) analysis was done using gas chromatography/mass spectrometry (GC/MS), as previously reported (Sasser, 2006) . FAMEs were separated using an Elite 5-MS column and monitored by mass spectrometry (Clarus 500- SQ 8 S, Perkin Elmer, Courtaboeuf, France). The spectral profile was compared with those in repertory databases using MS Search 2.0 operated with the Standard Reference Database 1A (NIST, Gaithersburg, USA) and the FAMEs mass spectral database (Wiley, Chichester, UK).

The antibiotic susceptibility of the described strain was assessed through the Minimum Inhibitory Concentration (MIC) determination method. Antibiotics were selected based on the recommendations of European Committee on Antimicrobial Susceptibility Testing (Matuschek *et al.*, 2014). The susceptibility to antimicrobial agents of strain was tested on 5% sheep blood-enriched Mueller Hinton agar (bioMérieux) under aerobic conditions. The following antibiotics were tested using E-TEST® strips (bioMérieux): daptomycin, imipenem, rifampicin, vancomycin, benzylpenicillin, amikacin, ceftriaxone, amoxicillin, tobramycin, linezolid, clindamycin, oxacillin, ceftazidime, ciprofloxacin, trimetho-sulphamethoxazole, doxycycline and colistin.

Genome sequencing and analyses

The genomic DNA was extracted using the EZ1 DNeasy Blood Tissue Kit (Qiagen GmbH, Hilden, Germany) according to the manufacturer's instructions (Anani et al., 2019). The whole-genome sequencing was performed using the Illumina MiSeq sequencer (Illumina, San Diego, CA, USA) as previously described (Caporaso *et al.*, 2012). The genome of strain Marseille-P4005 was assembled using Spades 3.5.0 software (Prjibelski *et al.*, 2020) and annotated using Prokka version 1.14.5 (Seemann, 2014). The genomic similarities between the studied species and their related taxon were calculated by the OrthoANI tool (OAT) version 0.93.1. The digital DNA-DNA Hybridization (dDDH) values were calculated using the DSMZ database on the following website (https://ggdc.dsmz.de, last accessed October 2022). A genome-based phylogenetic tree was generated with FastME 2.1.6.1 software (Meier-Kolthoff & Göker, 2019).

RESULTS

Identification and 16S rRNA phylogenies

Strain Marseille-P4005^T was unidentified using Maldi-TOF MS. Their spectra were uploaded to the local MALDI-TOF MS database. Blastn of the 16S rRNA gene sequence showed that strain Marseille-P4005^T had a 96.74% sequence similarity with *Agathobaculum desmolans* ATCC 43058^T and 95.01% with *Intestinibacillus massiliensis* strain Marseille-P3216^T. (**Fig.1**) revealed the phylogenetic relationship between strain Marseille-P4005^T and the related species.

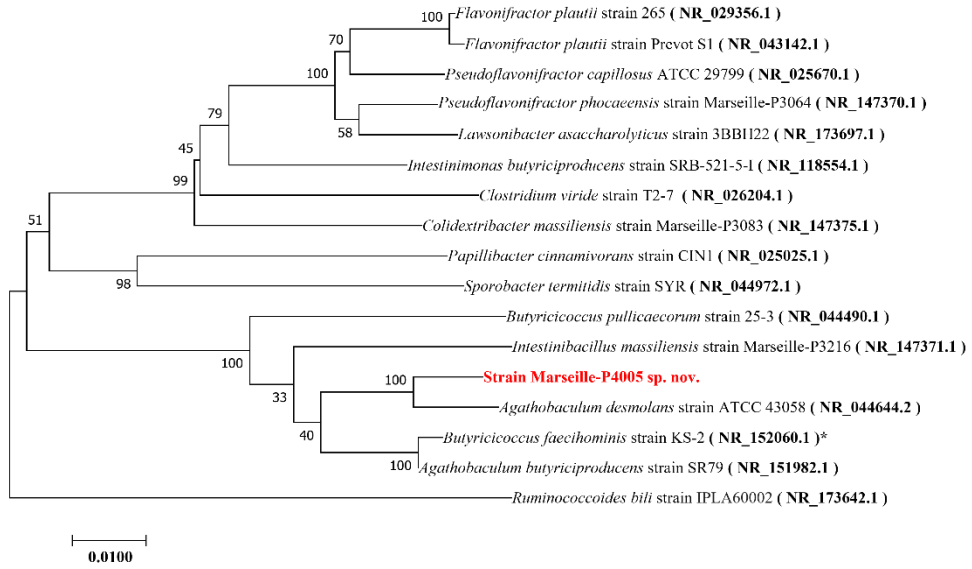

Fig.1 Phylogenetic relationship showing the position of strain Marseille-P4005^T compared to closely related species based on the 16S rRNA gene. Genbank accession numbers are indicated in parentheses. Sequences were aligned using MUSCLE. Phylogenetic inferences were obtained using the maximum likelihood method within the Mega software. Bootstrap values (mentioned at the nodes) were obtained by repeating the analysis 1000 times. *Ruminococcoides bili* strain IPLA60002 served as outgroup. The scale bar represents a 1% nucleotide sequence divergence. **Butyricicoccus faecihominis* species may be reclassified as *Agathobaculum* referring to LPSN (Ludwig *et al.*, 2021).

Phenotypic and biochemical characterizations

Bacterial colonies of strain Marseille-P4005^T were observed on COS agar (bioMérieux, France) at temperatures ranging from 28 to 45° C with optimal growth at 37 °C after 48 hours of incubation. The strain was able to grow in microaerophilic and anaerobic atmospheres with an optimal growth observed in an anaerobic atmosphere. No growth was observed in aerobic atmosphere at different temperature ranges. In the tested pH range, growth appeared at pH 7. Moreover, strain Marseille-P4005^T showed no salt tolerance. After 48 hours of incubation, bacterial colonies on COS agar were white, punctiform, slightly convex and nonhaemolytic. On COS agar, they have a diameter ranging from 0.1 to 0.15 mm. Cells were rod-shaped as revealed by the SEM micrographs and measured 1.03±0.21µm in length and 0.4±0.1µm in width (**Fig.2**).

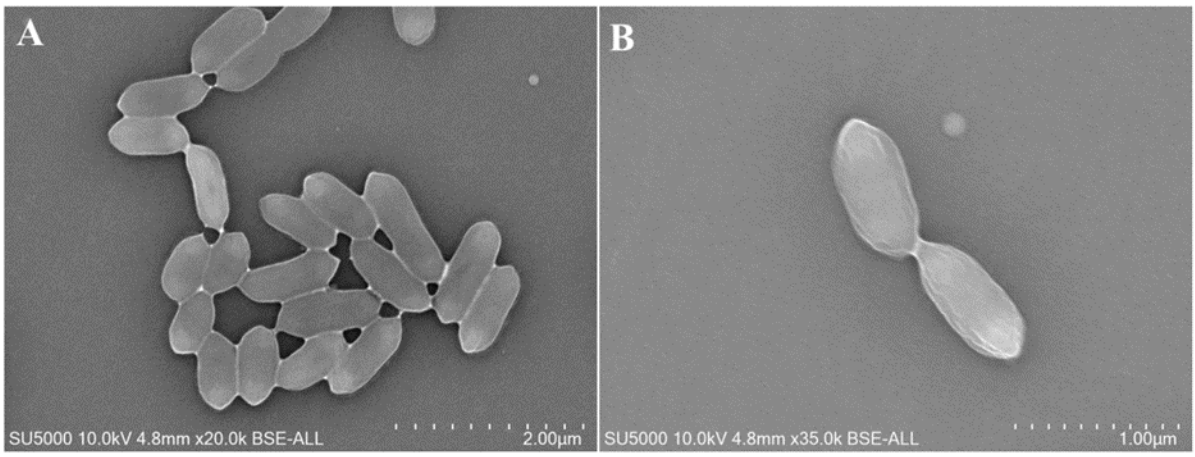

Fig.2 Scanning electron micrographs of *Agathobaculum massiliense* Marseille-P4005 (A-B) recorded on SU5000 SEM

The strain presented no catalase or oxidase activities. The following MICs were obtained for strain Marseille-P4005^T: 0.047 mg daptomycin, 0.032 mg imipenem, 0.1 mg rifampicin, 0.25 mg vancomycin, 0.75 mg benzylpenicillin, 256 mg amikacin, 0.38 mg ceftriaxone, 0.5 mg amoxicillin, 256 mg tobramycin, 2 mg linezolid, 256 mg clindamycin, 8 mg oxacillin, 256 mg ceftazidime, 256 mg ciprofloxacin, 32 mg trimetho-sulphamethoxazole, 8 mg doxycycline and 256 mg colistin.

The phenotypic characteristics of strain Marseille-P4005^T compared with those of their closest relatives are summarized in (**Table.1**). Using API® 50CH strip, positive reactions were obtained with glycerol, erythritol, dulcitol, D-mannitol, D-tagatose and potassium 5-cetogluconate. Using an API® ZYM strip, activities for the following enzymes were observed: alkaline phosphatase, lipase (C14), leucine arylamidase, trypsin, acid phosphatase, naphtol phosphohydrolase and β-galactosidase. The presence of a protease was also found using the API® 20A strip.

According to the proteomic analysis, the major fatty acids of strain Marseille-P4005 were saturated structures, namely hexadecanoic acid (25 %), octadecanoic acid (23 %) and tetradecanoic acid (20 %). A few unsaturated and branched fatty acids were also described with minor abundances (**Table.2**).

183 **Table.1** Phenotypic characteristics of strain Marseille-P4005^T compared with other closely related species

Properties	P4005	AD	AB	BP	BF	IM*
Gram stain	-	+	+	+	+	-
Cell shape	Rods	rods	short rod	coccid in pairs	coccoid-shaped	Rods
Motility	-	+	-	-	-	+
Cell diameter(µm)	0.8-1.3 x 0.3-0.4	NA	0.6–0.7 x 0.9–1.1	1.2–1.5	1.3×0.7	0.5-0.8 x 1.9-5
Endospore	-	-	-	NA	NA	-
Temperature	28°C- 37°C	37 °C	37 °C	42° C	37 °C	28°C- 37°C
Oxygen tolerance	Anaerobic	strictly anaerobic	strictly anaerobic	Anaerobic	strictly anaerobic	Anaerobic
Incubation (days)	2-3	2-3	3	1-2	3	2-3
Salt tolereance	-	-	0.5 %	NA	NA	-
Optimum pH	7	7	7	7	7	7
Alkaline Phosphatase	+	NA	NA	NA	+	+
Acid phosphatase	+	NA	NA	NA	+	+
Catalase	-	-	-	NA	NA	-
Oxidase	-	-	-	NA	NA	-
Indole	-	NA	NA	NA	+	-
Urease	-	-	-	-	-	-
α-galactosidase	-	NA	NA	NA	-	-
β-galactosidase	+	NA	NA	NA	-	-
Ribose	V	NA	NA	NA	NA	-
Mannose	-	+	+	+	-	-
Mannitol	+	+	+	-	-	-

Sucrose	-	+	+	+	-	-
Glucose	-	+	+	+	+	-
Fructose	-	NA	NA	NA	-	-
Maltose	-	+	+	+	-	-
Sorbitol	-	-	-	-	-	-
Starch	-	NA	NA	+	NA	-
Lactose	-	+	+	-	-	-
Source	Human stool	Cat faeces	Korean faecal sample	Chicken caecal content	Human faecal sample	Human left colon
Reference	-	(Ahn *et al.*, 2016)	(Ahn *et al.*, 2016)	(Eeckhaut *et al.*, 2008)	(Takada *et al.*, 2016)	(Ricaboni *et al.*, 2017)

+: Positive, -: Negative, V: Variable, NA: Not available

P4005: Strain Marseille-P4005^{T}; **AD:** *Agathobaculum desmolans* ATCC 43058^{T}; **AB:** *Agathobaculum butyriciproducens* NB2B-10-MRS; **BP:** *Butyricicoccus pullicaecorum* DSM 23266^{T}; **BF:** *Butyricicoccus faecihominis* JCM 31056^{T}; **IM:** *Intestinibacillus massiliensis* Marseille-P3216^{T}.

* API® 50CH, ZYM and 20A were performed in our lab.

Table.2: Cellular fatty acid composition (%)

Fatty acids	Name	Mean relative % [a]
16:00	Hexadecanoic acid	24.6 ± 4.1
18:00	Octadecanoic acid	22.8 ± 5.2
14:00	Tetradecanoic acid	20.1 ± 0.6
12:00	Dodecanoic acid	14.9 ± 6.7
18:1n9	9-Octadecenoic acid	3.4 ± 0.4
18:2n6	9,12-Octadecadienoic acid	2.2 ± 0.1
15:0 iso	13-methyl-tetradecanoic acid	2.1 ± 1.9
18:1n7	11-Octadecenoic acid	1.7 ± 0.5
13:00	Tridecanoic acid	1.6 ± 0.2
15:0 anteiso	12-methyl-tetradecanoic acid	1.6 ± 0.1
15:00	Pentadecanoic acid	1.3 ± 0.1
14:0 iso	12-methyl-Tridecanoic acid	1.1 ± 0.1
17:00	Heptadecanoic acid	1.0 ± 0.1
13:0 iso	11-methyl-Dodecanoic acid	TR
13:0 anteiso	10-methyl-Dodecanoic acid	TR
20:00	Eicosanoic acid	TR

a: Mean peak area percentage ; TR = trace amounts < 1 %

Genome characteristics and comparison

The genome was 3,212,687-bp- long with a G+C content of 56.4 mol%. It included 3,242 genes. Of them, 3,176 genes were protein-coding genes, and 67 genes were RNA (9 rRNA including 3 16S rRNA, 57 tRNA, 1 mRNA).

The number comparison of genes associated with a COG functional cluster for the strain with the closest species is represented in (**Fig.3**). A high proportion of genes assigned to transcription (10.19 %) and carbohydrate transport and metabolism (10.33 %) was observed in strain Marseille-P4005^T. The comparison of the genomic characteristics of strain Marseille-P4005^T with those of closely related strains is reported in (**Table.3**).

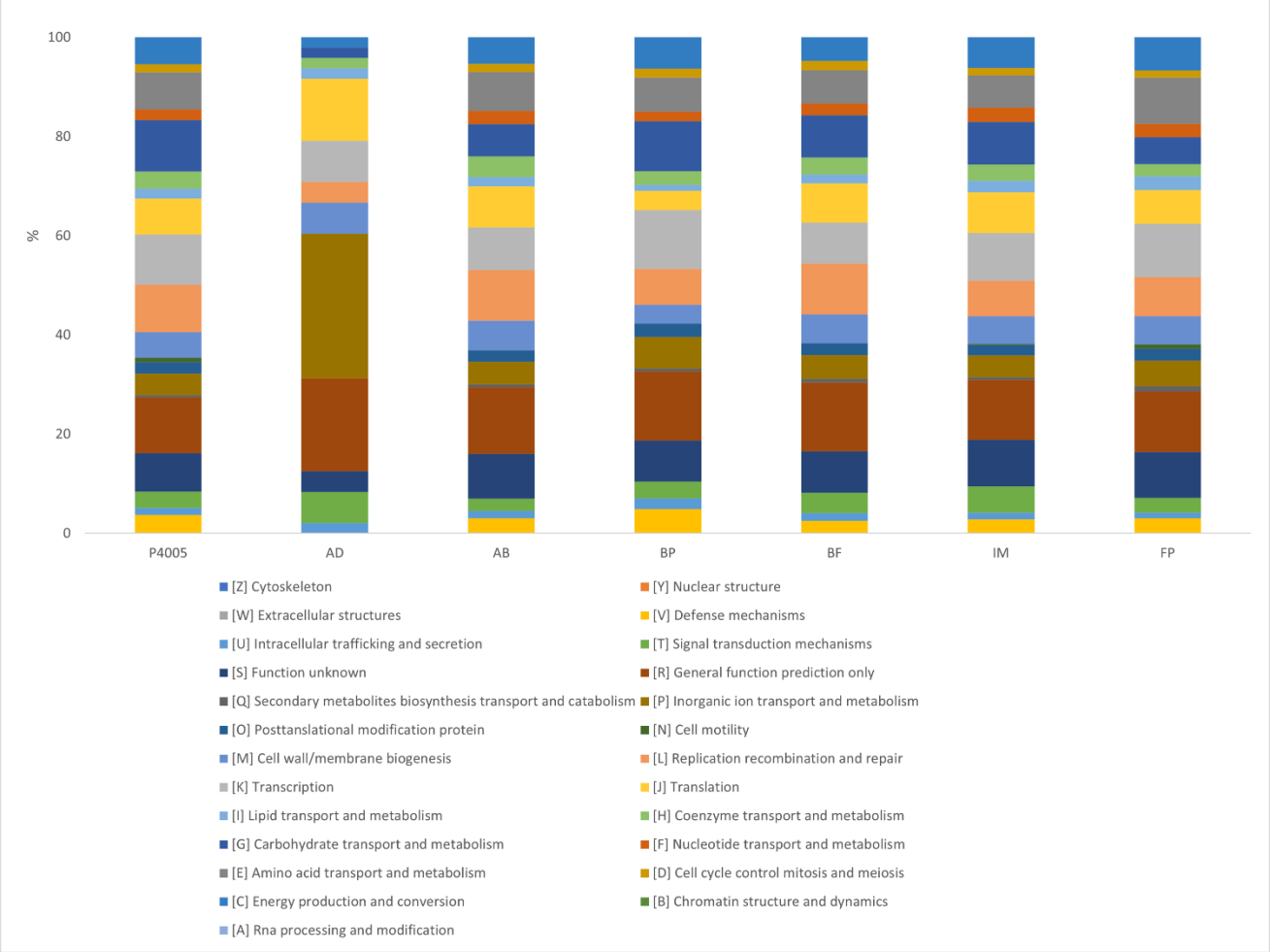

Fig.3 Comparison of the 25 general Cluster of Orthologous Groups (COGs) functional clusters of strain Marseille-P4005^T and closely related species.

P4005: Strain Marseille-P4005^T, **AD**: *Agathobaculum desmolans* ATCC 43058^T, **AB:** *Agathobaculum butyriciproducens* NB2B-10-MRS, **BP**: *Butyricicoccus pullicaecorum* DSM

23266^{T}, **BF:** *Butyricicoccus faecihominis* JCM 31056^{T}, **IM:** *Intestinibacillus massiliensis* Marseille-P3216^{T}, **FP:** *Flavonifractor plautii* ATCC 29863^{T}

Table.3 Genome comparison of strain Marseille-P4005^T with closely related species

Species	Genome accession number	Size (bp)	GC content (%)	Protein-encoding genes	Total no. of RNA genes	No. of proteins assigned to COGs	Total genes	Contigs
Strain Marseille-P4005^T	OMPN00000000.1	3,212,687	56.4	3,176	67	2148	3,242	2
Agathobaculum desmolans ATCC 43058^T	JNJN01000001.1	2,643,795	48.5	2,614	58	48	2,741	97
Agathobaculum butyriciproducens NB2B-10-MRS	JAMXVA010000001.1	3,002,197	52.9	2,837	102	1752	2,939	5
Butyricicoccus pullicaecorum DSM 23266^T	FUXW01000001.1	3,270,841	54.5	3,087	60	508	3,196	35
Butyricicoccus faecihominis JCM 31056T	BMQH01000001.1	2,995,907	55.6	2,880	73	1857	2,934	39
Intestinibacillus massiliensis Marseille-P3216T	FTLU00000000.1	2,814,054	NA	2,654	63	1822	2,817	109
Flavonifractor plautii ATCC 29863T	AGCK00000000.1	3,813,599	60.9	4,278	73	2279	4,296	344

NA: Not available

Using OrthoANI analysis, the strain exhibited the highest similarity (78.48%) with *Agathobaculum desmolans* strain ATCC 43058^{T} and the lowest one (67.58%) with *Flavonifractor plautii* strain ATCC 2986^{T} (**Fig.4**). Digital DDH (dDDH) values ranged from 20.1% between with *Intestinibacillus massiliensis* strain Marseille-P3216^{T} and *Agathobaculum desmolans* strain ATCC 43058^{T} to 29.1% between strain Marseille-P4005^{T} and *Butyricicoccus pullicaecorum* strain DSM 23266^{T} (**Table.4**).

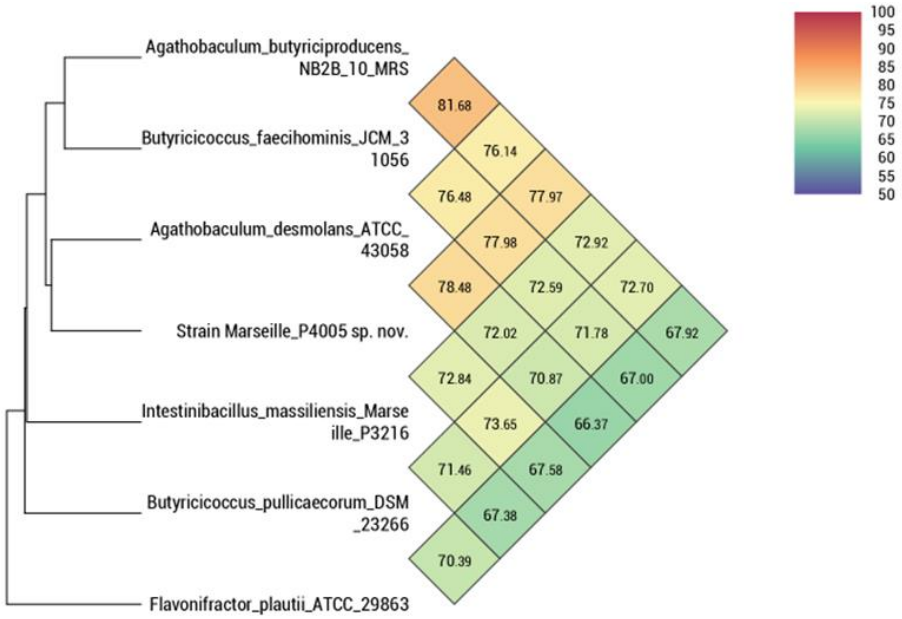

Fig.4 Heatmap generated with OrthoANI values using OAT software version 0.93.1 between Marseille-P4005 and the closely related species

Table.4 Digital DNA-DNA hybridization values (%) between strain Marseille-P4005 and the related species using formula 2 of the GGDC web server (Estimation was based on identities /HSP length)

Strains	AB	AD	BF	BP	FP	IM	P4005
AB	100	22	28.1	24.3	25.5	20.9	24.8
AD		100	23	23.8	19.4	20.1	22.7
BF			100	21.8	19.8	20.7	25
BP				100	32.5	20.9	**29.1**
FP					100	18.1	23.5
IM						100	20.8
P4005							100

P4005: Strain Marseille-P4005^T (OMPN00000000.1), **AD**: *Agathobaculum desmolans* ATCC 43058^T (JNJN01000001.1), **AB:** *Agathobaculum butyriciproducens* NB2B-10-MRS (JAMXVA010000001.1), **BP**: *Butyricicoccus pullicaecorum* DSM 23266^T (FUXW01000001.1), **BF:** *Butyricicoccus faecihominis* JCM 31056^T (BMQH01000001.1), **IM:** *Intestinibacillus massiliensis* Marseille-P3216^T (FTLU00000000.1), **FP:** *Flavonifractor plautii* ATCC 29863^T (AGCK00000000.1)

Values of OrthoANI and dDDH were lower than the critical values 95% and 70%, respectively, recommended to delineate a novel bacterial species (Ahn *et al.,* 2016; Ludwig *et al.,* 2021). The genome-based tree confirmed the close relationship of strain Marseille-P4005^T with *Agathobaculum* species (**Fig.5**).

Fig.5 Genome-based tree inferred using FastME 2.1.6.1 software. Scale bar represents 2% nucleotide divergence

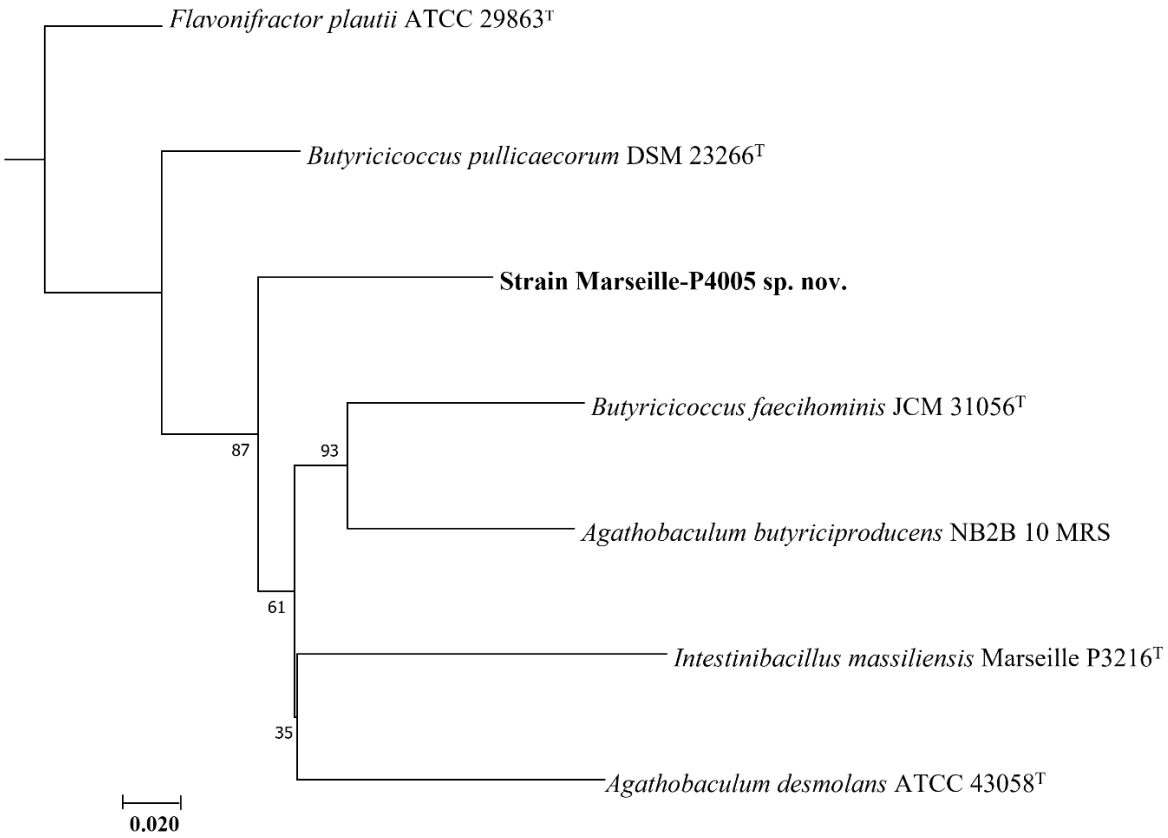

Conclusion

According to our findings, based on whole genome sequences analyses combined with the phenotypic data, we propose *Agathobaculum massiliense* sp. nov. as a novel species within the *Agathobaculum* genus, for which Marseille-P4005^T is the type strain.

Description of *Agathobaculum massiliense* sp. nov.

Agathobaculum massiliense (mas.si.li.en'se. L. masc. adj., massiliense, of Massilia, the latin name of Marseille, France, where the type strain was isolated). The type strain is Marseille-P4005^T (= CSUR P4005^T = CECT 9669^T). It was isolated from a stool of a healthy control. Optimal growth of strain Marseille-P4005 occurs at 37°C after 48h of incubation under strict anaerobic conditions on 5% sheep blood-enriched Columbia agar. Growth pH is 7. No salt

tolerance is observed. Colonies are punctiform, slightly convex, white and nonhaemolytic. It measures 1.03±0.21µm in length and 0.4±0.1µm in width. Using API® 50CH strip, positive reactions were obtained with glycerol, erythritol, dulcitol, D-mannitol, D-tagatose and potassium 5-cetogluconate. Using an API® ZYM strip, positive activities weare observed with Alkaline phosphatase, Lipase (C14), Leucine arylamidase, Trypsin, acid phosphatase, Naphtol phosphohydrolase and β-galactosidase. Strain Marseille-P4005 exhibited positive reaction only to gelatin when using API® 20A strip. The major fatty acids are the saturated structures as: Hexadecanoic acid (25 %), Octadecanoic acid (23 %) and Tetradecanoic acid (20 %). The genome was 3,212,687-bp- long with G+C content of 56.4 mol%. The pathogenic potential of strain Marseille-P4005^T is unknown. Strain Marseille-P4005^T was deposited in the Collection de Souches de l'Unité des Rickettsies (CSUR), as CSUR P4005 = CECT 9669.

Matrix-assisted laser desorption/ionization time-of-flight mass spectrometry (MALDI-TOF MS) spectrum

The MALDI-TOF MS spectrum of '*Agathobaculum massiliense*' strain Marseille-P4005^T is available online (https://www.mediterranee-infection.com/urms-data-base).

Collection deposite

Strain was deposited in the french collection (Collection de Souches de l'Unité des Rickettsies) as CSUR P4005= CECT 9669.

Accession numbers

The 16S rRNA and the genome of Marseille-P4005^T were deposited in Genbank under accession numbers LT985392.1 and OMPN00000000.1, respectively.

Acknowledgment

The authors thank Zouina Zahra MEKHALIF for her appreciated volunteering as a healthy donner in our study. The authors also thank Amael FADLANE for his technical assistance,

Ludivine BRECHARD for sequencing genome. We sincerely thank Takashi IRIE, Kyoko IMAI, Taku SAKAZUME, Yusuke OMINAMI, Hisada AKIKO and the Hitachi team of Japan (Hitachi High-Tech Corporation, Tokyo, Japan) for the collaborative study conducted together with IHU Méditerranée Infection, and for the installation of a SU5000 microscope at IHU Méditerranée Infection facility.

References

Ahn, S., Jin, T.-E., Chang, D.-H., Rhee, M.-S., Kim, H. J., Lee, S. J., Park, D.-S., & Kim, B.-C. 2016. *Agathobaculum butyriciproducens* gen. nov.; sp. nov., a strict anaerobic, butyrate-producing gut bacterium isolated from human faeces and reclassification of *Eubacterium desmolans* as *Agathobaculum desmolans* comb. nov. *International Journal of Systematic and Evolutionary Microbiology*, *66*(9), 3656–3661. https://doi.org/10.1099/ijsem.0.001195

Anani, H., Abdallah, R. A., Khoder, M., Fontanini, A., Mailhe, M., Ricaboni, D., Raoult, D., & Fournier, P.-E. (2019). *Colibacter massiliensis* gen. nov. sp. nov., a novel Gram-stain-positive anaerobic diplococcal bacterium, isolated from the human left colon. *Scientific Reports*, *9*(1), 17199. https://doi.org/10.1038/s41598-019-53791-1

Bellali, S., Haddad, G., Pham, T.-P.-T., Iwaza, R., Ibrahim, A., Armstrong, N., Fadlane, A., Couderc, C., Diallo, A., Sokhna, C., Million, M., Raoult, D., & Tidjani Alou, M. (2022). Draft genomes and descriptions of *Urmitella timonensis* gen. nov., sp. nov. And *Marasmitruncus massiliensis* gen. nov., sp. nov., isolated from severely malnourished African children using culturomics. *Antonie van Leeuwenhoek*. https://doi.org/10.1007/s10482-022-01777-x

BioMérieux France—Diagnostic Microbiologique clinique ou industriel Available online: Https://www.biomerieux.fr/ (accessed on June 8, 2022). (n.d.).

Caporaso, J. G., Lauber, C. L., Walters, W. A., Berg-Lyons, D., Huntley, J., Fierer, N., Owens, S. M., Betley, J., Fraser, L., Bauer, M., Gormley, N., Gilbert, J. A., Smith, G., & Knight, R. (2012). Ultra-high-throughput microbial community analysis on the Illumina HiSeq and MiSeq platforms. *The ISME Journal*, *6*(8), 1621–1624. https://doi.org/10.1038/ismej.2012.8

307 Eeckhaut, V., Van Immerseel, F., Teirlynck, E., Pasmans, F., Fievez, V., Snauwaert, C.,
308 Haesebrouck, F., Ducatelle, R., Louis, P., & Vandamme, P. 2008. *Butyricicoccus*
309 *pullicaecorum* gen. nov., sp. nov., an anaerobic, butyrate-producing bacterium isolated
310 from the caecal content of a broiler chicken. *International Journal of Systematic and*
311 *Evolutionary Microbiology*, *58*(12), 2799–2802. https://doi.org/10.1099/ijs.0.65730-0
312 Fontaine, B., Perrard, A., & Bouchet, P. (2012). 21 years of shelf life between discovery and
313 description of new species. *Current Biology: CB*, *22*(22), R943-944.
314 https://doi.org/10.1016/j.cub.2012.10.029
315 Kumar, S., Stecher, G., Li, M., Knyaz, C., & Tamura, K. (2018). MEGA X: Molecular
316 Evolutionary Genetics Analysis across Computing Platforms. *Molecular Biology and*
317 *Evolution*, *35*(6), 1547–1549. https://doi.org/10.1093/molbev/msy096
318 Lagier, J.-C., Armougom, F., Million, M., Hugon, P., Pagnier, I., Robert, C., Bittar, F.,
319 Fournous, G., Gimenez, G., Maraninchi, M., Trape, J.-F., Koonin, E. V., La Scola, B., &
320 Raoult, D. (2012). Microbial culturomics: Paradigm shift in the human gut microbiome
321 study. *Clinical Microbiology and Infection*, *18*(12), 1185–1193.
322 https://doi.org/10.1111/1469-0691.12023
323 Lagier, J.-C., Edouard, S., Pagnier, I., Mediannikov, O., Drancourt, M., & Raoult, D. (2015).
324 Current and past strategies for bacterial culture in clinical microbiology. *Clinical*
325 *Microbiology Reviews*, *28*(1), 208–236. https://doi.org/10.1128/CMR.00110-14
326 Lagier, J.-C., Hugon, P., Khelaifia, S., Fournier, P.-E., La Scola, B., & Raoult, D. (2015). The
327 rebirth of culture in microbiology through the example of culturomics to study human
328 gut microbiota. *Clinical Microbiology Reviews*, *28*(1), 237–264.
329 https://doi.org/10.1128/CMR.00014-14
330 Lagier, J.-C., Khelaifia, S., Alou, M. T., Ndongo, S., Dione, N., Hugon, P., Caputo, A.,
331 Cadoret, F., Traore, S. I., Seck, E. H., Dubourg, G., Durand, G., Mourembou, G.,

Guilhot, E., Togo, A., Bellali, S., Bachar, D., Cassir, N., Bittar, F., Raoult, D. (2016). Culture of previously uncultured members of the human gut microbiota by culturomics. *Nature Microbiology*, *1*, 16203. https://doi.org/10.1038/nmicrobiol.2016.203

Ludwig, W., Viver, T., Westram, R., Francisco Gago, J., Bustos-Caparros, E., Knittel, K., Amann, R., & Rossello-Mora, R. (2021). Release LTP_12_2020, featuring a new ARB alignment and improved 16S rRNA tree for prokaryotic type strains. *Systematic and Applied Microbiology*, *44*(4), 126218. https://doi.org/10.1016/j.syapm.2021.126218

Matuschek, E., Brown, D. F. J., & Kahlmeter, G. (2014). Development of the EUCAST disk diffusion antimicrobial susceptibility testing method and its implementation in routine microbiology laboratories. *Clinical Microbiology and Infection*, *20*(4), O255–O266. https://doi.org/10.1111/1469-0691.12373

Meier-Kolthoff, J. P., & Göker, M. (2019). TYGS is an automated high-throughput platform for state-of-the-art genome-based taxonomy. *Nature Communications*, *10*(1), 2182. https://doi.org/10.1038/s41467-019-10210-3

Morris, G. N., Winter, J., Cato, E. P., Ritchie, A. E., & Bokkenheuser, V. D. Y. 1986. *Eubacterium desmolans* sp. nov., a steroid desmolase-producing species from cat fecal flora. *International Journal of Systematic and Evolutionary Microbiology*, *36*(2), 183–186. https://doi.org/10.1099/00207713-36-2-183

Prjibelski, A., Antipov, D., Meleshko, D., Lapidus, A., & Korobeynikov, A. (2020). Using SPAdes De Novo Assembler. *Current Protocols in Bioinformatics*, *70*(1), e102. https://doi.org/10.1002/cpbi.102

Ramasamy, D., Mishra, A. K., Lagier, J.-C., Padhmanabhan, R., Rossi, M., Sentausa, E., Raoult, D., & Fournier, P.-E. 2014. (n.d.). A polyphasic strategy incorporating genomic data for the taxonomic description of novel bacterial species. *International Journal of*

Systematic and Evolutionary Microbiology, *64*(Pt_2), 384–391. https://doi.org/10.1099/ijs.0.057091-0

Ricaboni, D., Mailhe, M., Vitton, V., Cadoret, F., Fournier, P.-E., & Raoult, D. (2017). '*Intestinibacillus massiliensis*' gen. nov., sp. nov., isolated from human left colon. *New Microbes and New Infections*, *17*, 18–20. https://doi.org/10.1016/j.nmni.2016.12.008

Sasser, M. (2006). Bacterial identification by gas chromatographic analysis of fatty acids methyl esters (GC-FAME). *Newark, NY: Microbial ID*.

Seemann, T. (2014). Prokka: Rapid prokaryotic genome annotation. *Bioinformatics (Oxford, England)*, *30*(14), 2068–2069. https://doi.org/10.1093/bioinformatics/btu153

Seng, P., Drancourt, M., Gouriet, F., La Scola, B., Fournier, P.-E., Rolain, J. M., & Raoult, D. (2009). Ongoing revolution in bacteriology: Routine identification of bacteria by matrix-assisted laser desorption ionization time-of-flight mass spectrometry. *Clinical Infectious Diseases*, *49*(4), 543–551. https://doi.org/10.1086/600885

Takada, T., Watanabe, K., Makino, H., & Kushiro, A. 2016. Reclassification of *Eubacterium desmolans* as *Butyricicoccus desmolans* comb. nov., and description of *Butyricicoccus faecihominis* sp. nov., a butyrate-producing bacterium from human faeces. *International Journal of Systematic and Evolutionary Microbiology*, *66*(10), 4125–4131. https://doi.org/10.1099/ijsem.0.001323

Conflict of Interest

The authors would like to declare that Didier Raoult is a consultant in microbiology for the Hitachi High-Tech Corporation from March 2018 until March 2020. Otherwise, the authors declare no other conflict of interest.

Funding Resources

This work was supported by the French Government under the « Investissements d'avenir » (Investments for the Future) program managed by the Agence Nationale de la Recherche (ANR, fr: National Agency for Research), (reference: Méditerranée Infection 10-IAHU-03). This work was supported by Région Provence Alpes Côte d'Azur and European funding FEDER PRIMI.

Transparency Declaration

The authors declare that they have no competing interests. The stool samples used in this study are approved by the ethics statement of IFR48 (Marseille, France). Authorization number 09-022 with the consent of the subject.

Article 8

Description of *Ornithinibacillus timonensis* sp. nov.,*Thalassobacillus timonensis* sp. nov., *Sutcliffiella maliensis* sp. nov., *Pseudalkalibacillus massiliomalei* sp. nov., *Halobacillus maliensis* sp. nov., *Virgibacillus cacae* sp. nov., *Lentibacillus ihumii* sp. nov., *Rossellomorea faecium* sp. nov., eight moderate halophilic new species isolated from Malian healthy children

Salimata Konate, **Malak Zoaiter**, Aminata Camara, Ogobara Doumbo, Abdoulaye Djimde, Safiatou Niare, Abdoulaye Kassoum Kone, Issa Traore, Pierre-Edouard Fournier, Mahamadou Ali Thera, Maryam Tidjani Alou, Didier Raoult, Matthieu Million

-To be submitted-

Description of *Ornithinibacillus timonensis* sp.nov., *Thalassobacillus timonensis sp.nov.*, *Sutclifiella maliensis* sp.nov., *Halobacillus maliensis* sp.nov., *Pseudalkalibacillus massiliomalei* sp.nov., *Virgibacillus cacae* sp.nov., *Lentibacillus ihumii* sp.nov., *Rossellomorea faecium* sp.nov. eight moderate halophilic new species isolated from Malian healthy children

Salimata Konaté[1], Malak Zoaiter[3], Aminata Camara[1], Ogobara Doumbo[1], Abdoulaye Djimdé[1], Safiatou Niaré[1], Abdoulaye Kassoum Koné[1], Issa Traoré[2], Pierre-Edouard Fournier[3], Mahamadou Ali Théra[1], Maryam Tidjani Alou[4], Didier Raoult[4], Matthieu Million[4]

[1]Malaria Research and Training Center

[2]Centre de Santé de Reference de Kalaban-coro

[3] IHU Méditerranée Infection, IRD, AP-HM, SSA, VITROME, Marseille, France

[4] IHU Méditerranée Infection, IRD, MEPHI, Marseille, France.

[*]**Corresponding author**

Contact : Matthieu MILLION

IHU Méditerranée Infection, MEPHI, IRD, 19-12 Bd Jean Moulin 13005 Marseille, France.

Email : matthieumillion@gmail.com

Tel: +33 413 732 401, Fax: +33 413 732 402

DRAFT

Introduction

Culturomics is a new approach using matrix-assisted laser desorption/ionization time-of-flight (MALDI-TOF MS) for bacteria identification and aiming to cultivate individually all bacterial species from the human gut and also from other human mucosa microbiota (Senghor et al. 2017a). This approach allows to highlight the key role of gut microbiota in children nutrition by a dramatic decrease in anaerobic species (Tidjani Alou et al. 2017) the methanogen depletion and pathogen proliferation (Pham et al. 2019). However, exploring halophilic species remain under investigated in severe acute malnourished children but required for exhaustive gut exploration in severe acute malnutrition. Adding halophilic medium into usual axenic media in the context of culturomics approach allows us to discover eight news halophilic species belonging different genus as well as *Pseudalkalibacillus, Halobacillus, Lentibacillus, Ornithinibacillus, Thalassobacillus, Virgibacillus* and *Sutcliffiella*. This study aimed to describe the genomic and phylogenetic characteristics of these news species isolated from healthy Malian children.

DRAFT

Materials and methods

Isolation and identification

Ornithinibacillus timonensis sp. nov. (Q3649), *Thalassobacillus timonensis* (Q3652), *Halobacillus maliensis* (Q4110), *PseudalkaliBacillus massiliomalei* sp. nov (Q4114), *Virgibacillus cacae* (Q4221), *Lentibacillus ihumii* (Q4222), *Rosellomerea faecium* (Q4225) *Sutcliffiella maliensis* (Q4115) were isolated from healthy children under five years living in Mali in the context of case control study comparing severe acute malnourished children versus healthy children. The stool salinity was measured by the salinity refractometer (Thermo Scientific, Villebon-sur-Yvette, France) and performed as described in the previous study (Senghor et al. 2017b). Colonies were purified after subculturing for identification by MALDI-TOF MS. According grow conditions, stools were inoculated in the aerobic blood culture bottles (Becton Dickinson, Le Pont-de-Claix, France) and the halophilic bottle containing home medium which was developed at the IHU laboratory. Colonies were purified after subculturing for identification by MALDI TOF mass spectrometry.

DNA extraction and sequencing

Genomic DNA (gDNA) of all strains were extracted on the EZ1 biorobot (Qiagen, Hilden, Germany) using EZ1 DNA Tissue kit and then quantified by a Qubit assay (Thermofisher scientific). Sequencing was performed by two technologies on Miseq sequencer (Illumina Inc, San Diego, CA, USA) using the Nextera XT DNA sample prep kit (Illumina) and on GridION sequencer (Oxford Nanopore Technologies) using 1D genomic DNA by ligation kit (Oxford Nanopore Technologies).

DRAFT

16SrRNA phylogenetic analysis

16S rRNA sequences of the novel strains were extracted from genomes using contest16S (Ezbiocloud.net) (Lee et al. 2017) and then compared on Genbank database. The sequences of the related neighbors were downloaded from NCBI. Evolutionary analyses were inferred using the Mega software. Nucleotide sequences were aligned using clustal W. Phylogenetic distances were calculated using Maximum likelihood algorithm and the tamura-nei model. *Streptococcus pneumoniae* NCTC7465 was used as an outgroup (genome accession number: LN831051.1).

Genome annotation and comparison

The reads of the novel isolates were assembled using SPADES version 3.14.0 (Bankevich et al. 2012) and annotated by Prokka version 1.14.5 (Seemann 2014). Genome identities values were determined by the Average Nucleotide Identity (ANI) (Arahal 2014) and the digital DNA-DNA hybridization (Goris et al. 2007) tools. ANI was performed using pyani version 0.2.11 and dDDH using Genome-to-Genome Distance calculator version 3 (GGDC) available online https://ggdc.dsmz.de. The distance formula 2 was used to calculate dDDH values. Genome-based tree was constructed using IQ-tree (Minh et al. 2020) after an alignment with MAFFT software (Katoh et al. 2002).

Results

Identification and 16S rRNA and phylogenetic analysis

The isolated strains failed to be identified by MALDI-TOF MS, so we compared the 16S rRNA gene sequence with the closest related species. The blast of 16SrRNA genes in Genbank showed that strain Q3649 had 98.8% gene identity with *Ornithinibacillus californiensis* strain MB-9, Q3652 had 99.6% gene identity with *Thalassobacillus devorans* strain G-19, Q4110 had 98.1%

DRAFT

gene identity with *Halobacillus litoralis* strain SL-4, Q4114 had 98.4% gene identity with *Pseudalkalibacillus berkeleyi* strain KMM 6244, Q4115 had 99.2% gene identity with *Sutcliffiella horikoshii* strain DSM 8719, Q4221 had 97.5% gene identity with *Virgibacillus flavescens* strain S1-20, Q4222 had 96.9% gene identity with *Lentibacillus salicampi* strain SF-20, and Q4225 had 98.41% gene identity with *Rosellomorea aquimaris* strain TF-12. The 16SrRNA-based tree confirmed the affiliation of the strains Q3649, Q3652, Q4110, Q4114, Q4115, Q4221, Q4222 and Q4225 to *Ornithinibacillus, Thalassobacillus, Halobacillus, Pseudalkalibacillus, Sutcliffiella, Virgibacillus, Lentibacillus* and *Rossellomorea* genus, respectively. **Figure.1** revealed the phylogenetic relationship between the novel isolates and the closest related strains.

Genome comparison

The genome sizes of the novel isolates ranged from 3.27 to 4.53 Mb. The genomic DNA contents G+C ranged from 42.1 to 43.7 mol%. Data were showed in **Table.3.** ANI values between the eight species and the related species ranged from 69% to 92% **(Figure.2).** The highest values were obtained as following, 82% between strain Q3649 and *Ornithinibacillus californiensis* strain DSM 16628, 92% between strain Q3652 and *Thalassobacillus cyri* strain CCM7597, 73% between strain Q4110 is and *Halobacillus litoralis* strain SL4 and *Halobacillus halophilus* strain DSM 2266 , 74% between strain Q4114 and *Pseudalkalibacillus berkeleyi* KCTC 12718 , 81% between strain Q4115 and *Sutcliffiella horikoshii* strain DSM 8719, 77% between strain Q4221 and *Virgibacillus necropolis* strain LMG 19488, 79% between strain Q4222 and *Lentibacillus halodurans* strain CGMCC 1.3702 and *Lentibacillus salicampi* strain ATCC BAA 719, 73% between strain Q4225 and *Rossellomorea aquimaris* strain TF12 and *Rossellomorea marisflavi* strain JCM 11544. Digital DNA-DNA hybridization values ranged

DRAFT

from 17.3 % to 45.2%.The highest value was obtained between Q3652 and *Thalassobacillus cyri* strain CCM7597 **(Table.1).** ANI and dDDH values were lower than the critical thresholds 95% and 70%, respectively, to delineate a new species (Goris et al.). Genome-based phylogenetic tree showed the phylogenetic relationship between all isolated specie and their neighbors **(Figure.3).**

Conclusion

Based on our results, we propose to define Q3649, Q3652, Q4110, Q4114, Q4115, Q4221, Q4222, and Q4225 strains as new species within *Ornithinibacillus*, *Thalassobacillus*, *Halobacillus*, *Pseudalkalibacillus*, *Sutcliffiella*, *Virgibacillus*, *Lentibacillus* and *Rossellomorea* genus, respectively.

DRAFT

References

Arahal DR (2014) Chapter 6 - Whole-Genome Analyses: Average Nucleotide Identity. In: Goodfellow M, Sutcliffe I, Chun J (eds) Methods in Microbiology. Academic Press, pp 103–122

Bankevich A, Nurk S, Antipov D, et al (2012) SPAdes: a new genome assembly algorithm and its applications to single-cell sequencing. J Comput Biol J Comput Mol Cell Biol 19:455–477. https://doi.org/10.1089/cmb.2012.0021

Goris J, Konstantinidis KT, Klappenbach JA, et al (2007) DNA–DNA hybridization values and their relationship to whole-genome sequence similarities. Int J Syst Evol Microbiol 57:81–91. https://doi.org/10.1099/ijs.0.64483-0

Katoh K, Misawa K, Kuma K, Miyata T (2002) MAFFT: a novel method for rapid multiple sequence alignment based on fast Fourier transform. Nucleic Acids Res 30:3059–3066. https://doi.org/10.1093/nar/gkf436

Lee I, Chalita M, Ha S-M, et al (2017) ContEst16S: an algorithm that identifies contaminated prokaryotic genomes using 16S RNA gene sequences. Int J Syst Evol Microbiol 67:2053–2057. https://doi.org/10.1099/ijsem.0.001872

Minh BQ, Schmidt HA, Chernomor O, et al (2020) IQ-TREE 2: New Models and Efficient Methods for Phylogenetic Inference in the Genomic Era. Mol Biol Evol 37:1530–1534. https://doi.org/10.1093/molbev/msaa015

Pham T-P-T, Tidjani Alou M, Bachar D, et al (2019) Gut Microbiota Alteration is Characterized by a Proteobacteria and Fusobacteria Bloom in Kwashiorkor and a Bacteroidetes Paucity in Marasmus. Sci Rep 9:9084. https://doi.org/10.1038/s41598-019-45611-3

Seemann T (2014) Prokka: rapid prokaryotic genome annotation. Bioinforma Oxf Engl 30:2068–2069. https://doi.org/10.1093/bioinformatics/btu153

Senghor B, Khelaifia S, Bassène H, et al (2017a) “Gracilibacillus phocaeensis” sp. nov., “Sediminibacillus massiliensis” sp. nov. and “Virgibacillus ndiopensis” sp. nov., three halophilic species isolated from salty human stools by culturomics. New Microbes New Infect 20:51–54. https://doi.org/10.1016/j.nmni.2017.08.006

Senghor B, Seck EH, Khelaifia S, et al (2017b) Description of “Bacillus dakarensis” sp. nov., “Bacillus sinesaloumensis” sp. nov., “Gracilibacillus timonensis” sp. nov., “Halobacillus massiliensis” sp. nov., “Lentibacillus massiliensis” sp. nov., “Oceanobacillus senegalensis” sp. nov., “Oceanobacillus timonensis” sp. nov., “Virgibacillus dakarensis” sp. nov. and “Virgibacillus marseillensis” sp. nov., nine halophilic new species isolated from human stool. New Microbes New Infect 17:45–51. https://doi.org/10.1016/j.nmni.2017.01.010

DRAFT

149 Tidjani Alou M, Million M, Traore SI, et al (2017) Gut Bacteria Missing in Severe Acute
150 Malnutrition, Can We Identify Potential Probiotics by Culturomics? Front Microbiol
151 8:899. https://doi.org/10.3389/fmicb.2017.00899

152

DRAFT

Figure 1. The16S rRNA-based tree showing the taxonomic positions of all the eight isolates with the related neighbors. The tree was rooted using neighbor-joining method. Bootstrap values (%) were calculated from 1000 replicates. Accession numbers were indicated in brackets. Scale bar represents 2% nucleotide sequence divergence. *Streptococcus pneumoniae* strain NCTC 7465 was used as an outgroup.

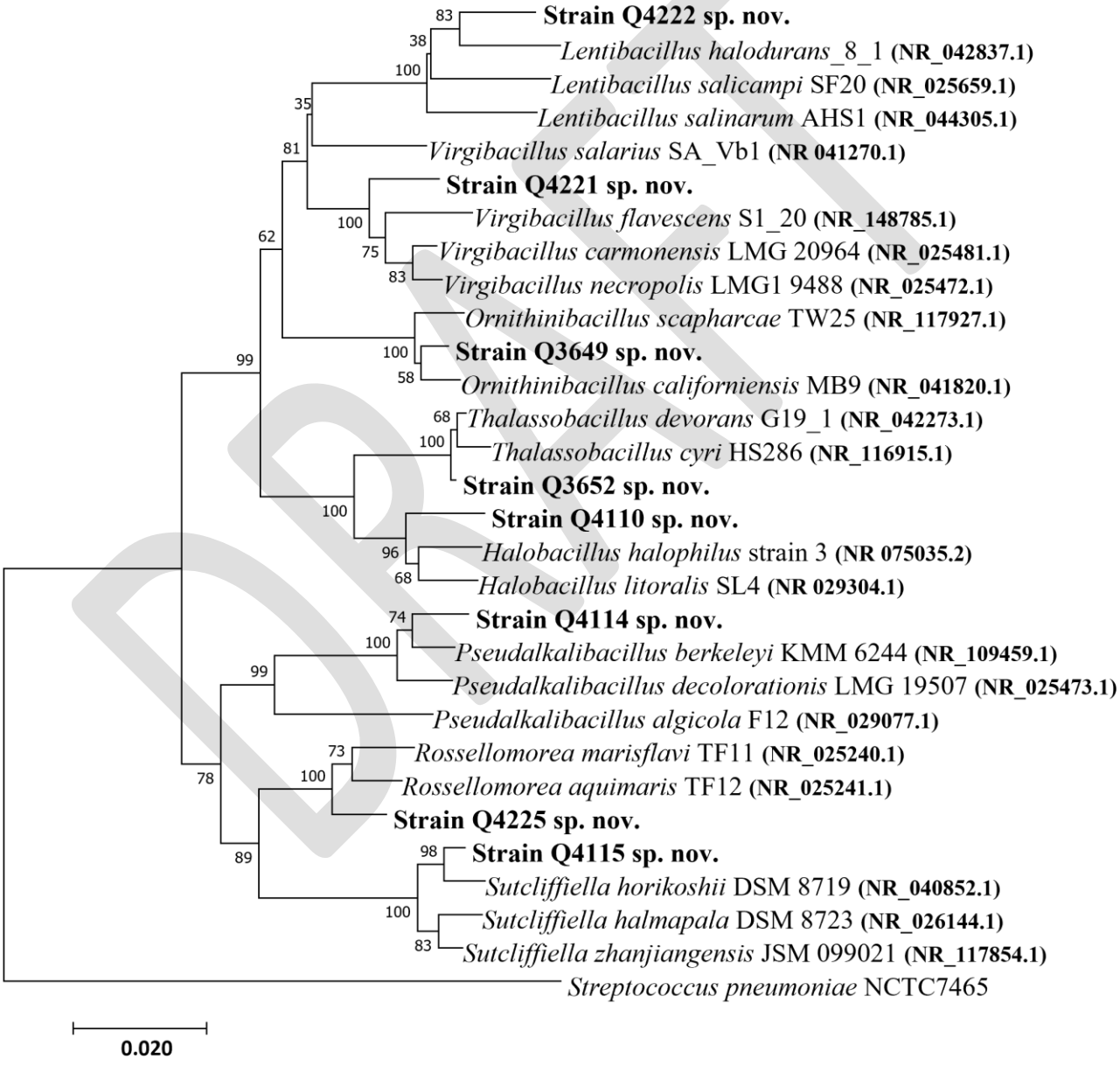

DRAFT

Figure 2 . ANI values between the eight strains and the related species. Values were calculated using PYANI software.

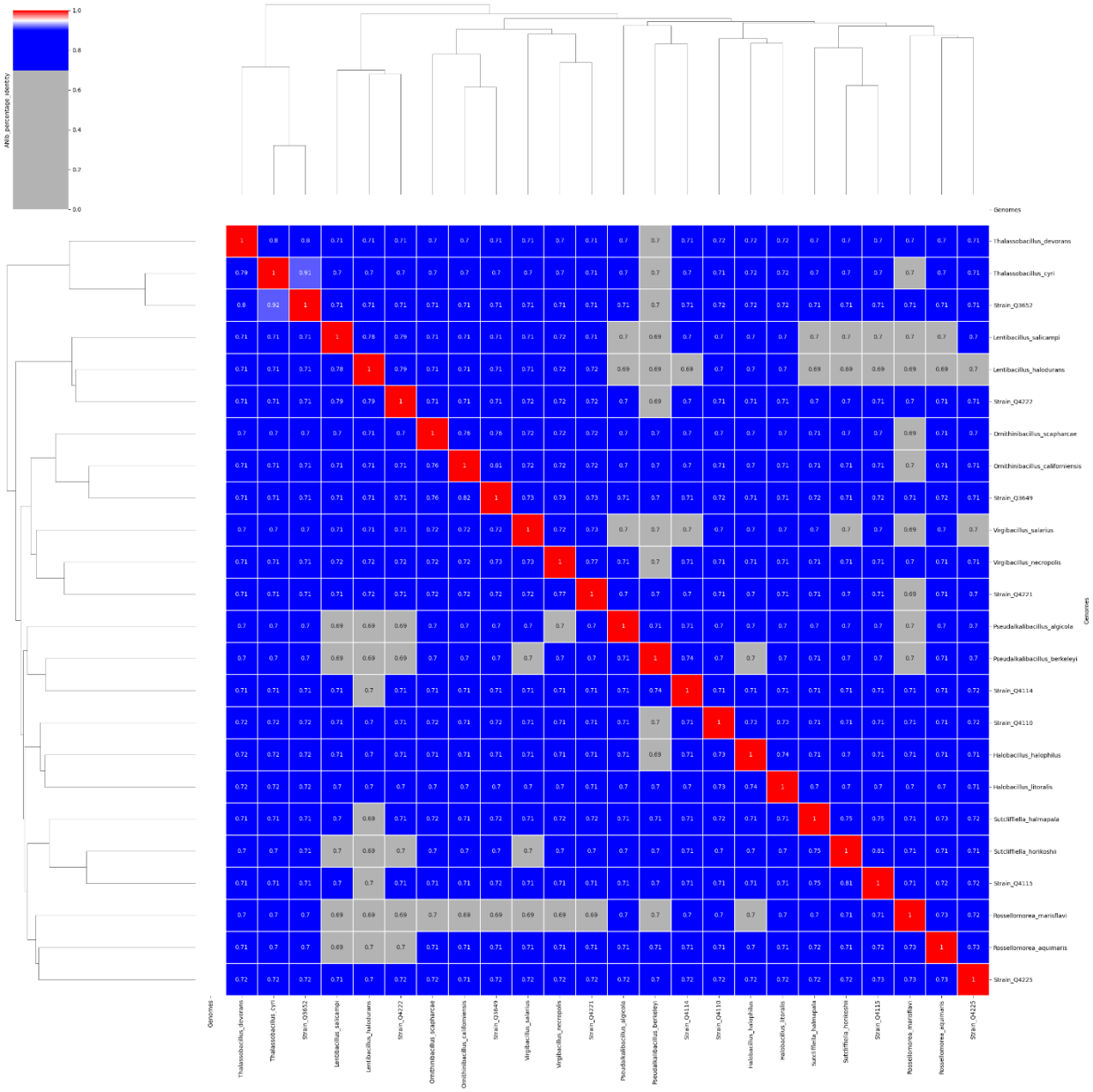

Table 1 . Genome size and DNA G+C content of each isolate.

Isolates	Nb of contigs	Size (bp)	G+C content
Q3649	2	3,680,869	37.10%
Q3652	16	4,293,610	42.60%
Q4110	5	3,268,807	43.70%
Q4114	7	4,444,057	42.10%
Q4115	5	4,052,493	40.90%
Q4221	10	3,830,934	36.80%
Q4222	3	3,522,964	42.80%
Q4225	1	4,530,265	42.10%

DRAFT

175 **Table 1.** Digital DNA-DNA hybridization values between our isolates and the related species.

176 Values were calculated using formula 2

DRAFT

	PA	PB	HH	HL	LH	LS	OC	OS	RA	RM	Q3649	Q3652	Q4110	Q4114	Q4115	Q4221	Q4222	Q4225	SP	SH	SHO	TC	TD	VN	VS
PA	**100**																								
PB	19.8	**100**																							
HH	23.1	18.7	**100**																						
HL	20.4	17.7	19.2	**100**																					
LH	30	26.5	20.4	20.8	**100**																				
LS	30.5	17.3	26.9	21.6	22.2	**100**																			
OC	22.1	20.9	25.8	22.3	18.8	21.6	**100**																		
OS	21.1	20.2	28.2	21.6	18.7	21.3	19.8	**100**																	
RA	22.1	19.8	22.3	20.8	26.1	30.4	22.4	27.4	**100**																
RM	21.6	18.5	22.7	24.9	25	32.8	22.8	22.4	18.6	**100**															
Q3649	25.2	23.6	31.6	26.3	20.8	23.2	24.6	20.1	22.4	25.2	**100**														
Q3652	23.9	17.3	22.2	21.7	20.9	26.4	25.2	25.5	26.5	27.2	30.4	**100**													
Q4110	32	20.2	20.4	20.6	21.4	27.8	27.9	27.7	22.1	23.2	33.3	22.9	**100**												
Q4114	25.8	19	27.9	24	24.6	23.7	31	29.6	27.7	23.7	36.4	27.3	27.1	**100**											
Q4115	26.1	18	35.7	28.6	28.3	25.3	22.3	34.6	23.7	23.1	28.8	26	25.2	31.3	**100**										
Q4221	22.7	18.9	25.3	20.8	18.8	20.8	21	20.6	23.6	29.9	22.7	24.9	27.5	34	24.6	**100**									
Q4222	37.3	30.1	28.4	35.6	22.9	23.8	24.6	25.1	32.3	30.3	25.7	37.6	36.1	37.8	32.4	23.7	**100**								
Q4225	27.3	20	32.9	24.8	26	32	26.4	26.7	23	22.5	37.4	29.2	29.3	38.4	28.6	27.4	35.9	**100**							
SP	28.8	33.1	26.2	23.1	24.9	25.4	28.3	27.4	24.3	28.1	27	27.3	26.5	26.8	26.2	24	25.5	25.3	**100**						
SH	30.3	18.6	27.4	31.7	31.9	32.1	31.2	35.2	23.2	24.4	28.1	26.2	26.1	31.5	20.1	26	27.3	30.3	26	**100**					
SHO	22.9	19	23.1	22.9	25.7	20.7	21.5	21.3	20	21.9	26.5	23.4	22.6	28.2	25	19.9	22.8	25.8	25	20	**100**				
TC	20.5	21.3	21	19.5	20.1	21.5	22.3	22	22.9	20	27.2	45.2	23.4	27.4	24	22.4	31.5	26.3	28	24	21	**100**			
TD	22.3	20.6	20.8	18.7	21.2	20.9	23.8	21.9	22	21.9	28.7	23.4	21	26.7	31	22.6	34	26.4	29	24	22	23	**100**		
VN	33.5	18.8	32.6	22.9	19.2	25.4	22.5	25.2	26.4	41.1	25.6	24.3	28	31.9	29.8	22.4	28.5	31.1	27	26	25	24	25.5	**100**	
VS	22	20.8	28.4	23.3	19.7	20	18.6	19.2	22.3	21.2	21	28.6	31.7	29.4	25.3	19.3	21.7	33.9	26	27	25	24	22.7	21	**100**

DRAFT

Figure 3. Genome-based phylogenetic tree inferred by IQ-TREE software. Genomes were aligned using MAFFT. Values at the node represents bootstrap values obtained 1000 replicates. *Streptococcus pneumoniae* NCTC 7465 was used as outgroup. Scale bar represents 5% nucleotide divergence.

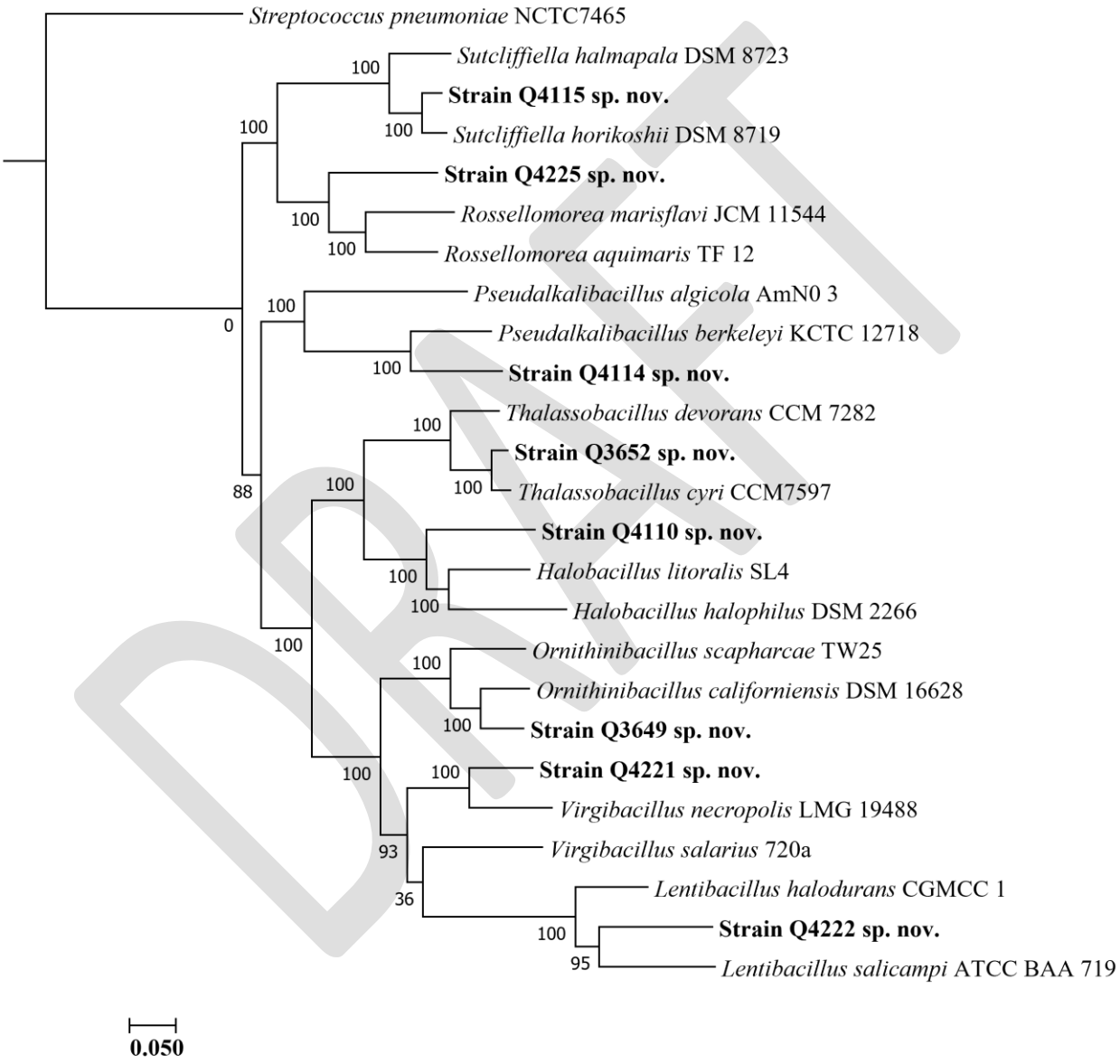

DRAFT

Bibliographie

Bibliographie

1. Whitman WB, Coleman DC, Wiebe WJ. Prokaryotes: the unseen majority. Proc Natl Acad Sci U S A **1998**; 95:6578–6583.

2. Hugon P, Dufour J-C, Colson P, Fournier P-E, Sallah K, Raoult D. A comprehensive repertoire of prokaryotic species identified in human beings. Lancet Infect Dis **2015**; 15:1211–1219.

3. Stewart EJ. Growing unculturable bacteria. J Bacteriol **2012**; 194:4151–4160.

4. Bollmann A, Lewis K, Epstein SS. Incubation of Environmental Samples in a Diffusion Chamber Increases the Diversity of Recovered Isolates. Appl Environ Microbiol **2007**; 73:6386–6390.

5. Kaeberlein T, Lewis K, Epstein SS. Isolating 'uncultivable' microorganisms in pure culture in a simulated natural environment. Science **2002**; 296:1127–1129.

6. Nichols D, Lewis K, Orjala J, et al. Short Peptide Induces an "Uncultivable" Microorganism To Grow In Vitro. Appl Environ Microbiol **2008**; 74:4889–4897.

7. Lagier J-C, Armougom F, Million M, et al. Microbial culturomics: paradigm shift in the human gut microbiome study. Clin Microbiol Infect **2012**; 18:1185–1193.

8. Greub G. Culturomics: a new approach to study the human microbiome. Clin Microbiol Infect **2012**; 18:1157–1159.

9. Lagier J-C, Khelaifia S, Alou MT, et al. Culture of previously uncultured members of the human gut microbiota by culturomics. Nat Microbiol **2016**; 1:1–8.

10. Dickson I. Culturomics: illuminating microbial dark matter. Nat Rev Gastroenterol Hepatol **2017**; 14:3–3.

11. Zha Y, Chong H, Yang P, Ning K. Microbial dark matter: from discovery to applications. Genomics Proteomics Bioinformatics **2022**; Available at: https://www.sciencedirect.com/science/article/pii/S1672022922000377. Accessed 18 September 2022.

12. Seng P, Drancourt M, Gouriet F, et al. Ongoing revolution in bacteriology: routine identification of bacteria by matrix-assisted laser desorption ionization time-of-flight mass spectrometry. Clin Infect Dis Off Publ Infect Dis Soc Am **2009**; 49:543–551.

13. Seng P, Abat C, Rolain JM, et al. Identification of rare pathogenic bacteria in a clinical microbiology laboratory: impact of matrix-assisted laser desorption ionization-time of flight mass spectrometry. J Clin Microbiol **2013**; 51:2182–2194.

14. Lagier J-C, Dubourg G, Million M, et al. Culturing the human microbiota and culturomics. Nat Rev Microbiol **2018**; 16:540–550.

15. Tvede M, Tinggaard M, Helms M. Rectal bacteriotherapy for recurrent Clostridium difficile-associated diarrhoea: results from a case series of 55 patients in Denmark 2000-2012. Clin Microbiol Infect Off Publ Eur Soc Clin Microbiol Infect Dis **2015**; 21:48–53.

16. Bannantine JP, Baechler E, Zhang Q, Li L, Kapur V. Genome Scale Comparison of Mycobacterium avium subsp. paratuberculosis with Mycobacterium avium subsp. avium Reveals Potential Diagnostic Sequences. J Clin Microbiol **2002**; 40:1303–1310.

17. Deurenberg RH, Bathoorn E, Chlebowicz MA, et al. Application of next generation sequencing in clinical microbiology and infection prevention. J Biotechnol **2017**; 243:16–24.

18. Fournier P-E, Raoult D. Prospects for the Future Using Genomics and Proteomics in Clinical Microbiology. Annu Rev Microbiol **2011**; 65:169–188.

19. Raoult D, Ogata H, Audic S, et al. Tropheryma whipplei Twist: a human pathogenic Actinobacteria with a reduced genome. Genome Res **2003**; 13:1800–1809.

20. Renesto P, Crapoulet N, Ogata H, et al. Genome-based design of a cell-free culture medium for Tropheryma whipplei. Lancet Lond Engl **2003**; 362:447–449.

21. Sentausa E, Fournier P-E. Advantages and limitations of genomics in prokaryotic taxonomy. Clin Microbiol Infect Off Publ Eur Soc Clin Microbiol Infect Dis **2013**; 19:790–795.

22. Schleifer KH. Classification of Bacteria and Archaea: past, present and future. Syst Appl Microbiol **2009**; 32:533–542.

23. Woese CR. Bacterial evolution. Microbiol Rev **1987**; 51:221–271.

24. Kim M, Oh H-S, Park S-C, Chun J. Towards a taxonomic coherence between average nucleotide identity and 16S rRNA gene sequence similarity for species demarcation of prokaryotes. Int J Syst Evol Microbiol **2014**; 64:346–351.

25. Jensen A, Scholz CFP, Kilian M. Re-evaluation of the taxonomy of the Mitis group of the genus Streptococcus based on whole genome phylogenetic analyses, and proposed reclassification of Streptococcus dentisani as Streptococcus oralis subsp. dentisani comb. nov., Streptococcus tigurinus as Streptococcus oralis subsp. tigurinus comb. nov., and Streptococcus oligofermentans as a later synonym of Streptococcus cristatus. Int J Syst Evol Microbiol **2016**; 66:4803–4820.

26. Glazunova OO, Raoult D, Roux V. Partial sequence comparison of the rpoB, sodA, groEL and gyrB genes within the genus Streptococcus. Int J Syst Evol Microbiol **2009**; 59:2317–2322.

27. Scholz HC, Pfeffer M, Witte A, et al. Specific detection and differentiation of Ochrobactrum anthropi, Ochrobactrum intermedium and Brucella spp. by a multi-primer PCR that targets the recA gene. J Med Microbiol **2008**; 57:64–71.

28. Moore WEC, Stackebrandt E, Kandler O, et al. Report of the Ad Hoc Committee on Reconciliation of Approaches to Bacterial Systematics. Int J Syst Evol Microbiol **1987**; 37:463–464.

29. Meier-Kolthoff JP, Göker M, Spröer C, Klenk H-P. When should a DDH experiment be mandatory in microbial taxonomy? Arch Microbiol **2013**; 195:413–418.

30. Goris J, Konstantinidis KT, Klappenbach JA, Coenye T, Vandamme P, Tiedje JM. DNA-DNA hybridization values and their relationship to whole-genome sequence similarities. Int J Syst Evol Microbiol **2007**; 57:81–91.

31. Ramasamy D, Mishra AK, Lagier J-C, et al. A polyphasic strategy incorporating genomic data for the taxonomic description of novel bacterial species. Int J Syst Evol Microbiol **2014**; 64:384–391.

32. Tindall BJ, Rosselló-Móra R, Busse H-J, Ludwig W, Kämpfer P. Notes on the characterization of prokaryote strains for taxonomic purposes. Int J Syst Evol Microbiol **2010**; 60:249–266.

33. Chun J, Oren A, Ventosa A, et al. Proposed minimal standards for the use of genome data for the taxonomy of prokaryotes. Int J Syst Evol Microbiol 68:461–466.

34. Nowrotek M, Jałowiecki Ł, Harnisz M, Płaza GA. Culturomics and metagenomics: In understanding of environmental resistome. Front Environ Sci Eng **2019**; 13:40.

35. Miller S, Naccache SN, Samayoa E, et al. Laboratory validation of a clinical metagenomic sequencing assay for pathogen detection in cerebrospinal fluid. Genome Res **2019**; 29:831–842.

36. Arango-Argoty G, Garner E, Pruden A, Heath LS, Vikesland P, Zhang L. DeepARG: a deep learning approach for predicting antibiotic resistance genes from metagenomic data. Microbiome **2018**; 6:23.

37. Nnadozie CF, Odume ON. Freshwater environments as reservoirs of antibiotic resistant bacteria and their role in the dissemination of antibiotic resistance genes. Environ Pollut Barking Essex 1987 **2019**; 254:113067.

38. Zhang L, Chen F, Zeng Z, et al. Advances in Metagenomics and Its Application in Environmental Microorganisms. Front Microbiol **2021**; 12. Available at: https://www.frontiersin.org/articles/10.3389/fmicb.2021.766364. Accessed 19 October 2022.

39. Lynch MDJ, Neufeld JD. Ecology and exploration of the rare biosphere. Nat Rev Microbiol **2015**; 13:217–229.

40. CDC. The biggest antibiotic-resistant threats in the U.S. 2022. Available at: https://www.cdc.gov/drugresistance/biggest-threats.html. Accessed 21 October 2022.

41. Résistance aux antibiotiques. Available at: https://www.who.int/fr/news-room/fact-sheets/detail/antibiotic-resistance. Accessed 21 October 2022.

42. Sommer MOA, Dantas G, Church GM. Functional Characterization of the Antibiotic Resistance Reservoir in the Human Microflora. Science **2009**; 325:1128–1131.

43. Boutin S, Dalpke AH. The Microbiome: A Reservoir to Discover New Antimicrobials Agents. Curr Top Med Chem **2020**; 20:1291–1299.

44. Jana B, Cain AK, Doerrler WT, et al. The secondary resistome of multidrug-resistant Klebsiella pneumoniae. Sci Rep **2017**; 7:42483.

45. Falgenhauer L, Waezsada S-E, Yao Y, et al. Colistin resistance gene mcr-1 in extended-spectrum β-lactamase-producing and carbapenemase-producing Gram-negative bacteria in Germany. Lancet Infect Dis **2016**; 16:282–283.

46. Towards a genomics-informed, real-time, global pathogen surveillance system | Nature Reviews Genetics. Available at: https://www.nature.com/articles/nrg.2017.88. Accessed 19 September 2022.

47. Andam CP, Carver SM, Berthrong ST. Horizontal Gene Flow in Managed Ecosystems. Annu Rev Ecol Evol Syst **2015**; 46:121–143.

48. Cabello FC, Godfrey HP, Buschmann AH, Dölz HJ. Aquaculture as yet another environmental gateway to the development and globalisation of antimicrobial resistance. Lancet Infect Dis **2016**; 16:e127–e133.

49. Stackebrandt E, Goebel BM. Taxonomic Note: A Place for DNA-DNA Reassociation and 16S rRNA Sequence Analysis in the Present Species Definition in Bacteriology. Int J Syst Evol Microbiol **1994**; 44:846–849.

50. Lee I, Ouk Kim Y, Park S-C, Chun J. OrthoANI: An improved algorithm and software for calculating average nucleotide identity. Int J Syst Evol Microbiol **2016**; 66:1100–1103.

51. Meier-Kolthoff JP, Auch AF, Klenk H-P, Göker M. Genome sequence-based species delimitation with confidence intervals and improved distance functions. BMC Bioinformatics **2013**; 14:60.

52. Monaco M, Giani T, Raffone M, et al. Colistin resistance superimposed to endemic carbapenem-resistant Klebsiella pneumoniae: a rapidly evolving problem in Italy, November 2013 to April 2014. Euro Surveill Bull Eur Sur Mal Transm Eur Commun Dis Bull **2014**; 19:20939.

53. Yu Z, Cai Y, Qin W, Lin J, Qiu J. Polymyxin E Induces Rapid Paenibacillus polymyxa Death by Damaging Cell Membrane while Ca2+ Can Protect Cells from Damage. PLoS ONE **2015**; 10:e0135198.

54. Moffatt JH, Harper M, Boyce JD. Mechanisms of Polymyxin Resistance. Adv Exp Med Biol **2019**; 1145:55–71.

55. Campos MA, Vargas MA, Regueiro V, Llompart CM, Albertí S, Bengoechea JA. Capsule polysaccharide mediates bacterial resistance to antimicrobial peptides. Infect Immun **2004**; 72:7107–7114.

56. Puja H, Bolard A, Noguès A, Plésiat P, Jeannot K. The Efflux Pump MexXY/OprM Contributes to the Tolerance and Acquired Resistance of Pseudomonas aeruginosa to Colistin. Antimicrob Agents Chemother **2020**; 64:e02033-19.

57. Teyssier C, Jumas-Bilak E, Marchandin H, et al. Identification d'espèce et épidémiologie moléculaire des bactéries du genre Ochrobactrum. Pathol Biol **2003**; 51:5–12.

58. Aghapour Z, Gholizadeh P, Ganbarov K, et al. Molecular mechanisms related to colistin resistance in Enterobacteriaceae. Infect Drug Resist **2019**; 12:965–975.

59. Baron SA, Rolain J-M. Efflux pump inhibitor CCCP to rescue colistin susceptibility in mcr-1 plasmid-mediated colistin-resistant strains and Gram-negative bacteria. J Antimicrob Chemother **2018**; 73:1862–1871.

60. Ni W, Li Y, Guan J, et al. Effects of Efflux Pump Inhibitors on Colistin Resistance in Multidrug-Resistant Gram-Negative Bacteria. Antimicrob Agents Chemother **2016**; 60:3215–3218.

61. Tang M, Wei X, Wan X, Ding Z, Ding Y, Liu J. The role and relationship with efflux pump of biofilm formation in Klebsiella pneumoniae. Microb Pathog **2020**; 147:104244.

62. Tian Z, Lu S, Jin D, et al. Streptococcus chenjunshii sp. nov. isolated from feces of Tibetan antelopes. Int J Syst Evol Microbiol 69:1237–1243.

63. Routy B, Le Chatelier E, Derosa L, et al. Gut microbiome influences efficacy of PD-1-based immunotherapy against epithelial tumors. Science **2018**; 359:91–97.

64. Vila A, Pagella H, Vera Bello G, Vicente A. Brucella suis bacteremia misidentified as Ochrobactrum anthropi by the VITEK 2 system. J Infect Dev Ctries **2016**; 10:432–436.

65. Elsaghir AAF, James EA. Misidentification of Brucella melitensis as Ochrobactrum anthropi by API 20NE. J Med Microbiol **2003**; 52:441–442.

66. Hördt A, López MG, Meier-Kolthoff JP, et al. Analysis of 1,000+ Type-Strain Genomes Substantially Improves Taxonomic Classification of Alphaproteobacteria. Front Microbiol **2020**; 11. Available at: https://www.ncbi.nlm.nih.gov/pmc/articles/PMC7179689/. Accessed 17 February 2021.

67. Moreno E, Blasco JM, Letesson JJ, Gorvel JP, Moriyón I. Pathogenicity and Its Implications in Taxonomy: The Brucella and Ochrobactrum Case. Pathog Basel Switz **2022**; 11:377.

68. Cox G, Wright GD. Intrinsic antibiotic resistance: Mechanisms, origins, challenges and solutions. Int J Med Microbiol **2013**; 303:287–292.

69. Manterola L, Moriyón I, Moreno E, et al. The Lipopolysaccharide of Brucella abortus BvrS/BvrR Mutants Contains Lipid A Modifications and Has Higher Affinity for Bactericidal Cationic Peptides. J Bacteriol **2005**; 187:5631–5639.

70. Campos MA, Vargas MA, Regueiro V, Llompart CM, Albertí S, Bengoechea JA. Capsule Polysaccharide Mediates Bacterial Resistance to Antimicrobial Peptides. Infect Immun **2004**; 72:7107.

71. Gogry FA, Siddiqui MT, Sultan I, Haq QMohdR. Current Update on Intrinsic and Acquired Colistin Resistance Mechanisms in Bacteria. Front Med **2021**; 8:677720.

72. Lin M-F, Lin Y-Y, Lan C-Y. Contribution of EmrAB efflux pumps to colistin resistance in Acinetobacter baumannii. J Microbiol **2017**; 55:130–136.

73. Wang Z, Bie P, Cheng J, Lu L, Cui B, Wu Q. The ABC transporter YejABEF is required for resistance to antimicrobial peptides and the virulence of Brucella melitensis. Sci Rep **2016**; 6:31876.